UNSW SYDNEY

Optimizing the Removal of Proteinaceous Foulants from Membranes

Author:
Norazman, Noreisham

Publication Date:
2010

DOI:
https://doi.org/10.26190/unsworks/14953

License:
https://creativecommons.org/licenses/by-nc-nd/3.0/au/
Link to license to see what you are allowed to do with this resource.

Downloaded from http://hdl.handle.net/1959.4/50257 in https://unsworks.unsw.edu.au on 2024-05-03

UNSW
>014954834

PLEASE TYPE

THE UNIVERSITY OF NEW SOUTH WALES
Thesis/Dissertation Sheet

Surname or Family name: Norazman
First name: Noreisham Other name/s: -
Abbreviation for degree as given in the University calendar: PhD
School: Chemical Sciences and Engineering Faculty: Chemical Engineering
Title: Optimizing the Removal of Proteinaceous Foulants from Membranes

Abstract 350 words maximum:

Characteristics of irreversible protein residues on cleaned membranes are a crucial issue during membrane operations as the build-up of residues following repeated fouling and cleaning reduces membrane performance, purity and safety. In this study, the residual deposition of various proteins along a flat-sheet 30kDa Molecular Weight Cut-off (MWCO) polyethersulphone membrane was investigated. One Dimensional Sodium Dodecyl Sulphate – Polyacrylamide Gel Electrophoresis (1D SDS-PAGE) and Lowry method were utilized to determine cleaning effectiveness. Whey protein isolate, Bovine Serum Albumin (BSA) and Beta Lactoglobulin (βLg) solutions were used as foulants while Hydrochloric acid (HCl), Sodium Hydroxide (NaOH), and Protease M Amano enzyme were used as cleaners.

The deposition was generally arbitrary due to the random nature of attachment and aggregation of the protein molecules. However these fluctuations can be reduced when a spacer was inserted in the channel resting above the membrane. When recovering the membrane flux, sequential cleaning with HCl and NaOH was more effective than NaOH cleaning alone. The inclusion of HCl was beneficial for severely fouled membranes with high amount of residues. The highest flux recovered through sequential cleaning for repeated fouling and cleaning cycles was 88%, while protease cleaning alone recovered 77%. Chemical cleaning leaves behind residues under the 20kDa molecular weight however these proteins were undistinguished due to the limitations of 1D SDS-PAGE. On the other hand, protease cleaning leaves behind a distinct 38kDa protease residue on the surface.

The cross-flow ultrafiltration of BSA solutions at various conditions was studied using empirical mass transfer models and Computational Fluid Dynamics (CFD) simulations. The CFD simulates the steady state flux and wall concentrations based on varying physical properties. The mass transfer study estimates individual resistances, mass transfer coefficients, and diffusivities through various models.

The CFD shows good agreement between simulated and experimental fluxes over time however the simulation response to the varied conditions was only qualitatively similar. The effect of concentration polarization towards flux decline was high however it was underestimated in the CFD. While theoretical wall concentrations varied with pH, measured depositions were constant. The estimated diffusivities between CFD and mass transfer study concurred.

Declaration relating to disposition of project thesis/dissertation

I hereby grant to the University of New South Wales or its agents the right to archive and to make available my thesis or dissertation in whole or in part in the University libraries in all forms of media, now or here after known, subject to the provisions of the Copyright Act 1968. I retain all property rights, such as patent rights. I also retain the right to use in future works (such as articles or books) all or part of this thesis or dissertation.

I also authorise University Microfilms to use the 350 word abstract of my thesis in Dissertation Abstracts International (this is applicable to doctoral theses only).

.....	.....	.....
Signature	Witness	Date 16.12.10

The University recognises that there may be exceptional circumstances requiring restrictions on copying or conditions on use. Requests for restriction for a period of up to 2 years must be made in writing. Requests for a longer period of restriction may be considered in exceptional circumstances and require the approval of the Dean of Graduate Research.

FOR OFFICE USE ONLY Date of completion of requirements for Award:

OPTIMIZING THE REMOVAL OF PROTEINACEOUS FOULANTS FROM MEMBRANES

A thesis submitted as partial fulfilment of the requirements for the degree of

Doctor of Philosophy

By

Noreisham Norazman

in

The School of Chemical Sciences and Engineering

University of New South Wales

2010

Copyright Statement

'I hereby grant the University of New South Wales or its agents the right to archive and to make available my thesis or dissertation in whole or part in the University libraries in all forms of media, now or here after known, subject to the provisions of the Copyright Act 1968. I retain all proprietary rights, such as patent rights. I also retain the right to use in future works (such as articles or books) all or part of this thesis or dissertation.
I also authorise University Microfilms to use the 350 word abstract of my thesis in Dissertation Abstract International (this is applicable to doctoral theses only).
I have either used no substantial portions of copyright material in my thesis or I have obtained permission to use copyright material; where permission has not been granted I have applied/will apply for a partial restriction of the digital copy of my thesis or dissertation.'

Signed .....

Date 16.12.10

Authenticity Statement

'I certify that the Library deposit digital copy is a direct equivalent of the final officially approved version of my thesis. No emendation of content has occurred and if there are any minor variations in formatting, they are the result of the conversion to digital format.'

Signed .....

Date 16.12.10

Originality Statement

'I hereby declare that this submission is my own work and to the best of my knowledge it contains no materials previously published or written by another person, or substantial proportions of material which have been accepted for the award of any other degree or diploma at UNSW or any other educational institution, except where due acknowledgement is made in the thesis. Any contribution made to the research by others, with whom I have worked at UNSW or elsewhere, is explicitly acknowledged in the thesis. I also declare that the intellectual content of this thesis is the product of my own work, except to the extent that assistance from others in the project's design and conception or in style, presentation and linguistic expression is acknowledged.'

Signed .....

Date 16.12.10

Abstract

Characteristics of irreversible protein residues on cleaned membranes are a crucial issue during membrane operations as the build-up of residues following repeated fouling and cleaning reduces membrane performance, purity and safety. In this study, the residual deposition of various proteins along a flat-sheet 30kDa Molecular Weight Cut-off (MWCO) polyethersulphone membrane was investigated. One Dimensional Sodium Dodecyl Sulphate – Polyacrylamide Gel Electrophoresis (1D SDS-PAGE) and Lowry method were utilized to determine cleaning effectiveness. Whey protein isolate, Bovine Serum Albumin (BSA) and Beta Lactoglobulin (βLg) solutions were used as foulants while Hydrochloric acid (HCl), Sodium Hydroxide (NaOH), and Protease M Amano enzyme were used as cleaners.

The deposition was generally arbitrary due to the random nature of attachment and aggregation of the protein molecules. However these fluctuations can be reduced when a spacer was inserted in the channel resting above the membrane. When recovering the membrane flux, sequential cleaning with HCl and NaOH was more effective than NaOH cleaning alone. The inclusion of HCl was beneficial for severely fouled membranes with high amount of residues. The highest flux recovered through sequential cleaning for repeated fouling and cleaning cycles was 88%, while protease cleaning alone recovered 77%. Chemical cleaning leaves behind residues under the 20kDa molecular weight however these proteins were undistinguished due to the limitations of 1D SDS-PAGE. On the other hand, protease cleaning leaves behind a distinct 38kDa protease residue on the surface.

The cross-flow ultrafiltration of BSA solutions at various conditions was studied using empirical mass transfer models and Computational Fluid Dynamics (CFD) simulations. The CFD simulates the steady state flux and wall concentrations based on varying physical properties. The mass transfer study estimates individual resistances, mass transfer coefficients, and diffusivities through various models.

The CFD shows good agreement between simulated and experimental fluxes over time however the simulation response to the varied conditions was only qualitatively similar. The effect of concentration polarization towards flux decline was high however it was underestimated in the CFD. While theoretical wall concentrations varied with pH, measured depositions were constant. The estimated diffusivities between CFD and mass transfer study concurred.

Acknowledgements

In the first part of carrying out this project, it became quite clear to me that a postgraduate student cannot complete his PhD thesis alone. Therefore, it is a huge pleasure to thank the following individuals who made this thesis possible.

First and foremost, I would like to thank Professor Vicki Chen for her supervision, enthusiasm, inspiration and guidance, throughout my research study. I would have been lost without her. I would also like to sincerely thank my Co-Supervisor, Dr Hongyu Li for providing help, advice, encouragement and good ideas. It was a pleasure working with the both of them and I am truly grateful. I would like to thank my colleagues at the membrane centre for all the companionship, entertainment, motivation and friendship they provided. Dr Pierre Le Clech, Dr Paul Schausberger, Dr Gustavo Fimbres, Dr Lee Nuang, Dr Deyan Guang, Vera Liany, Ebrahim, and Guangxi Dong deserve special mention. They have provided a stimulating and fun environment in which to learn and grow. Special thanks to visiting students Meir Hasbani and Alex Weldon of Princeton University, who I had a chance supervising and work with. And not forgetting visiting students Ilio from Rome and Florie from France, who I had fond memories with. I am grateful to all the administration staffs for assisting me in many different ways especially Ik Ling who was always helping.

Next, I wish to express my deepest gratitude to my parents, Eishah Abdullah and Norazman Hassan. They bore me, raised me and love me all my life. And to my siblings, Noreiskandar, Aqilah and Nabilah, who are all, close to me. A special thought is devoted to all of them for their never ending love and support.

Last but not least, a very big thank you to my wonderful wife, Nurulhuda, for her patience, understanding, and encouragement, especially during the thesis writing period. Without you, I would be a very different person today and it would have been harder to finish a PhD. All I can say is it would take another thesis to express my love for her. To her, I dedicate this thesis.

Publications and Conference Proceedings

Scientific Journals

H.B. Petrus, H. Li., V. Chen, N. Norazman, Enzymatic cleaning of ultrafiltration membranes fouled by protein mixtures solutions. Journal of Membrane Science, 2008. 325: p. 783.

P. Schausberger, N. Norazman, H. Li, V. Chen, and A. Friedl, Simulation of protein ultrafiltration using CFD: Comparison of concentration polarization and fouling effects with filtration and protein adsorption experiments. Journal of Membrane Science, 2009. 337: p. 1-8

N. Norazman, A.R.W.L. Wu, H. Li, V. Chen, and H. Zhang, The role of chemical cleaners in removal of protein components from ultrafiltration membrane fouled with whey protein mixtures. To be submitted to Journal of Membrane Science.

Conference Proceedings

N. Norazman, A.R.W.L. Wu, H. Li, and V. Chen. Fouling and Cleaning in PES Ultrafiltration Membranes Fouled by Whey Protein Isolates. in Proceedings of the North American Membrane Society. May 12-17, 2006. Chicago, USA.

P. Schausberger, N. Norazman, H. Li, and V. Chen. Modelling Mass Transfer in Cross flow Ultrafiltration of BSA Solutions. In Proceedings of the North American Membrane Society. May 15-17, 2006. Chicago, USA.

P. Schausberger, N. Norazman, H. Li, and V. Chen. Modelling Mass Transfer in Ultrafiltration of BSA Solutions. In Proceedings of the IMSTEC'07 Conference. 2007. Sydney, NSW, Australia.

N. Norazman, A.R.W.L. Wu, H. Li, and V. Chen. Cleaning Efficiency Evaluation for PES Membrane fouled with Whey Protein Isolate Solution. In Proceedings of the IMSTEC' 07 Conference. November 5 - 9, 2007. Sydney, NSW, Australia.

V. Chen, N.N., H. Li, H. Zhang. Residual Foulant Distribution After Chemical Cleaning of Ultrafiltration Membranes fouled with Whey Protein Isolate. In Proceedings of the Engineering with Membranes' 08 Conference. 2008. Vale de Lobo, Algarve, Portugal.

P. Schausberger, N. Norazman, H. Li, A. Friedl, and V. Chen. Simulation of Protein Fouling on UF Membranes by Computational Fluid Dynamics. In Proceedings of the Engineering with Membranes' 08 Conference. 2008. Vale de Lobo, Algarve, Portugal.

Table of Contents

List of Figures

List of Tables

6.5	Spatial boundary conditions	174
6.6	Channel geometry	175
6.8	Collected data, standard conditions printed bold	185

List of Abbreviations

According to alphabetical order

Symbols	Descriptions	Units
A	Rate constant	$m^{1.8}\ s^{-1}\ mol^{-0.6}$
A	Side area per volume, protein molecule	$m^2\ m^{-3}$
αLa	Alpha Lactalbumin (Protein)	-
B	Slope fouling resistance	$m\ mol^{-1}$
BSA	Bovine Serum Albumin (Protein)	-
βLg	Beta Lactoglobulin (Protein)	-
C, c	Concentration BSA solution	$mol\ m^{-3}$
CFD	Computational Fluid Dynamics	-
CP	Concentration polarization	-
D	Diffusivity, Diffusion coefficient	$m^2\ s^{-1}$
d_h	Hydraulic diameter	m
P	Density	$kg.m^{-3}$
F	Volumetric flow-rate	$mL.min^{-1}$
FESEM	Field Emission Scanning Electron Microscopy	-
FTA	Fatty acids	-
Gg	Gamma-Globulin	-
H	Slit height	m
HSA	Human Serum Albumin (Protein)	-
IEP, i.e.p, IP	Iso-electric point (pH)	-
J	Permeate flux	ms^{-1} or $Lm^{-2}h^{-1}$
K	Reaction order	-
K	Mass transfer coefficient	$m\ s^{-1}$
K(ϕ)	hydrodynamic interaction coefficient	-
L	Membrane length	m
LSZ	Lysozyme (Protein)	-
M, m	Molarity	$mol\ L^{-1}$
M	Molar mass BSA	$Da, gmol\ L^{-1}$
MALDI-MS	Matrix Assisted Laser Desorption Ionization Mass Spectrometry	-
MF	Microfiltration	-
MGB	Myoglobulin (Protein)	-
Milli-Q, MQ	Ultrapure Milli-Q™ water	-
MWCO	Molecular Weight Cut-Off	Da
N	Exponent fouling resistance	-
N_A	Avogadro Constant, 6.022E23	mol^{-1}
OP	Osmotic Pressure	Pa

P	Pressure	Pa, bar
PALL	Membrane manufactured by Pall Corporation (US)	-
Pe	Peclet number	-
pH	Power of hydrogen	-
PMA	Protease M Amano Enzyme (Protein)	-
Q	Protein deposition per membrane area	mol m^{-2}
R	Resistance	m^{-1}
$\mathcal{R}$	Gas constant, 8.3145	J mol^{-1} K^{-1}
Re	Reynold's Number	-
RO	Reverse Osmosis	-
SDS-PAGE	Sodium Dodecyl Sulphate Polyacrylamide Gel-Electrophoresis	-
Sc	Schmidt Number	-
Sh	Sherwood number	-
SYNDER	Membrane manufactured by Synder Filtration (US)	-
S(ϕ)	Thermodynamic coefficient	-
T	Temperature	K
T	Time	S
TMP	Trans-membrane pressure	Pa
U	Velocity	m s^{-1}
UF	Ultrafiltration	-
UV-Vis	Ultraviolet-Visible	-
M	Viscosity	Pa.s
V	Molar volume BSA	m^3 mol^{-1}
V	Volume flow	L h^{-1}
WPC	Whey protein concentrate	-
WPI	Whey Protein Isolate	-
x, y	Spatial coordinates	M
Z	Macro-ionic charge BSA	-
Greek letters	**Descriptions**	**Units**
$\prod$, π	Osmotic Pressure	Pa
M	Dynamic Viscosity	Pa s
P	Density	kg m^{-3}
Φ	Volume fraction BSA	-
Subscripts	**Descriptions**	**Units**
B, b	Bulk BSA concentration	-
C	Concentration	-
CP	Concentration polarization	-
Crit	Critical	-
F, f	Fouling	-
Gel	Gel	-
Id	Infinite dilution	-

M, m	Membrane	-
Ml	Monolayer	
NF, nf	Non-fouling	-
O	Initial conditions, at start of experiments	-
P, pass	Passive	-
S	Solute	-
S	Salt	-
Sim	Simulation	-
W	Wall	-
W	Water	-

Chapter 1: Introduction

1.1. Foreword

Membrane filtration is one of the largest and most diverse forms of separation technique. Ultrafiltration (UF) for instance, is widely utilized in the recovery and purification of protein products from a range of biological streams in food, pharmaceutical and biotechnological industry (Mulder, 2000; Ghosh, 2003). Continuous separation, absence of heat and low energy consumption are the main reasons why UF is employed to separate and fractionate labile and sensitive proteins. However, the application of UF is not trouble-free as the method is affected by fouling that reduces the membrane performance. Nevertheless, membrane fouling can be controlled and minimized through proper permeate flux control, membrane surface pre-treatment and periodic cleaning of the fouled membrane surface (Plett, 1985; Tragardh, 1989). Membrane cleaning study is necessary because most methods recommended by membrane manufacturers are unclear and trial-and-error base.

Further investigations are required for examining the nature of the protein deposits and residuals on the membrane surface after fouling and chemical cleaning, which initiates the decline in membrane performance. As a result, many researchers have performed various studies on membrane fouling using protein model solutions in the last few decades (Suki et al., 1983; Fane and Fell, 1987; Kim et al., 1992; Chan et al., 2002; Ye, 2005; Petrus, 2006; Chen et al., 2007). Subsequently, various membrane cleaning investigations were also done (Kim et al., 1993; Wu, 2007; Petrus et al., 2008). D'Souza and Mawson (2005) reviewed cleaning of membranes in the dairy industries while various characterization methods for analysing protein deposition on membrane surface were documented by Chan and Chen (2004). Not long ago, a study using Matrix Assisted Laser Desorption Ionization-Mass Spectrometry (MALDI-MS) was performed to describe the surface nature of the protein deposition along a cross-flow UF set-up (Chan et al., 2004). MALDI-MS analyses the immediate surface fouling layer, however, the overall composition in a relatively thicker fouling layer could be different from the surface composition. In addition, there were also issues related to the ionic excitation

that could interfere with the results. The limitation of the method motivates us to search for an alternative method to analyse the foulant layer on the membrane surface. In addition, the alternative method also needs to support and explain the source of fluctuations in protein deposition along the membrane channel experienced in MALDI-MS results.

The aim of this current study is to improve and optimize cleaning methods for membranes in protein based applications by understanding complex interactions that occur between the foulants and membranes, as well as foulants and cleaners. In this thesis, membrane fouling and cleaning is studied based on protein and residual deposition as well as distribution of protein species on the membrane. From this study, we can better understand the interaction that occurs between the foulants, membrane and cleaners under various operating conditions. The alternative method selected in this current study to examine protein deposition is One Dimensional Sodium Dodecyl Sulphate-Polyacrylamide Gel Electrophoresis (1D SDS-PAGE), which is a common technique used in biochemistry to separate proteins and peptides according to molecular weights (Hoefer, 1994). 1D SDS-PAGE was utilized to observe the characteristics of protein foulants and residues before and after chemical and enzymatic cleaning. However, its current use in the membrane field is relatively new. In addition, UF and Milli-Q fluxes were used as indicators to measure the extent of fouling and effectiveness of cleaning.

Another important study performed in this thesis is the application of Computational Fluid Dynamics (CFD) to model concentration polarization and flux decline during Bovine Serum Albumin (BSA) UF in a cross-flow set-up. In addition to CFD, mass transfer equations and empirical models were utilized to estimate wall concentration, diffusivity, and mass transfer coefficient during BSA UF at steady-state. Experimentally, the extent of fouling was measured using Milli-Q water flux and resistance measurements. The amount of protein deposits on the membrane surface were measured using the Lowry method (Hess et al., 1978). Using these methods, the deposition profile along the horizontal cross-flow membrane surface can be studied.

From this current study, a better understanding of the complex interactions that occur between the membrane, protein and cleaner during UF can be achieved. From this acquired knowledge, the cleaning of proteinaceous fouled membranes can be improved significantly and optimized.

1.2. Thesis Description

This thesis is sub-divided into seven chapters and an appendix. The brief description of each of these chapters is as follows.

Chapter 1 introduces the current study and realises the gaps that needs to be filled in the current study of membrane cleaning particular in applications involve proteineous solution.

Chapter 2 contains the literature review that highlights the relevant theories and principles towards formulation of research methods in fouling, cleaning and mass transfer modelling investigations that follows. These includes documentation on proteins, adsorption of proteins to surfaces, past studies in UF, membrane cleaning, cleaning mechanism of chemicals and enzymes, membrane characterization methods and mass transfer of proteins on membranes.

Chapter 3 contains information on the materials and methods applied in the current study on membrane fouling, cleaning and mass transfer modelling performed in the next following chapters. The characterization methods for evaluation of components in the membrane fouling layer and on the cleaned membrane surface compiled in this chapter are Lowry method, 1D SDS-PAGE, and Field Emission Scanning Electron Microscopy (FESEM).

Chapter 4 contains the fouling studies performed using binary BSA and Beta Lactoglobulin (βLg) solutions in a cross-flow set-up under constant pressure UF, under the influence of cross-flow velocity, pH, filtration duration, and spacer. The main objective of this study is to establish protein fouling characteristics in the particular filtration set-up so as to lay the foundation for the cleaning study. Novel studies include examining the horizontal distribution of binary protein species along the membrane surface in a cross-flow set-up under the presence and absence of spacer in the channel using the Lowry method and 1D SDS-PAGE. The

chapter contains findings of mass balance, critical flux, flux measurements and protein characterization. The results were compared with previous studies that uses similar feed solutions to typify fouling and flux decline.

Chapter 5 contains results of chemical and enzymatic cleaning studies of whey protein fouled membranes. Fluxes were measured and protein residuals at various stages of experiments were characterized using both the Lowry method and 1D SDS-PAGE. The effectiveness of single and sequential alkali-acid cleaning was tested under various conditions and the results were discussed.

Chapter 6 contains the application of mass transfer equations and fouling models to analyse the UF of BSA solution under various operating conditions. The contribution of concentration polarization and fouling are distinguished and the wall concentration, diffusivity and mass transfer coefficient are estimated. The results are compared to a parallel study using CFD to predict the flux decline in a cross flow set-up under the same operating conditions.

Chapter 7 contains the conclusions of the current study and recommendations to be considered for future study.

1.3. **Appendix Description**

The Appendix is sub-divided into Parts A, B, C and D.

Part A covers miscellaneous details from Chapter 3 which include methods and materials as well as results of MALDI-MS, information on the dead-end cell and gel-staining methods of 1D SDS-PAGE.

Part B covers supporting details from Chapter 4 which includes UV-Vis Spectrometry at 280nm, critical flux results at pH 3 for BSA solutions, analysis of surface protein deposition using MALDI-MS after 8 hours UF, analysis of feed protein using 1D SDS-PAGE, 4 hours of UF with no spacer, and the calculation of pressure losses in the UF rig.

Part C covers images of FESEM studies of BSA, βLg, and WPI fouled membranes. It also contains images of hydrochloric acid (HCl), sodium hydroxide (NaOH) and protease enzyme cleaned membranes.

Part D covers methods to derive stagnant-film equation, BSA rejection during UF and the effect of feed and flow on BSA deposition.

Chapter 2: Literature Review

2. Introduction

Ultrafiltration (UF) membrane systems are extensively applied in the fields of dairy and food processing where the feeds and products are heat sensitive and easily denatured (Meares, 1976). Two of the largest application of UF is in the fractionation of aqueous cheese whey and the pre-concentration of milk for cheese manufacturing (Cheryan, 1998). Although membranes are widely utilized, the main problems are the adhesion of proteinaceous substances onto the surface and fouling. Despite the significance of membrane fouling by proteins and its consequences towards membrane performance, it is surprising that protein removal was not given a great deal of attention.

Up till now, membrane cleaning has been performed with inadequate understanding on the cleaning mechanisms, residual characteristics and its consequences on membrane performance (D' Souza and Mawson, 2005). Moreover, an effective cleaning method saves substantial energy and production costs, reduce chemicals and wastewater usage and protect the membrane from degradation as a result of harsh cleaning methods. The principal objective of this current study is to analyse the foulants and irreversible residuals which is crucial towards building an effective cleaning strategy. Thus, all issues including the complex interactions between the proteins, membranes and cleaners are accounted for.

In this chapter, a literature review of the topics relevant to our current study was completed. This includes a brief introduction to proteins and proteins in solution. In addition, the review also covers the adsorption of protein molecules on solid surfaces including membranes, which discusses the interactions and bonds between protein molecules, surface and solution environment. The effects of pH charge, membrane type, critical flux and feed channel spacer on protein adsorption and fouling were also discussed. Other relevant topics include recent membrane cleaning investigations, methods of membrane characterization and mass transfer studies.

2.1. **Proteinaceous solutions**

2.1.1. A brief description of proteins

Proteins are chemical molecules that carry out the functions of living organisms in the processes of life. Understanding protein structures and functions are essentially chemical problems, and chemists have been involved in analysing their structures, purifying and investigating proteins for over a hundred years. Examples of proteins are enzymes, regulatory and transport proteins, immunoglobulin, muscle proteins, collagen and toxins.

A protein molecule is a linear biopolymer composed of basic building blocks called amino acids held together by peptide bonds (Streitwieser and Heathcock, 1976). Proteins are made from a set of nineteen amino acids and one amino acid Proline as shown in Figure 2.1.

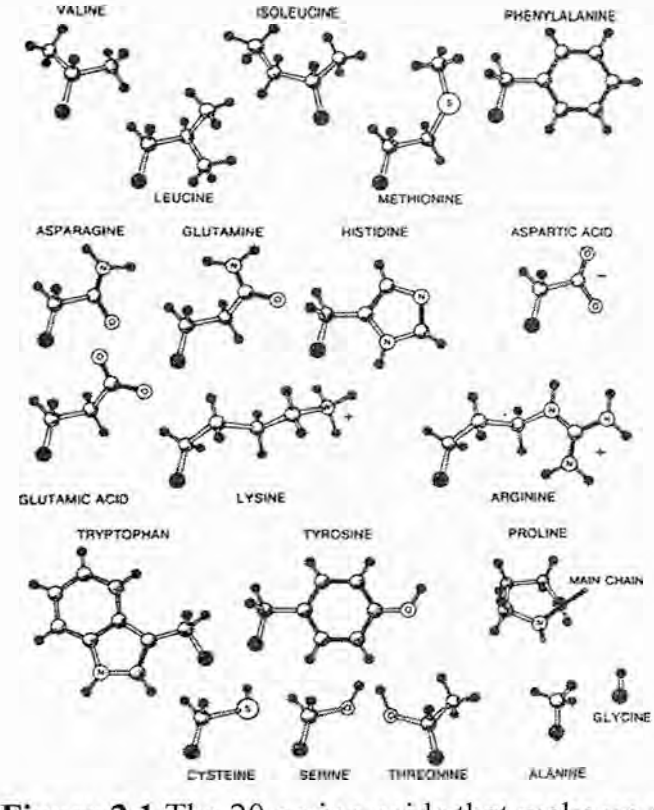

Figure 2.1 The 20 amino acids that make up proteins (Franks, 1993)

Proteins are also large molecules, with molecular weights ranging from 6 – 1000 Kilo Daltons. On the other hand, peptides are smaller proteins units formed between two molecules are called dipeptides while between three are called tri-peptides, and so on. As more units are added to the chain, a polymer of any length may be achieved and such polymers are known as polypeptides. Simply repeating this process leads to a generalized structure of a protein. A protein molecule can be a single poly-(amino acid) chain or may comprise of more than one poly (amino acid) chain, held together by covalent bonds or by non-covalent interactions. The three dimensional structure of protein is determined by a set of weak interactions – hydrogen bonding, charge and dipole interactions, van der Waals interactions – that each residue makes with its neighbours.

2.1.2. Protein coiling, folding and denaturation

Protein coiling, folding and denaturation are three important characteristics of proteins in aqueous solution. Protein coiling is caused by the intra-chain bonds (hydrogen bonding, van der Waals etc.) and interactions between these chains (Streitwieser and Heathcock, 1976). During protein coiling, the protein molecule orientates itself so that the non-polar side chains lie inside the bulk of the structure where they attract each other by van der Waals forces. The polar side chains tend to be on the surface of the molecule where hydrogen bond can take place between the protein molecule and water making it soluble. The inter-chain hydrogen bonds between the amide linkages inside the bulk of the molecule causes further coiling and compacting of the three dimensional structure.

Alternatively, protein folding is caused by disulphide bridges. Protein folding is spontaneous, and is driven by the increase in the entropy of the water that causes the hydrophobic side-chains to be removed from the solvent into the interior of the protein (Doonan, 2002). However, proteins can be unfolded by changes in conditions such as temperature, pH and addition of denaturing agents such as urea.

In the event of denaturation, the three dimensional structure can be permanently disrupted under extreme temperatures and pH and this affects the solubility of the proteins in water. One common example is the heating of skim milk at high temperature. However, protein denaturation and renaturation is reversible when the protein is subjected to the temperature and pH at a state where the protein is stable as shown Figure 2.2.

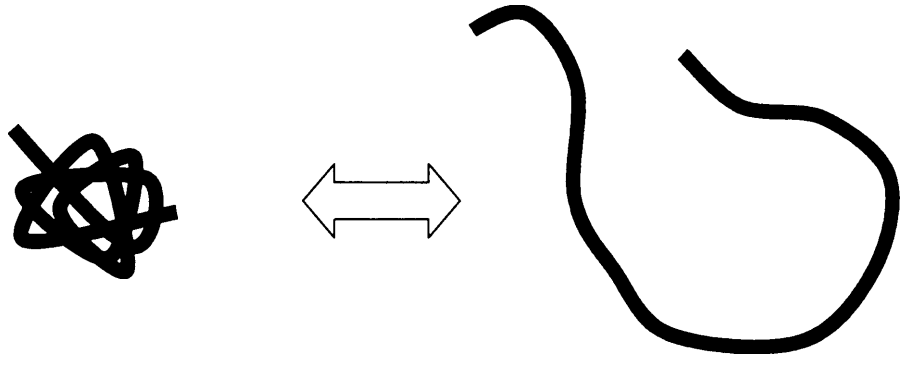

Figure 2.2 Schematic diagram of a globular protein, showing the reversible denaturation to random coil chain

2.1.3. Section synopsis

To summarize, this sections begins with an introduction to the basic properties of proteins, peptides and amino acids. Proteins are natural bio-molecules and complex in solution as their behaviours are influenced by their aqueous environment. The conditions of the aqueous environment, such as temperature, pH and hydrodynamics influences the state of the protein molecule i.e. folded or denatured. Extreme temperatures, pH as well as rough handling of proteinaceous solution can cause denaturation of the proteins resulting in the protein's insolubility and the elevation of membrane fouling. The protein's combined characteristics such as concentration, molecular weight, iso-electric points (IEP) and charge interactions are crucial to be understood as these influences the outcome of the product and performance of separation.

2.2. Protein adsorption

2.2.1. Passive adsorption of protein molecules on solid surfaces

Protein adsorption on surfaces is a natural phenomenon which occurs spontaneously when proteins in solution are exposed to a solid/liquid interface. The general trends in the adsorption of proteins on synthetic polymers surfaces are firstly, the adsorption attraction increases with increasing molecular mass. Secondly, adsorption can be enhanced by increasing the hydrophobicity of the protein and is related to structural stability ("hard" or "soft"). Thirdly, electrostatic interaction plays an important role especially in hydrophilic surfaces. Various authors state that the adsorption of protein on solid/liquid interface is influenced by the properties of protein molecules such as electrostatic charges, structural stability as well as solution environmental conditions such as pH and ionic strength (Arai and Norde, 1990a; Arai and Norde, 1990b; Norde and Anusiem, 1992; Norde and Favier, 1992; Bos et al., 1994).

Table 2.1, shows the molecular properties of Bovine Serum Albumin (BSA), Lysozyme (LSZ), Myoglobulin (MGB) and Alpha-lactalbumin (αLa) which are important for understanding and explaining the observed behaviour of proteins during protein adsorption on interfaces (Bos et al., 1994).

Table 2.1
Some physical-chemical properties of the proteins BSA, LSZ, MGB and αLa (Bos et al., 1994)

Parameters	Proteins			
	BSA	LSZ	MGB	αLA
Molar mass ($gmol^{-1}$)	67000	14600	17800	14200
Dimensions (nm^3)	11.6 × 2.7 × 2.7	4.5 × 3.0 × 3.0	4.5 × 3.5 ×2.5	3.7 × 3.2 × 2.5
Diffusivity (m^2s^{-1})	7.4×10^{-11}	1.04×10^{-10}	1.10×10^{-10}	1.06×10^{-10}
Gibbs energy of denaturation (Jg^{-1})				
Thermal	–	–4.1	–2.8	–1.5
By denaturant	–	–4.0	–3.1	–1.9
Iso-electric points (pH units):	4.7	11.1	7.0	4.3
Literature values	4.8	> 10	7.2	–
Measured				
Structural stability	Low "**Soft**"	Low "**Soft**"	High "**Hard**"	High "**Hard**"
Surface charge affinity	Hydrophilic and hydrophobic surfaces under all charges, attraction or repulsion	Hydrophilic and hydrophobic surfaces under all charges, attraction or repulsion	Hydrophobic surfaces under all charges. Hydrophilic if electro statically attracted	Hydrophobic surfaces under all charges. Hydrophilic if electro statically attracted
Charge at pH 7	– Ve	+ Ve	0	– Ve
Charge at pH 4	+ Ve	+ Ve	+ Ve	+ Ve

Information in Table 2.1, Bos et al. (1994) suggests that during protein adsorption on a surface, "hard" protein molecules with high internal stability and Gibb's energy are dominated by electrostatic and hydrophobic interactions between the proteins and surface. "Hard" protein molecules with high internal stability do not adsorb on hydrophilic surfaces unless there is an electrostatic attraction however on hydrophobic surfaces "hard" proteins adsorb and undergo structural changes upon adsorption. On the other hand, "soft" protein molecules with low internal stability, tends to adsorb on all surfaces regardless of electrostatic interactions and gains in structural entropy during adsorption.

At room temperature, negatively charged "hard" βLg molecules adsorbed on negatively charged hydrophilic surface i.e. silica gel and stainless steel (Nakanishi et al., 2001). While the amount of βLg adsorbed was small due to electrostatic repulsion, it could be increased by increasing the ionic strength of the solution. In the same reference, BSA and LSZ, both "soft" could adsorb on a surface irrespective of electrostatic interactions and the amount of "soft"

βSA adsorbed on hydrophilic silica gel was about twice compared to "hard" βLg under similar experimental conditions (0.01M and pH 7). Upon adsorption these "soft" proteins would change their structural conformation to a greater extent.

In conclusion, structurally stable "hard" proteins could adsorb on a surface with a charge opposite that of the proteins. However, "hard" proteins only adsorb on a surface of the same charge when there is hydrophobic interaction. On the other hand, the structurally unstable "soft proteins" seem to adsorb on any surfaces owing to a gain in conformational entropy.

The adsorption of protein molecules on surfaces is also affected by temperature. At room temperatures (20 – 22°C), Nakanishi et al. (2001) reported that the amount of proteins adsorbed was in the range of several milligrams per square meters varying with the type of proteins, surface and adsorption conditions and the amount adsorbed proteins was much higher at higher temperatures than at room temperatures due to conformational changes that results to aggregation of molecules on the surface and bulk. At pH 6.85, the amount of adsorbed βLg on stainless steel is constant up to 50°C and then starts to increase with the increase in temperature.

In milk processing, protein deposition on heat exchanging surfaces is a critical issue, as deposition results in fouling which reduces heat exchanging efficiency, pressure drop and economy of the processing plant (Bansal and Chen, 2006). In addition, milk fouling in heat exchangers also causes contamination and reduction in product quality.

When mixtures of soft proteins are exposed to an inert interface, sequential and competitive adsorption occurs, governed by electrostatic interactions. Previously, it was observed that when "hard" proteins competes with "soft" proteins during adsorption, "hard" proteins preferentially adsorbs even under repulsion (Arai and Norde, 1990b). However, the adsorption of "soft" proteins that has low structural stability structurally rearranges itself contributing to higher overall adsorption energy causing preferential adsorption over the "hard" proteins.

Structural rearrangements of the molecule outweigh the unfavorable contributions from hydrophilic dehydration and electrostatic repulsion.

Competitive adsorption or better known as "Vroman Effect" is a general behaviour of mixed proteins in solution during adsorption on surfaces. "Vroman Effect" involves sequential collision, adsorption, and species exchanging processes while forming protein layers (Leo and Adams, 1969; Lassen and Malmsten, 1996). Research on simultaneous adsorption of BSA molecules and βLG molecules on inert silica surface shows that βLG molecules was the dominant followed by a subsequent replacement by BSA molecules. In addition, Nakanishi et al. (2001) also stated that competitive nature for protein components is dynamic and depends on the proteins molecular size, structural stability, and degree of denaturation. The authors observed that proteins higher in concentration and diffusivity adsorbs first followed by subsequent exchange with less mobile proteins with higher binding attraction.

The adsorption kinetics, sequential and competitive adsorption of four different milk proteins, BSA, βLg, αLa, and β-casein was studied (Nasir and McGuire, 1998). In competitive adsorption of BSA and βLg, there was greater adsorbed mass and higher kinetic of adsorption on hydrophobic compared to hydrophilic surfaces. The adsorbed mass for binary protein is higher than single protein by itself indicating a mixed film consisting of more than one layer. βLg was the main protein adsorbed on the surface in the first hour however was replaced with BSA over time. Thus, after four hours, BSA adsorption increased while βLg adsorption decreases on the surface. This is consistent with Arai and Norde (1990b) who explains that "hard" proteins preferentially adsorb and after time "hard" proteins are taken over by "soft" proteins. Alternatively, in sequential adsorption of these three proteins, it was observed that there was an exchange of initially adsorbed BSA with the next proteins, βLg, αLa, and β-casein introduced.

2.2.2. Passive and dynamic adsorption of protein molecules on membranes

In membrane separation, adsorption of protein is an important issue that is influenced by the properties of protein molecules (i.e. molecular sizes, IEP and stability), environmental conditions (i.e. solution pH) and membrane type (i.e. porosity, morphology etc.). Thus, the adsorption of proteins on membrane surfaces is similar to solid surfaces except for the additional influence of membrane characteristics. In addition, due to the porous nature of membrane surfaces, the interfacial properties are sometimes altered when adsorption occurs. It is crucial to understand and control the adsorptive interactions between proteins and membrane interfaces that initiate many undesirable consequences such as fouling, biofouling and flux decline. Many studies were performed by various researchers on protein adsorption on membranes during UF.

Adsorption on membrane was defined as an equilibrium partitioning of solute between a solution and a membrane surface (Suki et al., 1984). Therefore, this refers to the solute molecules in direct contact with the membrane surface. Deposition is defined as the material irreversibly deposited on the membrane surface due to convection, protein-protein interactions and adsorption.

Protein adsorption has a very pronounced effect on the performance of partially permeable membranes (Suki et al., 1983; Waters et al., 1983). It was observed that the characteristics of UF membranes that govern fouling are physico-chemical properties of the membrane, porosity and morphology of the surface (Fane and Fell, 1987). Maximum deposition occurred at the IEP pH of the protein, where the protein molecules are less soluble. In addition, higher deposition also occurred on more heterogeneous membranes.

The effect of IEP was observed in a related study where during the UF of BSA and HSA in a cross-flow set-up and using ceramic membranes of higher MWCO than the two proteins, a rapid flux decline was observed at pH 3 and 5 (IEP pH 4.8), while slower deposition was

observed at pH 7 (Su et al., 2000). In addition, fouling also occurs very quickly at pH 5 and fouling is lowest at pH 7.

Therefore, the net charge of protein in solution is affected by pH of solution. When the solution pH is at IEP, the net charge of protein is zero (or neutral); when solution pH is higher than IEP of protein, the net charge of protein becomes negative and when solution pH is lower than the IEP, the net charge of the protein becomes positive. The net charge becomes more pronounced when the difference between solution pH and protein IEP pH is large.

Waters et al. (1983) explains that during the UF of proteins, permeate flux as well as solute rejection is time-dependent. The permeate flux decline of permeable membranes was very dramatic initially, followed by a gradual decline caused by a loss of porosity with time while in service due to internal adsorption and pore plugging. In addition, rejection is elevated initially due to significant protein adsorption at the beginning, and as the porosity disappears and surface adsorption occurs, rejection rises gradually. The highest permeate flux occurs when the protein is enlarged and most charged i.e. at extreme pH and non-ionic conditions. However, presence of added salts or in ionic solvents, the protein contracts and the charges are shielded, resulting in the formation of a less permeable deposit and a lower permeate flux.

The adsorption of proteins on an adsorptive, less adsorptive and retentive membranes is shown in Table 2.2 (Waters et al., 1983). In adsorptive and less adsorptive membranes, rejection is highest when protein is charged, while rejection is lowest when protein is uncharged. Minimum flux was observed at the IEP of the protein in non-ionic solution. In composite membranes, the effect of ions to the flux is more significant. In retentive membranes, the minimum flux occurs at the IEP of the proteins similar to adsorptive membranes.

Table 2.2
The comparisons of flux, rejection, resistance and adsorption between an adsorptive, less adsorptive and retentive membranes (Waters et al., 1983)

Membrane type	Flux decline	Rejection	pH and ionic strength
Permeable to proteins (Less adsorptive)	Lower final flux observed in adsorptive for proteins < pore size	Gradual increase in rejection.	In non-ionic, distinct minimum of flux at IEP of proteins. However, in ionic minima indistinct. Rejection lowest when protein is uncharged, adsorption is high Rejection highest when protein is charged, however adsorption is low
Permeable to proteins (Adsorptive)		Initial high rejection followed by a drop and a rise again to steady steep decline initially followed by gradual steady decline for proteins size < Molecular weight Cut-off (MWCO)	
Pre-used protein adsorbed membranes (Composite membranes)	Less dramatic change than the above and slow decline to a steady final flux	Comparable to retentive membranes	Ionic: Low flux Non-Ionic: High flux Same flux for ionic and non-ionic at IEP.
Retentive Membranes (Retain proteins larger than MWCO)	Steep decline in flux for proteins < (MWCO). Gradual decline for totally retained proteins Lower final flux for proteins < MWCO compared to retained proteins	Steep decline initially followed by gradual steady decline for proteins size < MWCO. Also rejection for these proteins.	Ionic: Low flux Non-Ionic: High flux Higher flux for Ionic at IEP In non-Ionic, distinct minimum of flux at IEP of proteins. The minimum flux for ionic solution is indistinct

In a study of the deposition and composition of fouling layer on the membrane surface after the UF of a single and mixed protein solution using Matrix Assisted Laser Desorption Ionization Mass Spectrometry (MALDI-MS), significant differences were observed between the deposition of single protein solution and multiple protein mixtures (Chen et al., 2007). The higher amount of proteins adsorbed on the membrane surface do not necessarily decreases the flux. In addition, the UF of multiple protein mixtures on a fully retentive membrane resulted in the adsorption of large proteins initially in short term filtration and later superseded by smaller

proteins in long term filtration. This was caused by protein exchange and displacement phenomena in deposition layer caused by the differences in structure and diffusivity of different protein molecules in the mixture.

2.2.3. Section synopsis

The adsorption and deposition of proteins on surfaces is both complex and dynamic. Investigations in protein adsorption on solid surfaces are not new and many experiments were performed to understand this phenomenon. We may conclude that the important factors affecting protein adsorption on solid surfaces are structural stability of the protein, pH and solution charge, ionic concentration and the hydrophilic or hydrophobic properties of the surface. Proteins are being categorised into "hard" and "soft". Hard proteins are proteins with high structural stability and adsorb strongly on hydrophobic surfaces. On the other hand, soft proteins have low structural stability and adsorb strongly on both hydrophilic and hydrophobic surfaces. In addition, competitive adsorption is also observed on surfaces exposed to mixtures of proteins. During competitive adsorption, proteins higher in concentration and diffusivity adsorbs first followed by subsequent exchange with less mobile proteins with higher binding attraction. Past findings have shown that "hard" proteins preferentially adsorb on surfaces and taken over by "soft" proteins with time. Similarly, protein adsorption on membrane surfaces is also affected by protein characteristics and solution environment however membrane characteristics such as morphology and porosity are important influence. The adsorption of protein molecules on membranes was found to result in the lost of porosity with time. The nature of membranes used i.e. adsorptive, composite or retentive, affects the protein deposition, permeate flux and protein rejection. In addition, the highest flux during filtration occurs at pH extremes (i.e. away from the IEP) where the protein is enlarged and the deposit is more permeable. All these studies are very relevant to our present investigation and may provide an explanation to the results during membrane fouling and cleaning.

2.3. Protein fouling on surfaces

Milk processing which includes pasteurization and sterilization results in fouling on heat transfer equipment and other surfaces. Proteins make up about 50% of the milk deposits formed making it a major foulant in dairy processes (Tissier et al., 1984). Other than dairy, proteins also make up most of the foulants in the production of chocolate desserts and tomato pastes. Protein deposits are formed from denatured proteins which agglomerate together and/or stick together to form a compact or porous layer on the surface. In addition, this layer may contain other organic and inorganic deposits such as carbohydrates, salts and minerals (Gillham et al., 1999). In the heat exchangers of milk processing, the main protein foulant identified is βLg (Fryer et al., 2006). Irreversible fouling on surfaces by these denatured proteins is an inevitable phenomenon in food processing mainly in the dairy industries. Without cleaning, the flux will never increase to the original when the membrane was severely fouled. Water is insufficient to solubilise heat-induced dairy fouling deposits or gels, and a reactive agent is required. Cleaning-In-Place (CIP) is a method using the hydraulic circulation of formulated detergents to remove these foulants. The contributions of chemical reactions and hydraulics in foulant removal are shown in Table 2.3. Chemical cleaning is discussed further in Section 2.7 of the literature.

Table 2.3
Effects of chemical and hydraulic processes on foulant removal (Grabhoff, 1997)

Factors	Effects
Chemical reaction	Swelling of the deposit matrix – Change of voidage Dissolution – Erosion Ageing – Change in deposit composition and structure over time
Hydraulic action of reagent flow	Mass transfer of reagent and reaction products from deposit interface to bulk solution Lift – Removal of particulate foulants from surfaces Scouring – Entrained particulates Surface shear stress – Mechanical erosion

2.4. Membrane fouling

An understanding of the fundamental mechanisms of membrane fouling is essential if the optimum performance of the technique is to be achieved (Kim et al., 1993). Membrane fouling is the result of concentration polarization and component deposition on the membrane surface and pores. Concentration polarization is the development of a concentration gradient of the retained components near the membrane surface. Concentration polarization is dependent on hydrodynamic conditions and independent of the membrane's physical properties. The unwanted build-up of deposits on the membrane surface and pores causes membrane fouling. Consequently, membrane fouling causes an irreversible flux decline, reduces productivity, shortens membrane life and alters the separation performance of the membrane.

2.4.1. Fouling mechanisms by proteins

The causes of membrane fouling in dairy industry are (1) protein adsorption (2) protein or particle deposition (including casein or cheese fines, microorganisms, and protein aggregates and (3) deposition of fats and minerals especially calcium phosphate (D' Souza and Mawson, 2005). In dairy feeds like milk or whey, protein adsorption plays a significant part in membrane fouling. The physico-chemical properties including membrane-protein and protein-protein interactions influence protein fouling characteristics. Different fouling mechanisms are presented in Figure 2.3.

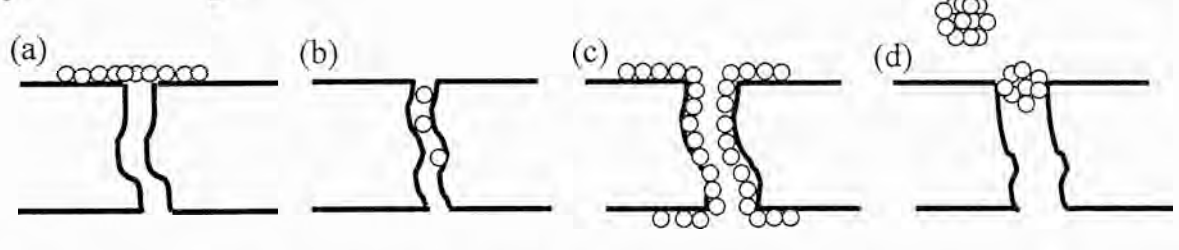

Figure 2.3 Different membrane fouling mechanisms: a) accumulation of particles on the membrane top surface, b) pore blocking by an individual particle, c) pore size constriction due to adsorption to the pore walls, d) pore blocking by an aggregate.

As shown in Figure 2.3 (a), the accumulation of proteins on the membrane surface during UF (cake filtration) may produce a dynamic membrane that controls the membrane behaviour. During the UF of whey proteins, βLg and BSA formed protein sheets on the surface while γ-globulin formed granules of irregular sizes. These granules agglomerate randomly stacking into layers as the concentration of protein increases (Lee and Merson, 1975; Lee and Merson, 1976). In the UF of cottage cheese whey, larger components (microorganisms, γ-Globulin and protein polymers) binds together to form lattice-like structures on the surface of the membrane. The spaces in the lattice network are then filled with the smaller proteins which are then trapped to form a second "protein membrane". Therefore, in multi-protein component solutions like milk and whey, smaller proteins tend to deposit in protein lattices formed by the larger proteins. In another study, BSA granules were observed using FESEM developing on the membrane surface until they combine to form a protein cake that blocks the pores. Aggregates are formed at high initial permeate flux that causes rapid super-saturation at the pores and higher pressure of 100kPa compared to 50kPa (Kim et al., 1992). Therefore, in the UF of whey proteins, dynamic membrane can occur on the membrane surface, controlling the UF performance.

Protein deposition within the membrane structure as shown in Figure 2.3 (b) and (c) is more significant with MF membranes compared to UF due to the larger pores. Using FESEM, Kim et al. (1992) detected no proteins within the UF membrane pores however by pore radius change calculation one or two layers of proteins would have caused the experimental flux decline. In BSA static adsorption, pore blocking was seen to occur on 50kDa and 100kDa membrane preventing BSA to reach the internal pore structure (Robertson and Zydney, 1990). In another study, proteins were identified within the UF membrane structure however the amount of protein deposits in the pores was much smaller than on the surface (Labbe et al., 1990; Sheldon et al., 1991). Studies have shown that the amount of proteins that adsorbs within the membrane surface was 100-400 times less than the surface (Hanemaaijer et al., 1989). Therefore, we may conclude that protein deposition within the pores is less significance for UF membranes.

Initial flux decline is generally associated with internal fouling while the long-term flux decline is considered to be due to membrane surface fouling (Metsamuuronen, 2003). For larger particles (> 1 μm) shear induced diffusion and inertial lift effects dominate and fouling is mainly by pore blocking and cake formation (Bacchin et al., 1995). For smaller particles (10 – 100 nm) short range inter-particle forces including electrostatic and Van der Waals forces dominate and coagulation and adsorption dominate fouling (Harmant and Aimar, 1998). It was observed that pore constriction and pore blocking are typical fouling mechanisms for solutions containing solutes that are relatively small compared to the mean pore size of the membrane (Belfort et al., 1993).

The deposition of material on the surface of the membrane must obstruct the pore entrances reducing membrane porosity as shown in Figure 2.3 (d). However in protein fouling, the concept of molecules blocking and unblocking the pores is highly unlikely for protein adsorption as the process is irreversible.

2.4.2. Effect of protein feed concentration, pH and ionic strength

The effect of concentration is dependent on the dominating mechanism of fouling i.e. surface or internal fouling. When surface fouling dominates, increasing feed concentration increases the total membrane resistance, reversible fouling and flux (Daufin et al., 1991). However, increasing concentration would not affect membrane fouling and irreversible fouling. In addition, the decrease in permeate flux is mainly due to concentration polarization. When internal fouling dominates, increasing the concentration results in a more rapid loss of permeate flux with time i.e. rate of membrane fouling (Bowen and Gan, 1991). At high concentrations, cake or surface fouling is likely to occur.

The protein solution pH and ionic strength changes the protein conformation and stability, effective size, and charge difference between the protein solution and membrane surface. Therefore, the tendency of the protein adsorption and deposition on the membrane surface is

affected by pH and ionic strength. The effect of pH and ionic strength is explained in Section **2.2.2.**

2.4.3. Effect of membrane properties and temperature

Proteins adsorb less on hydrophilic membranes than hydrophobic membranes. Most UF membranes have a wide pore size distribution. Higher deposition occurs on membranes of lowest porosity or highest heterogeneity. The more heterogeneous the membrane surface, the higher the local velocity normal to the surface. This results in higher local concentration polarisation and more rapid initial deposition. Membrane fouling changes the pore size distribution and pore density of the membrane.

Increasing the temperature generally increases the permeate flux due to the lowering of viscosity, increasing diffusivity and reducing concentration polarization during fouling on the membrane surface for both UF and MF. Increasing temperature from 20°C to 50°C reduced the viscosity of the raw milk reducing the thickness of the cake layer (Vetier et al., 1988). However, increasing temperatures may also cause a higher rate of flux decline caused by the precipitation of calcium phosphate (van Boxtel et al., 1991). However calcium and phosphate fouling increases at 50°C for skim milk, resulting in lower final flux than at a lower temperature.

2.5. **Identification of critical flux**

In theory, critical flux is the flux on start-up that exist below which a decline of flux with time does not occur (Field et al., 1995; Howell, 1995). A strong form of the critical flux is a flux can exist below which the same TMP is required to maintain it when filtering a colloid as for clean water at the same flux. On the other hand, a weak form of critical flux is when the TMP required is greater than for clean water but the TMP still increases linearly with the flux up to critical flux. Constant flux filtration has advantages over constant pressure filtration as it prevents over fouling and reduces the severity of fouling.

Critical flux was commonly evaluated using a flux stepping procedure, in that the flux was imposed and maintained constant at given time span (20 min to 1 hour) while the TMP respond to the imposed flux. At below critical flux, TMP does not change very much at the imposed flux. When the flux was increased to a level close to the critical flux, the increase in TMP becomes significant. When the flux was increased above the critical flux, the TMP increase becomes very steep.

Most of the critical flux studies were performed in the microfiltration of larger colloid suspensions other than protein solutions. A microscope was utilized to watch yeast particles being deposited on the membrane and observed a critical flux for mass deposition (Li et al., 2000). The authors found that a modified shear-induced diffusivity model predicted critical fluxes for particles of 5 – 12 μm. Critical flux increased with pore size and decreased with increasing concentration of protein in filtration of 0.1 – 1% BSA with permeable membranes (Chen, 1998). The critical flux was also the lowest at the IEP of the protein. The influence of individual proteins in a binary feed mixture upon the measured critical flux and found that the larger protein controlled the critical flux while the transmitted protein decreases near the apparent critical flux where minimum fouling occurs (Chan et al., 2002). The finding is useful in fractionating mixtures of proteinaceous solutions and the manipulation of flux could possibly influence the rejection and transmission of the solutes.

In summary, this section reviews past studies on critical flux. In our study, the purpose of identifying critical flux is to establish a standard filtration or fouling procedure to form sufficient fouling layer for subsequent cleaning study. Flux stepping will be performed for various solution pH and protein feed components.

2.6. **Effect of feed channel spacer**

One of the most effective approaches to reducing concentration polarization and fouling is to increase the hydrodynamic shear near the membrane surface by means of 'net-like' turbulent promoter known as spacers. A spacer is an important component of spiral wound membrane is

occasionally held against the topside of a membrane in a flat sheet channel in research studies to mimic spiral wound conditions. The effects of spacers on pressure drop and mass-transfer for spiral-wound and spacer-filled flow channels was investigated (Miquel and Schock, 1987). Following that, mass transfer correlations for spacer-filled channels for UF of dextran solutions for non-fouling solutes (Da Costa et al., 1991). According to these authors, mass transfer is described by laminar flow correlation while channel pressure loss is described by laminar flow condition. In spite of improving flux, it is arguable that under certain operating parameters, spacers could also generate localised stagnant zones that lead to high levels of solute deposition on the membrane surface. The effect is a critical under distribution of solvent flux for solutes that have a tendency to cause foul easily.

Following non-fouling conditions, the effect of spacers for whey that has high fouling potential for UF was investigated (Da Costa et al., 1993). The authors discovered that tighter spacers produces higher velocities at the membrane surface and spacers with thick filaments that have a bigger interval behind the strands performed better and 90 degrees was the optimal angle for higher mass transfer.

In a later study, channel spacers were characterized by Mesh-Length (distance between filaments in either axial of the transverse direction), Filament diameter, Internal angle (the acute angle formed between intersecting filaments) and Orientation (the way in which filaments touching the membrane is oriented with respect to the axis of the channel) (Neal et al., 2003). The authors observed that the spacers enhance the critical flux of latex beads.

Computational fluid dynamics (CFD) was used to model the behaviour of fluid flowing through a range of spacer-filled channel geometries (Cao et al., 2001). It was discovered that the stress peaks generated by the filaments travelled only a short distance downstream from them. In addition, the significant flux will improve when the inter-filament distance is reduced and an overlap of regions of high stress occurs. Eddy currents were also formed in front and behind the filaments.

In summary, spacer influences the deposition profile of proteins on the membrane surface by creating turbulence and flow vortices. Spacer is useful in reducing protein deposition however spacer also increases the pressure drop across the system. Moreover, inappropriate flow settings might also cause increase in deposition due to the formation of dead volumes. In our study, a spacer will be placed in the cross-flow channel directly above the membrane during filtration and cleaning. The influence of spacer towards protein and residual deposition will be the focus of our investigation.

2.7. **Removal of protein foulants from membrane surface**

There has been much effort in minimizing membrane fouling such as tailor-make less fouling membranes, design of membrane module with better hydrodynamic situation and optimized operational conditions. However, membrane fouling is almost always unavoidable and ultimately membranes need to be chemically cleaned to restore its productivity and selectivity. Membrane cleaning is particularly important in dairy and food applications as membrane fouling in those applications are much rapid and intense than other applications such as water treatment.

The cleaning agents commonly used for cleaning membrane plants are alkalies, acids, enzymes, surface-active agents, formulated cleaning agents, combined cleaning and disinfecting agents, and disinfectants (Ghosh, 2003).

2.7.1. Water rinsing of protein fouled membranes

According to Tragardh (1989), a typical cleaning cycle generally includes the following stages: product removal from the system, rinsing with water to remove product, cleaning in one or more steps, rinsing with water to remove detergents and any remaining soils, and final disinfection. The rinsing of the cleaning solution is an important part of the cycle as it prepares the membrane for the next step, especially since the residues may reduce the efficacy of the subsequent step or sanitizing agent (D' Souza and Mawson, 2005). Membrane rinsing

consumes large quantity of high quality water, free from impurities such as mineral salts, ions and organic matter.

In one study, 90% rinsing efficiency (i.e. reduction of membrane resistance) was achieved after 15 minutes of rinsing with tap water at 50°C, for whey fouled membranes (Cabero et al., 1999). In addition, water rinsing is also best performed at the same temperature as chemical cleaning to avoid compaction of the foulant (i.e. 54°C) for whey fouled UF membranes (Bohner and Bradley Jr, 1992). Rinsing can recover a small part of the membrane flux by removing loose foulants on the membrane surface. It was reported that a 5% flux recovery of membranes fouled with BSA (Kuzmenko et al., 2005). Rinsing can remove up to one third of the total protein removed by rinsing and cleaning and achieved 80% rinsing efficiency (Matzinos and Alvarez, 2002). In addition, ionic strength of the water aids calcium removal from the membranes. The duration of water rinsing is dependent on the size of the membrane, but it is usually performed between 5 to 20 minutes (Tragardh, 1989; Petrus et al., 2008).

2.7.2. Chemical cleaning of protein fouled membranes

This section reviews past studies by researchers on membrane cleaning of protein fouled membranes. Various cleaning agents, methods of cleaning, and parameters affecting cleaning are also discussed.

Daufin et al. (1991) have investigated acid-disinfectant (HNO_3 and NaOCl) and acid-alkali (HNO_3 and NaOH) combinations to clean inorganic membrane fouled by defatted whey protein concentrate and milk. HNO_3 was effective in removing inorganic material containing bases such as calcium phosphates while NaOCl dissolve organic materials that include bacteria. The authors found that acid-disinfectant cleaner was better than acid-alkali. This is because hypochlorite is a strong oxidant which promotes the swelling of the pores and breaks the binding between the foulant and membrane. Using NaOCl exclusively is not effective as HNO_3 is required to remove the inorganic deposits first. Chemical cleanliness was not

completely achieved as irreversible protein and inorganic residues were detected on the membrane surface after cleaning.

Bohner and Bradley Jr (1992) cleaned and sanitized polysulphone (PS) membranes fouled by Cheddar cheese whey and had developed a procedure in removing the foulants. The authors have used a mixture of NaOH (pH 11) and a non-ionic surfactant (0.1%), followed by a 1:1 mixture of HNO_3 and HPO_4, and lastly NaOH (pH 11) and NaOCl (200ppm) at 54°C. The cleaning steps incorporate 2 minutes of rinsing at 54°C. Lastly, chlorine based cleaners were used to remove all bacteria from the surface. Their protocol did not damage the membrane even after prolonged cleaning and had effectively removed whey residues and sanitized the membrane.

Kim et al. (1993) has found that modifying the charge effects of the cleaning solution is significant during membrane fouling (by BSA) and cleaning in terms of flow conditions and TMP, pH, membrane properties and cleaning agents (HCl or NaOH). The reversing of charges by adding acid gave a better cleaning effect than an increase in charge. Thus, it was considered essential to take into consideration the solute properties of the cleaning agents that influence the electrostatic interactions between the fouled layer and the cleaner.

Kuzmenko et al. (2005) claims that during multiple cycles of BSA fouling and hypochlorous acid cleaning of polyethersulphone membranes, higher concentration of cleaner used in the initial cleaning step leads to a complete recovery of flux. However, this led to a more severe fouling long term due to alteration in the membrane structure. In addition, chlorine oxidation also occurred in the first layer of the absorbed protein molecules on the surface, forming hydrophilic hydrolyzates that covered the internal surface of the pores. This alteration of hydrophilicity and surface charge of the membrane surface facilitates the transport of water molecules along with the suspended BSA molecules to the membrane surface resulting in severe membrane fouling. In comparison, NaOH cleaning did not recover the flux as efficiently as hypochlorous acid.

Field et al. (2008) applying multi-photon microscopy has found that NaOH Cleaning of BSA and ovalbumin fouled 22μm pore size microfiltration membrane was less effective compared to Ultrasil 53. Large aggregates were found unremoved by NaOH even after 1 hour of cleaning resulting in only 50% flux recovery.

Previous studies have shown that NaOH was able to remove whey proteins from membranes efficiently (Bartlett et al., 1995; Bird and Bartlett, 1995). NaOH has the ability to saponify fats and solubilize proteins to some extent (peptidization). Bird and Bartlett (1995) found the optimum concentration for NaOH was 0.2% and 0.4% for stainless steel and ceramic membranes respectively. Alkali/acid or acid/alkali sequences have little effect on the final flux obtained.

Using NaOH and HNO_3 sequentially, the authors discovered that the alkali was responsible for improving flux recovery however the acid was detrimental to the membrane (Blanpain-Avet et al., 2004). During repeated fouling and cleaning cycles, protein retention was observed to increase in the last few cycles due to changes in selectivity and irreversible residual deposition. The measured amount of residual proteins deposited onto the membrane was close to 20 mg per unit membrane surface area, showing that chemical cleanliness was incomplete.

2.7.3. Cleaning mechanism of sodium hydroxide on proteins

Understanding cleaning requires the knowledge of how the deposits are removed as well as the effects of process parameters and plant design on cleaning. In general, cleaning is a heterogeneous reaction between the detergent solution and the fouled layer. As described by (Plett, 1985), cleaning consists of six stages as shown in Table 2.4. Any of the following may be involved in cleaning of dairy deposits: Melting, mechanical break-up, wetting, swelling, desorption, emulsification, hydrolysation, saponification and dispersion. Removal may be governed by a combination of mass transfer, diffusion and reaction, any of which may be controlling (Bird and Fryer, 1991).

Table 2.4
Cleaning reaction steps (Plett, 1985)

Cleaning Steps	Cleaning Actions
Bulk reaction of detergents	The unstable foulant that consumes the detergent and reduces the amount of available detergent is removed.
Transport of detergents to the fouled surface	The mass transport of the detergent to the fouling layer is dependent on hydrodynamics and flow conditions.
Transport of detergent to the fouled layer	The adsorption into the surface is assisted by capillarity, molecular diffusion and cleaner adsorption characteristics.
Cleaning reactions	In the reaction, soluble products would be produced and the cohesion forces between the foulant and the membrane are reduced.
Transport of cleaning reaction products back to the interface.	-
Transport of products to the bulk solution	The transport is controlled by diffusion or turbulence

Alkali-based solutions frequently based on NaOH are usually employed to remove proteinaceous foulants from surfaces due to their ability to destroy the gel matrix and solubilise proteins. Protein deposits on surfaces swell when they absorb water and NaOH solutions can reinforce this swelling and dissolve the deposit. Cracks are form which consequently increases the penetration of the cleaning solution into the deposit.

Visualization of protein deposit response to NaOH treatment on surfaces revealed three phases of protein deposit removal (Grabhoff, 1989; Bird, 1992; Bird and Bartlett, 1995; Grabhoff, 1997; Gillham et al., 1999). These protein deposit phases are shown schematically in Figure 2.4 (Adapted from (Gillham et al., 1999)). "Swelling" where the alkali solution contacts the deposit and causes swelling, forming a matrix of high void fraction; "Erosion" where uniform

removal of deposit by shear stress forces and diffusion occurs. There may be a plateau region of constant cleaning rate, but this depends on the balance between swelling and removal; and "Decay" where the swollen deposit is thin and no longer uniform, so the removal of isolated islands occurs by shear stress and mass transport.

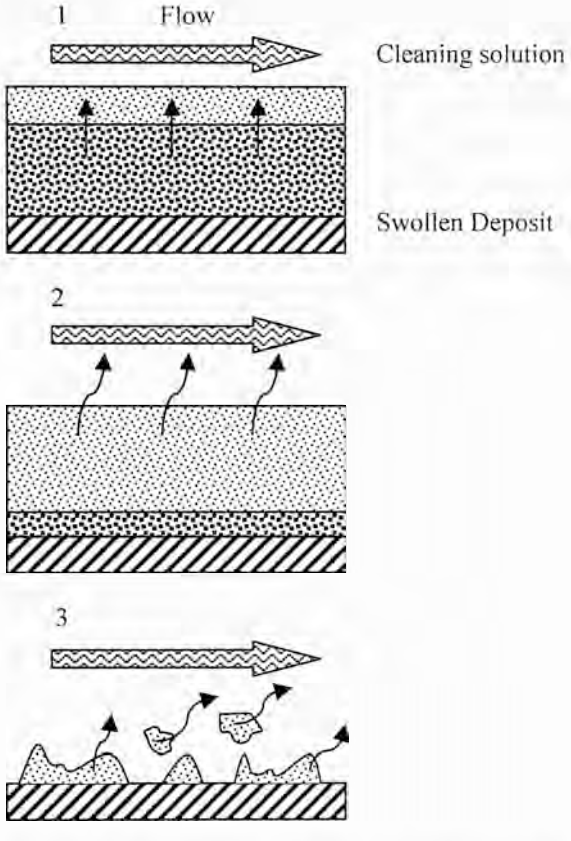

Figure 2.4. Schematic of the stages involved in removal of whey protein deposits (a) swelling phase; (b) uniform erosion phase; (c) decay phase.

In a study of cleaning mechanisms of alkali on heat-induced milk fouling deposits using whey protein gels as models, has found that the cleaning mechanisms were identified as (1) NaOH diffusion, acid-base reaction, and swelling of the proteinaceous deposit (2) Reactions that break down the gel structure (3) Mass transfer of removable clusters into the bulk solution (Xin et al., 2002). In a later study, the rate of dissolution was found to be controlled by an external mass transfer mode (Xin et al., 2004).

The key step in the dissolution process is the disengagement of protein clusters. Dissolution at low temperatures and in the absence of erosion is limited by the disentanglement of protein aggregates through the swollen layer, and the cleavage of the disulphide bridges. In order for disentanglement to occur, the chemical reactions that break down the gel structure have to be slow to yield large cluster sizes. In addition, the presence of cations in ionic solution also decreases the dissolution rate due to screening effect of the cations.

2.7.3.1. Effect of sodium hydroxide pH, concentration and flow velocity

An optimum cleaning pH and concentration specific to a cleaning application often exist in alkali cleaning. The dissolution of whey gels occurs in a few steps (Mercade-Prieto et al., 2007; Mercade-Prieto et al., 2008). These steps are: (1) Fast diffusion of the alkali from the bulk solution into the gel. (2) Swelling of the deposit due to the increased inter-protein repulsion in the NaOH penetration zone. (3) Dissolving the deposit.

The swelling of whey gels occurs at pH > 10 while the breaking down occurs at pH > 11.2. In addition, gelation pH or temperature have a significant influence on the cleaning rate of NaOH (Mercade-Prieto and Chen, 2006). The dissolution of protein gels in alkali is not simply controlled by the diffusion of reaction products through the boundary layer. Thus, an external mass transfer model does not describe the mechanism controlling cleaning. The structure of the βLg gel is an important limiting factor in the NaOH dissolution of the gel (Mercade-Prieto et al., 2006). At pH 13, dissolution is dependent on the conditions under which the gel is formed. Dissolution rate decreases with extended gelation time and gelation temperature, thus

dependent on the amount of cross-linked proteins present in the gel. On the other hand, above pH 13, relatively low dissolution rates are observed, highly independent on gelation conditions. Above pH 11.5 – 12, dissolution is only significant for βLg gels that are swollen over a minimum degree (Mercade-Prieto et al., 2008).

Plett reported a near linear increase in cleaning rate with increasing detergent concentration (Plett, 1985). Some authors also reported an optimal alkali concentration and surface shear that minimizes cleaning time (Bird and Fryer, 1991). 0.5% NaOH cleaner concentration was the optimum for whey fouled microfiltration membranes (Bird and Bartlett, 1995). Above that concentration, the protein deposits become harder to be removed due the formation of a less open structure that is not susceptible to fluid shear.

In all cleaning situation, shear force is provided by fluid flow on the surface and increasing the flow rates induce greater surface shear on the deposit. However, cleaning solution must remain in contact with the foulant long enough to take effect. Boundary layer thickness controls cleaning, more deposit is protruding into the turbulent flow and is removable. Bird and Fryer observed no significant change in the cleaning rate when moving from laminar to turbulent flow while Bird found no minimum flow velocity (Bird and Fryer, 1991; Bird, 1992).

2.7.3.2. Effect of temperature and cleaning duration on alkali cleaning

The rate of cleaning increases as the temperature increases. Increasing temperature improves diffusion, increases the solubility of both cleaning agents and foulants, and increases reaction rates, thus aid the removal of foulants (D' Souza and Mawson, 2005). Shorter time is required to achieve maximum flux recovery for alkali solutions at increased temperatures. However, an optimum temperature has been observed at about 50 – 55°C, beyond which overall flux recovery declines (Bartlett et al., 1995). This is caused by the change in the nature of the foulants (i.e. swelling) at high temperatures, making it less amenable to loosening and breaking. The swelling of the deposit inhibits transportation at higher concentration (Plett, 1985).

In addition, it was found that the length of "Decay" phase (in Figure 2.4) decreases when cleaning temperature exceeds 50°C. In addition, during the uniform "Erosion" phase, the protein removal rate is dependent on the conditions at the deposit/solution interface, while in the non-uniform "Decay" phase the removal rate is sensitive to flow rate i.e. shear stress (Gillham et al., 1999).

2.7.4. Enzymatic cleaning of membranes

With the increasing environmental concern, the uses of enzymes for cleaning are a promising alternative to traditional chemicals (Grabhoff, 2002). The enzymatic and detergent cleaning of polysulphone UF membrane fouled by BSA and whey was investigated and the cleaners cleaved specific points of the protein strands. Detergents dissolve small loose proteins after the cleaving effect of enzymes (Munoz-Aguado et al., 1996). The authors found that cleaning was effective when enzymes were used prior to the application of detergents, with a condition that the two do not interact. A concentration that results in the cleavage of protein strands is sufficient and excess amount of enzymes have no effect in increasing the cleaning efficiency. In a related study, thermophilic proteinase when combined with sodium dodecyl sulphate (SDS) increased the performance of cleaning UF membranes fouled by whey (Coolbear et al., 1992). The method utilized successfully removes whey residues and sanitized the membrane from microorganism. In addition, the procedure did not damage the membrane. Maartens et al. (1996) studied the application of enzymatic cleaners that targets lipids and proteins in the cleaning of UF membranes fouled by abattoir effluent and achieved high cleaning efficiencies.

2.7.5. Section synopsis

The section discusses the various methods, protocols and results achieved by researches investigating the removal of proteinaceous foulants from solid surfaces and membranes. Generally removal of protein foulants from surfaces involves chemical reactions and mass-transfer. In addition, βLg was identified as the main protein foulant in milk and whey processing where heat-transfer is involved.

The section also includes an in-depth review on the cleaning mechanisms of NaOH. The cleaner attacks protein deposits on surfaces in phases. The combination of alkali-disinfectant was identified as the best cleaner of membranes fouled by whey proteins leaving it "residual free". However, NaOH, when employed as a cleaner on its own is questionable on its effectiveness in removing protein aggregates from the membrane surfaces. Enzymes also make a good cleaner for protein fouled surfaces however residual enzymes on the surface may be detrimental for the product quality.

In this current study, the protein residuals on the membrane surface following NaOH and enzyme cleaning will be characterized. In addition, the nature of residual deposition will provide an explanation to the incomplete recovery of flux after cleaning.

2.8. **Characterization of protein-fouled membranes**

Flux and rejection studies were traditionally used to characterise protein fouling and cleaning on membranes. However current methods are more sophisticated and fascinating. Chan and Chen (2004) had reviewed the current development in membrane characterization methods as applied to protein-fouled membranes.

2.8.1. Field Emission Scanning Electron Microscopy (FESEM)

Scanning electron microscope (SEM) has been by various authors to characterize protein fouled membranes (Lee and Merson, 1974; Kim et al., 1992; Kim and Fane, 1994). Lee and Merson (1974) studied the structures of individual whey protein deposits formed during UF. Gamma-globulin (Gg) formed granules formed granules which agglomerated and formed layers to form a porous matrix, while βLg and BSA both formed sheets and multimers which were identified by gel electrophoresis. In addition, βLg also formed strands where deposits are not thick and α-lactalbumin formed smooth spherical particles that did not hinder water permeation greatly. It was found that βLg and Gg were the most significance in causing permeation flux decline by surface fouling. Kim et al. (1992) employed FESEM to examine the deposits formed during UF of albumin solution. Fouling was found to be mainly on the

surface, and no proteins can be observed in the pores. Cake multilayer and aggregation are the two different deposits observed on the membrane surface. High initial flux resulted in the formation of aggregating foulants while low initial flux causes cake formation. Thus, there is a crucial need to control the initial start-up flux in order to obtain the required rejection and transmission. Kim and Fane (1994) investigated the factors affecting the image qualities when using SEM such as voltage and coating. Chromium coating gives a superior quality image to platinum for protein fouled membranes, and low voltage SEM is useful for investigating surface morphology of finely porous membranes and interactions between membranes and solutes at the interface. They reminded us of the importance of sample preparation that neither alter nor damage the solute on the sample.

2.8.2. The Lowry Method

Protein determination method of Lowry has been used to measure protein concentration with ease, sensitivity, as well as accuracy (Lowry et al., 1951). These authors investigated the use of Folin phenol reagent and had successfully discovered the foundation of general protein assay procedure. However, the method has its disadvantages such as lack of specificity, slow reaction rates, instability of reagents and non-linearity of the standard curve. Therefore, the Lowry method was modified by correcting the non-linearity of Lowry method by using high concentration of folin reagent as well as incorporating sodium dodecyl sulphate (SDS) in the analysis (Hess et al., 1978). In this current study, the Lowry method will be used for the quantitative determination of proteins on the membrane surface and pores.

2.8.3. MALDI-MS

Matrix-assisted laser desorption ionisation mass spectrometry (MALDI-MS) is a mass spectrometry method used for analysing biological material with mass ranges above 10,000 Daltons (Karas and Hillenkamp, 1988; Larsen and McEwen, 1998). The method requires femtomoles (10^{-15}) or less material and consumes only a small fraction of analyte on the target making it highly sensitive. MALDI-MS is an efficient process as it allows a number of

samples to be prepared on a target. The sample is co-crystallised with a matrix compound and the ionisation occurs when the dried matrix is irradiated with a focused beam in the mass spectrometry. Our Membrane group and collaboration with Bioanalytical Mass Spectrometry group has done an extensive study on analysing proteins on membranes (Chan et al., 2002; Chan et al., 2004; Chen et al., 2007). A useful method of quantitative analysis and calibration for MALDI-MS can be found in Chan's Thesis (Chan, 2002).

Although previous studies were performed on the deposition profile of mixed protein mixtures by MALDI-MS were successful, there were still limits to how reliable this method is (Chan et al., 2002; Chen et al., 2007). Patchiness in the measured protein deposition and the irregularity of crystallization of matrix in MALDI-MS analysis were experienced in previous studies and further optimization for the process is required for each membrane and foulant system. Quantification of protein components on the membrane is difficult since the analysis of the protein is mainly on the top fouling layer. The reliability of desorption also needs more rigorous examination. Thus, additional studies are performed in the current study to verify the patchy deposition using Lowry and 1D SDS-PAGE. The method also provides with another supportive and reliable method of analysis.

2.8.4. 1D SDS-PAGE

Electrophoresis is defined as the movements of charged particles such as macromolecular ions under the influence of an electric field (Deyl, 1979; Andrews, 1986; Hoefer, 1994). It refers to the movement of ions through a medium such as polyacrylamide gel, cellulose acetate or agarose gel. As proteins are zwitterions or large macromolecules containing both cationic and anionic groupings, the dissociation constants (pK values) of these groups differ widely, the net charge on such a molecule will depend upon the pH of its environment and pH affects the mobility of the molecule. The electrokinetic potential is affected by the ionic strength that reduces the net charge of the effective charge and the mobility of the charged particle is inversely proportional to the square root of the ionic strengths.

Starch gel was introduced in 1955 for the electrophoresis of protein mixtures according to particle size using the sieving effect of the gel. In the 1960s, starch gels were replaced by polyacrylamide gels and in 1967 gel electrophoresis with sodium dodecyl sulphate (SDS) was introduced. The method allows the determination of the subunit molecular weight of reduced and carboxymethylated proteins by comparison of their mobility with those of standard proteins of known molecular weight (ladder). SDS binding produces proteins of nearly constant charge to mass ratio and identical mobility in free solution. SDS electrophoresis is very suitable for the analysis of multi-component systems such as membranes and viruses. The proportion of the components in the system and the subunit molecular weights are also readily available.

Polyacrylamide gel is formed by the polymerization and cross-linking of monomeric substances, acrylamide (CH_2=CH–$CONH_2$) and a cross-linking agent, N, N'–methylenebisacrylamide (Bis). The reaction produces a three-dimensional network determined by the concentration of acrylamide and Bis. The polymerization of the monomeric mixture of acrylamide and Bis is accelerated by the catalytic action of suitable redox systems, ammonium persulphate with N,N,N',N'–tetramethylethylenediamine (TEMED).

2.8.5. Section synopsis

All these membrane characterisation methods mentioned in Section 2.8 will be applied in studying the protein deposition before and after cleaning. When these methods are utilized concurrently, the components of the protein species, before and after cleaning can be clearly represented. Lowry method measures the total protein deposited on the membrane (Surface and pores), while MALDI-MS accounts for the individual protein species on the surface of the membrane. 1D SDS-PAGE represents the detailed protein component deposition on the membrane.

2.9. Mass transfer in protein ultrafiltration

This section will cover some terminologies, definitions and equations involved during the UF of protein solutions (Cheryan, 1998).

2.9.1. The Resistance Model

Transport models are being used to relate the permeate flux to the effect of concentration polarization. A basic transport model that describes permeate flux in UF systems is Darcy's law [Eq. (2.1)], relating the decline in permeate flux by decreased driving forces and/or increased resistances.

$$J_v = \frac{Driving\ force(e.g.\Delta P, \Delta C, or \Delta T)}{Viscosity \times total\ resistance} = J_v = \frac{\Delta P - \Delta \pi}{\mu(R_M + R_F + R_{CP})} \qquad (2.1)$$

where

ΔP is the transmembrane pressure
$\Delta \pi$ is the osmotic pressure
μ is the dynamic viscosity

The resistances occurring in membrane systems are caused by the membrane, concentration polarization, internal pore fouling, cake fouling and gel-layer formation. Concentration polarization arises from the solute retention by the membrane when the solvent transport is facilitated. Solute accumulates on the membrane surface and forms a layer at the membrane interface with a relatively high concentration. The resistance due to the concentration polarization layer (R_{cp}) increases during membrane filtration until the system reaches steady state, concentration polarization also causes the increase in osmotic pressure ($\Delta \pi$), causing a reduction in the driving force.

2.9.2. Gel Polarization Model

Gel-polarization model [Eq. (2.2)] is a transport model which assumes that beyond a certain value of applied pressure, the membrane permeation rate is limited by the presence of a gel-layer deposited on the membrane surface which increases the effective membrane thickness and so reduces its hydraulic permeability (Blatt et al., 1970).

$$J_v = -D\frac{dC}{dx} \tag{2.2}$$

Where D is the diffusion coefficient for the solute transport through the solvent, C is the concentration of the rejected species and dC/dx is the solute concentration gradient. C_m, C_b and C_g are the concentrations at the membrane surface, bulk, and gel respectively. After integration [Eq. (2.2)] becomes [Eq. (2.3)], using the boundaries of C_g as an upper limit and C_b as the lower limit.

$$J_v = \frac{D}{\delta} ln\left(\frac{C_g}{C_b}\right) \tag{2.3}$$

Where δ is the thickness of the boundary layer over which the concentration of the solute varies. In most cases, D/δ is replaced by mass transfer coefficient k that provides the insight on how geometry and flow conditions can affect flux. Also, to improve flux, is to increase the boundary layer thickness as well as k.

At high TMP, the membrane wall concentration, c_w, reaches a maximum value that is determined by the physical characteristics of the solute. This maximum value coincides with the point of gelation, precipitation and/or aggregation of the solute at the membrane wall (Zeman and Zydney, 1996). The gel layer forms an additional resistance adjacent to the membrane wall, and for a fully retentive membrane the flux is expressed as [Eq. (2.4)].

$$J_v = k\ ln\left(\frac{C_g}{C_b}\right) \tag{2.4}$$

The concentration of macromolecules has osmotic pressure which can be of the same magnitude as the applied pressure used in the UF. Gel polarization model make it possible to calculate the flux on the basis of the mass transfer of rejected species from the membrane surface to the bulk. The dynamic gel layer has a fixed gel concentration but is free to adjust its thickness and porosity.

Osmotic pressure as shown in causes counter pressure due to the accumulated rejected solute near the membrane surface.

2.9.3. Sherwood Mass Transfer Model

The hydrodynamic conditions prevalent in membrane filtration give rise to concentration polarisation, producing a concentration profile established within an interfacial film as shown in Figure 2.5.

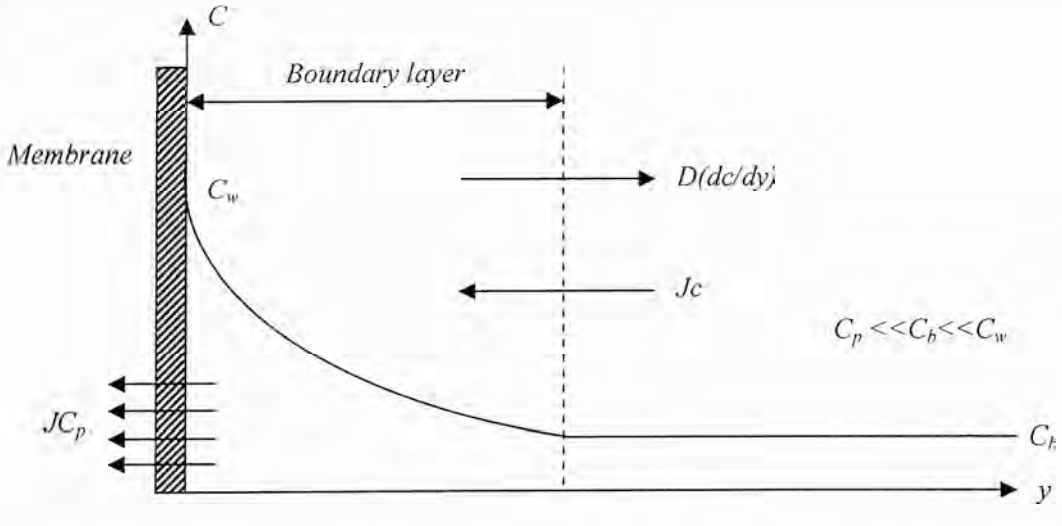

Figure 2.5. Concentration profile generated by hydrodynamic conditions at a membrane surface.

Where J is the permeate flux, D is the diffusion coefficient of the solute and c, c_p, c_b and c_w are the boundary layer, permeate, bulk and membrane wall concentrations, respectively (Bowen and Jenner, 1995).

Convection of solute toward the interface, *Jc*, is balanced by back transport into the bulk solution due to diffusion, *D (dc/dy)*. Therefore, a solute mass balance may be expressed as Eqn. (2.5).

$$Jc = D\frac{dc}{dy} + Jc_p \tag{2.5}$$

Integrating Eqn. (5) over the boundary layer thickness, δ, using the boundary conditions

$$c(y = \delta) = c_b \qquad c(y = 0) = c_w$$

Gives the film model, Eqn. (2.6)

$$J = kln\left(\frac{c_w - c_p}{c_b - c_p}\right) \tag{2.6}$$

Where the overall mass transfer coefficient of the solute in the boundary layer, $k = D/\delta$. The mass transfer coefficient can be evaluated using experimental correlations of the form:

$$Sh = \beta Re^{\alpha} Sc^{b} \left(\frac{d_h}{L}\right)^{c} \tag{2.7}$$

Where,

Sh, the Sherwood number = kd_h/D;
Re, the Reynolds number = $\rho U d_h/\mu$;
Sc, the Schmidt number = $\mu/\rho D$;
L = the channel length;

β, a, b, and c are the parameters specific to the system geometry and flow conditions;
ρ and μ are the solution density and viscosity;
d_h is the hydraulic diameter.

Sherwood number (Sh) is a measure of the ratio of convective mass transfer to molecular mass transfer. It can be looked at as the ratio of the channel dimensions (in terms of equivalent hydraulic diameter dh) to the boundary layer thickness δ (Gekas and Hallstrom, 1987). The Reynolds number is a measure of inertia effects to viscous effects and the state of turbulence in a system. In general, $Re < 1800$ are considered laminar while $Re > 4000$ is turbulent flow.

Another Sherwood correlation was obtained from UF and MF Hand-book (Cheryan, 1998) and shown below [Eq. (2.8)]

$$Sh = A(Re)^{\alpha}(Sc)^{\beta} \tag{2.8}$$

For laminar flow systems, if both velocity and concentration profiles are fully developed, both α and β are zero. If velocity profile is fully developed while concentration boundary is developing along the entire channel, the Graetzor Leveque solutions can be used with α = 1/3 and β = 1/3. If both are developing, α = 1/2 and β = 1/3. For turbulent flow, the Chilton-Colburn or Dittus-Boelter correlation can be used with α = 0.8 and β = 0.33. The constant A generally reflects physical property variations and other conditions of the system that one cannot explicitly account for from first principles. Sherwood number will also be a function of the channel length, L. For laminar flow models,

$$Sh = A'(Re)^{\alpha}(Sc)^{\beta}\left({}^{d_h}/_{L}\right)^{\omega} \tag{2.9}$$

A' is 0.664 in the Grober correlation and 1.86 in the Leveque solution, the value of ω is 0.33 in the developing boundary layer and 0.5 for fully developed velocity profiles. Thus in summary,

- For turbulent flow, when Re > 4000

$$Sh = 0.023(Re)^{0.8}(Sc)^{0.33} \quad (2.10)$$

For laminar flow, when Re < 1800, Lv < L and Lc < L

$$Sh = 1.86(Re)^{0.33}(Sc)^{0.33}\left({}^{d_h}/_{L}\right)^{0.33} \quad (2.11)$$

For overall *Sh* number, integrate [Eq. (11)], over length (0 - 0.5m), and divide the integral by length (0.5). We get [Eq. (12)],

$$Sh = 3.49(Re)^{0.33}(Sc)^{0.33}(d_h)^{0.33} \quad (2.12)$$

- For laminar flow, when Lv>L and Lc>L

$$Sh = 0.664(Re)^{0.5}(Sc)^{0.33}\left({}^{d_h}/_{L}\right)^{0.5} \quad (2.13)$$

This section summarises the transport equations that describes the mass transfer occurring during the UF of proteins. These equations will be used to describe the observations occurring during the UF of binary and whey protein feeds used in the current study. The experimental results can be correlated to the known transport models and conclusions can be developed from the findings. The equations show the importance of flux J and the mass transfer coefficient k in relation to concentration polarisation. The mass transfer coefficient is dependent on the hydrodynamics of the system, thus can be varied and optimized. Therefore the concentration polarization effect can be reduced by manipulating the J and k.

2.10. Research needs and expected outcomes

This study aimed to improve the understanding of cleaning mechanism for complex protein foulants using whey protein isolates as model feed by using alkaline and acids as well as enzyme cleaners to identify cleaning procedure through observation of flux recovery as well as components of foulants remained on the membrane after cleaning in cross-flow filtration membrane module which simulates spiral wound module conditions. Surface analysis techniques including the Lowry method and gel electrophoresis would be applied to examine the protein content on the membrane before and after cleaning procedures. Foulant distributions along the membrane channel at various cleaning procedures will also be examined. Membrane performance and residual foulants on the membrane after repeated cleaning cycles were evaluated to provide insight information on the membrane cleaning process.

Whey protein isolates, a by-product from the conversion of milk into cheese and consists of more than 90% of proteins was selected as a complex feed in UF process and representative of the conditions of the UF processes in the dairy industry. The major protein components in WPI powder include β-Lactoglubulin (βLG) (42%), while Glycomacropeptide (GMP) (18%), and α-Lactalbumin (aLA) (13.8%) are also significant components. Polyethersulfone (PES) membrane, a commonly used membrane in UF processes in the dairy industry with MWCO of 30kDa was selected in this study. PES membranes have a wide temperature limit of up to 125°C, wide pH tolerance, good chemical and chlorine resistance, easy fabrication and availability in a wide range of pore sizes. However, PES membranes are somewhat hydrophobic, which makes it more prone to fouling as compared to hydrophilic membranes such as cellulose acetate membranes. Surface analysis of fouled and cleaned membrane was conducted using the Lowry method to evaluate the total protein amount and Gel-electrophoresis for protein composition.

- While high temperatures would increase protein fouling on the membrane the temperature effect on fouling will be not be evaluated in this study since the filtration experiments will

be conducted at room temperatures. However as high temperatures would assist the cleaning process, the effect of NaOH cleaning of whey fouled membranes at 50°C will be evaluated.

- Given that some protein components in whey (αLA and βLG) are smaller than the nominal MWCO of the selected membrane of 30kDa, it is possible that some protein molecules may be trapped in the membrane pores during filtration process. Surface analysis methods applied in this study using Lowry and gel-electrophoresis, which extract foulant from membrane and the pores would account for the proteins that remained in the membrane pores.
- While the spacer placed in between the channel would reduce deposition due to the turbulence it produces, the effect of spacer on the membrane cleaning efficiency has not been fully understood and this work will evaluate the extent of spacer effect on the membrane cleaning efficiency.
- There is lack of investigation on the protein residuals on the membrane surface following chemical and enzymatic cleaning of protein fouled membranes. The irreversible protein residuals on the membrane surface are responsible for the incomplete recovery of flux and continuous decline in membrane performance after successive fouling and cleaning processes.
- The residual deposition after repeated fouling and cleaning will be evaluated to understand the effect of accumulated foulants on the membrane performance due to possible incomplete cleaning and the effect of chemical agent on those accumulated foulants.
- Chemical and enzymatic cleaning results of binary and WPI fouled membranes will be compared
- Suggestions towards an effective cleaning protocol in the removal of irreversible protein foulants from the membranes will be developed.

Chapter 3: Materials and Methods

3. Introduction

Chapter 3 explains in detail the materials and methods applied in the current study on membrane fouling, cleaning and mass transfer modelling performed in the following chapters. The characterization methods for evaluation of components in the membrane fouling layer and on the cleaned membrane surface compiled in this chapter are Lowry method, One Dimensional Sodium Dodecyl Sulphate Polyacrylamide Gel Electrophoresis (1D SDS-PAGE), and Field Emission Scanning Electron Microscopy (FESEM).

Other supporting materials are presented in Appendix A, which includes chemical lists and procedures for Matrix Assisted Laser Desorption Ionization Mass Spectrometry (MALDI-MS), information on dead-end stirred-cell, and trypsin digestion.

3.1. Model protein feed

3.1.1. BSA and equimolar BSA and βLg mixed protein feed solution

In the current study, Bovine Serum Albumin (BSA, 68kDa, 14.0 × 4.0 × 4.0 nm) solutions were used to study the effect of operating conditions on the foulant deposition on the membrane surface. BSA is a common model protein applied when studying concentration polarization, fouling and cleaning of UF membranes applied in protein related filtration. Binary protein solutions, containing equimolar BSA and Beta Lactoglobulin (βLg, 18.4kDa, 6.9 × 3.6 × 1.8 nm) were utilized to investigate the interactions between two different proteins and the membrane during adsorption and fouling process. The fouled and cleaned membrane surface were analysed for their presence using characterization methods explained in greater detail in the following sections.

BSA, reagent grade pH 5.0, was purchased from Moregate Biotech, Australia. Feed concentrations ranging from 0.01wt% to 0.1wt% BSA were prepared. These solutions were prepared fresh using ultrapure Milli-Q water (Milli-Q), and the pH was adjusted by drop wise addition of dilute 0.1M hydrochloric acid (HCl) or sodium hydroxide (NaOH) prior to filtration tests. In preparing binary protein solutions, βLg A & B from bovine milk with 80% PAGE purity purchased from Sigma Aldrich was used along with BSA. Equimolar 1.16×10^{-5}M each of BSA and βLg in the solution (0.1wt% total proteins, 0.394g BSA and 0.107g βLg, 500mL Milli-Q water), was prepared fresh. In some instances, 1.015×10^{-5}M BSA and βLg solution was also used. The IEP of BSA and βLg are 4.8 and 5.2 respectively. The pH of the protein solution was set to 4 in most protein filtration experiments.

3.1.2. Whey protein isolates UF feed solution

Whey Protein Isolates (WPI) is a complex protein mixture representing dairy UF feeds such as milk and Whey Protein Concentrate (WPC). WPI contains various proteins and peptides, and it was used as a model feed solution during fouling and cleaning experiments for cleaning efficiency evaluation study. WPI was purchased from BodyScience Australia Pty Ltd. A concentration of 0.1 wt% (0.5g of WPI in 500 mL Milli-Q water) was prepared immediately prior to performing the experiments to ensure freshness and to avoid bacterial growth. Dilute HCl or NaOH was added to adjust the pH of the solution to 6. Table 3.1 shows the various protein ingredients that make up the WPI.

Table 3.1
The protein content of WPI used in the experiments. Source: BodyScience (Aust) Pty Ltd.

Protein	Composition (%)	Relative Molecular Mass (kDa)
βLg	42.4	18.4
Glycomacropeptide (GMP)	18.7	20 – 24
α-Lactalbumin (αLa)	13.8	14.5
Proteose Peptones (PP)	6.7	13
Immunoglobulin (Igb)	5.9	120 – 250
BSA	1.1	68
Lactoferrin	0.06	77

3.2. Experimental set-up

All the experiments performed utilized a cross flow rig shown in Figure 3.1 and 3.2. The membrane filtration cell consists of acrylic cross flow filtration module with a dimension of 657 by 99 mm and a filtration area of 0.02 m^2. The module has been constructed with an O-ring and a flat rubber gasket (Clark Rubber, Australia) to ensure a good seal. 22 bolts, screws and wing nuts are used to tighten the module halves together during the filtration. A peristaltic pump (Masterflex, Model 7529-00) from Cole Parmer, Australia, deliver the feed pressure and maintain a constant cross flow velocity. An electronic balance (Mettler PM 6000, Australia) was used to monitor the flux by timed permeate collection. The pressure transducers used in the experiments were a pair of identical model PDCR 810 from Druck (Davidsons, Australia). The flow meter and pressure transducer measured the feed flow rate and pressure difference respectively and the signals for pressure transducers, cross flow rates and balance (permeate flux) were connected to a personal computer installed with Labtech^{TM} Notebook Program Version 7.20. Generally, oscillatory flow may reduce membrane fouling tendency and this reduction could be affected by the frequency and the amplitude of the oscillatory in feed flow. Insertion of the damper significantly reduced the amplitude of the feed oscillation thus the effect of feed oscillation on membrane fouling was significantly minimised.

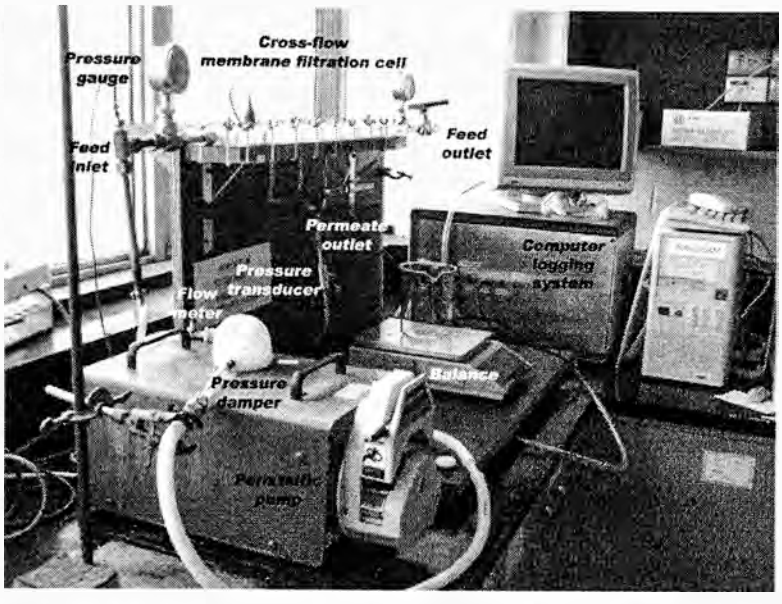

Figure 3.1 A captioned photograph of the UF Membrane cross-flow Rig.

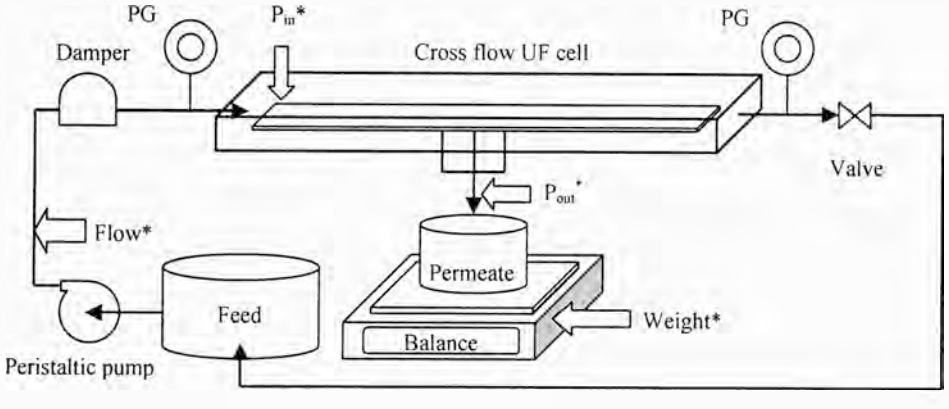

Figure 3.2 Schematic diagram of the UF Membrane cross-flow Rig.

3.3. Polyethersulphone Membrane

Polyethersulphone (PES) membranes of 30kDa Molecular Weight Cut-Off (MWCO) purchased from Synder Filtration™ (SYNDER) and Pall™ (PALL) from USA was used in all the experiments. Both membranes exhibit a hydrophobic behaviour and are negatively charged

(-mV) at pH range of 3 to 14 when analysed using an Electrokinetic Analyser (EKA) by Anton Parr. PES hydrophobic membrane were also applied in previous studies (Chan, 2002). According to the manufacturer, the membrane is resistant towards HCl and NaOH up to 35% and 22% respectively. No change in the flux and selectivity was reported in the literature when using diluted HCl for cleaning fouled PES membranes. These membranes were designed for milk concentration and the attributes are durability and long lastingness.

SYNDER flat sheet membranes were cut out from a commercial spiral wound module as shown in Figure 3.3 that includes feed channel spacers and permeate channel spacers. For storage and preservation, the SYNDER membranes were sliced into strips of 600 by 40 mm and then immersed in a preservative solution of Milli-Q water (78%), sodium metabisulphite (2%) and glycerol (20%) adjusted by HCl to pH 4. This preservative solution was recommended by the manufacturer from Synderfiltration^{TM} to prevent bacterial growth. Sodium metabisulphite when dissolved in water makes sodium bisulphite solution is known to neutralize chlorine and ozone, as well as prevents the degradation of membranes. No evidence was found that the preservative solution may adversely affect the membrane properties, and supported by good reproducibility of pure water flux. The membranes were kept in zip-lock bags and refrigerated to prevent bacterial growth while maintaining the moisture within. Prior to usage, the membranes were thoroughly cleaned with Milli-Q water followed by a Milli-Q water flux test under 50kPa TMP to remove all preservatives from the surface.

On the other hand, PALL membrane was provided as dry flat sheets (coated with glycerol) supplied from the manufacturer, and the membranes were soaked and rinsed thoroughly with Milli-Q water prior to running the experiments.

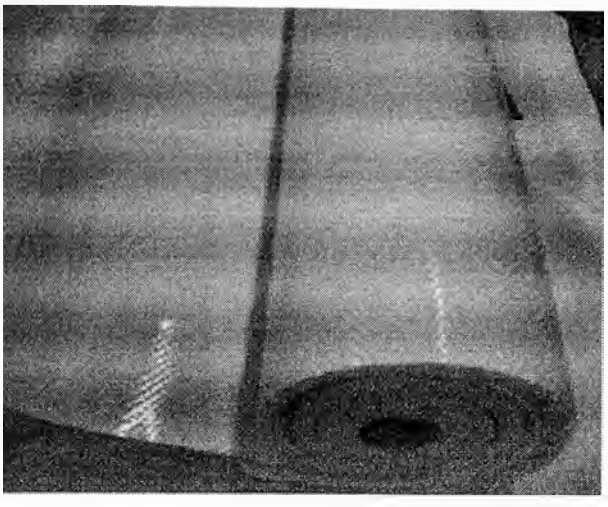

Figure 3.3 Commercial Spiral Wound Module with one leaf in its unwound state (SYNDER) – Consist of membrane, spacer mesh and permeate collector.

One distinct difference between the PALL membrane and SYNDER was PALL membrane has a higher Milli-Q water flux than SYNDER membrane at the same applied TMP, which was common for membranes from different sources. These membranes are not very homogeneous with direct eye inspection, therefore prior to experiments, the initial Milli-Q water fluxes under constant TMP were measured and only membranes within a certain range of flux (±10%) are accepted to be used in the fouling and cleaning experiments.

3.4. Feed Channel Spacer

Spacers as shown in Figure 3.4 are characterised by mesh-length, distance between filaments in the axial or traverse direction, filament thickness and internal angle (Neal et al., 2003). The spacer-filled channel in the cross-flow rig was normally used to simulate spiral wound modules by placing the feed channel spacer semi-tightly against the membrane.

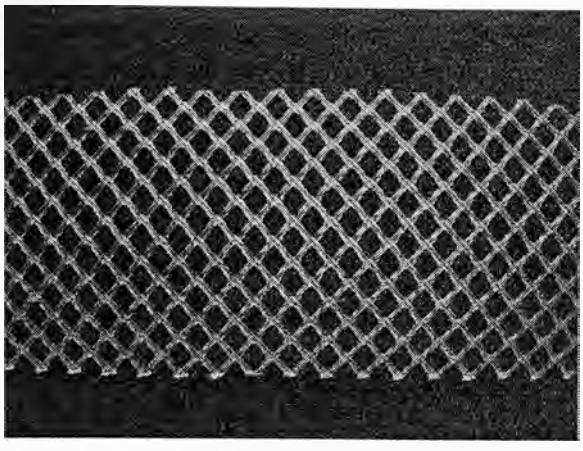

Figure 3.4 Photograph of the plastic net-like feed spacer against a red colour backdrop.

In addition, mass transfer and pressure drop can be calculated from these spacer-filled channels (Miquel and Schock, 1987). Table 3.2 contains the characteristics of the spacer used in the experiments.

Table 3.2
Spacer characteristics

Spacer characteristics	Dimensions
Filament thickness, d_f	4.064×10^{-4} m
Mesh length, l_m	2.794×10^{-3}
Volume of spacer, V_{sp}	7.2486×10^{-3} m^3
Spacer thickness, h_{sp}	7.874×10^{-4} m

The hydraulic diameter (d_h) was found to be 1.415×10^{-3} m and 2.9×10^{-3} m, for a spacer-filled channel and an empty (no spacer) channel respectively. The equations to calculate d_h and Reynolds number (Re) is shown in Table 3.3. The voidage (ε) of the spacer-filled channel was calculated to be 0.88. The calculated Re for an empty and a spacer-filled channel is shown in Figure 3.5. The Re numbers for the spacer filled channel are 250.29, 500.57 and 750.86, at 500, 1000, and 1500 mL.min^{-1} volumetric flows respectively. In addition, the Re numbers for an empty channel are 451.2, 902.5 and 1353.7, for 500, 1000 and 1500 mL.min^{-1} respectively. Currently, the experiments were performed in the laminar flow region of 500 – 600 mL.min^{-1}.

Table 3.3
Equations used to calculate Reynolds number for spacer-filled channels

	Mass transfer equations for spacer-filled cross flow channel
Re number	$Re = {v \cdot d_h \cdot \rho}/{\mu}$
Hydraulic diameter	$d_h = {(4 \cdot \varepsilon)}/{\left({2}/{h} + (1-\varepsilon) \cdot S_{v,Sp}\right)}$
	where,
	$S_{v,Sp}$ is the specific surface: ${4}/{d_f}$
	ε is the spacer porosity: $1 - {V_{Sp}}/{V_{Tot}}$
	V_{Tot} is the total volume: ${l_m}^2 \cdot h_{Sp}$

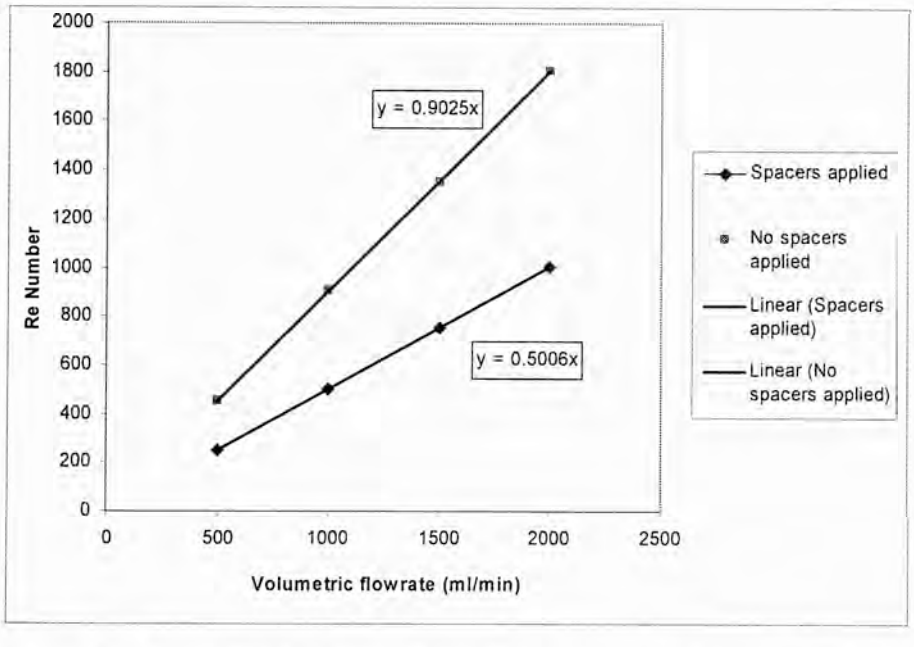

Figure 3.5 Graph of Re number of an empty and spacer-filled channel Vs volumetric flow

3.5. Experimental procedures

3.5.1. Ultrafiltration of protein feed solution

Prior to each filtration tests, the initial Milli-Q flux of a membrane was measured by circulating Milli-Q water in the rig at 50 kPa for 15 minutes. The protein solution was then used as feed and the filtration was conducted at constant TMP for the duration of 4 or 8 hours with or without spacers inserted in the membrane module. During continuous filtration, permeate and retentate streams were recycled back into the bulk feed. Typical initial water flux and the flux at the end of filtration for the two types of membranes are shown in Table 3.4. While the two membranes were made with the same polymer material (PES) and have the same nominal MWCO, due to possibly different membrane fabrication procedures and post-treatment processes, it's not uncommon that the initial water flux was different for those two membranes.

Table 3.4
Initial and final Milli-Q water flux after 4 hours UF of binary BSA and βLg

Membrane Source	Flux ($Lm^{-2}h^{-1}$)	
	J_i(±10%)	J_{uf}(±10%)
SYNDER	77.6	13.8
PALL	240	17.3

3.5.2. Cleaning of membranes fouled with whey proteins

In cleaning studies, the fouled membranes were rinsed with Milli-Q water to remove loosely bounded proteins followed by chemical cleaning. HCl, NaOH and Protease M. Amano (purchased from Sigma Aldrich, Australia) are used as cleaners. NaOH was prepared at a concentration of 0.1 M by dissolving sodium hydroxide in Milli-Q water. The pH of the NaOH solution was at pH 12.5. HCl was prepared at a concentration of 0.1 M and pH 1.3 by diluting the stock solution with Milli-Q water. The protease solution was prepared at pH 7.5 and cleaning was performed at 30°C.

3.6. Membrane preparation for surface analysis

The fouled and cleaned membranes were dissected according to the diagram shown in Figure 3.6. The dried membranes were sliced with a sharp razor blade on a cutting board pre-wiped with 70% ethanol. The membranes were sliced down to sizes of about $4mm^2$ to increase the surface area for analysis. Only longitudinal effects of deposition were studied. The membrane were analysed with Lowry and gel-electrophoresis per surface area. The total membrane length was divided into five sections and each section were analysed using both Lowry and Gel Electrophoresis methods. For MALDI-MS, samples were taken from the immediate entrance and exit as well as intersections from each section of the membrane. The methods and procedures for MALDI-MS are explained in Appendix A.

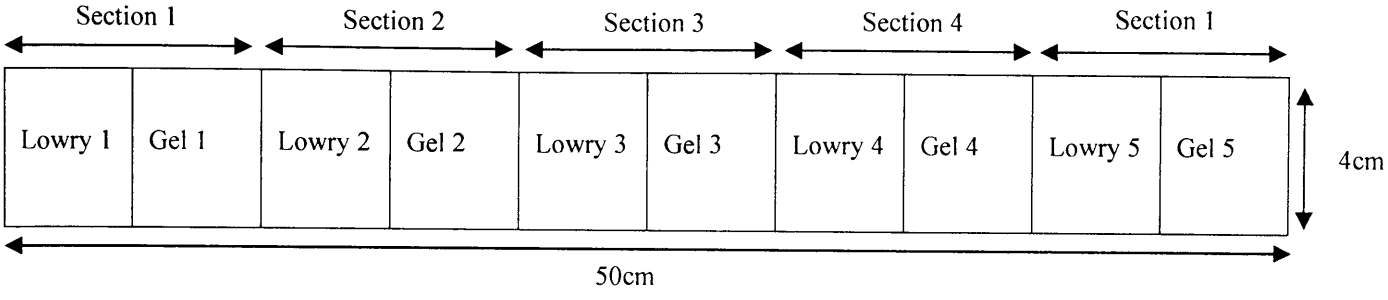

The rectangle on the bottom indicates the sections for Lowry (Lowry 1–5) and Gel electrophoresis (Gel 1–5) analysis respectively. In some experiments, only half of the gel sections are being used.

Figure 3.6 The dissection of the cross-flow membrane.

3.7. The Lowry Method

3.7.1. Chemicals and equipment

Several chemicals were used in making the reagents for Lowry assay and they were anhydrous sodium carbonate (Na_2CO_3), copper sulphate ($Cu_2SO_4.5H_2O$), 2 M folin ciocalteu (Phenol reagent), sodium docedyl sulphate (SDS), NaOH and sodium tartrate (Hess et al., 1978). All chemicals were obtained from AJAX Chemicals and Sigma Aldrich, Australia. The membrane samples are then subjected to a series of reagents as shown in Table 3.5 to facilitate a chain of reactions to allow the proteins to be detected by the Cary UV-Vis Spectrophotometer at wavelengths of 650nm and 750nm. A pair of black quartz cuvettes with a volume of 0.8 mL was used in all spectrophotometry measurements.

Table 3.5
Ingredients of Lowry Reagents

Lowry reagents	Ingredients
Reagent A	0.2 g of sodium tartrate and 10 g of Na_2CO_3 added to 55 mL of 1 M NaOH. Milli-Q water was added to make 100 ml of solution.
Reagent B	2 g of sodium tartrate and 1 g of $CuSO_4.5H_2O$ mixed in 10 mL of 1 M NaOH and 90 mL of Milli-Q water.
Reagent C	1 mL of Folin Ciocalteu (Phenol reagent) mixed with 2 mL of Milli-Q water. This solution had to be prepared fresh daily prior to usage.
Reagent D	5 g of SDS dissolved in 90 mL of 0.5 M NaOH at 90°C with the aid of a stirrer. Milli-Q water was added to produce 100 mL of the solution.

3.7.2. The Lowry Procedure

The procedure of the analysis is shown in Table 3.6. An accurate 1 mL calibrated auto-pipette was used in all the experiments. 0.15mL samples were taken from each of the 2mL solution for Lowry method.

Table 3.6
The Lowry method procedure

Steps	Lowry Procedure
1	Soak dissected membranes in 2 mL of Reagent D under agitation for two hour
2	Extract 0.15mL of Reagent D containing proteins into three different sets of glass sample tube.
3	Add 0.10mL of 2N NaOH in each of the sample tubes containing Reagent D and proteins, Shake/stand
4	Add 0.18mL of Reagent A. Shake/stand for 30 minutes
5	Add 0.02mL of Reagent B (Blue). Shake/stand for 20 minutes
6	Add 2 portions 0.30mL of Reagent C (fresh), while shaking
7	Stand and shake for 1 hour or until there's no change in colour

The calibration graph for the Lowry method is shown in Figure 3.7. All results in the following chapters are reported per area of membranes e.g. $\mu g\ cm^{-2}$. If the samples were too dark, dilution of the samples were performed when using the calibration graph and 1.05mL of Milli-Q water was added per dilution.

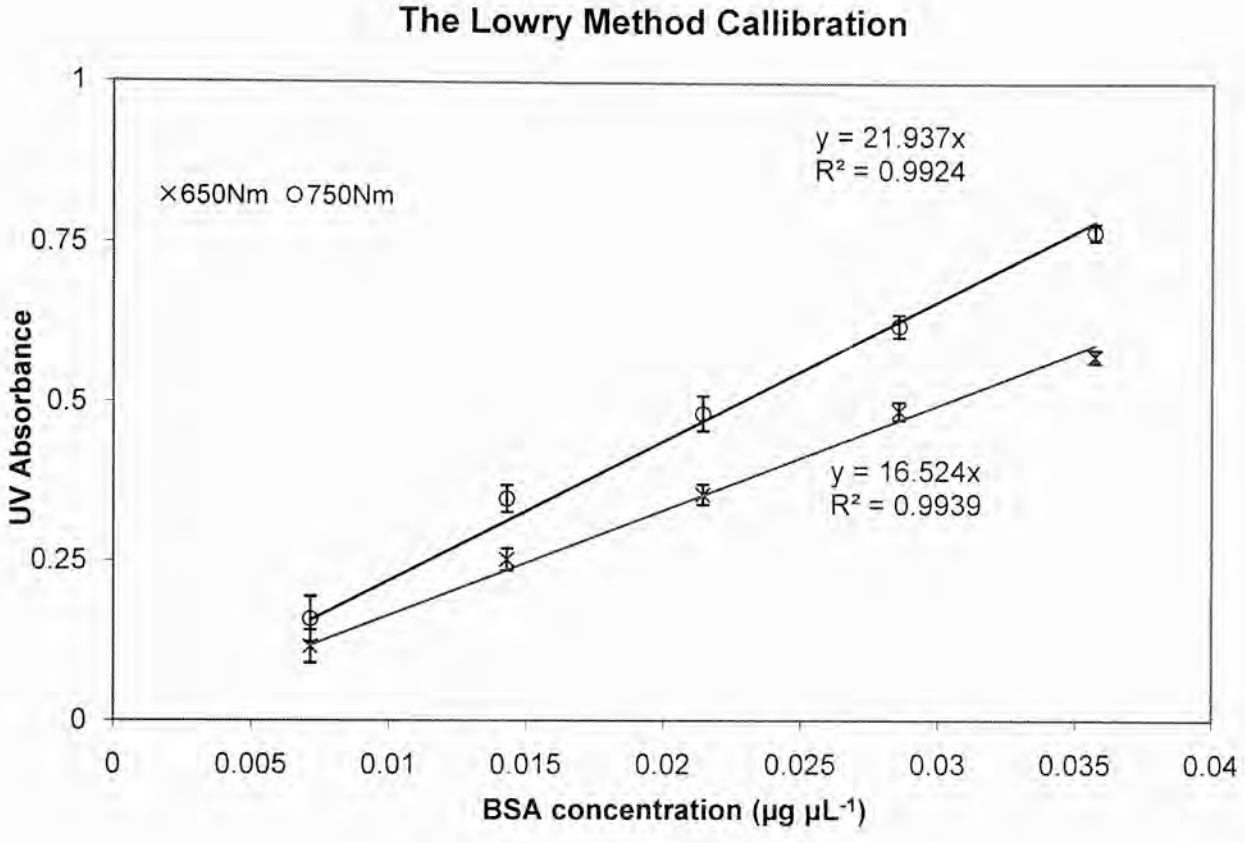

Figure 3.7 Calibration graph of Lowry method. Total volume is 1050µl of sample and reagents.

3.8. 1D SDS-PAGE Method

3.8.1. The chemicals and equipments

The main chemicals for 1D SDS-PAGE are bromophenol blue, glycerol, 2 mercaptoethanol, sodium docedyl sulphate (SDS), 40% Acrylamide/Bis, 10% ammonium persulphate (APS) and tetramethylethylenediamine (TEMED). Other chemicals are tris-hydrochloric acid, ethanol, methanol, anhydrous sodium carbonate and acetic acid. These chemicals were obtained from AJAX Finechem. Sodium thiosulphate, silver nitrate ($AgNO_3$) and 37% formaldehyde (H_2CO) were acquired from Sigma-Aldrich, Australia. The benchmark protein ladder was from Invitrogen, while the running buffer solution was from Garvan Institute. The

ingredients for making the gel are shown in Table 3.7 while the chemicals required to make the lysis solution is shown in Table 3.8.

Table 3.7
Ingredients of Acrylamide stack gels

Ingredients	12.5%T	4%T
Acryl/Bis 40%	3.13mL	0.5mL
1.5M Tris-HCl pH 8.8	2.5mL	1.26mL (0.5M Tris-HCl pH 6.8)
SDS 10%	0.1mL	50μL
Make up Milli-Q	10mL (4.24mL)	5mL (3.16mL)
APS 10% (add 2nd to last)	25μL	25 μL
TEMED (add last)	5μL	5 μL

Table 3.8
Ingredients of sample boiling solutions (Not in SI units)

Ingredients	Final Concn	Volume (10mL)
SDS	10% w/v	4
Glycerol	87% w/w	2
Bromophenol blue	0.1% w/v	50μL
Tris-HCl 0.5M, pH 6.8	0.125 M	2.5
2 mercaptoethanol	2 – 5% v/v	200 μL
Milli-Q (make up)		10mL (1.25mL)

The equipment used for running the gels is Amersham Pharmacia Biotech Hoefer miniVE vertical electrophoresis system (Figure 3.8) with the Electrophoresis Power Supply Unit (EPS-1001) to carry out the analysis by SDS-PAGE. A 'mighty small' mould can also be used to make a maximum of three gels at a time (Figure 3.9).

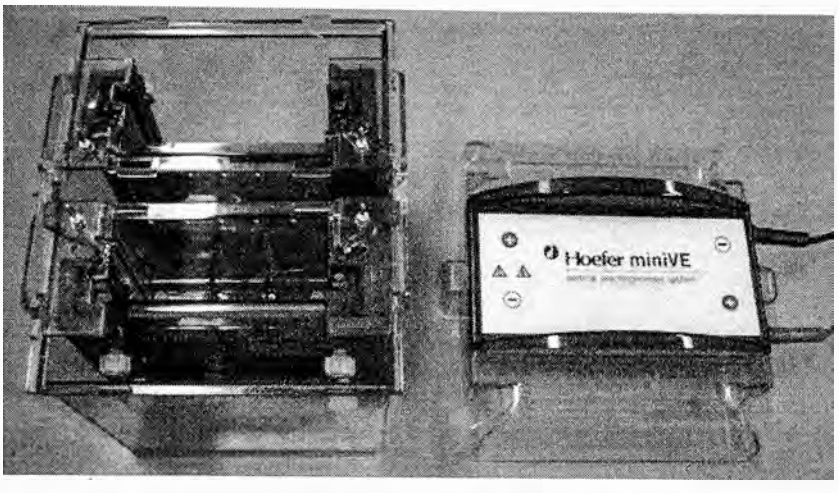

Figure 3.8 Amersham Pharmacia Biotech Hoefer miniVE Vertical Electrophoresis System and loaded with polyacrylamide solution.

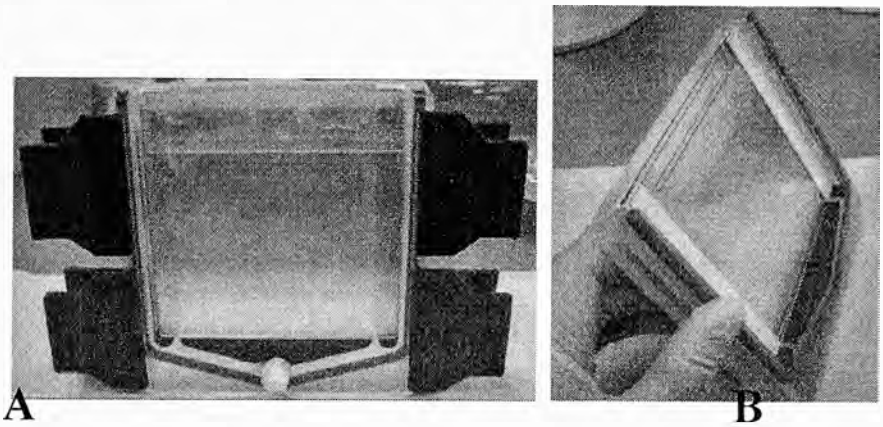

Figure 3.9 Hoefer Mighty small gel caster. A: Front view; B: Four plates separated by plastic spacers (white).

3.8.2. 1D SDS-PAGE Procedure

The general procedure for performing 1D SDS-PAGE is shown in Table 3.9 and is rigorously explained in the next two sections that follow.

Table 3.9
General 1D SDS-PAGE procedures

Number	Procedures
1	Prepare polyacrylamide stack gel in the MiniVe cartridge or multiple gel casters. The bottom 3/4 of the gel is 12.5%T while the top 1/4 is 4%T.
2	Prepare sample boiling solution for protein elution from membrane surface.
3	Soak dissected membranes in 1 mL of boiling solution and ultrasonicate for 2 hours. Extract the protein containing boiling solution into eppendorf boiling tubes. Boil for 5 minutes.
4	Inject 10 or 20μLof the hot samples into each of the gel wells.
5	Run the gels at 180V, 30mA, and 5W for 1 hour to separate the proteins
6	Stain the gels to visualize the separated protein and peptides bands

All gels were prepared fresh as polyacrylamide gels degrade in the open environment resulting in a poor separation of proteins. 12.5%T Acrylamide gel were made for the bottom stack (3/4) followed by 4.5%T Acrylamide gel for the upper stack (1/4) (Hoefer, 1994). A small layer of butanol is used to make the gels horizontally straight at the very top. A 'comb' was placed into the top stack in the 4.5%T gel to create wells for samples.

The dissected membranes were soaked in 1 or 2 mL of sample boiling solution for 2 hours under intermittent ultrasonication to prevent the sonicator machine to overheat and fail. Samples solution containing the proteins and boiling solution were dispense into 1.5 mL Eppendorf tubes. The Eppendorf tubes were then heated in water bath at 100°C held by white-circular holders for 5 minutes prior to injection into the gel. All samples were heated except the protein markers (ladders) which was stored in the freezer and thawed before use. The tank of the miniVE system was filled with 1× running buffer solution while the cartridge well contains 2× running buffer. Following that, the boiled samples (while hot) were injected into the formed wells of the gel. The power supply was tuned to deliver an output of 180 V, 30

mA, 5 W for about 1 hour to the miniVE system when running a single gel. Additionally, a setting of 180V, 60mA, and 5W can be set for running two gels simultaneously.

Finally, the gel was carefully removed from the glass plates and immersed in Milli-Q water to hydrate the gel and minimise breakages.

3.8.3. Post electrophoresis gel staining

The gels were stained with CBB-R, CBB-G, or silver nitrate method to detect and quantify the protein in the gels. CBB is disulfonated triphenylmethane textile dye. In acidic solutions, the dye sticks to the amino groups of the proteins by electrostatic and hydrophobic interactions. The chemicals used for staining and the procedures are explained in the Appendix A (Miller et al., 2006)

3.8.4. BSA, βLg and WPI standards for protein quantification

Relative measurements of mass in a stained band can be performed by correlating its intensity to a standard band of known mass and intensity. The standard band was prepared using an equimolar solution of BLG and βLg of 1.16 $\times 10^{-5}$ M concentration. In 10 mL MQ H_2O, 0.00107 g βLG and 0.00394 g BSA is dissolved. 20μl of the solution was injected into the gel, which is equivalent to 1.972μg and 0.5336μg of BSA and βLg respectively. In making the WPI standard, 20 μl known mass of WPI with concentration of 0.01wt% (1 μg WPI), 0.1wt% (10 μg WPI) and 1 wt% (100 μg WPI) are injected into the gel to characterize the separated protein species. Table 3.10 describes the calculated masses of αLa, BSA and βLg in the three 20μl standards.

Table 3.10
The mass of αLa, βLg and BSA injected in the gel as reference intensity for other bands

Protein Type	Normalised mass concentration in whey solution (%)	0.01wt%	0.1wt%	1wt%
		Total mass (μg)		
αLa	15.565	0.1557	1.5565	15.5651
BSA	1.241	0.01241	0.1241	1.2407
βLg	47.823	0.4782	4.7823	47.8231

3.8.5. Trypsin digestion with LC-MS.

Trypsin digestion was used to identify unknown protein and peptides bands found on the stained gel from fouled and cleaned membrane surface. The procedures for trypsin digestion are shown in Table 1.5 and 1.6 in Appendix A. The peptide extraction methods are shown in Table 1.7 and 1.8 in Appendix A. The settings for liquid chromatography mass-spectrometry (LC-MS) are shown in Section 1.4.1 in Appendix A.

3.9. FESEM

FESEM was used to establish the foulant location either on or in the membrane structure as well as identify the foulant morphology at high resolution and low beam. The specimen preparation procedure is shown in Table 3.11.

Critical drying was carried out on the membranes. The dried membranes were carved into a suitable size (1mm by 0.5mm) and mounted on bronze stubs using carbon tape and the sides were smeared with a shallow area of silver paint prior to coating with 150 angstrom of chromium using sputter coating device (Emitech K575-High Resolution Sputter Coater). Membranes were subsequently examined using a Hitachi S-900 FESEM at an accelerating voltage of 4kV. The magnifications operated were ×10, ×500, ×5k, ×50k, ×70k and ×100k.

Table 3.11
SEM specimen preparation protocol

	Protocol Steps	Actions	Duration
1.	Fixation	2.5% glutaraldehyde in 0.1M cacodylate buffer, pH 7.2	2 hrs
2.	Buffer wash	0.1M cacodylate buffer, pH 7.2	3 × 5 min
3.	Dehydration		
		30% ethanol	10 min
		50% ethanol	10 min
		70% ethanol	
		80% ethanol	10 min
		95% ethanol	10 min
		100% ethanol	10 min
		100% ethanol	10 min
		100% ethanol	10 min
4.	Drying	Critical point dry	2 hrs
5.	Mounting	Onto stubs	5 min
6.	Coating chromium		30 min

Chapter 4: Fouling Study of Single and Binary Protein Solutions in a Cross-Flow Ultrafiltration System

4. Introduction

The adsorption of proteins on the membrane surface and the interactions between protein and the membrane surface and between the deposit proteins are a major concern in membrane separation process especially in the biotechnology and food processing applications. An in-depth study in membrane cleaning is of great interest as effective cleaning saves substantial energy, reduces chemicals and wastewater while protecting the membrane from degradation resulted from cleaning (D' Souza and Mawson, 2005). Since the adherence of these protein foulants to the membrane surface affects cleaning process, prior investigation on the behaviour between protein and membrane surface with respect to operating conditions is important.

Single or binary protein mixtures are commonly used to characterize membrane fouling and cleaning in dairy applications. However in many industries, the mixtures such as whey are complex and may consist of multiple proteins. Earlier studies using Matrix Assisted Laser Desorption Ionisation - Mass Spectrometry (MALDI-MS) have reported that membrane pore size, duration of UF and molecular weight influenced the foulant distribution and composition along the membrane channel on the surface after Ultrafiltration (UF) of mixed protein mixtures (Chan et al., 2002; Chen et al., 2007). Uneven deposition of individual protein species observed in the fouling layer previously was believed to be caused by surface in-homogeneity and initial deposition. The study on protein adsorption and fouling on a membrane surface in cross-flow UF with spacer in the channel, observed significant differences between deposition of single protein solution and multiple protein mixtures. As usual, most studies were performed on single proteins due to the complexities of characterizing multi component protein mixtures (Chan and Chen, 2004). By using MALDI-MS to study the spatial distribution along the membrane, it was found that the deposition and composition of mixed proteins along the channel was influenced by molecular weights of different protein molecules and duration of filtration (Chen et al., 2007).

Although previous studies on the deposition profile with mixed protein mixtures on fouled membranes using MALDI-MS were successful, there were still limits to how reliable this method was (Chen et al., 2007). Patchiness in the measured protein deposition and the irregularity of crystallization of matrix in MALDI-MS analysis were experienced in previous studies and further optimization for the process was required for each membrane and foulant system. Quantification of actual protein components on the membrane was difficult since the analysis of the protein was mainly on the top fouling layer. Also, there is an urgent need to explain the principal cause of uneven protein deposition on the surface.

The main objective of the study in this chapter is to establish protein fouling characteristics in the particular filtration set-up so as to lay the foundation for the cleaning study which will be presented in Chapter 5. The combined effects of membrane properties, feed composition, and the interactions between the membrane and foulants are examined in this chapter. The degree of membrane fouling and protein deposition profiling along the membranes channel analysed with Lowry method (Hess et al., 1978) and 1D SDS-PAGE were presented. The effects of critical flux, filtration duration (4 or 8 hours), hydrodynamics (spacer or no spacer), and pH environment are investigated. Flux comparison before and after filtration was used to measure the degree of fouling while the deposition profile of BSA and βLg along cross-flow length of the membrane was obtained using a combination of Lowry method and 1D SDS-PAGE. The experimental aims, methods and purpose are summarised in Table 4.1 presenting the sections in this thesis. Additional observation using MALDI-MS and FESEM on the membrane surface was also performed and presented in Appendix A.

Table 4.1
Summary of experiments – Experiments, methods and aims

Sections	Experiments	Methods	Aims
• 4.2.1	• Protein mass balance	• Lowry and UV Spectrophotometer	• The integrity of the characterization methods
• 4.2.2	• Flux observation and spacer influence	• Flux studies	• The effect of spacer towards deposition and flux
• 4.2.3	• Critical flux	• Constant flux stepping mode	• The effect of pH, single or binary protein feed on critical flux
• 4.2.4 – 4.2.5	• Deposition profile on the membrane	• The Lowry Method	• The protein components
		• UV Spectrophotometer	• The effect of fouling duration, membrane and spacer
		• 1D SDS-PAGE	

4.1. Materials and methods

Binary protein feed solution containing 0.1wt% equimolar BSA and βLg (1.16×10^{-5}M each) was used in the fouling studies. The quantities are equivalent to 0.3944 g BSA and 0.1067 g βLg dissolved in 500mL of Milli-Q^{TM} water (Milli-Q). In some cases, 0.07wt% equimolar BSA and βLg (1.05×10^{-5}M each) was also used as the feed similar to a previous study (Chan, 2002). The pH of the feed solution was adjusted to pH 4 using diluted HCl or NaOH. The fouling experiments are performed on two different PES 30kDa MWCO membranes generally employed in dairy industries, one supplied by Synder Filtration^{TM} (SYNDER) while the other by Pall Inc. (PALL), USA. The feed solution and permeate was recycled throughout the fouling duration.

In addition, many past studies have also utilized PES membranes and BSA in studies of cleaning and fouling (Kuzmenko et al., 2005; Chen et al., 2006). The UF and filtration/fouling protocols, as well as procedures for surface protein characterizations were provided in Chapter 3.

4.2. Results and discussions

4.2.1. Mass balance of protein solution during UF

Mass balance of protein was carried out on the UF of binary proteins to verify protein assay methods in determining the total protein in the system. The concentration of protein in the feed solution before and after UF was determined by measuring the solution absorbance at 280nm while the protein deposition on the membrane was measured using the Lowry method. The calibration curve of BSA concentration and absorbance using UV-Vis Cary Spectrophotometer is shown in Appendix B. The results for the protein mass balance performed for PALL membrane are shown in Table 4.2. The UV Absorbance of the initial feed solution and final feed solution is indicated as IN and OUT respectively. The percentage of feed deposited (%) is the amount of initial protein (0.5025g) in the feed deposited on the membrane surface. The percentage (%) loss is the difference in protein mass between Feed In (IN), 0.5025g and Feed Out (OUT).

Table 4.2
Mass balance of protein with and without spacer after different UF duration (PALL)

Flow Condition	Protein on Surface (g)	OUT (g)	% of feed deposited on membrane	% losses
8 hours no spacer	8.7×10^{-5}	0.4857	0.01737	3.362
4 hours spacer	3.1×10^{-5}	0.4442	0.006096	11.63
4 hours no spacer	3.8×10^{-5}	0.4964	0.007574	1.243

Abs = 0.6283 × Ca. ($\mu g\ \mu L^{-1}$). Total feed in (IN) measured using UV-Vis at 280nm = 0.5025g at the start. Actual feed (IN) = 0.5011g total in 500mL Milli-Q. Total feed (OUT) measured using UV-Vis at the end of filtration.

The total measured mass of proteins in the feed (IN) was 0.5011g ± 0.005g and the corresponding mass measured by UV-Vis Spectrophotometer was 0.5025g ± 0.002g. These two readings demonstrated excellent agreement, indicating the accuracy of the calibration curve. The low protein deposition on the surface indicated that the concentration of the feed remained almost constant throughout the experiment. In addition, it can be seen that, there

were more protein deposition on the membrane after 8 hours than 4 hours of UF without spacer. Also spacer in the membrane channel did not reduce the amount of protein deposition after 8 hours of filtration (Not shown in Table 4.2) as the deposition amount measured on the surface with spacer in the channel was 1.413×10^{-4} g. The results of mass balance for SYNDER membranes are shown in Table 4.3.

Table 4.3
Mass balance of protein with and without spacer after different UF durations (SYNDER)

Condition	Protein on surface (g)	Total OUT (g)	% of feed deposited on membrane	% losses
8 hours spacer	0.000330	0.4457	0.06832	7.844
8 hours no spacer	0.000317	0.4457	0.06555	5.7694

Abs = 0.6283 × Ca. ($\mu g\ \mu l^{-1}$). Total feed in (IN) measured using UV-Vis at 280nm = 0.4833g at the start. Actual feed (IN) = 0.4536g total in 500mL MQ-water. Total feed out (OUT) measured using UV-Vis at the end of filtration.

The total mass of proteins in the feed was 0.4536g ± 0.005g and the corresponding mass measured by UV-Vis Spectrophotometer was 0.4833g ± 0.0007g. The mass fraction of protein from feed that deposits on the membrane surface is 0.06832% to 0.0655% for 8 hours filtration with spacer and 8 hours filtration without spacer respectively. The small difference shows that the effect of spacer was minimal in reducing deposition in long term UF.

In conclusion, the mass balance tests confirmed the reliability of combining the Lowry method and UV-Vis Spectrophotometer to evaluate the mass of protein in feed, permeate and surface. The small amount of protein losses (less than 12%) observed could be due to errors in UV measurements, adherence of proteins to the spacer and proteins trapped in the dead volume and piping system. However, adherence of proteins to the spacer seems to be a major influence. Overall, the amount of protein deposited on the membrane are very small (< 0.1% of feed) compared to that in the feed, indicating that protein deposition on the membrane do not reduce the feed concentration at the end of filtration.

4.2.2. Observation of flux and the influence of spacer

The average initial Milli-Q fluxes (J_{wi}) for 30kDa PALL and SYNDER membranes was 240 ± 24 $Lm^{-2}h^{-1}$ (10% error, average of 4 readings) and 96 ± 6 $Lm^{-2}h^{-1}$ (2% error, average of 5 readings) respectively measured at 50kPa constant TMP. It should be noted that although both membranes were 30kDa MWCO, the initial Milli-Q flux differed greatly.

The UF final fluxes (J_{uf}) for binary BSA & βLg feed mixture for PALL and SYNDER membranes were reported in Figure 4.1 and Figure 4.2 respectively (50kPa, 4 hrs or 8 hrs duration, 0.1wt%, pH 4, 500mLmin^{-1}, with or without spacer). There was an average of 94.7% flux decline at the end of UF for PALL membranes and an average of 85.6% flux decline in the final measured flux with SYNDER membrane (8 hours, 50kPa, without spacer). For both PALL and SYNDER membranes, the longer the duration of UF, the lower the final UF flux of the membrane. The measured flux with spacer was higher compared to that without spacer for the same UF duration, indicating the effectiveness of the spacer in minimizing concentration polarization and reducing the rate of fouling. Although both PALL and SYNDER membranes have different initial Milli-Q fluxes, the final fluxes after 8 hours of UF were agreeable with small differences (~ ± 3 $Lm^{-2}h^{-1}$).

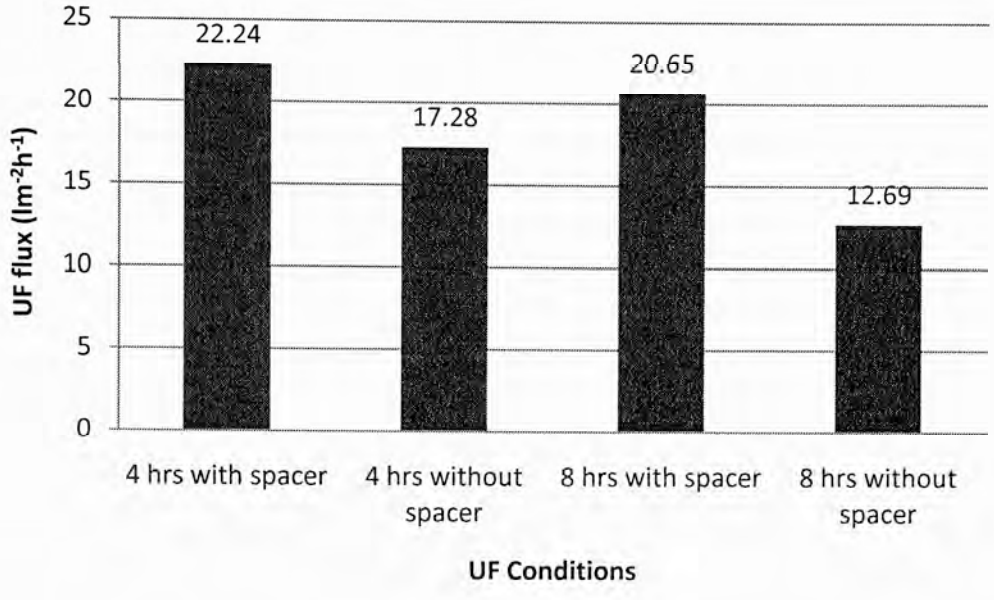

Figure 4.1 Measured UF fluxes at the end of filtration of 0.1wt% equimolar BSA and βLg (± 3 $Lm^{-2}h^{-1}$).
(UF conditions: 50kPa, pH 4, 500mLmin^{-1}, 4 and 8 hours UF, with and without spacer, PALL)

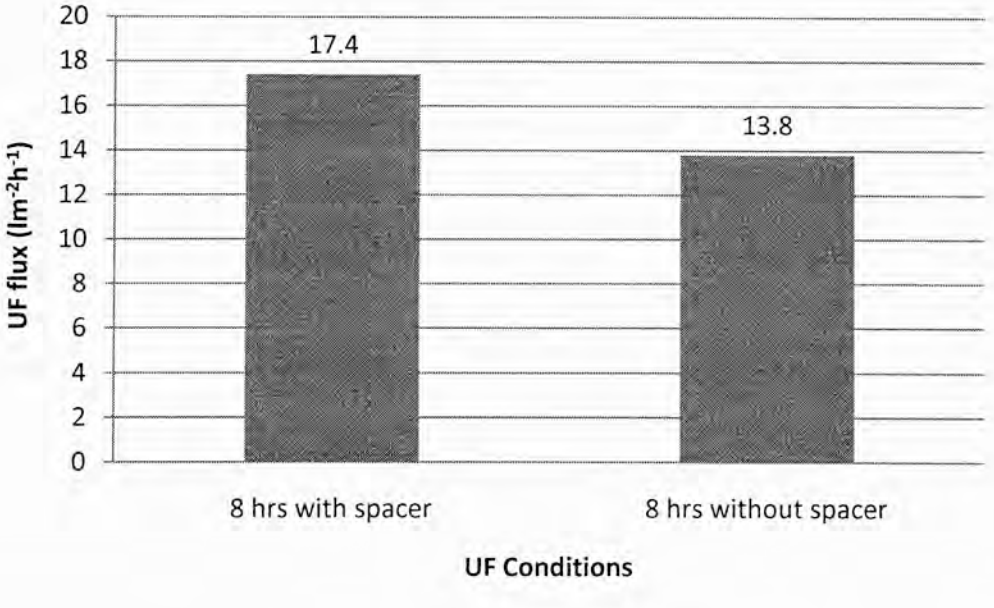

Figure 4.2 Measured UF flux at the end of filtration of 0.1wt% equimolar BSA and βLg (± 2 $Lm^{-2}h^{-1}$).
(UF conditions: 50kPa, pH 4, 500mLmin^{-1}, 8 hours UF, with and without spacer, SYNDER)

A spacer inserted in the membrane channel reduced the flux decline in both membrane types. Therefore spacer was useful during the operation of UF systems in reducing flux decline and increasing productivity despite little difference in deposited protein. A comparison between the measured Milli-Q flux after rinsing (J_{ww}) with and without spacer for PALL membrane is shown in Table 4.4.

Table 4.4
Influence of spacer on the measured final flux ($Lm^{-2}h^{-1}$) after 4 hours of UF and after Milli-Q rinsing.

	Spacer	No spacer
Flux type	Flux ($lm^{-1}h^{-1}$)	
J_i	240.00	240.00
J_{uf}	22.24	17.28
J_{ww}	45.41	49.91

(UF conditions: 0.1wt% equimolar BSA and βLg, pH 4, 500mLmin^{-1}, PALL)

Table 4.4 shows that the flux recovered $(J_{ww} - J_{uf})/J_{uf}$ after rinsing without spacer is 45% higher than the flux recovered with spacer. This shows that the spacer present in the channel can reduce rinsing efficiency and protein removal. This could also suggest that the foulant on the membrane without spacer in the membrane channel was probably looser and easier to be removed in the rinsing stage. This finding was supported by authors who explained that spacer could create localised stagnant zones at the membrane surface resulting in high levels of proteins deposited in that zones (Da Costa et al., 1993). Some authors found that this discrepancy was caused by spacer that results in higher protein deposition (Chen et al., 2007). The proteins might be trapped in stagnant zones or adhere to the spacers and when rinsing occurs re-deposition takes place. Also, 80% loss in permeate flux (J_{ww}/J_{wi} %) was observed during the filtration process indicating the need for chemical cleaning to recover the flux back to the initial membrane flux.

In conclusion, 4 hours of filtration fouling with BSA and βLg binary mixture feed was sufficient to cause irreversible changes to the flux and the need to involve chemical cleaning to improve the flux back to normal. Based on final UF flux, SYNDER membranes were fouled more than PALL membranes under the same set-up. Differences between final flux after 4

hours and 8 hours filtration was less than 5 $Lm^{-2}h^{-1}$ showing small difference caused by of duration of fouling with and without spacer (Figure 4.1). Although insertion of spacers reduced concentration polarization and protein deposition on the membrane, spacer did not improve the flux more than the non spacer case at rinsing process due to possible re-deposition of the stagnant and loose proteins (Table 4.4).

4.2.3. Determination of critical flux

Critical flux was estimated with SYNDER membranes to identify the flux where fouling starts to occur using constant flux stepping mode and monitoring the increase in TMP (Chen, 1998; Metsamuuronen and Nystrom, 2000; Metsamuuronen et al., 2002; Chan and Chen, 2004). In addition, the effect of pH and spacer towards critical flux was also studied.

In Figure 4.3, it can be observed that at the imposed flux of about 12 $Lm^{-2}h^{-1}$, the TMP remained constant, and at increased flux of 17 $Lm^{-2}h^{-1}$, TMP increased steadily over time, this indicates that this flux was above the critical flux. At the further increased flux of 23 $lm^{-2}h^{-1}$ severe fouling had occurred with a much higher increase rate in TMP (1.05×10^{-5}M BSA, pH 4, Pin=60kPa, flux stepping mode, No spacer).

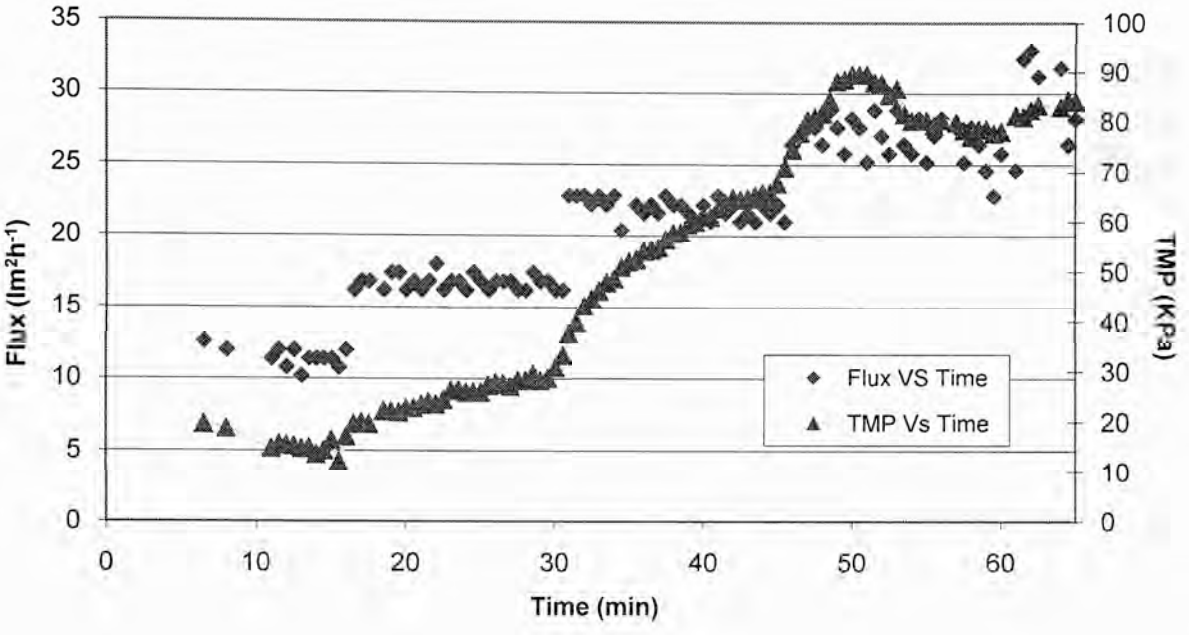

Figure 4.3 Critical flux in the UF of BSA at pH 4 with no spacer (Flux stepping mode, Pin = 60kPa, 1.05×10^{-5}M, 500mLmin^{-1}, pH 4, no spacer inserted) (Electrostatic charge: membrane – ve / BSA +ve)

In Figure 4.4, critical flux was estimated at pH 4 with a spacer in the membrane channel (1.05×10^{-5}M BSA, pH 4, Pin = 60kPa, flux stepping mode, spacer inserted). In Figure 4.4, it can be observed that at the imposed flux of about 23 Lm^{-2}h^{-1}, the TMP remained constant, and at increased flux of 32 Lm^{-2}h^{-1}, TMP increased steadily over time, this indicates that this flux was above the critical flux. The spacer in the membrane channel increased the critical flux of BSA UF by reducing the rate of adsorption of BSA and decreases localised concentration on the membrane surface.

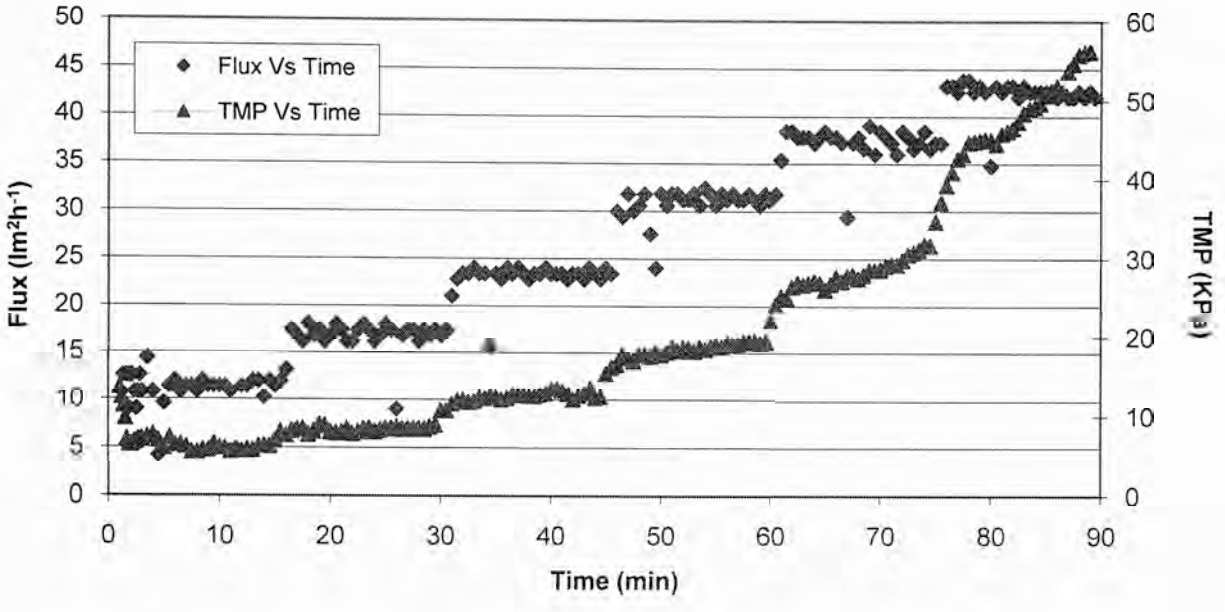

Figure 4.4 Critical flux in the UF of BSA at pH 4 with spacer (Flux stepping mode, Pin=60kPa, 1.05×10^{-5}M BSA, 500mLmin^{-1}, with spacer (Electrostatic charge: membrane –ve / BSA +ve)

In Figure 4.5, the critical flux was exceeded at the imposed flux of 17 Lm^{-2}h^{-1} for equimolar BSA and βLg mixed solution and fouling occurred (1.05×10^{-5}M BSA and βLg each, pH 4, Pin=60kPa, flux stepping mode, No spacer). By comparing Figure 4.3 and Figure 4.5, the critical flux of equimolar BSA and βLg mixed solution is very similar to the critical flux of single BSA feed due to similar iso-electric point (IEP) of BSA (IEP 4.8) and βLg (IEP 5.2).

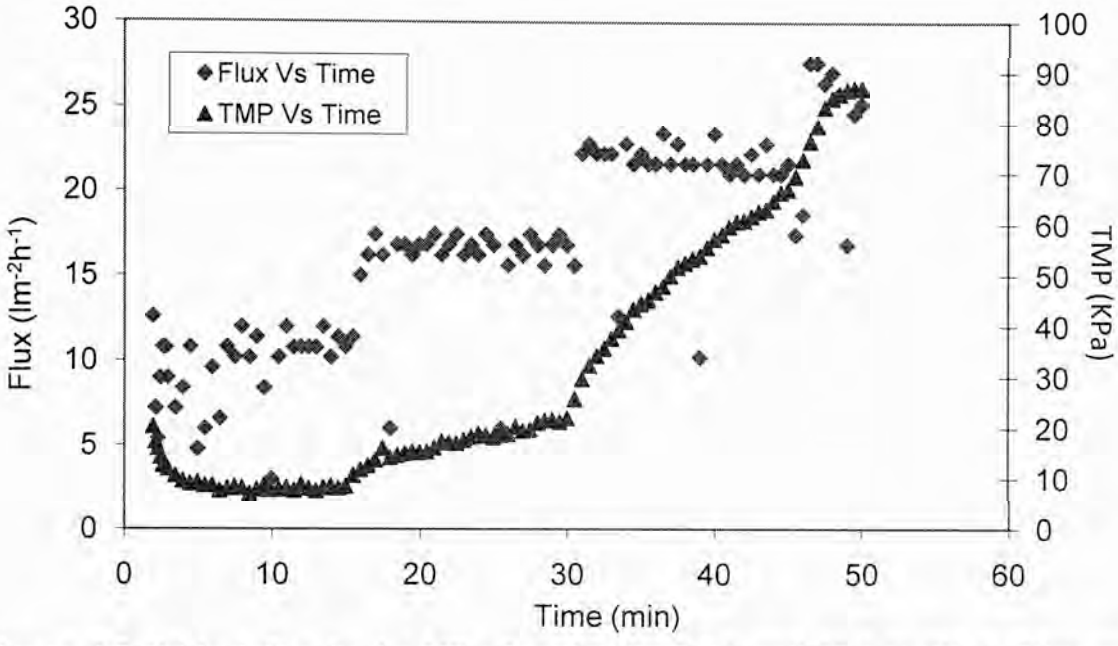

Figure 4.5 Critical flux in the UF of equimolar BSA and βLg at pH 4 (Flux stepping mode, Pin=60kPa, 1.05×10^{-5}M each, 500mL.min^{-1}, with no spacer) (Electrostatic charge: membrane –ve / BSA + ve / βLg +ve)

The critical flux at pH 6 was exceeded at the imposed flux of 30 Lm^{-2}h^{-}1 in Figure 4.6 (1.05×10^{-5}M BSA, pH 4, Pin=60kPa, flux stepping mode, No spacer). By comparing the results of Figure 4.3 and 4.6, the critical flux at pH 6 was higher than at pH 4. At pH 6, both the membrane and BSA were negatively charged and electrostatic repulsion between the BSA and membrane occurred. Thus, it was harder to obtain an irreversible fouling at pH 6 due to electrostatic repulsion between the protein and membrane when compared to pH 4. These results were expected as the critical flux is the lowest at pH closest to the IEP, and the critical flux increases with pH on either side of the IEP (Chen, 1998; Metsamuuronen et al., 2002). An additional test of estimating the critical flux at pH 3 and the results are shown in Figure 2.2 in Appendix B. At pH 3, TMP increase was not observed during the flux stepping of constant flux.

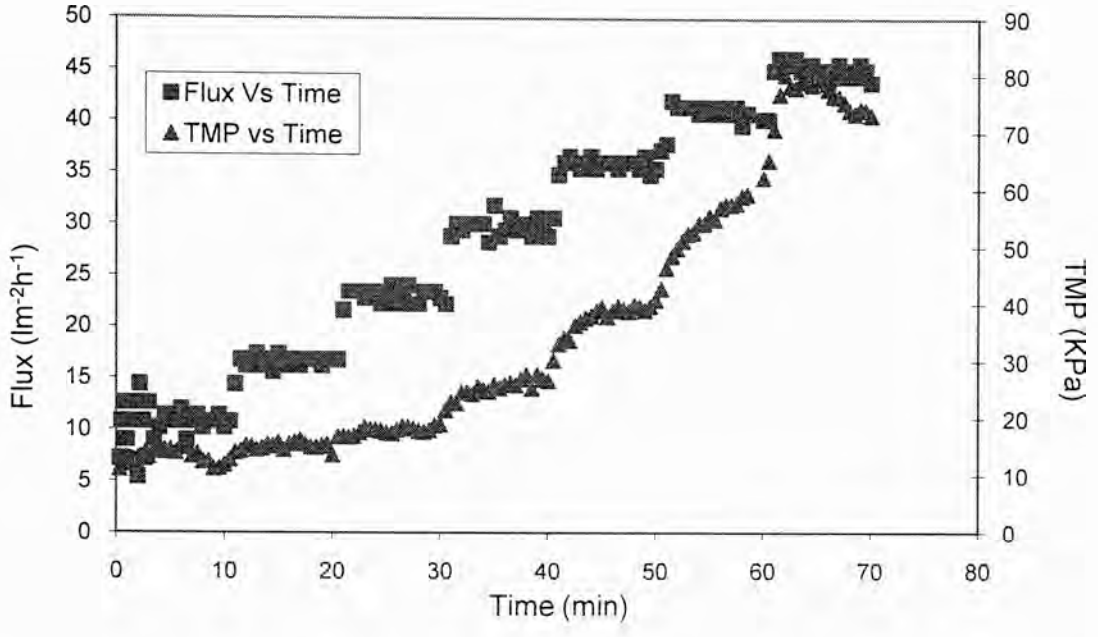

Figure 4.6 Critical flux in the UF of BSA at pH 6. (Flux stepping mode, Pin=60kPa, 1.05×10^{-5}M, 500mL.min^{-1}, with no spacer) [Electrostatic charge: membrane –ve / BSA –ve]

The Flux-TMP relationship of the critical flux experiments are plotted in Figure 4.7. The diagram shows a weak form of critical flux, as the TMP is greater than that for pure water and the slope differs from that of the pure water (Field et al., 1995; Howell, 1995).

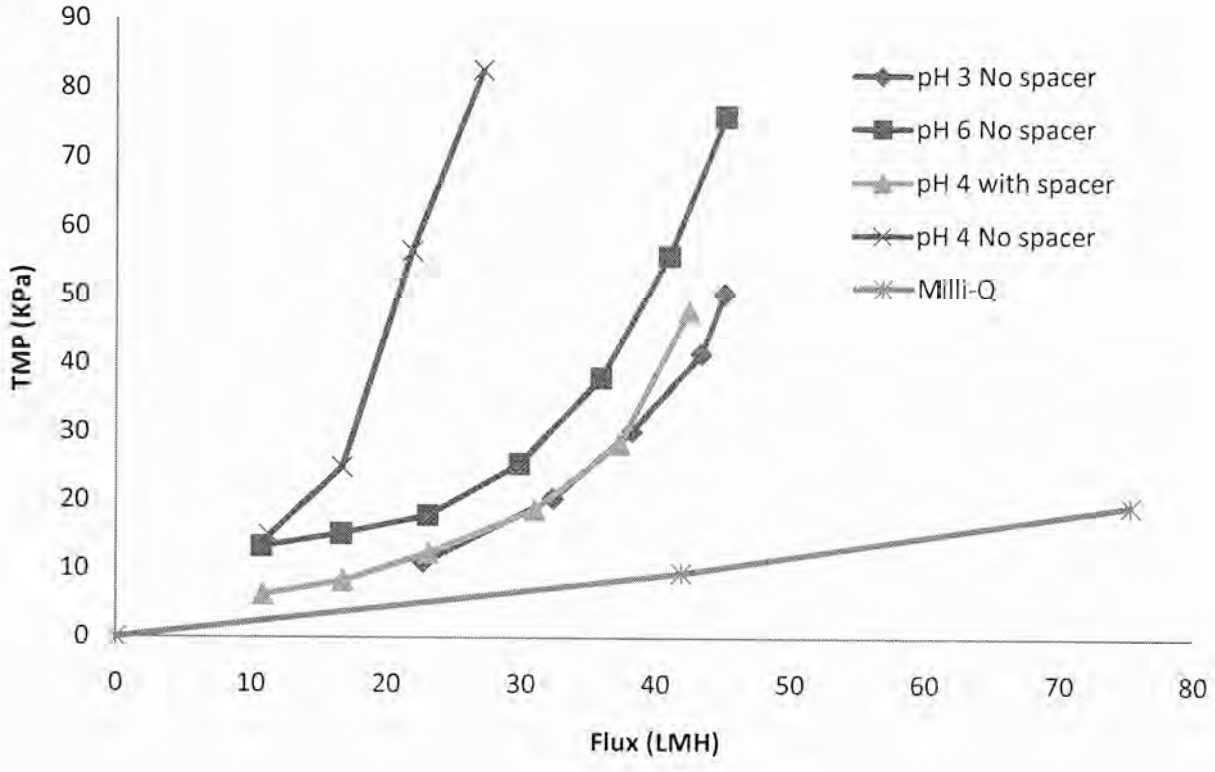

Figure 4.7 Summary of critical flux or TMP at imposed flux vales observed in the UF of equimolar BSA and/or βLg feed solutions (Conditions: various pH values, 500 mL.min^{-1}, with and with no spacer inserted in the channel)

In conclusion, the critical flux experiments revealed that setting the pH to 4 and running at a TMP of 50kPa and above can ensure irreversible fouling to occur. This pH and TMP is the main condition of fouling for the subsequent cleaning chapter that follows. The critical flux differences between spacer (Figure 4.4) and no spacer (Figure 4.3) at pH 4 was high showing the effectiveness of spacer in reducing concentration polarization and fouling on the membrane surface.

4.2.4. Measurements of surface deposition using Lowry method

4.2.4.1.Protein deposition after 4 hour of UF

Spatial distribution of BSA and βLg deposition on SYNDER membrane surface was measured using Lowry method at the end of UF (0.1wt% equimolar BSA and βLg, pH 4, 4 hrs,

500mL.min^{-1}, SYNDER). Shown in Figure 4.8, we can observe that less than 2μg cm^{-2} proteins per membrane section were deposited on each section of the surface and the deposition of the proteins were uneven. These uneven protein deposition was experienced in past studies using MALDI-MS (Chen et al., 2007). Many factors were thought to cause the unevenness of distribution along the membrane horizontal surface. These factors includes the random nature of protein aggregate deposition, uneven membrane surface, and local inhomogeneities in matrix crystallization during MALD-MS analysis. However, as the deposition were observed to be uneven when using a different technique that is the Lowry method, it can be safely conclude that the limitation of the MALDI-MS technique was not solely responsible for these uneven deposition. Thus, for our study, this observation was the result of uneven membrane and protein aggregate formation along the surface. This randomness of deposition was not concentrated on the fouling surface but on the entire deposition which includes the pores.

Although the deposition of proteins on the membrane surface was small, the flux decline was considerable as experienced in both SYNDER and PALL membranes. Standard deviation (σ) of the protein deposition per membrane sections with and without spacer was measured to analyse the influence of spacers to the spatial deposition along the membrane surface. The measured standard deviations with and without spacer are 0.137 μgcm^{-2} and 0.176 μgcm^{-2} respectively. The lower standard deviation with spacer in the channel indicates that spacer reduces the patchiness in the deposition along the membrane surface.

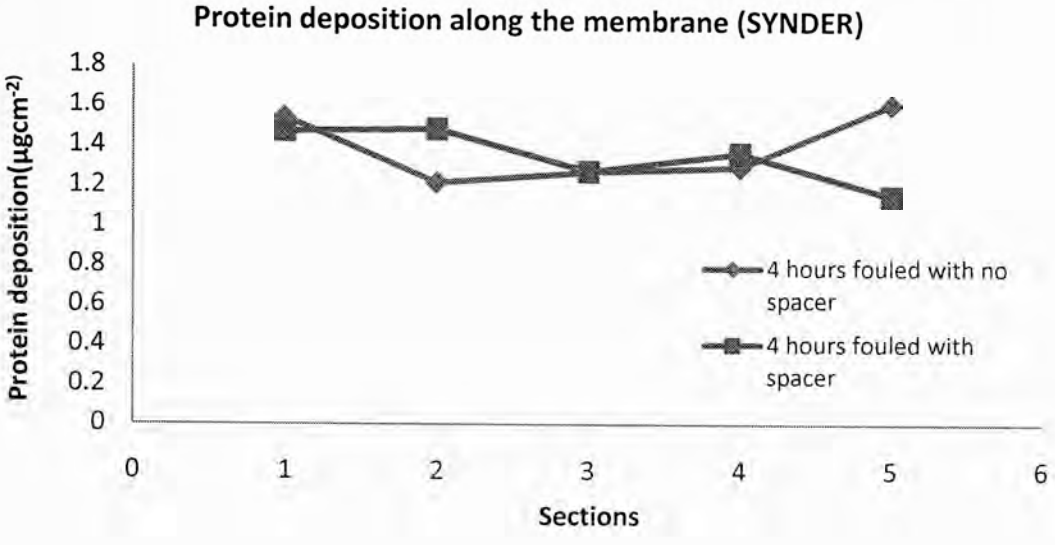

Figure 4.8 Total protein deposition along the membrane after 4 hours of UF with and without spacers in the membrane channel measured by Lowry method (UF conditions: 0.1wt% equimolar BSA and βLg, pH 4, 4 hrs, 500mL.min^{-1}, SYNDER).

Alternatively, Figure 4.9 shows the spatial distribution of BSA and βLg deposition on the PALL membrane surface at the end of UF (0.1wt% equimolar BSA and βLg, pH 4, 4 hrs, 500mL.min^{-1}, PALL). Having a higher initial Milli-Q flux when compared to SYNDER, PALL membrane experiences less overall deposition compared to SYNDER membrane. There was less than 0.5μgcm^{-2} of proteins detected per section of membrane. Therefore, although the molecular weights cut off (MWCO) are the same, under similar operating conditions SYNDER membranes are more susceptible to fouling compared to PALL membrane. The measured standard deviations for protein deposition per section with and without spacer are 0.035 μgcm^{-2} and 0.110 μgcm^{-2} respectively and respectively. Similar to SYNDER membrane in Figure 4.8, lower standard deviation of protein deposition per section were experienced with spacer present. The sames findings are also obtained after 8 hours of UF for PALL membranes in Figure 4.11 where the deviation for protein deposition with spacer is lower. One noticable difference between the deposition on PALL (Figure 4.8) and SYNDER (Figure 4.9), was the higher deposition of proteins at the inlet section of the channel.

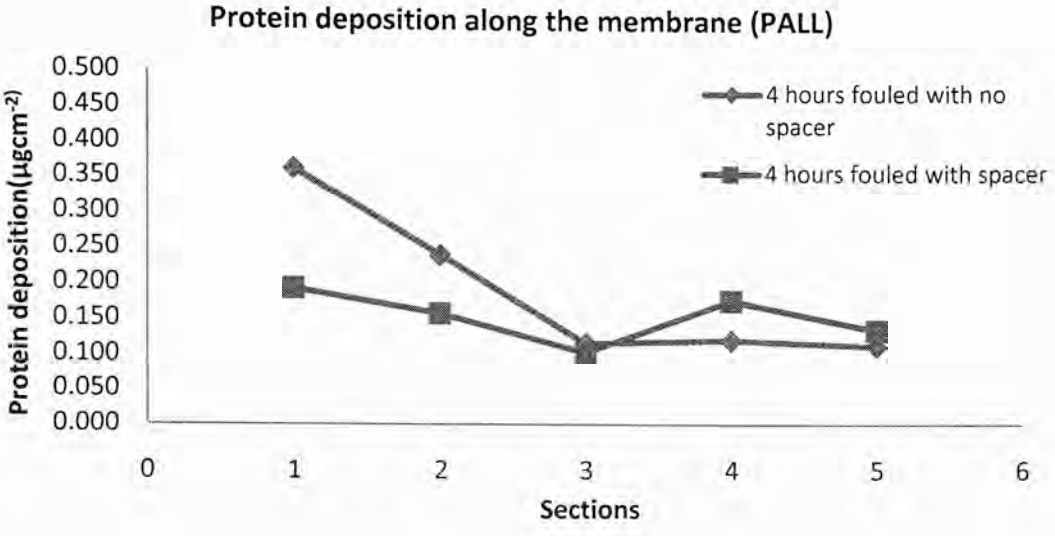

Figure 4.9 Total protein deposition along the membrane after 4 hours of UF with and without spacers in the membrane channel measured by Lowry method (UF conditions: 0.1wt% equimolar BSA and βLg, pH 4, 4 hrs, 500mL.min^{-1}, PALL).

Although there was high critical flux difference between no spacer (Figure 4.3) and spacer (Figure 4.4) inserted in the channel, the spatial deposition differences are small (Figure 4.8). Therefore, deposition still occurs whether a spacer is inserted or not however concentration polarization and fouling was reduced.

4.2.4.2.Protein deposition after 8 hours of UF

Similarly, spatial distribution of BSA and βLg deposition on the SYNDER and PALL membrane surface was measured using Lowry method at the end of 8 hours UF (0.1wt% equimolar, pH 4, 8 hrs, 500 mL.min^{-1}). The spatial deposition results are shown in Figures 4.10 and Figure 4.11 for SYNDER and PALL membrane respectively. Similar to 4 hours UF, the total protein deposition on SYNDER membrane was also more than PALL membrane after 8 hours of UF.

By comparing effect of spacer in the channel on protein deposition after 4hrs and 8hrs of UF using PALL membranes in Figures 4.9 and 4.11 respectively, we can observe that spacer increased the average protein deposition (μg cm^{-2}) on the membrane by 362% while without spacer, the increase was 129%. Therefore, spacer did not help to reduce the deposition on the membrane surface after longer duration of UF. This phenomena was also observed in past studies involving multiple protein feeds where in some cases spacer has not reduced protein deposition (Chen et al., 2007).

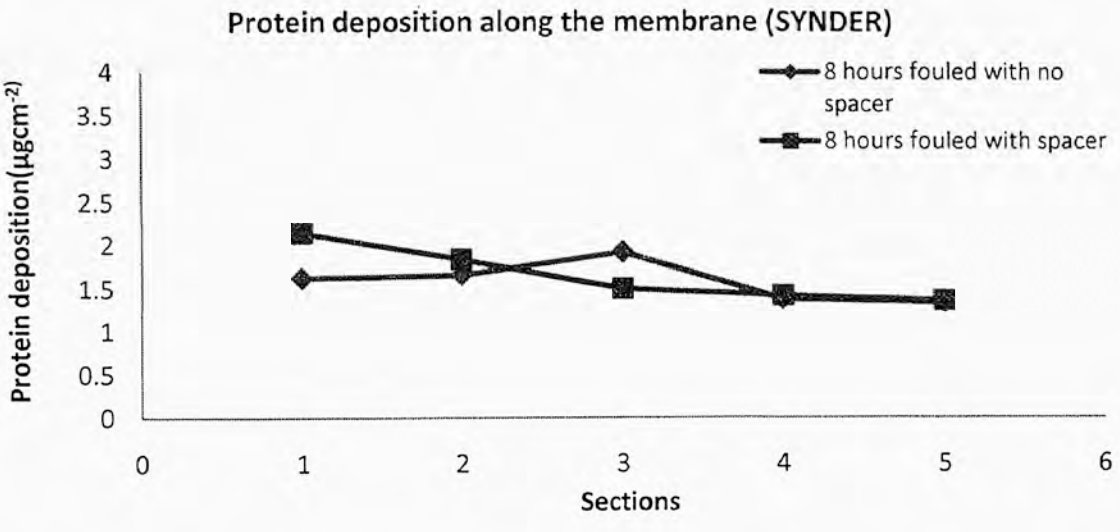

Figure 4.10 Total protein deposition along the membrane after 8 hours of UF with and without spacers in the membrane channel measured by Lowry method (UF conditions: 0.1wt% equimolar BSA and βLg, pH 4, 8 hrs, 500mL.min^{-1}, SYNDER).

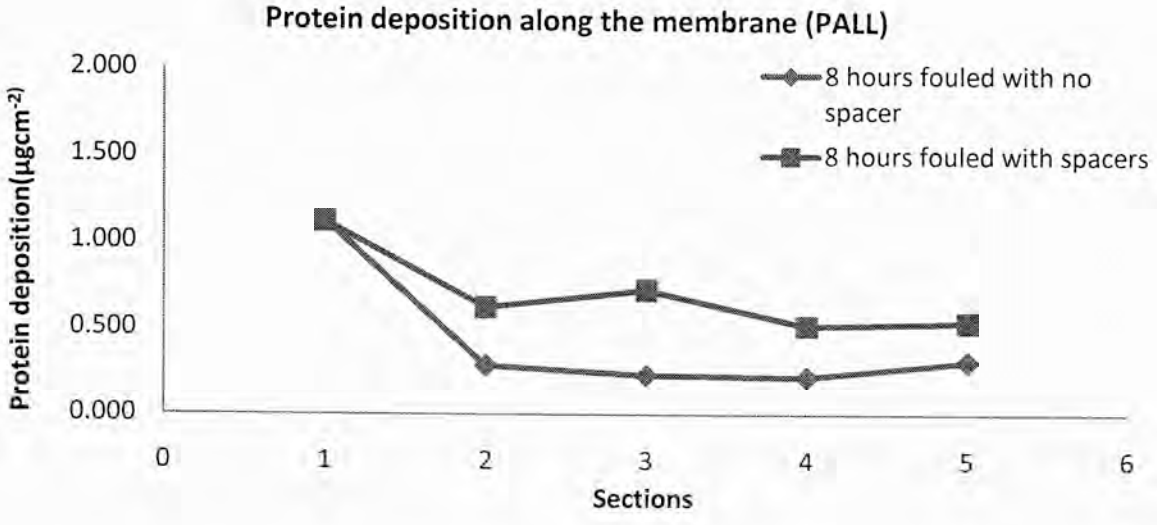

Figure 4.11 Total protein deposition along the membrane after 8 hours of UF with and without spacers in the membrane channel measured by Lowry method (UF conditions: 0.1wt% equimolar BSA and βLg, pH 4, 8 hrs, 500mL.min^{-1}, PALL)

The distribution of protein deposition along the membrane surface for PALL membrane showed higher protein deposition at the entrance section of the channel (Figure 4.9 and 4.11). This was probably caused by uneven pressure losses along the membrane channel during UF at constant pressure of 50kPa TMP (Holland and Bragg, 1995). The calculated localised pressure losses at the entrance ΔP_{ent}, along the channel (ΔP_f) and at the exit (ΔP_{ex}), are 4.547 Pa, 231.933 Pa and 8.115 Pa respectively. The calculations are described in Appendix B, Section 2.6. The low pressure loss at entrance causes maximum TMP at this region which could result in higher protein deposition on the membrane surface. At the exit, the total pressure losses should be the highest and therefore causing the lowest pressure drop. Adding to that, spacer also helps to dampen the fluctuations of protein deposition along the membrane as shown in Figures 4.9 and 4.11.

There was a slight descending profile of deposition after 8 hours of fouling for both SYNDER (Figure 4.10) and PALL membranes (Figure 4.11). Also, when using PALL membrane, the longer the duration of UF, the higher the protein deposition (Figures 4.9 and 4.11). On the

other hand, when using SYNDER membranes for longer UF duration, smoother deposition was observed along the membrane surface (Figures 4.8 and 4.10).

4.2.5. Measurements of surface deposition using 1D SDS-PAGE

4.2.5.1.Protein deposition after 8 hours of UF (PALL)

1D SDS-PAGE was used to characterize the individual protein species in the individual sections along the membrane surface after UF (0.1wt% equimolar BSA and βLg, pH4, 8 hrs, 50kPa). The detailed procedures for running this method are explained in Chapter 3, Section 3.8.

Figure 4.12 shows the silver stained gel of feed injected into the gel. The BSA and βLg are present as a mixture of peptides of different molecular weights which can influence the fouling and cleaning of the UF membranes.

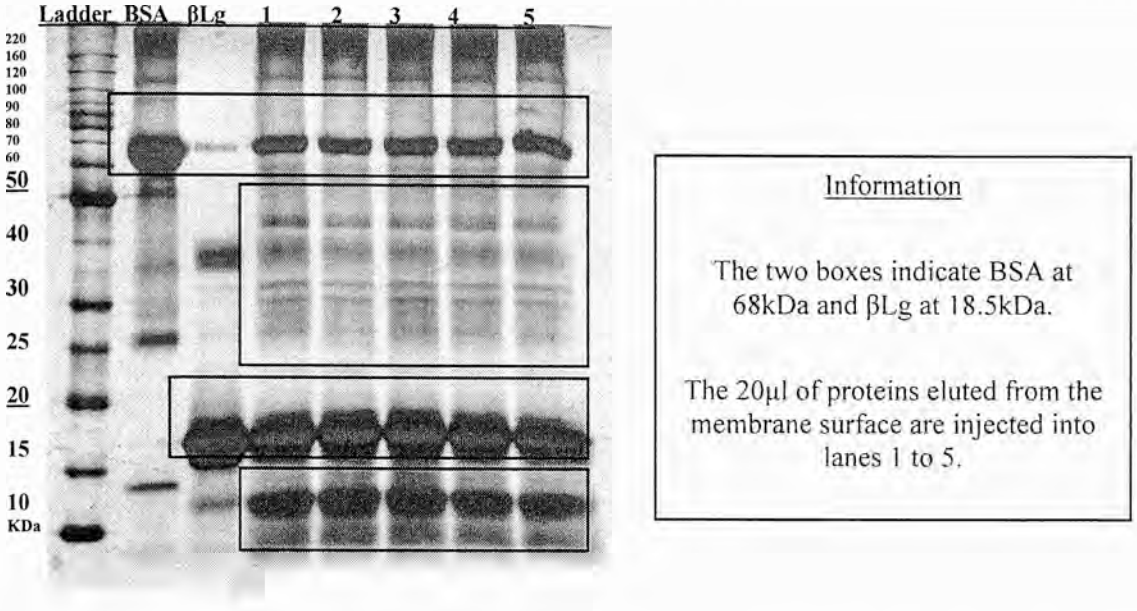

Figure 4.12 1D SDS-PAGE of BSA and βLg spatial distribution along the membrane after UF of 8 hours (UF conditions: 0.1wt% equimolar BSA and βLg, pH 4, 8 hrs, 500mL.min^{-1}, PALL, spacer)

The composition of protein deposits on PALL membrane after 8 hours of UF with and with no spacer was shown in Figure 4.13 and Figure 4.14 respectively (0.1wt% equimolar BSA and βLg, pH4, 8 hrs, 50kPa). Figure 4.13 and Figure 4.14 shows that βLg was the dominant protein that fouled the membrane surface from the intensities of the gel stained by silver. The finding was similar to the surface analysis obtained by MALDI-MS after 8 hours of fouling where βLg was the major foulant (Appendix B, Section 2.3). The results agree favourably with a past study in the constant pressure UF of lysozyme, BSA, βLg and Ovalbumin, where BSA preferentially adsorbs followed by βLg displacement as the duration increased from 2 hours to 6 hours (Chen et al., 2007). This unique observation shows the exchange and displacement phenomena between proteins of different structural stability, where on solid surface proteins of higher concentration adsorbs first, while less mobile proteins with higher binding affinity subsequently exchange with the initially absorbs proteins (Nakanishi et al., 2001). In other words, when "hard" proteins such as βLg compete with "soft" proteins such as BSA during adsorption, hard proteins preferentially adsorbs even under electrostatic repulsion (Arai and Norde, 1990b). As observed in the spatial deposition of protein along the membrane surface

measured using Lowry method (Figures 4.9 and 4.11), the deposition of BSA and βLg was also randomly distributed along the membrane surface.

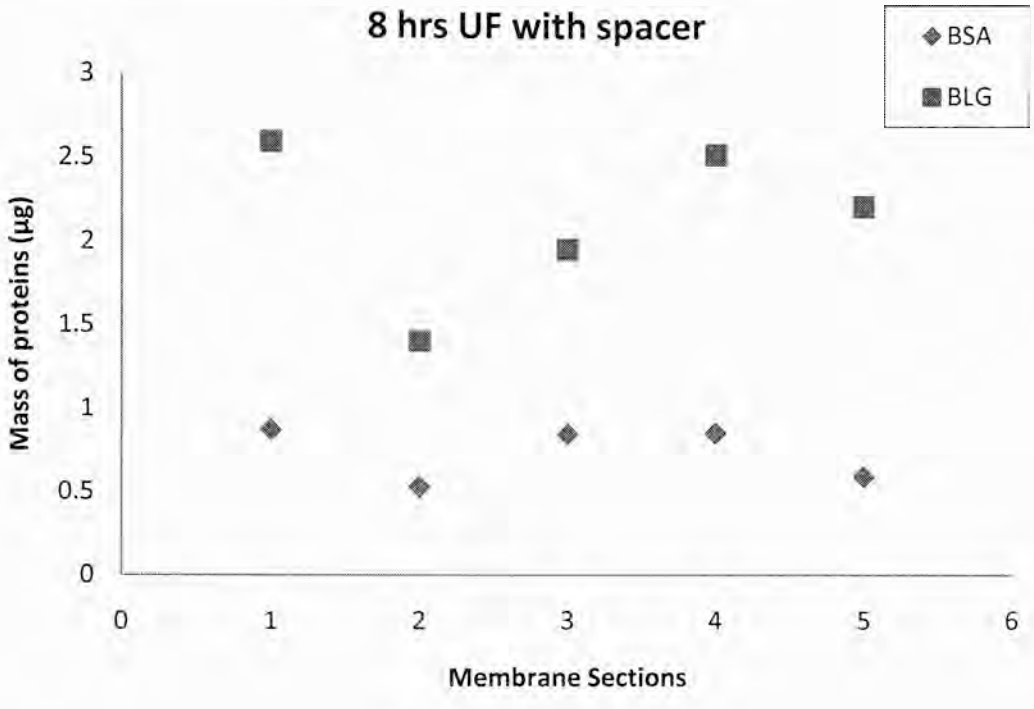

Figure 4.13 Amount of BSA and βLg along the membrane strip after 8 hours of UF with spacer measured by 1D SDS-PAGE (UF conditions: 0.1wt% equimolar BSA and βLg, pH 4, 8 hrs, 500mL.min^{-1}, PALL, Spacer).

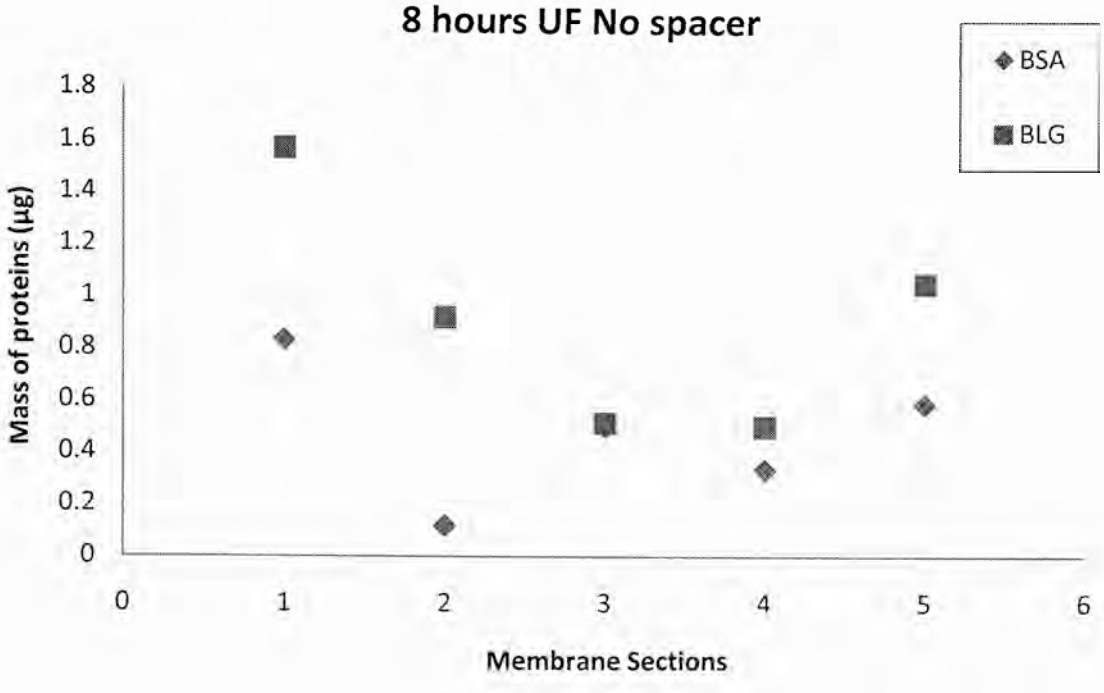

Figure 4.14 Amount of BSA and βLg along the membrane sections after 8 hours of UF with no spacer estimated measured by 1D SDS-PAGE (UF conditions: 0.1wt% equimolar BSA and βLg, pH 4, 8 hrs, 500mL.min^{-1}, PALL, No Spacer).

Also in Section 2.4 of Appendix B, we show the analysis of permeate and the feed solution after 4 and 8 hours of UF. We can observe that no proteins are detected in the permeate solution after both durations proving that most of the proteins are retained on the membrane and feed/recycle solution.

By observing Figures 4.14 and 4.15 again, there was higher deposition at the end of the 8 hours UF when spacer is present in the channel. This was similar to Figure 4.11 when spacer did not help to reduce deposition on the membrane surface after a longer duration of fouling.

Standard deviations for BSA and βLg deposition per membrane section were measured to determine the smoothness or unevenness of deposition along the membrane surface. The standard deviations for BSA and βLg deposition per membrane sections are 0.164 and 0.557

respectively with a spacer present (Spacer inserted, Figure 4.13). On the other hand, the standard deviations for BSA and βLg deposition per membrane sections are 0.269 and 0.443 respectively with no spacer present (No spacer inserted, Figure 4.14). Generally, the standard deviation for BSA deposition was less than βLg demonstrating a smoother deposition of BSA along the membrane surface.

4.2.5.2.Protein deposition after 8 hours of UF (SYNDER)

The composition of protein deposits on SYNDER membrane after 8 hours of UF with and with no spacer was shown in Figures 4.15 and 4.16 respectively (0.1wt% equimolar BSA and βLg, pH4, 8 hrs, 50kPa). Both BSA and βLg deposition is relatively evenly along the surface when spacer was inserted in the channel, as observed in Figure 4.13. In addition, BSA and βLg deposition was almost similar in mass quantity. By comparing Figures 4.13 (PALL, 8 hours UF, Spacer) and Figure 4.15 (SYNDER, 8 hours UF, Spacer), BSA deposition was evenly distributed along the membrane surface, indicating the dampening effect of spacer to the fluctuations. By looking at Figure 4.15 (SYNDER, 8 hours UF, Spacer) and Figure 4.16 (SYNDER, 8 hours UF, No spacer), and comparing them to Figure 4.10 (SYNDER, 8 hours UF, spacer and no spacer), we can observe that there was higher deposition on the surface at the inlet of the channel. Therefore, the phenomenon was not coincidental but was caused by the hydraulic effect in the channel.

Figure 4.16 (SYNDER, 8 hours UF, No spacer) shows that BSA has a higher deviation in deposition compared to βLg and on some sections of the membrane, BSA has more coverage than βLg. This was similar to the observations on PALL membranes in Figure 4.14 (PALL, 8 hours UF, No spacer). Therefore, spacer dampens the fluctuations of BSA deposition along the membrane surface.

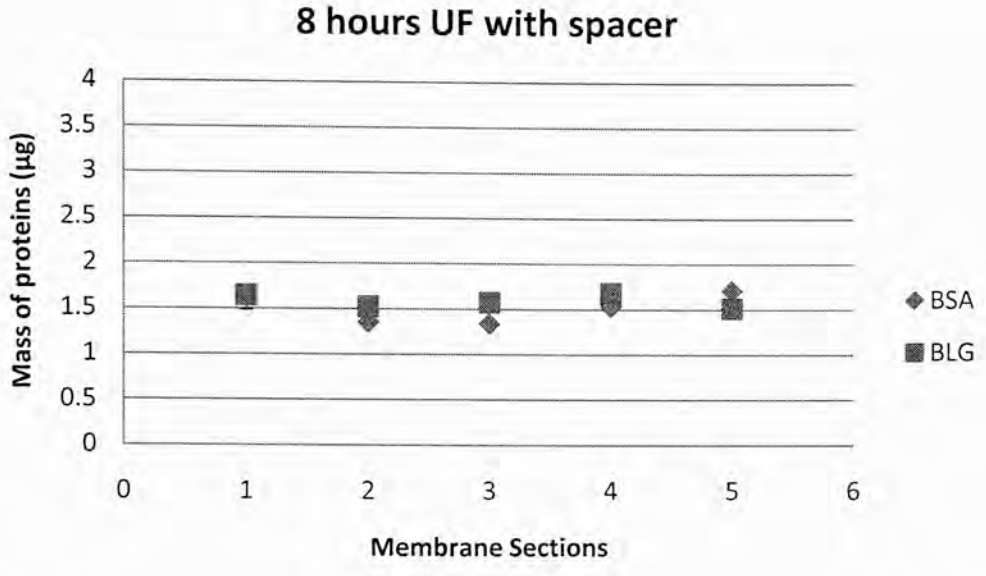

Figure 4.15 BSA and βLg profile along the membrane after 8 hours of UF with spacer measured by 1D SDS-PAGE (UF conditions: 0.1wt% equimolar BSA and βLg, pH 4, 8 hrs, 500mL.min^{-1}, SYNDER, Spacer).

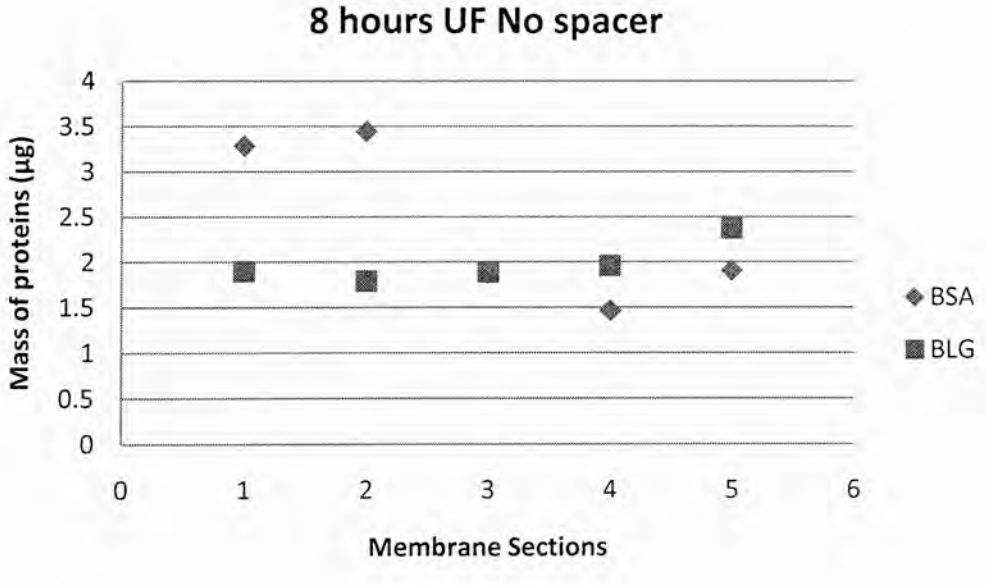

Figure 4.16 BSA and βLg profile along the membrane after 8 hours of UF with no spacer measured by 1D SDS-PAGE (UF conditions: 0.1wt% equimolar BSA and βLg, pH 4, 8 hrs, 500mL.min^{-1}, SYNDER, No Spacer)

4.2.6. Conclusion

The parameters that were examined in this study are the effects of feed channel spacer, interactions between BSA and βLg, effects of solution environment and hydrodynamics of the channel. These physico-chemical properties are crucial in designing the membrane cleaning methods in the next chapter.

Milli-Q flux before and after fouling, as well as final UF flux were measured to analyse the degree of fouling during UF. Under the selected conditions (0.1% equimolar BSA and βLg each, pH 4, 500 $mL.min^{-1}$, 50kPa, 4 and 8 hours), the UF final flux results shows that although the amount of proteins adsorbed on the membrane surface was small i.e. less than 1%, compared to the feed, the final UF flux decline was high (≈ 90% of initial Milli-Q flux) (Table 4.2 and 4.3). The final flux with a spacer in the channel was higher than with no spacer (Figure 4.1). This indicates the effectiveness of spacer in reducing the flux decline. In spite of this, the flux recovered after Milli-Q rinsing (J_{ww}) (15min, 500mL.min-1) was higher without a spacer in the channel under the selected conditions. Thus, the spacer did not assist in improving the flux of the membrane during rinsing due to its ineffectiveness in reducing deposition (Table 4.4). To conclude, spacer inserted in the channel reduces flux decline during UF however the flux recovery was less with a spacer than without a spacer present due to re-deposition of proteins during rinsing.

Therefore, the selected constant pressure fouling condition (50kPa, 0.1wt% Equimolar BSA and βLg each, 4 hours, 500$mL.min^{-1}$) was sufficient to cause an irreversible loss of flux that requires cleaning intervention to recover the flux. In addition, the amount of protein adsorbed along the cross-flow membrane surface after fouling was sufficient for both qualitative and quantitative conclusions.

The critical flux studies at the selected conditions (pH 4, flux stepping mode, Pin = 60kPa, 0.1wt% BSA or BSA and βLg) shows that the critical flux for BSA to be at 17 $lm^{-2}h^{-1}$ without a spacer. With a spacer, the critical flux was 30$lm^{-2}h^{-1}$ indicating the effectiveness of spacers

in reducing adsorption on the membrane surface. A Flux-TMP summary of critical flux experiments for pH 6 and 4, with and with no spacer are shown in Figure 4.7. From this study, the selected conditions for fouling (50kPa, 0.1wt% Equimolar BSA and βLg each, 4 hours, 500mL.min^{-1}) would sufficiently cause irreversible fouling to occur on the membrane surface.

The distribution of protein deposition along the membrane was observed to be random and uneven and was caused by uneven membrane surface and random protein aggregate formation (Figure 4.8 – 4.9) (0.1wt% equimolar BSA and βLg, pH 4, 4 hrs, 500mL.min^{-1}, PALL and SYNDER). From standard deviations measurements of protein deposition per sections for both membranes (PALL and SYNDER), the spacer in the channel reduces the patchiness in the protein deposition along the membrane. Two obvious characteristic of deposition on PALL membranes (Figures 4.9 – 4.11) was higher deposition at the inlet of the channel. This phenomenon was probably cause by uneven pressure losses along the cross-flow channel, the lowest at the entrance and exit, while the highest at the centre of the channel (Measured, Appendix B). Higher pressure loss in the section resulted in lower amount protein deposition in that particular section. There was also a slight descending profile of deposition after 8 hours of UF for both PALL and SYNDER membranes. Although both were fouled, SYNDER was fouled more severely than PALL membrane from measured flux after fouling. The finding was supported by the total protein deposition measured by the Lowry method.

There was a random deposition of BSA and βLg along the membrane when performing the Lowry method to analyse deposition of the two protein species. Also, after 4 and 8 hours of UF using PALL membranes, there was a higher deposition of protein at the entrance of the channel due to initial deposition and accumulation and the amount gradually decreases along the channel.

1D SDS-PAGE of membranes fouled under same conditions (0.1wt% equimolar BSA and βLg, pH 4, 4 hrs, 500mL.min^{-1}, PALL and SYNDER) also shows randomness in the deposition of proteins along the membrane. However, βLg was found to be dominant over BSA in terms of mass for both membranes (Figure 4.13 and 4.14). The findings were similar

to past studies that found the exchange and displacement of proteins occurring on solid surfaces and membranes due to differences in structural stability.

When we compare the Lowry method results (Figures 4.9 and 4.11) and 1D SDS-PAGE results of PALL membrane (Figures 4.13 and 4.14) (0.1wt% equimolar BSA and βLg each, pH 4, 4 and 8 hrs, 500mL.min^{-1}, PALL), we can observe that the longer the duration of fouling resulted in greater deposition in the entrance section of the membrane rig. This was due to initial deposition and accumulation of the proteins at the entrance region.

MALDI-MS showed that the deposition on the top layer of SYNDER membrane was mainly βLg (Appendix B, Section 2.3). MALDI-MS interprets the surface deposition while 1D SDS-PAGE characterizes the total deposit on the membrane surface. The finding is possible as the BSA and βLg deposited itself on the membrane in a "sheet-like" manner. The finding is similar to 1D SDS-PAGE for 8 hours of UF on PALL membranes which shows that βLg is the dominant foulant. In addition, 1D SDS-PAGE showed βLg is identified as the dominant foulant in PALL and SYNDER after 8 hours of UF.

In conclusion, the deposition of proteins on membrane surfaces depends highly in the structural stability, hydrodynamics and fouling duration. The shear stress and turbulence induced by the spacer was found to influence the deposition characteristics of total proteins on the membranes. The uneven membrane and random aggregate formation on the surface seems to cause the random deposition profile of BSA and βLg along the surface. However, the total protein deposition was smoother compared to individual protein species deposition. The current settings of UF (0.1wt% equimolar BSA and βLg, pH 4, 4 hrs, 500mlmin^{-1}, PALL and SYNDER) can irreversibly foul the membrane that is an important requirement for cleaning studies to be performed in the following chapter.

Chapter 5: Cleaning of Ultrafiltration Membrane Fouled with Whey Protein Solutions

5. Introduction

Protein fouling of membranes in food processing is an inevitable phenomena and it results in significant flux and performance reduction and it requires chemical or enzymatic cleaning and disinfection to restore membrane performance, productivity and selectivity. Cleaning if poorly performed in dairy industry can be a costly procedure that consumes time, energy, chemicals and water. Therefore, it's crucial that cleaning is efficient, easy and rapid with minimum risk to the environment and installation, while simultaneously meet sanitary standards (Changani et al., 1997; D' Souza and Mawson, 2005; Fryer et al., 2006). The most commonly used cleaning agents in industry are caustics, acids, enzymes, surface-active agents, formulated cleaning agents, combined cleaning and disinfecting agents, and disinfectants (Ghosh, 2003). Cleaning-In-Place (CIP) method is commonly used in the food industries where the fouling is severe and daily cleaning is often a requirement (Romney, 1990; Bird and Bartlett, 1995; Gillham et al., 1999). Membrane cleaning processes are described by a couple of reviews and they are comparable to general cleaning in food processing (Zeman and Zydney, 1996; D' Souza and Mawson, 2005).

While cleaning can be effective in some circumstances, cleaning cannot restore membrane performance to its original, leaving behind irreversible foulant residuals which slowly degrade the membrane flux. Understanding the characteristics of the residual deposits on the membrane after fouling and cleaning is important for optimizing operation and cleaning process. The current investigation focuses on characterization of those residuals that cause continuous reduction in flux after successive cleaning and fouling as observed from the majority of previous cleaning studies. From this study, we seek to better understand cleaning mechanism and effects of residuals while identifying the reasons for incomplete cleaning at some cleaning conditions.

5.1. Materials and methods

5.1.1. Whey protein foulants

In this study, 30kDa Molecular Weight Cut-Off (MWCO) Polyethersulphone (PES) Ultrafiltration (UF) membranes provided by Pall Australia were fouled with either 0.1wt% Whey Protein Isolate (WPI) or binary 0.1wt% equimolar Bovine Serum Albumin (BSA) and Beta Lactoglobulin (βLg) solutions. BSA was purchased from Moregate Biotech, Australia while βLg, was purchased from Sigma Aldrich, Australia. The filtration operating conditions when using 0.1wt% WPI as feed foulants was either pH 6 (HCl added) or pH 7.5, constant pressure cross-flow UF at 50kPa and 100kPa for 4 hours with WPI feed solute on and permeate recycled during the experiment. On the other hand, when utilizing binary BSA and βLg as the feed in UF, the pH was set at 4 while the other conditions were similar with using WPI feed. βLg, a whey protein, is selected as the feed as it was identified as the main protein foulant deposits on the equipment in milk processing and often used as a model protein in food and dairy studies (Burton, 1968; Changani et al., 1997; Hoffmann and Van Mil, 1997; Hoffmann and Van Mil, 1999; Mercade-Prieto et al., 2007).

5.1.2. Cleaning agents

The chemical agents used to clean the WPI fouled membranes are enzyme Protease M Amano, NaOH and HCl. In food industries, NaOH is commonly used in two-stage cleaning techniques usually followed with nitric acid (HNO_3) or phosphoric acid or as an ingredient in formulated detergents (Timperley and Smeulders, 1987). NaOH swells protein deposits and gels, forming a protein matrix of high void fraction (Jeurnik and Brinkman, 1994; Mercade-Prieto et al., 2008). Previous studies also reported that dilute HCl (0.1% – 0.5%) to be effective in removing proteins like 0.1% BSA and 1% whey from UF membranes and improved flux (Kim et al., 1993; Madaeni and Sharifnia, 2000). In the dairy industries, HCl is mainly used in cleaning scale compounds and metals oxides in the foulant deposits. In addition, HCl also dissolve precipitates formed during cleaning procedure and is usually used in sequential

cleaning following alkaline cleaning i.e. in CIP. While long term exposure to chlorine ions could degrade PES membranes, the experimental work conducted in this study is normally short period of time and the membrane degradation would not have been manifested. Various concentrations and cleaning durations were applied during this study, as indicated in the sections of this chapter. The HCl, NaOH and enzyme were purchased from Sigma-Aldrich Australia. Enzymatic cleaning was performed at pH 7.5 and 30°C, the recommended optimum cleaning condition by the enzyme manufacturer.

5.1.3. Mathematical equations

Milli-Q fluxes (J) were measured throughout the experiments to measure the extent of fouling and efficiency of protein removal by the cleaning agents. Equations (5.1) and (5.2) were used to measure cleaning efficiency and solute resistance removal.

$$Cleaning\ Efficiency\ (\%) = {}^{J_{wc}}/_{J_{wi}} \times 100 \qquad (5.1)$$

Cleaning efficiency is also labelled as Flux Recovery (%),

$$Solute\ Resistance\ Removal\ (\%) = {}^{(R_{SW} - R_{SC})}/_{R_{SW}} \qquad (5.2)$$

where,

J_{wc} is Milli-Q flux after chemical or enzymatic cleaning

J_{wi} is Milli-Q flux before cleaning (Virgin membrane)

R_{SW} is the membrane resistance after Milli-Q rinsing following fouling

R_{SC} is the membrane resistance after chemical or enzymatic cleaning

For multiple fouling and cleaning cycles,

Equation (3) is Flux recovery increment, FRI_i for sequential cleaning

$$Flux\ Recovery\ Increment, FRI_i\ (\%) = {(J_i - J_{i-1})}/{(J_w - J_F)} \times 100 \qquad (5.3)$$

where,

J is Milli-Q flux

i = 1, 2, 3 represent stages i.e. Milli-Q rinsing, NaOH cleaning and HCl cleaning respectively

J_w is the Milli-Q flux before cleaning

For multiple cycles, $J_W = J_3$

J_F is the Milli-Q flux after fouling

Equation (4) is Total Flux Recovery, FR, at the end of each cycle of sequential cleaning

$$FR = FRI_1 + FRI_2 + FRI_3 \qquad (5.4)$$

The methods and protocols of fouling and cleaning were discussed in greater detail in Sections 3.5.1 and 3.5.2 of Chapter 3.

5.1.4. Experiments

The current study consists of fouling and cleaning experiments under controlled conditions. The deposition of residual proteins and peptides on the membrane surface following UF and cleaning treatment were investigated. The experimental aims, methods and results are summarised in Table 5.1.

Table 5.1
Summary of experiments – Experiments, methods and results

Sections	Experiments	Methods	Results
• 5.2.1 – 5.2.3	• Analysis of the protein foulant feed solution and residues	• 1D SDS-PAGE	• Figure 5.1 – 5.3
• 5.2.4	• NaOH cleaning of BSA and βLg, and WPI fouled membrane	• 1D SDS-PAGE • Flux measurements	• Figure 5.4 – 5.5
• 5.2.5	• Residual deposition after NaOH and HCl cleaning	• 1D SDS-PAGE	• Figure 5.6 – 5.7
• 5.4.4	• Sequential cleaning of WPI fouled membranes	• Flux measurements • Lowry method • 1D SDS-PAGE	• Figure 5.8 – 5.21
• 5.4.5	• Enzyme cleaning of BSA and βLg fouled membrane	• Flux measurements • Lowry method • 1D SDS-PAGE	• Figure 5.22 – 5.26
• Appendix C	• FESEM study of fouled and cleaned membranes	• Critical drying and FESEM	–

5.2. Results and discussion

5.2.1. Characterization of whey protein solutions

Whey protein isolate and 0.1wt% equimolar BSA and βLg proteins were characterized using 1D SDS-PAGE and the gel scans are shown in Figure 5.1. The figure consist of Lane A (10μg WPI) and Lane B (0.1wt% equimolar BSA and βLg i.e. 7.87μg BSA and 2.13μg βLg). In Lane A, the size and intensity of the bands shows that βLg makes up the greatest amount of protein available in the WPI solution, followed by Glycomacropeptide (GMP) and BSA. It is expected that Immunoglobulin (Ig), BSA and Lactoferrin which makes up of 7% of the total protein isolates, can be easily retained on the 30kDa MWCO polyethersulphone membrane. On the other hand, the molecular weight of βLg and Alpha Lactalbumin (αLa), which makes up a total of 56.2% of the total proteins, was smaller than the molecular weight cut off of the membrane. Proteins of molecular weights smaller than 30kDa could contribute to internal fouling of the membranes and not easily removed by cleaning agents. In lane B, BSA was present in larger quantity compared to βLg, however in terms of molar units, BSA was equal to βLg, and therefore the size and intensity of both bands appears the same. In both Lane A and B, there were presence of smaller peptides and amino acids however they were not easily identified using 1D SDS-PAGE.

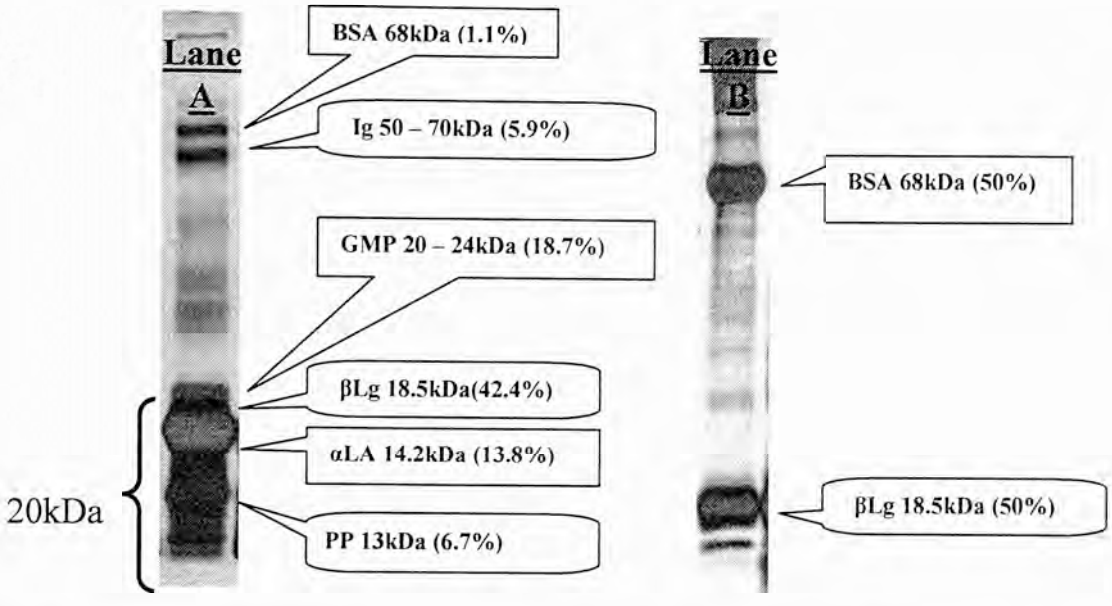

Figure 5.1 1D SDS-PAGE gel scans. (Lane A) 10μg of fresh WPI and (Lane B) 10μg of fresh equimolar BSA and βLg. The molecular masses (kDa) and mass percentages (%) are also shown.

5.2.2. Whey protein isolate deposition on the membrane surface

Figure 5.2 consists of Lane I (Feed solution before UF), Lane II (WPI deposited on membrane) and Lane III (Feed recycle solution). The UF conditions shown in Lane II are 4 hours cross-flow, 50kPa TMP, 0.1wt% WPI, pH 6, 500mL.min^{-1}.

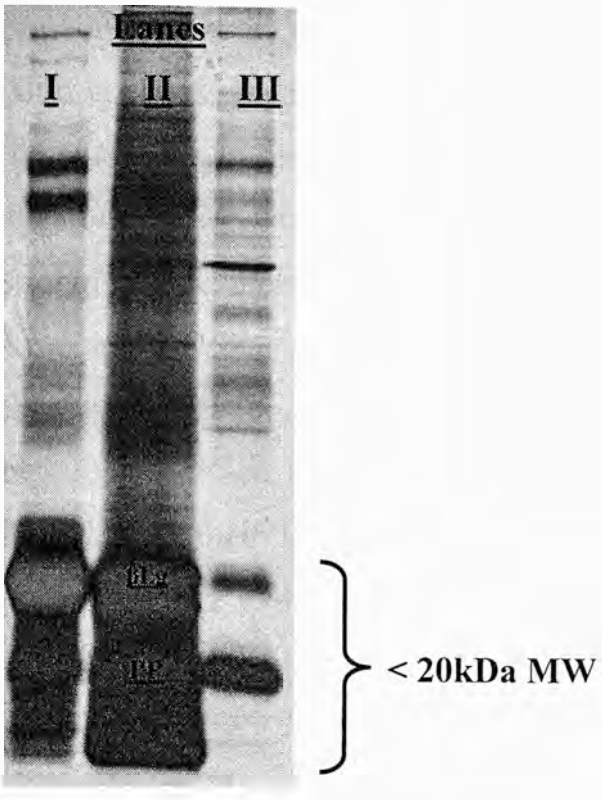

Figure 5.2 1D SDS-PAGE gel scans of various feeds. (Lane I) WPI feed solution, (Lane II) Adsorbed WPI on membrane (Lane III) Feed-recycle solution. (Fouling conditions: 4 hours of cross-flow UF, 50kPa TMP, 0.1wt% WPI, pH 6, and 500mL.min^{-1})

In Figure 5.2, WPI eluted from the membrane surface (Lane II) is different from the feed solution (Lane I) as more peptide bands appeared in the foulant after filtration. Unknown peptides, fragmentations from the original WPI were introduced in Lane II. These artifacts originate from the denaturizing protein desorption processes that uses SDS and Mercaptoethanol to extract the deposited proteins from the membrane surface when performing 1D SDS-PAGE. The extraction process involves dissecting dried and fouled membranes followed by soaking and ultra-sonicating the dissections in boiling solution to dissolve the proteins (Discussed in Chapter 3). In addition, these proteins are residuals from the denaturation of the WPI on the surface caused by flow and shear force.

In Figure 5.2, most of the peptides in Lane II (Adsorbed WPI) were under 20kDa MW. αLa and βLg did not change significantly during the UF and denaturizing protein desorption process due to its high stability in solution (Bos et al., 1994). βLg is the dominant whey

protein foulant in dairy processing especially in the heat exchangers of milk processing (Burton, 1968; Fryer et al., 2006). Analogous to this knowledge, the same was happening to βLg on the membrane surface. As a globular protein, and at pH 4, where the membrane is negatively charged while βLg molecules are positively charged, the molecules absorbs strongly on the membrane surface. Upon denaturation, βLg molecules congregates and forms a structurally strong deposit on the hydophobic membrane surface. Shear stresses caused by flow and filtration may not be able to break the hard deposit that forms directly on the membrane surface. On the other hand, BSA deposition on the membrane was less compared to βLg due to their larger molecular size as well as being structurally soft and weaker in attraction to the hydrophobic surface (Bos et al., 1994).

In Lane III (Feed-recycle solution), there were less bands of proteins and peptides detected compared to the fouled membrane surface Lane II (Adsorbed WPI). Thus, most of the proteins are strongly bonded to the membrane surface. Lanes I and III were also different in profile, as most of the proteins have transferred to the membrane surface.

No proteins were detected in the permeate stream after 4 hours of continuous UF indicating total rejection. Negligible absorbance from UV-Vis measurements of permeate solutions at 280nm confirms that no proteins have passed through the membrane during UF of BSA and βLg (Discussed in Chapter 4).

5.2.3. Binary protein deposition on the membrane surface

Figure 5.3 shows the deposition of equimolar 0.1wt% BSA and βLg mixture along the horizontal membrane surface after 4 hours UF (d – h lanes in the left photo image) and 8 hours UF (di – hi lanes in the right photo image). The depositions were similar for both duration of UF and unknown peptides were observed in the sections (d – h) and (di – hi) along the membrane surface along with the known BSA (70kDa) and βLg (18 kDa). The unknown peptides appeared consistent in both images of 4 and 8 hours filtration durations. By visualizing the intensity of the bands after 8 hours of UF seems to be stronger than after 4

hours of UF, showing higher deposition with longer duration of UF. These unknown peptides was also observed when performing MALDI-MS to analyze the top-layer deposition on the membrane later identified as protein-based fragmentations (Chan et al., 2002; Chen et al., 2007).

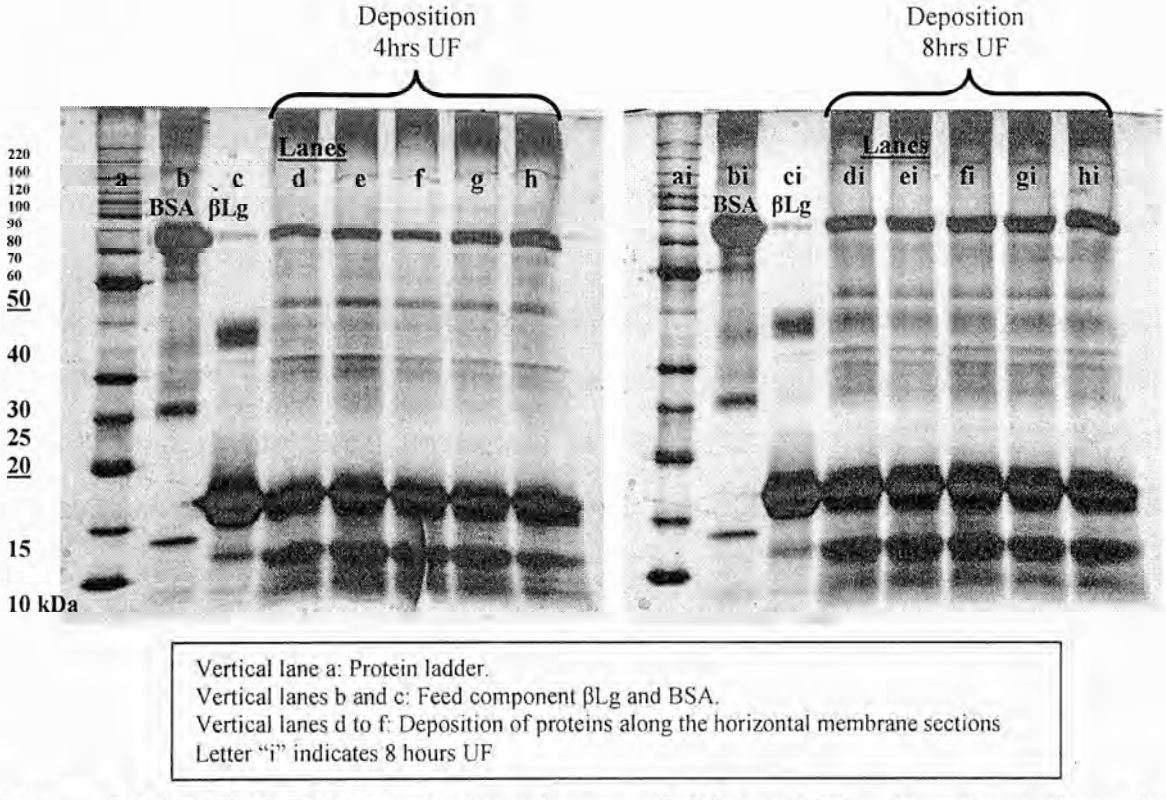

Figure 5.3 1D SDS-PAGE gel photo image of BSA and βLg deposition along the membrane surface after 4 hours of UF duration (Left photo) and 8 hours UF duration (Right photo) of UF with spacer present (Fouling conditions: 0.1wt% BSA and βLg, 50kPa, pH 4, Flow rate 500mLmin^{-1}).

In conclusion, the proteins extracted from the membrane surface underwent denaturation during the extraction process prior to 1D SDS-PAGE as shown in Figure 5.2 and 5.3. The unknown peptides are present in the region of less than 15kDa, and between 50kDa and 30kDa. Thus, complications may have been produced in procedure of 1D SDS-PAGE which caused changes to the original protein deposited on the membrane surface. Therefore,

measuring the relative masses of individual proteins based on intensities using 1D SDS-PAGE was not very sensitive.

5.2.4. NaOH cleaning of whey fouled membranes

NaOH is known to chemically attack protein deposits and increase the electrostatic repulsion between the foulants and membranes (Sayed Razavi et al., 1996). NaOH initiates hydrolysis of proteins by addition of extensive charge on few sites within the macromolecule, resulting in strong electrostatic repulsion between the molecules patches (Dee et al., 2002). An optimum concentration and temperature when the swelling of the protein deposit occurs were determined in the past (Bartlett et al., 1995).

In our current study, we have performed NaOH cleaning on both BSA and βLg binary mixture fouled or WPI fouled membranes. The experimental set-up and Milli-Q fluxes – Initial, fouling, and rinsing are summarised in Table 5.2. The cleaning results for binary fouled membranes are shown in Figures 5.4 while for WPI fouled membranes are shown in Figure 5.5.

Table 5.2
Cleaning study for NaOH cleaning for membranes fouled by WPI and equimolar binary protein solutions

Protein feed solution	Fouling set-up	Milli-Q Fluxes ($lm^{-1}hr^{-1}$)	Cleaning treatment	Diagrams
0.1wt% BSA and βLg	Flowrate = 500mL.min^{-1}, Spacer inserted in membrane channel, 50kPa, pH 4, 4 hours UF	J_{wi} = 248.50 J_{uf} = 36.89 J_{ww} = 45.41	0.1M NaOH cleaned, 15, 30, 60 and 120 min	Figure 5.4
0.1wt% WPI	Flowrate = 500mL.min^{-1}, No spacer, 100kPa, 0.1wt% WPI, pH 6, 4 hours UF	J_{wi} = 402.11 J_{uf} = 14.30 J_{ww} = 52.41	0.1M NaOH cleaned, 15, 30, 45 and 60 min	Figure 5.5

The results of cleaning efficiencies and solute resistance removal calculated using equations (5.1) and (5.2) are shown in Figure 5.4 and 5.5. The trends in Figure 5.4 clearly shows that "cleaning efficiency" results were not as sensitive to cleaning durations as "solute resistance removal" results. The cleaning efficiency was at a range of 43% to 48% while the solute resistance removal was at a range of 64% to 88%. The highest cleaning efficiency was achieved at 48% after 60 min of cleaning while the highest solute resistance removal was 88% after 30 min of cleaning for binary fouled membrane. Maximum protein removal occurred at 30 minutes corresponded to the swelling of BSA deposits that gave the highest voidage, where the protein matrix was easily fractured by shear. Beyond 30 minutes, the swelled protein deposits become difficult to remove.

In the past, much higher cleaning efficiencies was achieved in a similar study using whey protein concentrate as foulants due to the higher temperatures used during NaOH cleaning (Bartlett et al., 1995). Another study achieved only 10% gain in flux recovery over BSA fouled membranes (Kuzmenko et al., 2005). The reason for a low flux recovery was that NaOH was unable to remove large aggregates from the membrane surface. Most recently, a similar NaOH cleaning recovery of 50% was obtained for BSA fouled membranes (Field et al., 2008).

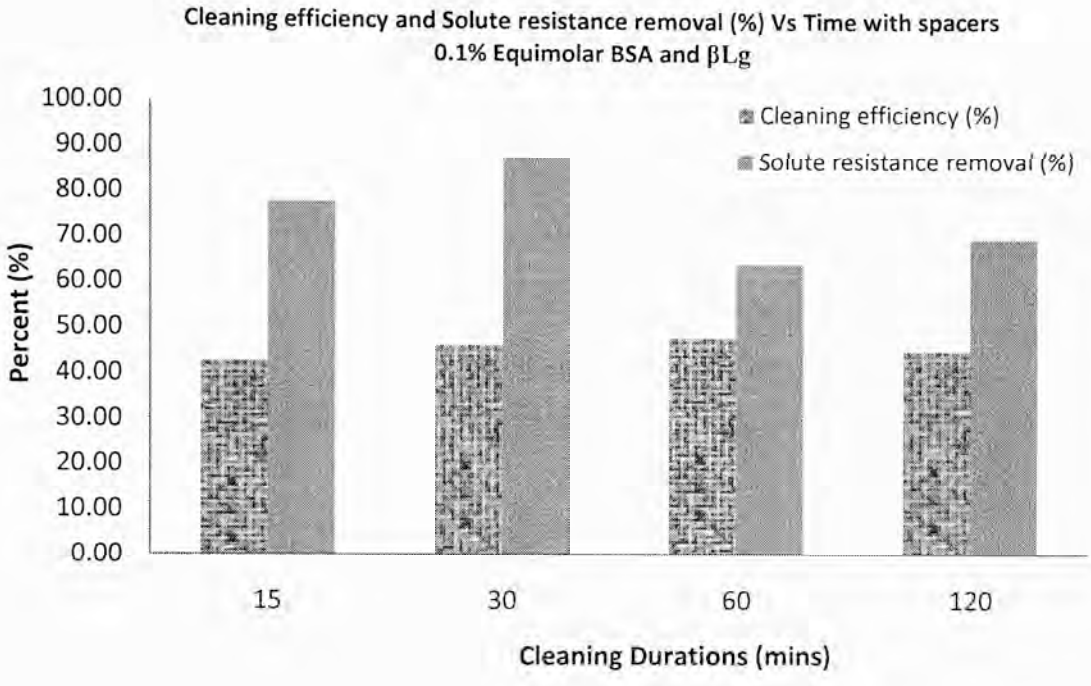

Figure 5.4 The solute resistance removal and flux recovery of NaOH cleaned membranes at various cleaning durations in a cross-flow set-up. (Fouling conditions: 0.1wt% equimolar BSA and βLg, 50kPa, 500mL.min^{-1}, pH 4, Cleaning conditions: 0.1M NaOH, flow rate 500 mL.min^{-1})

Figure 5.5 shows the NaOH cleaning results obtained from membranes fouled with WPI as feed solution. Once more, the cleaning efficiency results were not sensitive to cleaning durations as solute resistance removal results. The cleaning efficiency ranges from 28% to 33% while the solute resistance removal ranges from 57% to 75%. The highest solute resistance removal was 75% after 60 min of cleaning.

When comparing Figures 5.4 and 5.5, the cleaning efficiencies and resistance removal of WPI fouled membranes are generally lower than that for binary BSA and βLg fouled membranes. This was because of the multiple proteins present in the WPI which makes them harder to be removed by NaOH. In addition, longer duration of cleaning was also required for WPI compared to BSA and βLg mixture. Therefore, at 60 minutes the maximum voidage and fracturing of the gel matrix had occurred resulting to the highest flux recovery.

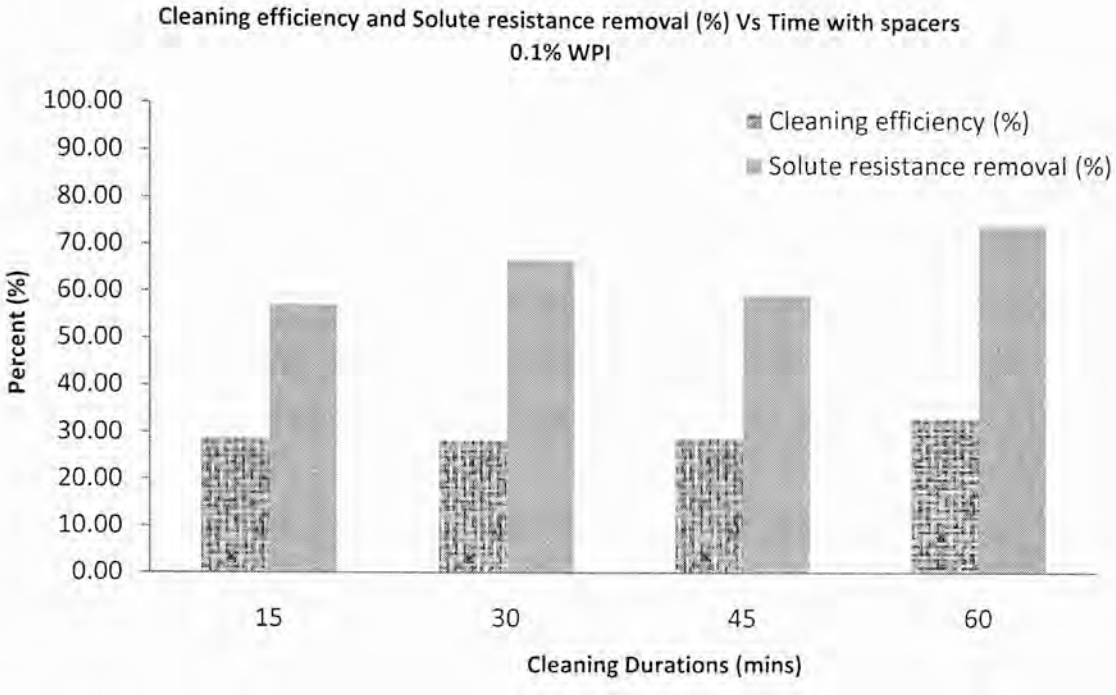

Figure 5.5 The solute resistance removal and flux recovery of NaOH cleaned membranes at various cleaning durations in a cross-flow set-up. (Fouling conditions: 0.1wt% WPI, 100kPa, 500mL.min^{-1}, pH 6. Cleaning conditions: 0.1M NaOH, flow-rate 500 mL.min^{-1})

Similar results of low flux recovery and high solute resistance were obtained in a past study performed for 0.1M NaOH cleaning for 0.1% BSA (Kim et al., 1993). A study also shows that NaOH may induced gelation of whey protein resulting in an increased resistance of the deposit to the alkali (Mercade-Prieto and Chen, 2005). Therefore, the gelation of the protein deposit may have reduced the effectiveness of removal by NaOH.

In a previous study using a stirred-cell set-up, a flux recovery of 60% flux recovery and 75% solute resistance removal was achieved after 60 min of cleaning (0.1M NaOH, 1gL^{-1} equimolar BSA and βLg, 100kDa MWCO polysulphone membrane) (Chen et al., 2006). In their case, NaOH was maybe able to remove the foulants more efficiently because of the larger pore size and the effective surface area of the stirred-cell is larger than the cross-flow set-up for the same concentration of cleaner. Similar to the cross-flow set-up, the flux was not recovered completely due to the residuals that were not removed from the surface after

cleaning. A later study by a colleague from our group using a stirred-cell set-up have achieved a higher flux recovery of 50% and a solute removal of 80% after 60 min of 0.1M NaOH cleaning (0.1 wt% WPI, 100kPa, pH 6, 400 rpm) (Wu, 2007).

In conclusion, NaOH was not able to recover membrane flux when used on its own. This is because NaOH was unable to remove irreversible foulants or fragments from the membrane surface effectively. In the following sections, we will investigate the use of sequential cleaning, NaOH followed by HCl, to recover the loss flux after fouling.

5.2.5. Protein residuals deposition after NaOH and HCl cleaning

The gel scans of protein residuals after 30 min (Lane i) and 60 min (Lane ii) of NaOH cleaning are shown in Figure 5.6. Comparing the bands in between 30min and 60min of cleaning, we can observe that after 60 min more protein bands have disappeared and they appear more diffused than after 30 min of cleaning. The absence of residuals resulted in the slightly higher flux recovery achieved after 60 min of NaOH cleaning of BSA and βLg fouled membranes in Figure 5.4. The longer the duration of cleaning (i.e. chemical contact between the protein deposit and NaOH) resulted in more proteins removed from the membrane.

- Membrane Fouled: 0.1wt% equimolar BSA and βLg, 100kPa, 500mLmin^{-1}, pH 4, 4 hours UF
- Membrane Cleaned: 0.1M NaOH, 500 mlmin^{-1} Lane (i): 30 min, Lane (ii): 1 hr,

< 20KDa MW

Figure 5.6 1D SDS-PAGE gel scans of (Lane i) 30min NaOH treated membrane and (Lane ii) 1 hour NaOH treated membrane (Fouling conditions: 0.1wt% equimolar BSA and βLg, 100kPa, Flow rate 500mL.min^{-1}, pH 4, 4 hours UF)

As concluded in Section 5.4.3.1 earlier, NaOH is not an effective cleaner when used by its own for protein fouled membranes. Therefore, a better solution would be the incorporation of mixed cleaners that targets the lower molecular weight residues. The combined effects of sequential cleaning with NaOH and HCl were studied in Section 5.4.4 to observe its effectiveness in comparison to single NaOH cleaning.

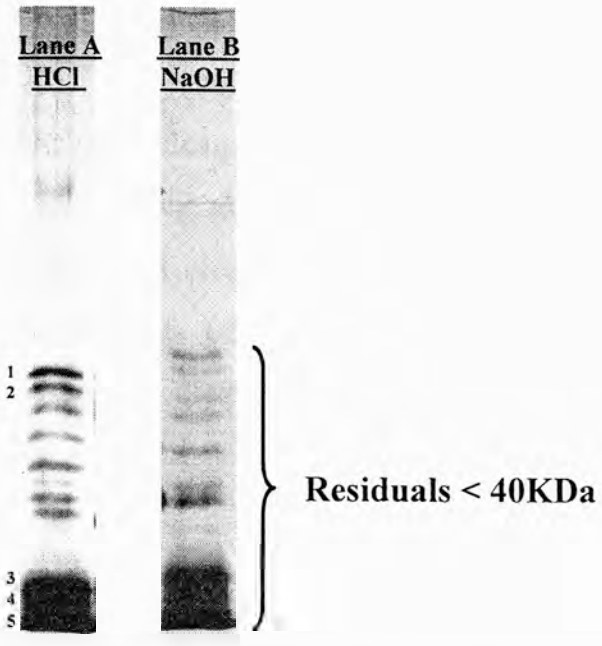

Figure 5.7 The residuals identified after HCl (Lane A) and NaOH (Lane B) cleaned membranes at various cleaning durations in a dead-end stirred cell set-up. (Fouling conditions: 0.1 wt% WPI, 100kPa, pH 6, 400 rpm Cleaning conditions: 0.1M NaOH, 400 rpm)

Figure 5.7 shows the 1D SDS-PAGE of protein residuals after HCl and NaOH cleaning in a stirred-cell set-up. The cleaning and fouling experiment was performed by a colleague (Wu, 2007). Residuals of molecular masses < 40kDa was found deposited (Figure 5.7, Lanes A and B). These bands are residuals originating from the cleaving of WPI on the membrane surface.

Trypsin in-gel digestion followed by mass spectrometry (LC-MS) was performed on the residuals (Bands 1 – 5 in Figure 5.7) to identify the unknown protein bands. The results showed that Beta Casein (gi|115660) of mass 25.13kDa was the protein detected in Bands 1 to 5 (indicated left of Lane A, Figure 5.7). Beta Casein A2 variant (gi|248147) of mass 5.11kDa was also detected in Band 1, while Beta Casein (gi|1366102) of mass 16.44kDa was detected in Band 5. Thus Beta Casein was the protein found in the WPI that was not easily removed by HCl and NaOH at 0.1M.

5.2.6. HCl and NaOH sequential cleaning of whey fouled membranes

The prior cleaning studies in Section 5.4.2 and 5.4.3 showed that single NaOH or HCl cleaners were unable to recover flux completely after cleaning. Therefore an investigation using a constituted cleaning agent was performed on the fouled membranes. The summary of the experiments on sequential cleaning are shown in Table 5.3. The selected conditions for sequential cleaning is 30 min 0.1wt% NaOH cleaning followed by 15min 0.1wt% HCl cleaning.

Table 5.3
Sequential Cleaning study

No.	Experimental setup
1	WPI fouling for 2 hours (30°C, 50kPa, 500 mL.min^{-1})
2	WPI fouling (2 hours) + MQW rinsing (15min)
3	WPI fouling + MQW rinsing + NaOH treatment (15 min)
4	WPI fouling + MQW rinsing + NaOH (30 min) + HCl (15 min)
5	WPI fouling + MQW rinsing + NaOH (30min) + HCl (15 min) at 50°C
6	WPI fouling for 6 hours
7	WPI fouling (6 hours) + MQW rinsing + NaOH + HCl
8	4 cycles (6 hrs WPI fouling + MQW rinsing + NaOH + HCl)

During HCl and NaOH sequential cleaning, the Milli-Q fluxes were measured after WPI fouling, Milli-Q rinsing, HCl cleaning and NaOH cleaning and the results are shown in Figure 5.8. The fouling and cleaning conditions are shown in Table 5.3, Experiment 4. The Milli-Q flux gradually increases following rinsing and cleaning. The flux increases by 4.6% after rinsing (FRI_1), 35% after NaOH cleaning (FRI_2) and 11% after HCl cleaning (FRI_3).

Rinsing with Milli-Q water removes the loose proteins from the membrane surface and the equipment through shear flow resulting to a rinsing efficiency of 23% (J_{WF}/J_{WI}%). In the past, Kuzmenko et al. (2005) achieved 5% flux recovery from rinsing alone of BSA fouled membranes which was much smaller. Cleaning with NaOH resulted in a flux recovery of about 50% and cleaning with HCl resulted in a total flux recovery of 52%.

The flux recovery results are shown in Figure 5.9 (2 hours WPI fouled). The total flux recovery (*FR*) was 52% after the whole rinsing and cleaning process. The flux was not recovered totally after sequential cleaning however HCl adds 11% to the total flux recovery. Although the flux recovery after the introduction of HCl after NaOH cleaning was marginal, it was effective in improving the flux. HCl was able to solubilise the large protein fragments that were not removed during NaOH cleaning resulting in more flux recovery.

In the past, it was found that sequential cleaning did not make much difference to the final flux (Bartlett et al., 1995). Interestingly, in a past study, it was found that sequential cleaning reversed, HCl followed by NaOH achieved the highest resistance removal for BSA fouled membranes (Kim et al., 1993).

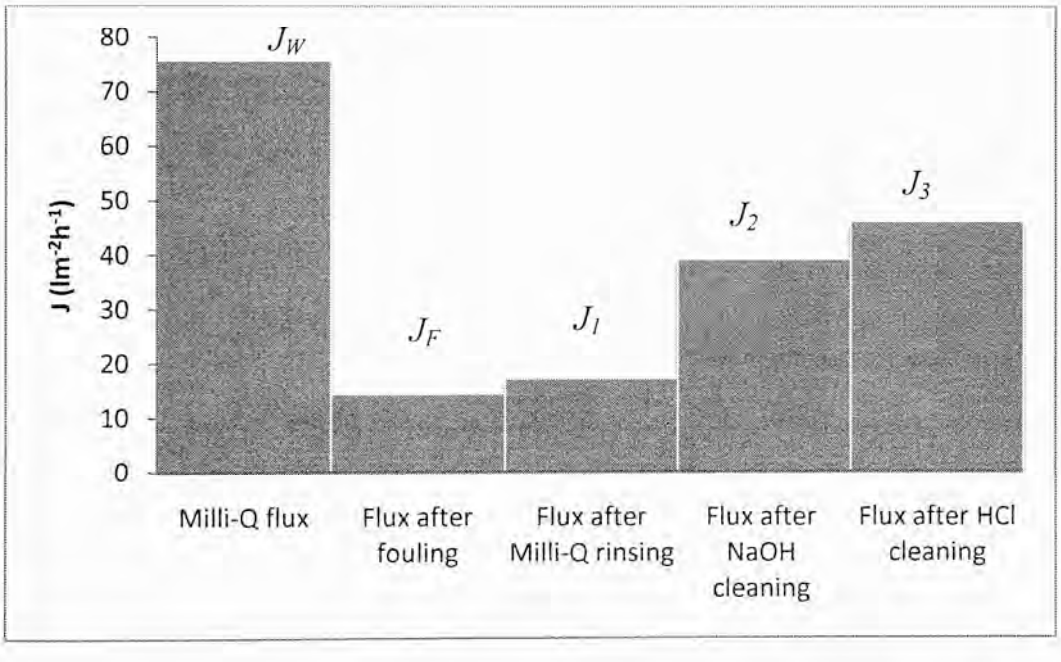

Figure 5.8 The measured Milli-Q flux of sequential cleaning of WPI fouled membrane. (Fouling conditions: 1wt% WPI, 2 hours, 100kPa, 500mL.min^{-1}. Cleaning conditions: 0.1% NaOH (30 min) + 0.1% HCl (15 min), flow-rate 500 mL.min^{-1})

The effect of WPI fouling durations (2 and 6 hours UF) on flux recovery increments after sequential HCl and NaOH cleaning was investigated and the results are shown in Figure 5.9. The total flux recovery for 6 hours fouling is slightly less than 2 hour fouling by 5.4%. The

lower total flux recovery for 6 hours fouling (FR = 46.5%) compared to 2 hours (FR = 51.9%) fouling indicates that there were more irreversible residuals not removed after sequential cleaning. One crucial observation is the decrease in NaOH cleaning recovery (FRI_2) and increase in HCl cleaning recovery for 6 hours fouling (FRI_3). Therefore, HCl is more effective in recovering the flux for longer fouling duration. The corrosive effect of HCl helps to solubilize and remove the leftover foulants after NaOH cleaning. The flux recovery after sequential NaOH (30min) and HCl (15 min) cleaning was 18% higher than single 0.1%NaOH (60min) cleaning in Figure 5.5.

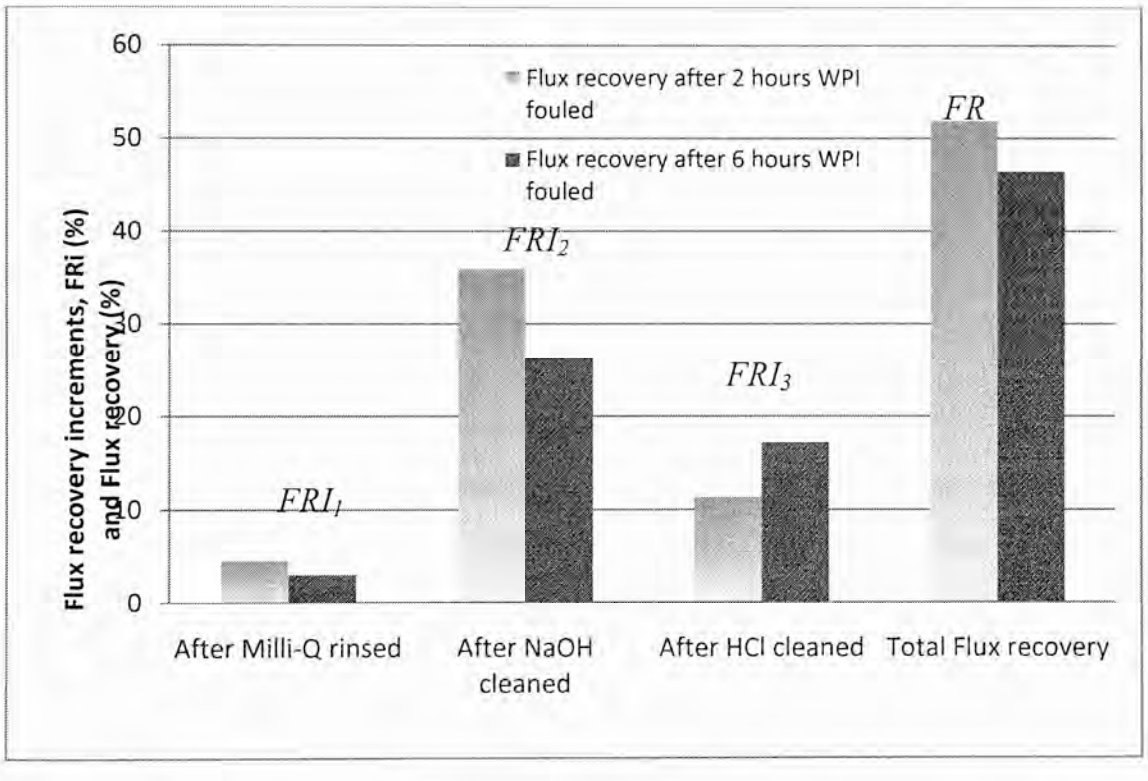

Figure 5.9 The flux recovery increment (FRI_i)) and flux recovery (FR) of sequential cleaning of 2 hours and 6 hours WPI fouled membrane. (Fouling conditions: 1wt% WPI, 100kPa, 500mL.min^{-1}; cleaning conditions: 0.1% NaOH (30 min) + 0.1% HCl (15 min), flow-rate 500 mL.min^{-1})

Flux recovery increments and flux recovery of sequential cleaning at 30°C and 50°C is shown in Figure 5.10. The flux recovery increments were higher for both NaOH and HCl cleaning at

50°C compared to 30°C. This was because temperature helps to improve protein solubilisation and removal during the cleaning process.

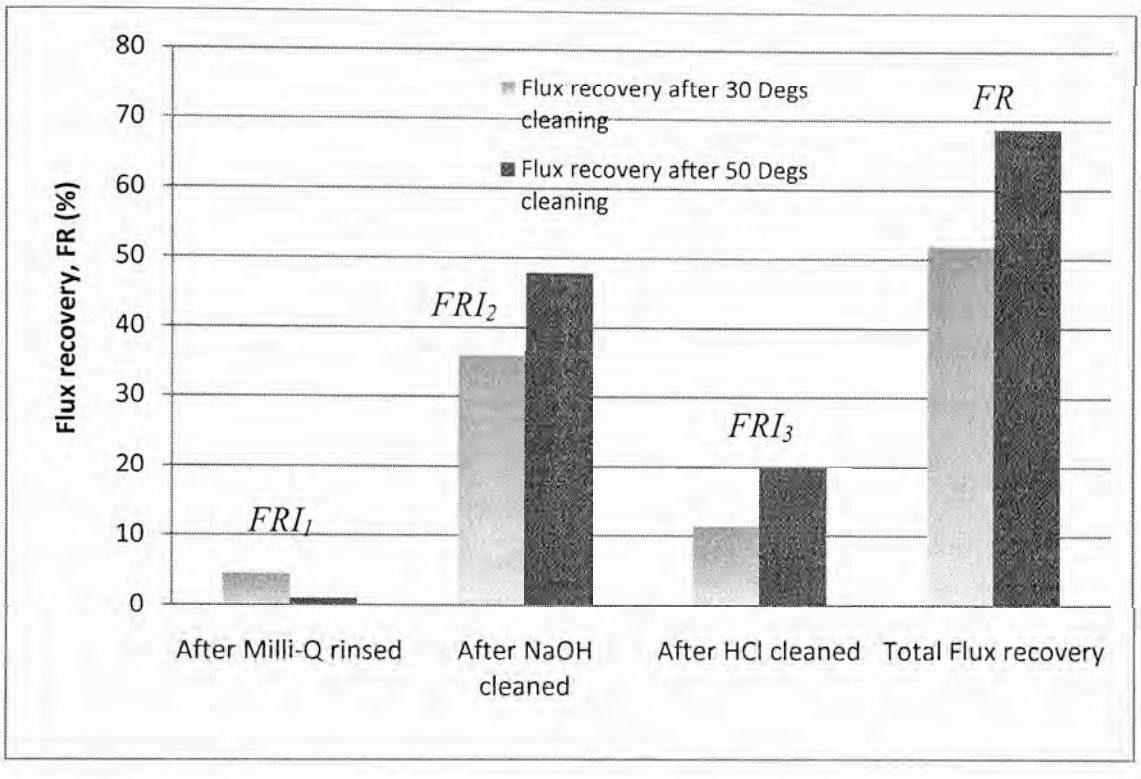

Figure 5.10 The flux recovery increment (FRI_i)) and flux recovery (FR) of sequential cleaning at 30°C and 50°C. (Fouling conditions: 1wt% WPI, 100kPa, 500mL.min^{-1}; cleaning conditions: 0.1% NaOH (30 min) + 0.1% HCl (15 min), flow-rate 500 mL.min^{-1})

The effect of repeated fouling and sequential cleaning cycles (4 cycles) to the final flux and flux recoveries during rinsing, NaOH cleaning and HCl cleaning are investigated. The flux (J_i) and flux recovery (FRI_i and FR) results at each of the cycles are shown in Figure 5.11 and 5.12 respectively. The flux after fouling and rinsing decreases very gradually after each successive cycle. However, the flux decreases significantly after each cycle. Figure 5.12 shows that the flux recovery increment after NaOH cleaning remained stable for 2nd, 3rd and 4th cycle (Average FRI_i = 52.7%). However, the flux recovery after HCl cleaning increases after 1st – 4th cycle (FRI_3, Figure 5.12). This shows that HCl is more effective in the recovering the flux for longer duration of fouling, which was also observed in Figure 5.9 for 6 hours fouling duration.

The total flux recovery also increases to a maximum of 89% after the 4th cycle (*FR*, Figure 5.11).

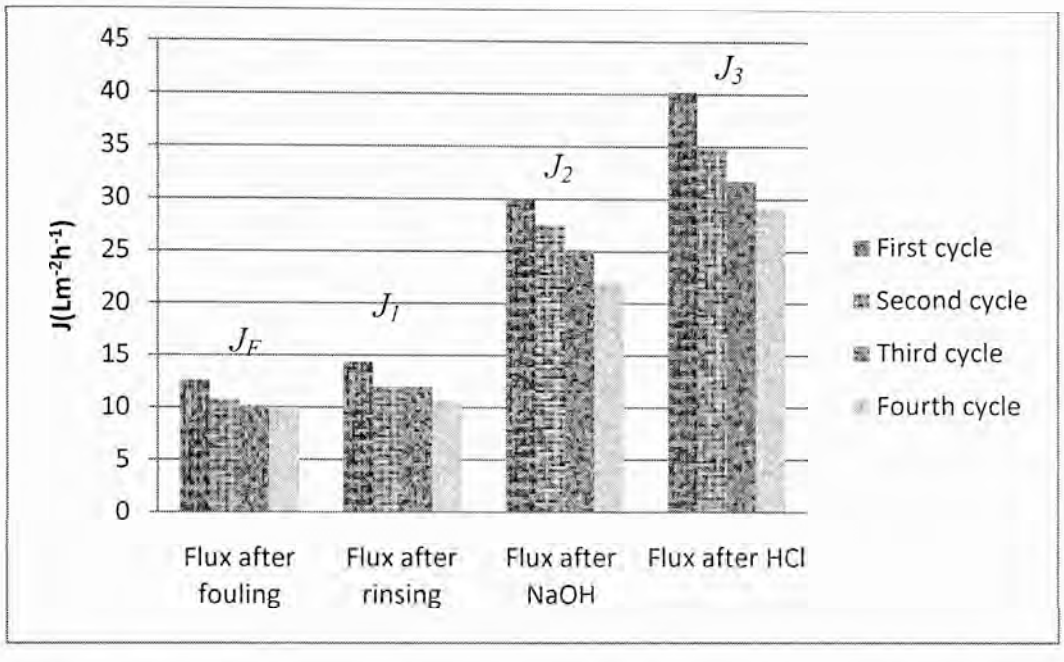

Figure 5.11 The measured Milli-Q flux of four repeated cycles of fouling and sequential cleaning (Fouling conditions: 1wt% WPI, 6 hours, 100kPa, 500mL.min^{-1}. Cleaning conditions: 0.1% NaOH (30 min) + 0.1% HCl (15 min), flow-rate 500 mL.min^{-1})

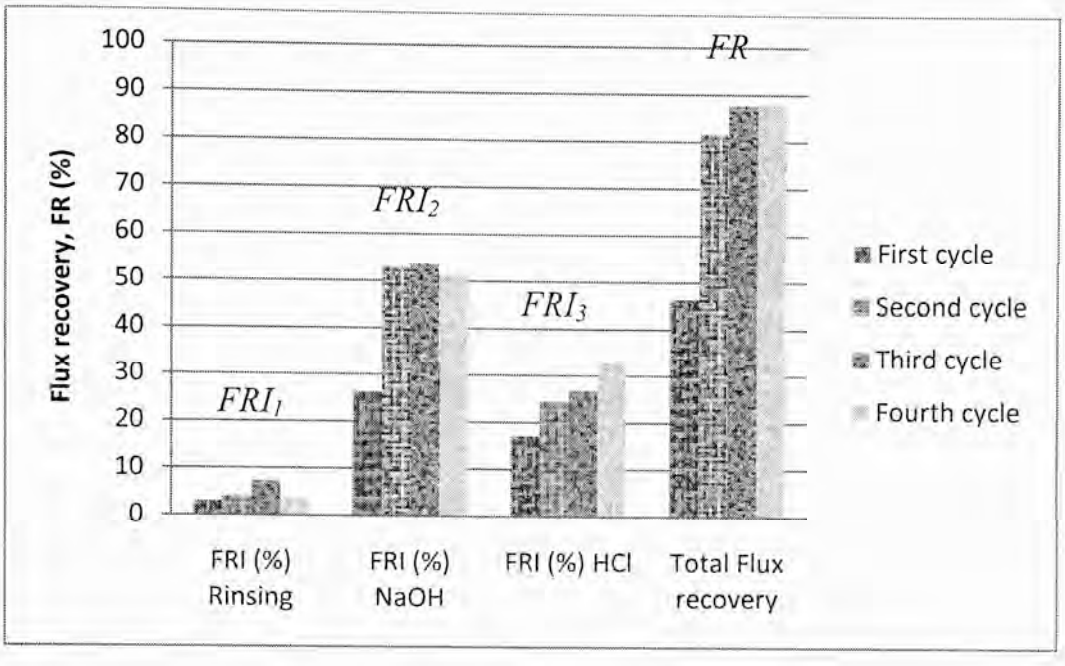

Figure 5.12 The flux recovery increment (FRI_i)) and flux recovery (FR) of four repeated cycles of fouling and sequential cleaning. (Fouling conditions: 1wt% WPI, 6 hours, 100kPa, 500mL.min^{-1}; cleaning conditions: 0.1% NaOH (30 min) + 0.1% HCl (15 min), flow-rate 500 mL.min^{-1})

The total quantity of proteins and residuals measured by the Lowry method after fouling, rinsing and cleaning under the various experimental set-ups (Table 5.3 (Experiment 1 – 8)), are shown in Figure 5.13 (Bar chart 1 – 8). 6 hours WPI fouling (Bar 6) resulted in a 50% increase in the amount of protein deposition in the membrane when compared to 2 hours fouling (Bar 1). Milli-Q rinsing reduces the deposition after 2 hours fouling by 9% (Bar 2). NaOH cleaning (Bar 3) and sequential cleaning (Bar 4) reduced the deposition by 55% and 50% respectively. Thus, sequential cleaning did not further improve the removal of the deposited proteins however the flux was improved as shown in Figure 5.8. The amount of protein deposited after sequential cleaning is 6% more than single NaOH cleaning. The reason for a lower residual removal may be due to re-deposition of residuals to the surface after sequential cleaning. HCl cleaning may create a more open layer of deposit resulting in a higher flux recovery. Sequential cleaning at 50°C (Bar 5) did not remove the protein as effectively as NaOH cleaning (Bar 3) and sequential cleaning at 30°C (Bar 4). Sequential

cleaning after 6 hours of fouling (Bar 7) has a higher amount of residual than 2 hours fouling (Bar 4). However the reduction of deposit from 6 hours fouling to cleaning (Bar 6 and 7) was higher than 2 hours fouling and cleaning (Bar 1 and Bar 4) i.e. 53% for 6 hours and 50% for 2 hours of fouling and cleaning. 4 cycles of repeated fouling and cleaning (Bar 8) resulted in a higher deposition compared to 1 cycle of fouling and cleaning (Bar 7). This shows that the irreversible residuals layers increases as the cycle increases. However, the increased in residuals did not affect the flux as the flux recovery (FRI_i and FR) improves with the cycles as shown in Figure 5.12.

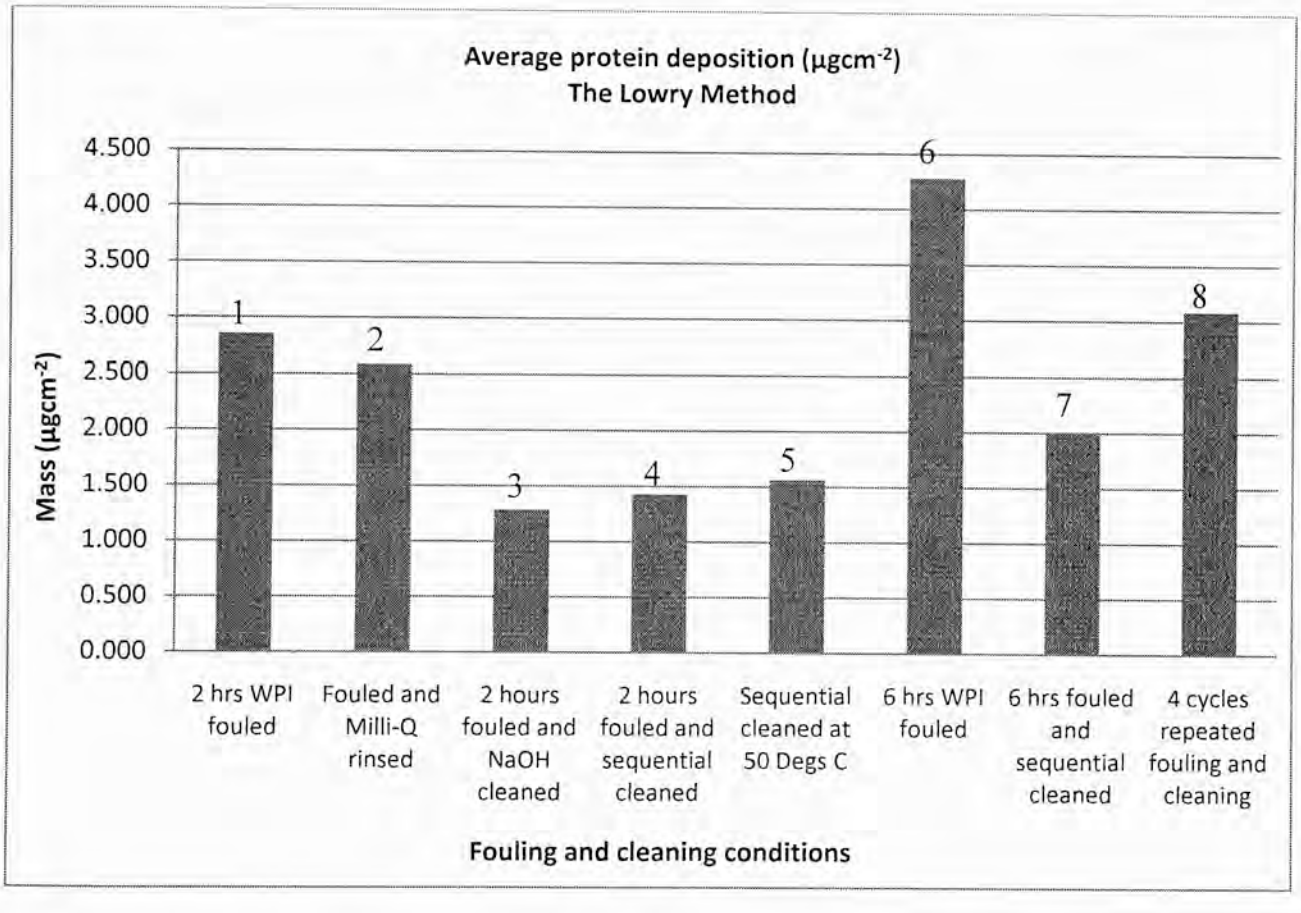

Figure 5.13 The average protein deposition on the membrane after different treatment quantified by Lowry method (Fouling conditions: 1 wt% WPI, 4 hours UF, 50kPa, 500mL.min^{-1}. Cleaning solutions: HCl (15 min) and NaOH (30 min). The numbers indicate the experimental set-ups as described in Table 5.3.

The horizontal distribution of proteins along the membrane surface after fouling was investigated using Lowry method and the results are shown in Figure 5.14. It can be adsorbed that more protein was deposited after 6 hours of fouling. The deposition profile was stable along the horizontal surface for 2 hours fouling however the amount of deposition was higher at the centre of the cross-flow rig which was also observed in past studies (Chan et al., 2002). For total protein amount on the membrane evaluation, the whole length of membrane sections (indicated in Fig. 3.16) was being dissected and soaked into solution C of the Lowry method. The main error could originate from the UV Spectroscopy measurements at 650nm. At the moment, the standard errors are less than 0.01 for each section.

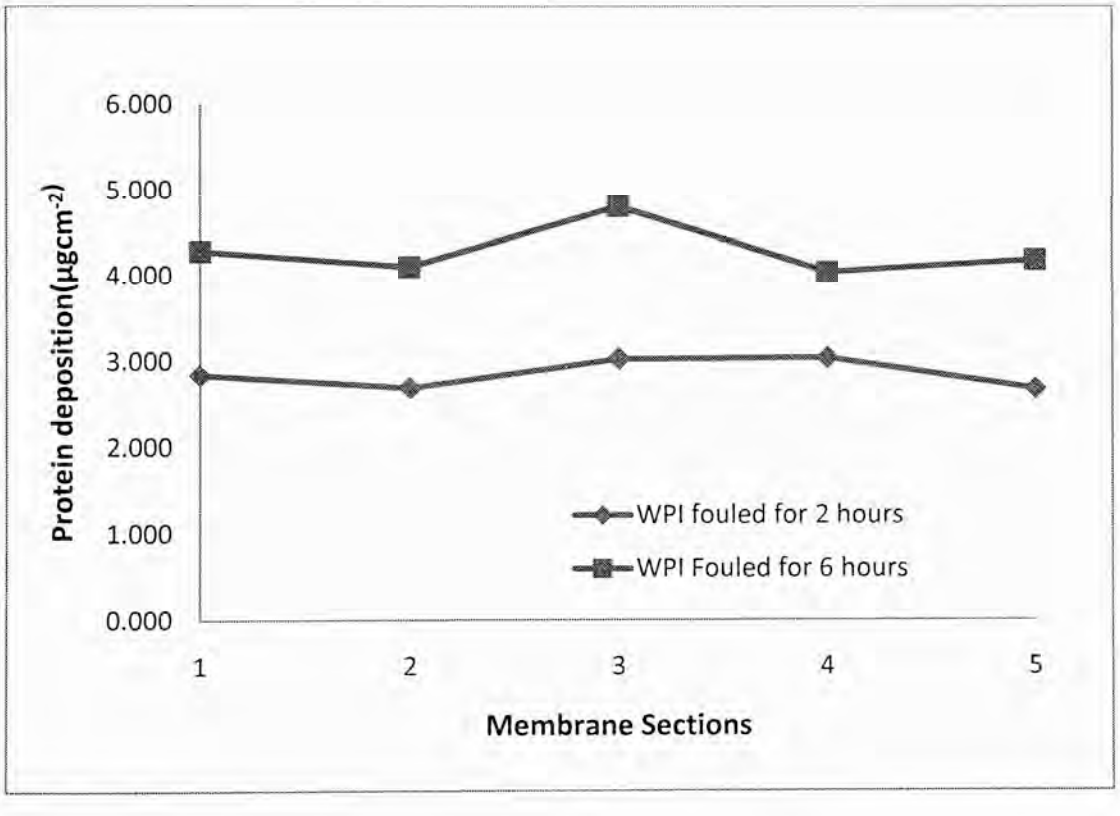

Figure 5.14 WPI deposition after 2 and 6 hours fouling durations (Fouling conditions: 1 wt% WPI, 50kPa, 500mL.min^{-1})

Figure 5.15 shows the deposition profile along the membrane after NaOH cleaning and sequential cleaning which resulted in an almost similar amount of deposition and profile on the membrane. The increased in residual deposition by sequential cleaning mainly occurs at

the entrance of the cross-flow rig. Thus, sequential cleaning may have caused re-deposition at the entrance of the rig.

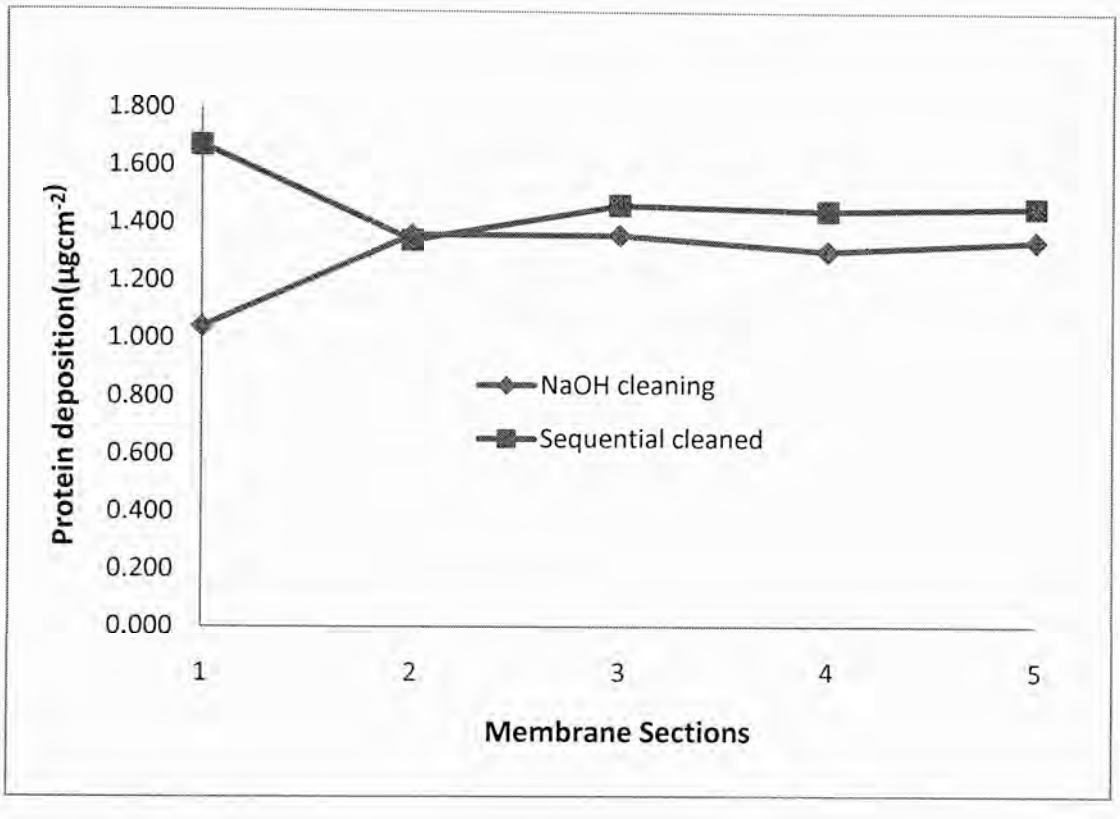

Figure 5.15 Single and sequential cleaning deposition (Fouling conditions: 1 wt% WPI, 50kPa, 500mL.min^{-1}. Cleaning conditions: Sequential: HCl (15 min) and NaOH (30 min), and single: NaOH (30min) at 30°C)

Figure 5.16 shows the deposition profile along the membrane for 6 hours WPI fouling, 1 cycle of sequential cleaning and 4 cycles of repeated fouling and cleaning. The deposition along the membrane surface for 1 cycle of sequential cleaning causes a gradual increase of deposition along the cross-flow surface while the opposite, i.e. gradual decrease of deposition was observed for 4 cycles of repeated fouling and sequential cleaning.

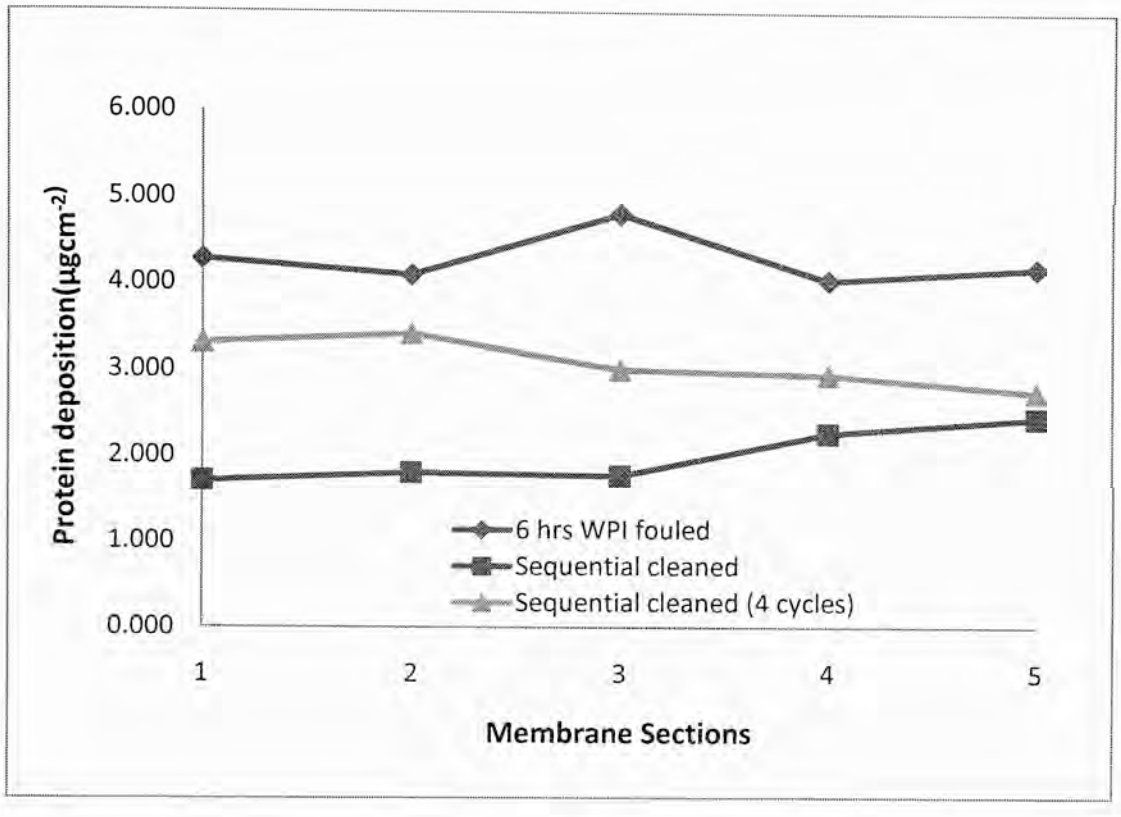

Figure 5.16 The comparison between sequential cleaning deposition of 1 and 4 cycles of fouling and cleaning (Fouling conditions: 1 wt% WPI, 50kPa, 500mL.min^{-1}. Cleaning conditions: Sequential: HCl (15 min) and NaOH (30 min))

Figure 5.17 shows the deposition profile along the horizontal cross-flow membrane surface after sequential cleaning at 30°C and 50°C. An increased temperature shows higher deposition at the end of the rig, however the flux recovery was improved as shown in Figure 5.10. An optimized cleaning temperature of 50°C and concentration of 0.5wt% for NaOH cleaning of reconstituted whey protein fouled membranes resulted in 80% flux recovery (Bartlett et al., 1995). Extensive studies were later conducted by the same authors for alkaline cleaning of whey fouled membranes (Bird and Bartlett, 2002). Warm temperatures were also found to assist in the NaOH hydrolysis of proteins (D' Souza and Mawson, 2005). Therefore, we should be able to achieve higher recoveries for our set-up if the temperature is increased during the cleaning process.

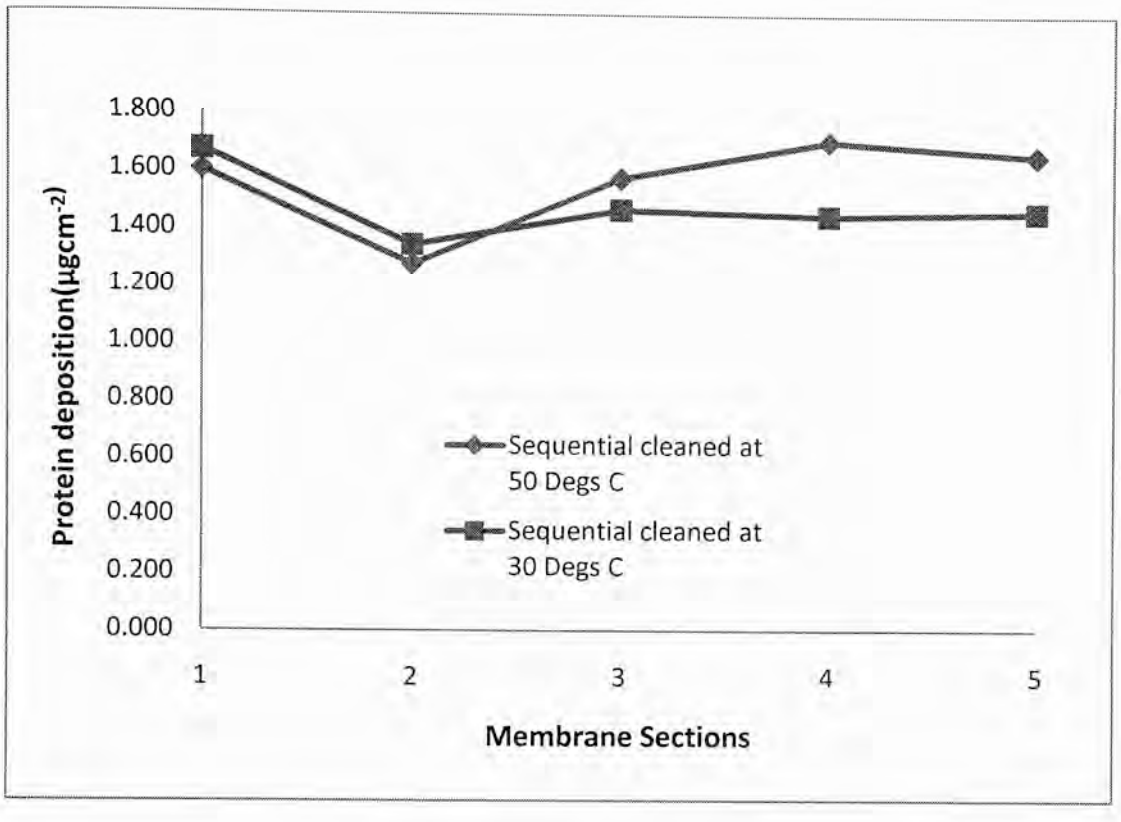

Figure 5.17 The comparison between deposition after sequential cleaning at 30°C and 50°C (Fouling conditions: 1wt% WPI, 50kPa, 500mL.min^{-1}. Cleaning conditions: Sequential: HCl (15 min) and NaOH (30 min))

Figure 5.18 shows that sequential cleaning for 6 hour fouled membranes has a higher residual deposition at the exit region of the rig. On the other hand, for 2 hours fouled membranes the residual deposition was constant along the membrane surface. The higher residual deposition at the exit could be due to accumulation of protein deposition initiated at the exit end of the membrane channel, caused by uneven cross-flow or localised dead flow zones caused by the location of the exit port not at the very end of the flow channel due to fabrication limitations of membrane module. The same pattern was also observed in the previous study using the same membrane module (Chen et al., 2007).

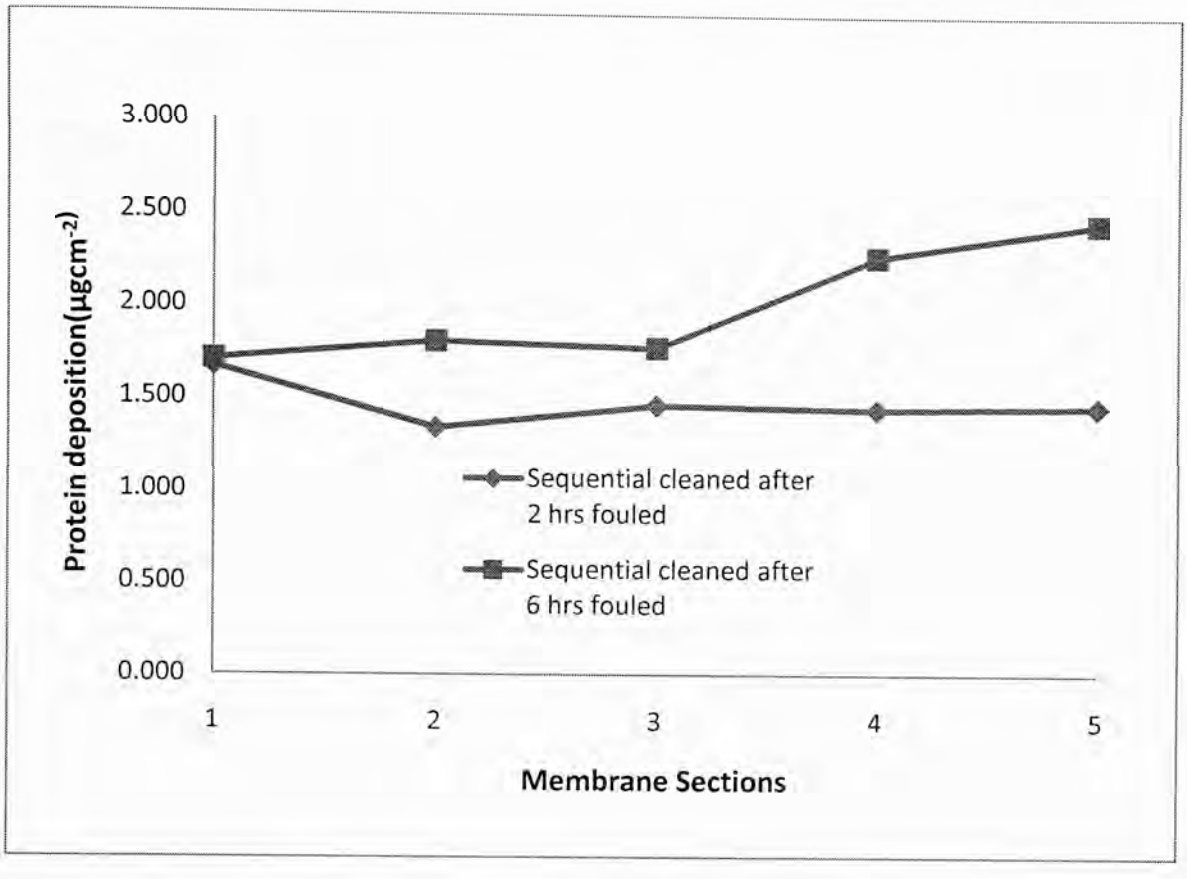

Figure 5.18 The comparison between deposition after sequential cleaning following 2 hours and 6 hours fouling (Fouling conditions: 1wt% WPI, 50kPa, 500mL.min^{-1}. Cleaning conditions: Sequential: HCl (15 min) and NaOH (30 min))

The protein residuals along the membrane surface after single and sequential cleaning were investigated using 1D SDS-PAGE. Observation of residual deposition along the membrane surface (Section 1 to 5) after single 0.1 wt% HCl for 30 min cleaning is shown in Figure 5.19. The amount of residues increases along the membrane channel with S5 containing the most amount of deposition. Most residues were removed from the membrane surface at the entrance region of the rig as that is the initial region where the cleaning solution comes into contact with. No residues above 50kDa molecular weight detected from the experiment.

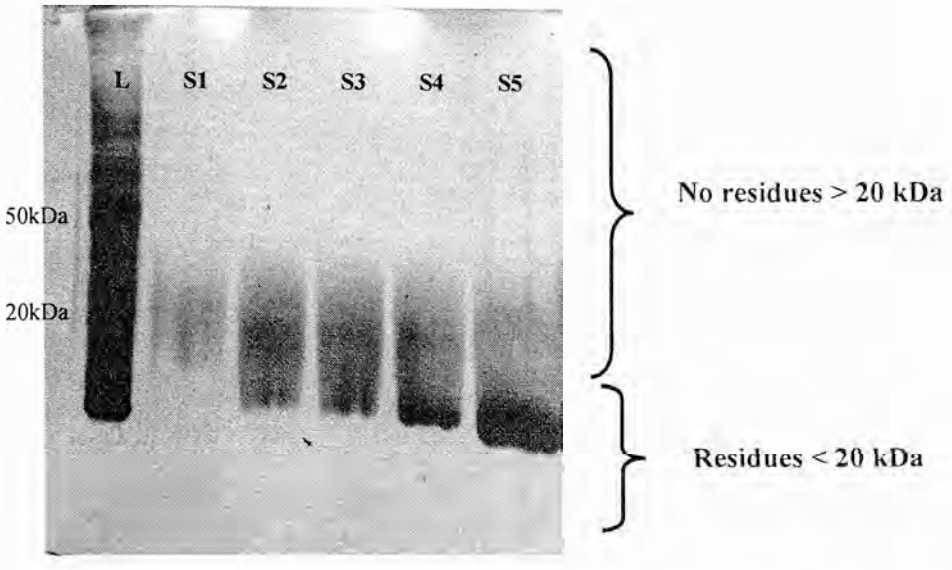

Figure 5.19 The gel scan of protein residuals eluted from membrane surface after 30min HCl treatment following 4 hours of fouling with 1wt% WPI at 50kPa. Letter "S" indicates sections along the membrane while "L" is the protein ladder.

The residual deposition along the membrane surface after single cleaning with 0.1wt% NaOH for 30 min is shown in Figure 5.20. It can be observed that residues of molecular weights of less than 20kDa were left on the membrane. Most peptides above 50kDa were removed. From the comparison of residuals between Figure 5.19 and 5.20, HCl seems to be a better cleaner than NaOH. Trypsin Digestion and LC-MS of HCl cleaned membrane indicated that the lower molecular weight bands in the gel for membranes cleaned with HCl were not whole proteins, but smaller fragments left on the membrane when HCl had cleaved main structure of proteins in the fouling layer. Those low molecular weight bands on the fouled and rinsed membranes were from materials comprised mainly the fragments of proteins produced by the breakage of protein molecules during the 4 hours filtration.

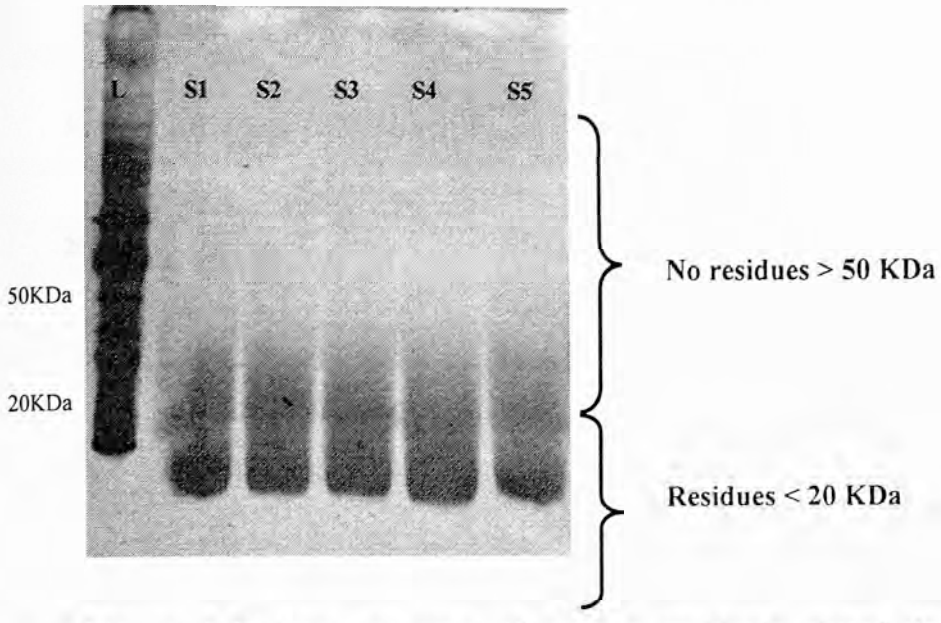

Figure 5.20 The gel scan of protein residuals eluted from membrane surface along the membrane cross-flow length after 30min NaOH treatment following 4 hours of fouling with 1wt% WPI at 50kPa. Letter "S" indicates sections along the membrane while "L" is the protein ladder.

Figure 5.21 shows the residuals along the membrane surface after sequential cleaning with NaOH followed by HCl. Remaining low molecular weight fragments of proteins on the membrane can be seen on the surface. In Figure 5.21, 1D SDS-PAGE results shows that the bands after sequential cleaning seems to be more intense and bigger than the bands in NaOH or HCl only treatments (Figures 5.19 and 5.20). The bands are accumulation of un-detached foulants on the membrane surface which consist of low MW fragments. The re-deposition was also observed previously in the Lowry results of Figure 5.13.

1D SDS-PAGE did not resolve the protein residuals along the membrane surface as the bands were indistinct. This may be caused by NaOH and HCl residues on the membrane after cleaning interfering with the protein extraction process and the electrophoresis. However, qualitative conclusions regarding the effect of cleaning with single and sequential cleaners can be performed.

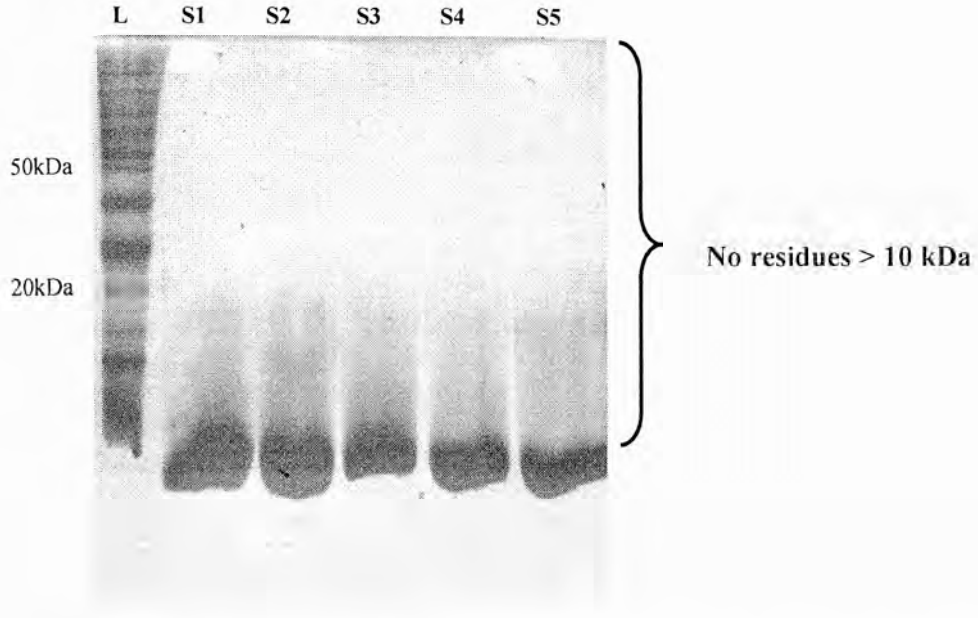

Figure 5.21 The gel scan of protein residuals eluted from membrane surface after 30min NaOH and 15 min HCl following 4 hours of fouling with 1wt% WPI at 50kPa. Letter "S" indicates sections along the membrane while "L" is the protein ladder.

5.2.7. Protease cleaning of binary protein fouled membranes

Enzymatic cleaning using Protease M Amano was performed on 0.1wt% BSA and βLg binary mixture fouled membranes with spacer in the membrane channel, to compare its effectiveness with HCl and NaOH cleaners. The UF of 0.1wt% equimolar BSA and βLg was carried out at 50kPa TMP, pH 4, 500mL.min^{-1} flow rate and 4 hours duration to ensure irreversible fouling of the membrane. Table 5.4 summarizes the cleaning conditions performed using Protease M Amano at various operating conditions. Cleaning duration (min), protease concentrations (wt %) and cross-flow rate (mL.min^{-1}) were the experimental conditions investigated. The results of these experiments in Table 5.3 are shown in Figures 5.22 – 5.25. Cleaning efficiencies was

evaluated according to equations (1) while resistance removal was calculated using equation (2). Equation (3) and (4) was used to calculate flux recovery increments and total flux recovery respectively. The residual deposition after cleaning was evaluated using the Lowry method.

Table 5.4
Cleaning studies for protease on membranes fouled with BSA and βLg, 4hrs, 50kPa, 500mL.min^{-1}

	Experimental setup	
No.	Cleaning Duration (Min)	Protease Concentration
1	60 min,	0.01wt%
2	40 min (Standard)	0.01wt%
3	20 min,	0.01wt%
4	40min, High Conc.	0.1%,
5	40 min, Low Conc.	0.001%,
6	40 min, 1000mL.min^{-1} (High Flow)	0.01%,
7	40 min, 200 mL.min^{-1} (Low Flow)	0.01%,

The flux recovery after protease cleaning at various operating conditions in Table 5.4 was investigated and the results are shown in Figure 5.22. By looking at Figure 5.22, a cleaning efficiency of 60% was obtained after 40 min of 0.01wt% protease treatment (Bar 2). In addition, increasing the protease concentration to 0.1wt% and cross-flow rate to 1000mL.min^{-1} (Re = 903) resulted in an elevated cleaning efficiency of 73% (Bar 4) and 77% (Bar 6) respectively. As expected, the lowest cleaning efficiency was obtained at 0.001wt% protease (Bar 5). Thus concentration and cross-flow rate has a direct influence in the removal of protein residuals from the membrane surface. Previous studies have also achieved high efficiencies using protease enzymes, 85% cleaning efficiency in removing abattoir foulants (Maartens et al., 1996) and more than 90% resistance removal for mixed BSA and βLg foulants (Petrus et al., 2008).

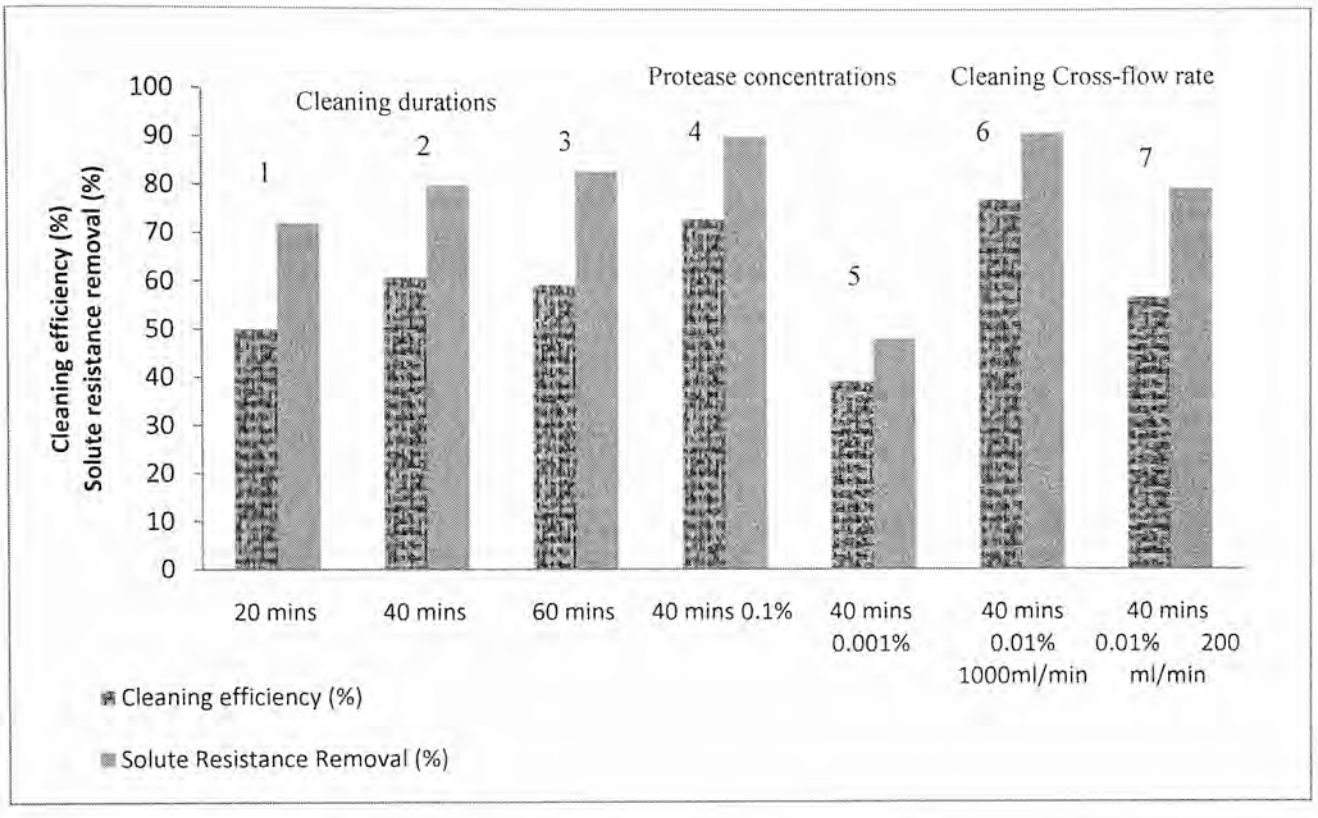

Figure 5.22 Solute resistance removal and cleaning efficiency of protease cleaned membranes at various cleaning durations in a cross-flow set-up. (Fouling conditions: 0.1 wt% equimolar BSA and βLg, 50kPa, pH 4, 500mL.min^{-1}. Cleaning conditions: Protease M Amano, pH 7.5, 30°C) The numbers above the bars indicate the experimental set-ups as described in Table 5.4.

Figure 5.23 shows the residual protein deposition (μgcm^{-2}) on the membrane surface measured using the Lowry method after protease treatment under various cleaning durations, concentrations and flow rates.

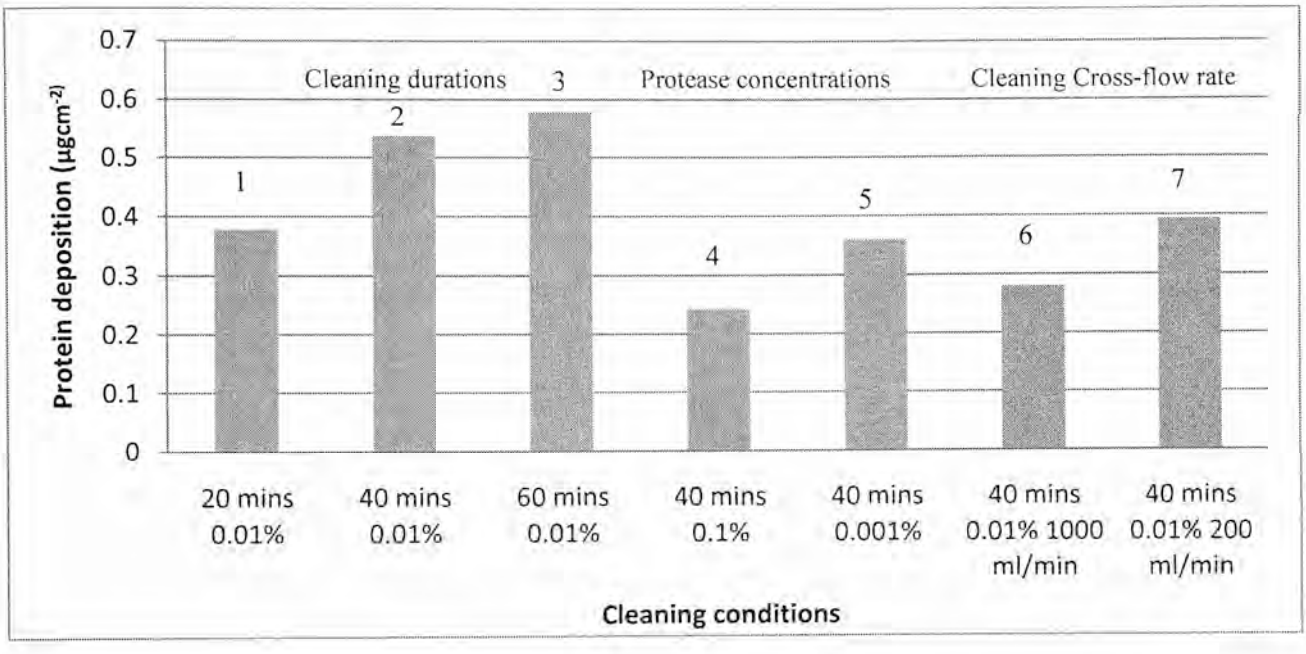

Figure 5.23 Total protein deposition measured by Lowry method of protease cleaned membranes at various durations, concentrations and flow rates. (Fouling conditions: 0.1wt% BSA and βLg, 50kPa, pH 4, 500mL.min^{-1}. Cleaning conditions: Protease M Amano, pH 7.5, 30°C). The numbers above the bars indicate the experimental set-ups as described in Table 5.4

The highest cleaning efficiencies that was achieved at 40 min (0.1wt % protease, Bar 4) and 1000mL.min^{-1} cross-flow rate (0.01 protease, Bar 6), resulted in low total protein residues per area. Also, the protein residues increase as the duration of cleaning increases from 20 min to 60 min (Bars 1 – 3) demonstrating the additional protein deposition provided by the protease. However, it is observed that these residues did not affect the cleaning efficiencies and solute resistance removal. However, it is important that these residues are removed completely to prevent interference with the following process cycle.

Figure 5.24 shows the effect of three cycles of fouling and protease cleaning in terms of initial Milli-Q flux after fouling (J_F), Milli-Q flux after rinsing (J_1) and Milli-Q flux after protease

cleaning (J_2). The final cleaning flux (J_2) decreases successively after each runs although the fluxes (J_F) for the second and third runs are stable.

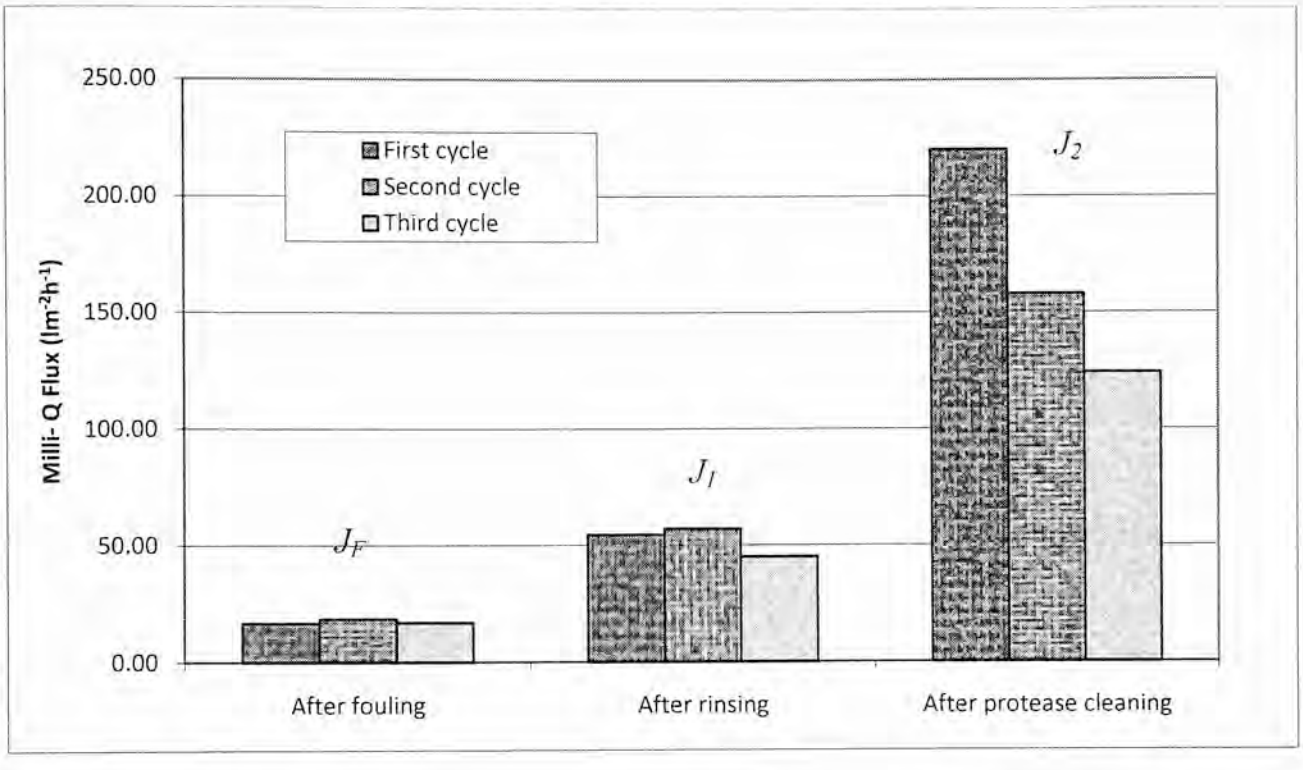

Figure 5.24 Milli-Q flux of 3 cycles of fouling and cleaning (Fouling conditions: 0.1 wt% BSA and βLg, 50kPa, pH 4, 500mL.min^{-1} Cleaning conditions: Protease M Amano, pH 7.5, 30°C, 0.01wt%, 40 min)

Figure 5.25 shows the flux recovery increments (FRI_i) and total flux recovery (FR) after three successive fouling and protease cleaning cycles. FR decreases as the cycle increases which was caused by the increase in residues.

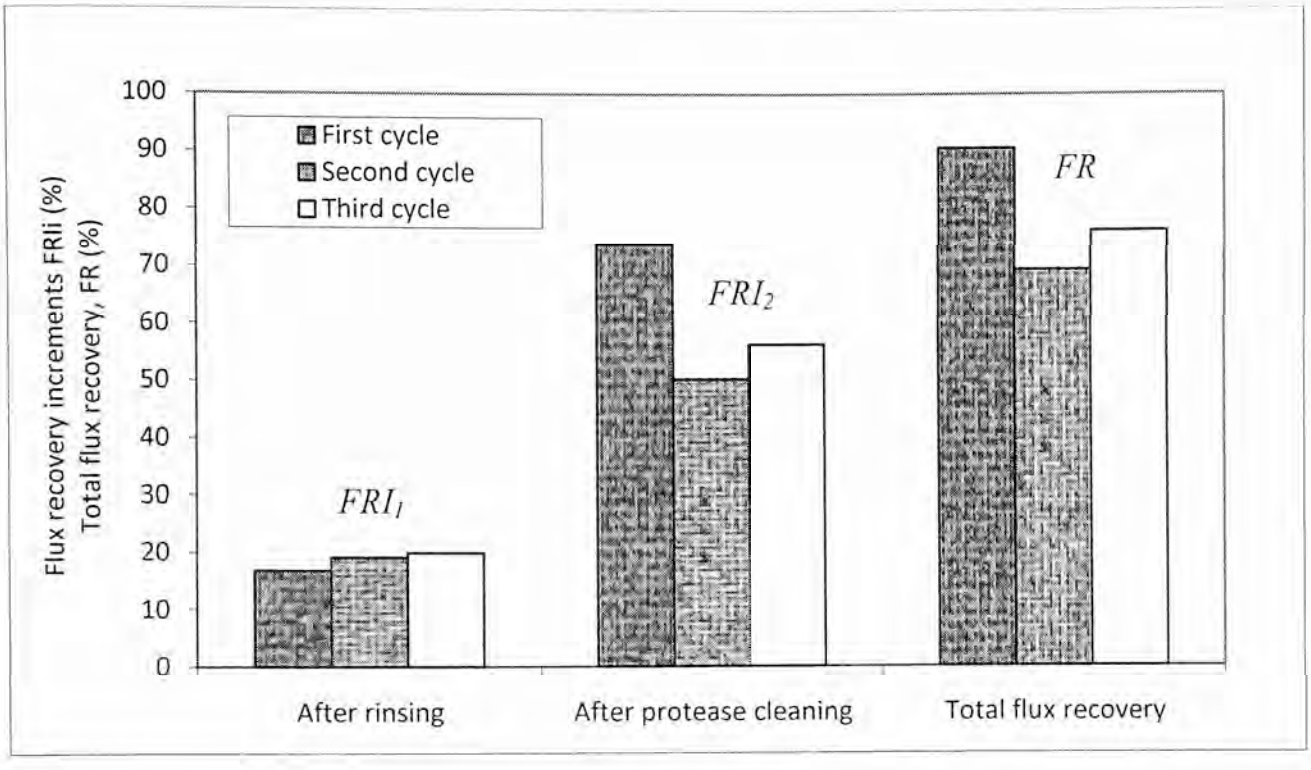

Figure 5.25 Flux recovery increments and flux recovery after 3 cycles of fouling and cleaning (Fouling conditions: 0.1 wt% BSA and βLg, 50kPa, pH 4, 500mL.min^{-1} Cleaning conditions: Protease M Amano, pH 7.5, 30°C, 0.01wt%, 40 min)

Figure 5.26 shows the residuals after protease cleaned of WPI (Left side) and equimolar BSA and βLg (Right side) fouled membranes. A band at 30 – 40 kDa was detected in both treatments showing that the band originated from protease, and it was a residue from the enzyme and not the protein foulants.

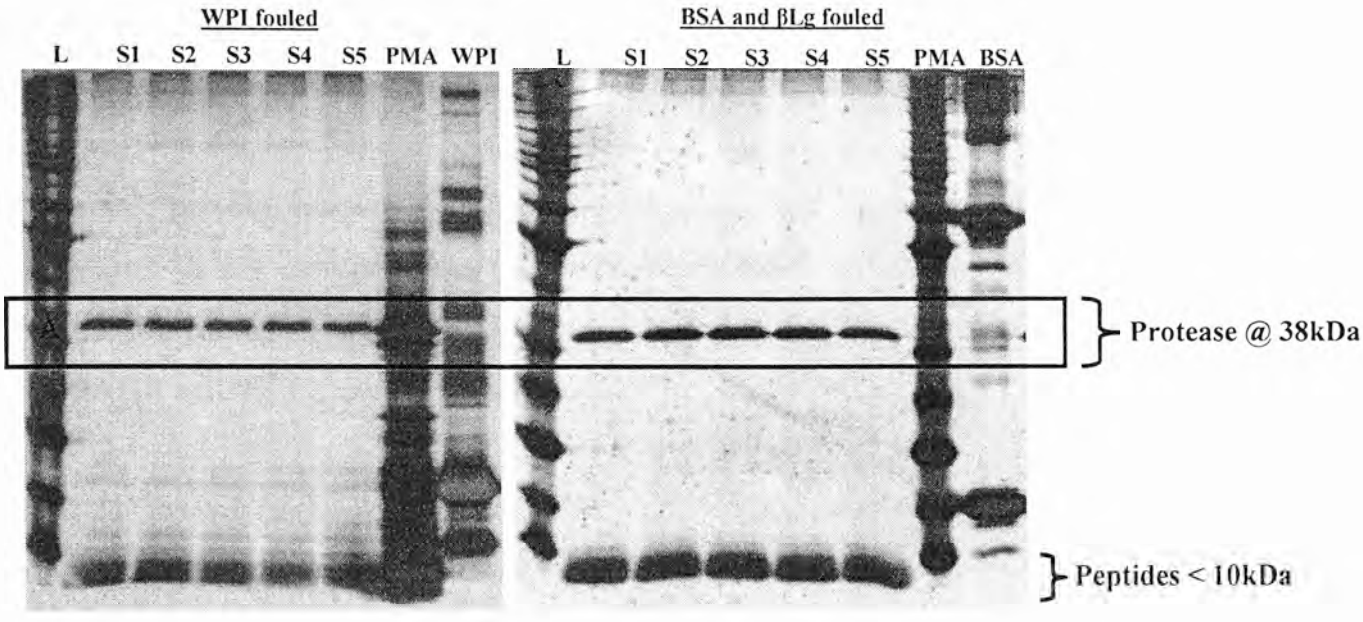

Figure 5.26 Gel scan of protease treated membranes after 3 cycles of fouling and cleaning (Fouling conditions: 0.1% WPI (Left) and 0.1% BSA and βLg (Right), 50kPa, pH 4, 500mL.min^{-1} Cleaning conditions: Protease M Amano, pH 7.5, 30°C, 0.01wt%, 40 min)

Trypsin 'in-gel' digestion followed by mass spectrometry was performed on the residuals to identify the unknown protein band at 38 kDa (Box A) in Figure 5.26. The results showed the peptide was Oryzin Precursor (Alkaline Proteinase) (gi|464318) of mass 871.56kDa which is an enzyme residual.

5.3. Conclusions

Irreversible protein deposition on membranes after cleaning is a crucial issue in membrane separation. In this current study, the residual deposition following NaOH, HCl and Protease M Amano cleaning of whey protein fouled membranes was successfully assessed using 1D SDS-PAGE and the Lowry method.

Using 1D SDS-PAGE, we observed that WPI is made up of a complex mixture of whey proteins. The proteins deposited on the membrane surface following UF was different from the original protein feed as "new" peptides were introduced during the extraction process due to denaturation prior to analysis using 1D SDS-PAGE. Although, several bands were distinct such as BSA, βLg and αLa, most other bands were unknown, and were made up of peptides and amino-acids. For WPI UF, αLa and βLg were not denatured significantly due to its high stability in solution. On the other hand, binary mixtures of pure BSA and βLg remained stable on the membrane after UF.

Cleaning of whey protein fouled membranes with NaOH was effective in recovering a fraction of the membrane flux of WPI fouled membranes. The cleaning efficiency for BSA and βLg fouled membranes are higher than WPI fouled membranes under the same operating conditions. 60 minutes of cleaning resulted in the highest cleaning efficiency of 48% for BSA and βLg fouled membranes, and 33% for WPI fouled membranes. Lower efficiency was obtained in the cleaning of WPI fouled membranes because of the presence of low molecular weight proteins smaller than the MWCO of the membrane i.e. 3kDa.

The residues after HCl and NaOH cleaning in a dead-end set-up were the same because of the similar cleaning reactions provided by these two chemicals to the proteins. After HCl and NaOH treatment, residues of less than 40kDa MW were detected and there were no residues detected above 40kDa MW.

The sequential cleaning of WPI fouled membranes using NaOH followed by HCl, led to new exciting discoveries. HCl cleaning after NaOH cleaning improved the flux recovery for longer

duration of WPI fouling and repeated cycles of fouling and cleaning. Incorporating HCl cleaning during sequential cleaning added 11% to the flux recovered by NaOH cleaning. In addition, the flux recovered by HCl improves as the number fouling and cleaning cycles increase. The highest flux recovery obtained through sequential cleaning was 89% in repeated fouling and cleaning cycle. Although sequential cleaning improved flux, however the amount of residual deposition was higher than single NaOH cleaning measuring $0.143\mu gcm^{-2}$ more. Thus, the higher protein residuals did not reduce the flux of the membrane. Sequential cleaning at higher temperatures also resulted in a higher flux recovery.

The residuals after NaOH, HCl, and NaOH and HCl cleaning were analyzed using 1D SDS-PAGE. The bands were indistinct, however from the electrophoresis bands, HCl cleaning seems to be a better remover of residuals compared to NaOH and sequential cleaning.

Following 1D SDS-PAGE, the residual protein molecules was further characterized up to its amino-acid fragments by trypsin digestion and liquid chromatography and mass spectrometry (LCMS). We found that casein was the protein not removed by HCl and NaOH in 2 hours under dead-end filtration, however in most cases, the proteins and peptides are totally removed.

From protease cleaning experiments, we have found that 0.01wt% protease can effectively recover to almost 60% of initial membrane flux after cleaning after 40min of cleaning. Cleaning efficiency was affected by cross-flow rate and concentrations. The highest efficiency was achieved at 77% after 40 min cleaning at $1000mL.min^{-1}$ and 0.01% protease. A higher protease concentration of 0.1% also resulted in a similar cleaning efficiency of 73%. In addition, high efficiency resulted in lower residual concentration on the membrane surface.

Protease cleaned membranes resulted in residues of less than 10kDa and a single protein residue at 38kDa. Increasing protease concentration and cleaning time resulted in increased total residual protein level on the membrane after cleaning which may be carried forward to the subsequent process cycle. This confirms earlier observation of re-adsorption of protease on

the membrane surface however no fouling occurs. We have to ensure that this residue be removed by using an appropriate treatment.

Using sequential cleaning resulted in re-deposition of removed peptides from the membrane where there was a small increase in deposition measured by Lowry after sequential cleaning compared to single NaOH cleaning, where 1D SDS-PAGE shows more deposition with sequential cleaning compared to single NaOH and HCl treatment.

Studying residual protein fragments using the methods involved after cleaning is useful for dairy and milk processing industries that encounter protein fouling in their membrane systems. Understanding this deposition allows better control in reducing foulants and producing an efficient cleaning protocol.

Chapter 6: Investigating concentration polarization and fouling on the steady state flux in cross-flow UF of BSA solutions

6. Introduction

CFD is a tool applied to model flow and concentration polarization in membrane separation units (Rosen and Tragardh, 1993; Geraldes et al., 2000; Neal et al., 2003). The various techniques to improve membrane processes by applying CFD was reviewed recently (Ghidossi et al., 2006). Ideally, when physical properties are constant, the resistances caused by concentration polarization and fouling can be easily described by in-series resistances according to Darcy's Law (Eqn. 6.6) with minimum deviations. However, this is not the case for aqueous BSA solution which is well known for its complex physical behaviour. As the transport properties and physical properties of complex BSA solutions depend strongly on the BSA concentration, pH and salt concentration, simple mass transfer models such as the film theory are not applicable as considerable errors are to be encountered. While the effect of pH on flux decline is well documented, the relative contribution of concentration polarization and fouling (i.e. reversible and irreversible respectively) towards flux decline in UF under different pH conditions is unclear. In addition, the sensitivity of flux losses and protein adsorption towards various operating conditions i.e. pH, feed concentration, and cross-flow rate with and without added salt are unknown. Thus, the current study investigates the implications of concentration polarization and fouling towards flux decline through CFD simulation and mass transfer study.

A CFD program was developed in collaboration with Dr Paul Schausberger from Vienna University of Technology to simulate flux, concentration polarization and fouling by taking varying operating conditions and surface adsorption during BSA UF into account (Schausberger et al., 2009). While the CFD simulation was set-up and performed by Schausberger, the fouling experiments and mass transfer study were conducted by me. In the mass transfer study, empirical models were utilized to estimate the diffusivity, mass transfer coefficient and wall concentration. In addition, the contribution of polarization and fouling

(based on individual resistances) towards flux decline were also distinguished. The agreement between mass transfer models (constant physical properties) and CFD (variable operating conditions) were discussed.

6.1. Modelling and mass transfer study

6.1.1. Physical properties of BSA in solution

The physical properties required in our CFD and mass transfer study are dynamic viscosity (μ), density (ρ), osmotic pressure (Π), and gradient diffusion coefficient or diffusivity (D). These physical property models applied are listed in Table 6.1 and are explained in the following paragraphs.

Table 6.1
Physical property models – viscosity, density, osmotic pressure, and diffusivity used in the study

Empirical Models	Eqn.	Ref.	Units
$\mu(c) = \mu(0) \cdot e^{\left(0.0024 \cdot \left[\frac{c}{10^4}\right] \cdot M\right)^2}$	**(6.1)**	(Kozinski and Lightfoot, 1972)	[Pa s]
$\rho(c) \approx \rho(0) = \rho_w$	**(6.2)**	(Gill et al., 1988)	[kgm^{-3}]
$\Pi(c) = \mathcal{R}T\left(2\sqrt{\left(\frac{Zc}{2 \cdot 10^3}\right)^2 + m_s^2} - 2m_s + \frac{c}{10^3} + A_2\left(\frac{c}{10^3}\right)^2 M + A_3\left(\frac{c}{10^3}\right)^3 M^2\right)$ $Z(pH) = -497.512 - 37.913 \cdot pH + \frac{2896.079}{pH^2} + 352.129 \cdot ln(pH)$	**(6.3)**	(Vilker et al., 1984)	[Pa]

$A_2(Z) = -5.625e-4 - 2.41e-4 \cdot Z - 3.664e-5 \cdot Z^2$ $A_3(Z) = 2.95e-5 - 1.051e-6 \cdot Z + 1.762e-7 \cdot Z^2$			
$D(c) = D_{id} \cdot \frac{\mu_w}{\mu(c)} \cdot \sqrt{\frac{1}{\mathcal{R}T} \cdot \frac{\partial \pi(c)}{\partial c}}$	**(6.4)**	(Gaigalas et al., 1995)	$[m^2s^{-1}]$

Dynamic viscosity (μ) of aqueous BSA solutions strongly increases with increasing BSA concentration (c). The viscosity model, Eqn. (6.1) was obtained from (Kozinski and Lightfoot, 1972), who reported negligible dynamic viscosity dependence on pH and buffer. Newtonian behavior was confirmed for BSA concentrations of up to 6.61 $molm^{-3}$, which is also the point of agglomeration or gel formation.

The density (ρ) equation, Eqn. (6.2) applied in this study was constant which is valid for our BSA feed concentration. The density of BSA solution is approximately linearly dependant on the BSA mass fraction at mass fractions below 0.15wt% (Gill et al., 1988).

The osmotic pressure model used in this study was taken from Eqn. (6.3) (Vilker et al., 1984) on Page 160 of the revised text. Figure 6.1, shows the plot of osmotic pressure (Y-axis) against pH (X-axis) of BSA concentrations 1, 2 and 3 $molm^{-3}$ at pH range of 4 to 7.5 for 0.15M and 0.005M NaCl (No added salt). The range of pH values of 4 to 7.5 brings about the Z values. Following that the Z values were used to calculate the virial coefficients A_2 and A_3 at either 0.15M or 0.005M NaCl. The virial coefficients was then used to calculate the corresponding osmotic pressure at the specific pH.The osmotic pressure of aqueous BSA solutions shows strong dependence on concentration and pH as well as salt concentrations. Most of the osmotic pressure data available refers to BSA in either NaCl or KCl solution. The calculated osmotic pressure for solutions with no added salt shows a very distinct minimum at the protein i.e.p. pH 4.9 while for added salt solutions at low protein concentrations the minimum vanishes due

to the buffering effect of NaCl. In addition, at elevated BSA concentrations the minimum shifts to a lower pH value.

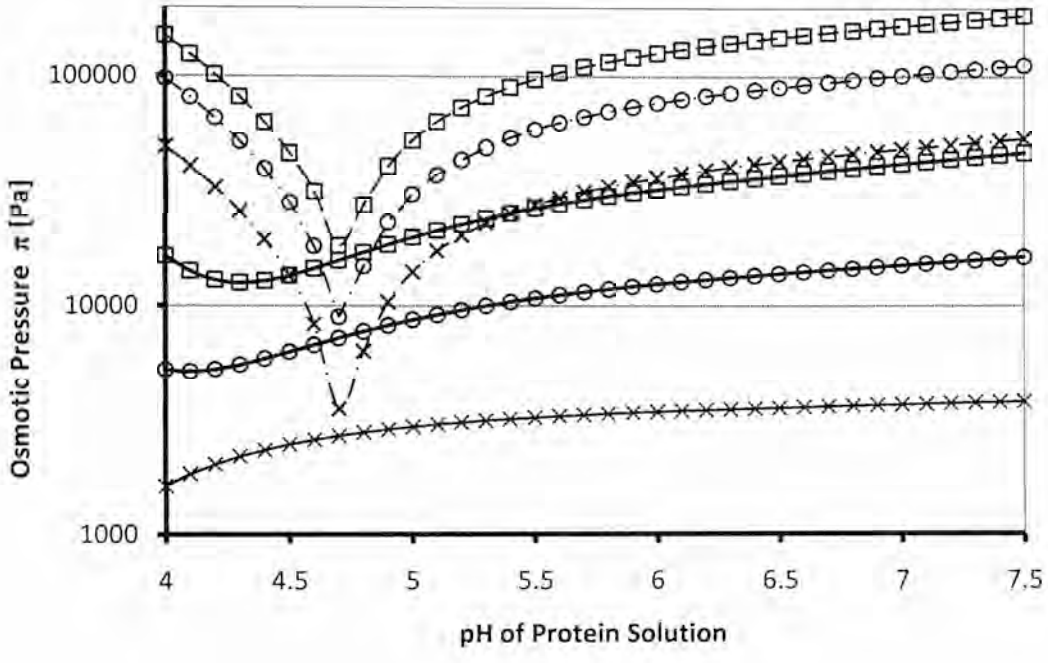

Figure 6.1 Osmotic pressure of BSA solutions dependant on pH, protein and salt concentration, full/dotted lines represent NaCl concentrations of 0.15/0.00 [moll^{-1}], crosses/circles/squares represent BSA concentrations of 1/2/3 [molm^{-3}]

The diffusivity (D) of BSA in aqueous solutions shows strong dependence on the system's thermodynamic state (i.e. BSA concentration, ionic strength and pH value). The diffusion process addressed here is gradient diffusion (elsewhere referred to as mutual, cooperative or collective mass diffusion), meaning that the macroscopic flux of particles (macromolecules) is induced by Brownian motion in the presence of a gradient in the total number density of particles (Bowen et al., 2000). The generalized Einstein relation (Eqn. 6.5) describes the corresponding diffusion coefficient for use with Fick's law of diffusion

$$D(\phi) = D_{id} \cdot \frac{K(\phi)}{S(\phi)} \tag{6.5}$$

Here, D_{id} is the diffusion coefficient at infinite dilution, $K(\phi)$ is the hydrodynamic interaction coefficient and $S(\phi)$ is the thermodynamic coefficient. Whereas $S(\phi)$ is derivable from osmotic pressure data, no universally accepted form to describe $K(\phi)$ for charged ellipsoid BSA molecules is available.

In the CFD, diffusivity was estimated using the theoretical framework (Eqn. 6.4) (Gaigalas et al., 1995) which relates hydrodynamic contribution $K(\phi)$ to the solution viscosity.

The properties of BSA used in this study are shown in Table 6.2.

Table 6.2
BSA properties

BSA properties	Abbreviations	Value	Unit	References
Molecular Weight	M	69000	$gmol^{-1}$, (Da)	(Vilker et al., 1984)
Iso-electric point	i.e.p	4.9	(pH)	(Vilker et al., 1984)
Molecular size	Size (at i.e.p.)	4×4×15	nm	(Nakanishi et al., 2001)
Gel concentration	c_{gel}	~7	$molm^{-3}$	(Kozinski and Lightfoot, 1972)
Diffusivity at infinite dilution	D_{id}	$6.7x10^{-11}$	m^2s^{-1}	(Shen and Probstein, 1977)

6.1.2. Fouling Model

There are a number of models that correlate flux to operating parameters and they are based on three models, which is film theory, resistance in series theory and the osmotic pressure theory. In general, flux is proportional to trans-membrane pressure (TMP) however at higher fluxes, mass balance governs its characteristics. The three regions that describe the flux-TMP relationship are pressure-controlled region, transition region, and mass-transfer controlled region.

In the pressure controlled region, the permeate flux can be described by Darcy's Law that is also known as the resistance in series model (Eqn. 6.6). According to this law, permeate flux decline is caused by decreased driving forces and/or increased resistances. In other words, the flux is directly proportional to the applied pressure and inversely proportional to the viscosity and the total resistance of the system. Thus, in our system, the membrane flux (J_{UF}) can be described as,

$$J_{UF} = \frac{\Delta P - \Delta \pi}{\mu(R_M + R_F)} = \frac{\Delta P}{\mu(R_M + R_F + R_{CP})} = \frac{\Delta P}{\mu(R_{Total})} \quad (6.6)$$

The resistances occurring in membrane systems are caused by the membrane (R_M), concentration polarization (R_{CP}), and fouling (R_F). Concentration polarization arises from the solute retention by the membrane when the solvent transport is facilitated. When solute retention occurs, solute accumulates on the surface and forms a layer at the membrane interface with a relatively high concentration resulting in concentration polarization. The resistance due to the concentration polarization layer (R_{CP}) increases during membrane filtration until the system reaches steady state. In addition, concentration polarization also causes the increase in OP ($\Delta\pi$), causing an increase in resistance. In our study, we mainly utilized traditional Darcy's Equation (Eqn. 6.6) and other mass transfer equations to estimate steady-state resistances and theoretical flux.

6.1.3. Concentration polarization

The primary reason for flux decline during the initial period of UF is concentration polarization of the solute at the membrane surface. Concentration polarization occurs in combination with fouling and gel layer formation which is irreversible and reversible respectively. An excellent review on concentration polarization in UF and RO and recommended models and experimental methods to better address this phenomenon was presented (Sablani et al., 2001).

In this study, a mass balance equation (Eqn. 6.7), known as a stagnant-film model was used to describe the change in concentration during UF near the membrane wall at steady state conditions,

$$J_{UF} = \frac{D}{\delta} ln \frac{C_w}{C_b} = k ln \frac{C_w}{C_b} \tag{6.7}$$

where k represents the mass transfer coefficient, δ is for layer thickness for solute transport, D for diffusivity, and C_w and C_b represents concentration at the wall and bulk solution respectively. The method of deriving this equation is shown in Appendix D.

6.1.4. Sherwood model

In the mass transfer controlled region, the stagnant-film model (Eqn. (6.7)) and Sherwood correlation best describes the permeate flux (Eqn. (6.8) and (6.10)). Sherwood correlations can be applied assuming constant physical properties at steady state. To describe laminar flow in a thin channel, Sherwood correlation is shown in Eqn. (6.8) (Cheryan, 1998). Eqn. (6.8) to Eqn. (6.10) are combined to obtain Eqn. (6.11) that relates diffusivity to Schmidt's number (Sc), and Sh.

$$Sh = 1.86(Re)^{0.33}(Sc)^{0.33}\left(d_h/L\right)^{0.33} \tag{6.8}$$

$$Sc = \frac{\mu}{\rho D} \tag{6.9}$$

$$Sh = \frac{kdh}{D} \tag{6.10}$$

$$D = \left(\frac{k \cdot dh}{1.86 \cdot \left[Re\ \mu\ dh / \rho\ L \right]^{0.33}} \right)^{1/0.67} \tag{6.11}$$

6.2. Experiments

Throughout the study, 30 kDa Nominal MWCO flat sheet PES (Synder Filtration^{TM}, US) membranes were used. The study utilises the same acrylic cross-flow filtration rig used in all previous studies with a filtration area of 0.02 m^2. Reagent grade pH 5.0 BSA (Moregate Biotech Pty Ltd, Australia) was used as the model protein throughout the study. The protein was dissolved in either in Milli-Q water or 0.15M NaCl and Milli-Q water solution at room temperature. The required pH was adjusted using dilute HCl or NaOH solution. The fouling and flux measurement techniques are explained in Chapter 3.

Experiments were performed to obtain the steady-state flux (J_{UF}) at 1 hour under various operating conditions i.e. solution pH, flow and concentration. From these studies, the controlling factors that affect the flux decline and the effect of operating conditions to BSA deposition can be determined. BSA deposition on the membrane surface was measured using the Lowry method as performed in the previous chapters (Hess et al., 1978).

The UF membranes were fouled at 50kPa TMP for 1 hour under different operating conditions. The standard (STD) conditions were flow = 500 $mL.min^{-1}$, pH = 5.4, feed Concentration (Ca.) = 1.05×10^{-5} M. The feed concentration, pH and flow variations are shown in Table 6.3, keeping the other two parameters at standard values (STD).

Table 6.3
Operating conditions in the test series (Added or no added salt)

	pH	Feed Ca.	Flow ($mL.min^{-1}$)
–	4.5	1.05×10^{-6}M	15
STD	5.4	1.05×10^{-5}M	500
+	7.4	1.05×10^{-4}M	1400

The initial Milli-Q flux was measured at 50kPa and 500$mL.min^{-1}$ for 15 min prior to running the UF test series. The Milli-Q flux (J_i) for membranes used in the added salt BSA solutions studies was 97 ± 3 Lm^2h^{-1} (9 repeats). On the other hand, the initial Milli-Q flux for pure BSA

solution studies was 68 ± 4 Lm^2h^{-1} (7 repeats). The lower initial Milli-Q flux value obtained from studies without added salt was due to a different batch of 30kDa PES membrane used. Thus, some care must be taken when comparing the results for added salt and without added salt solutions as the membrane permeability were differing substantially.

Following that, the effect of concentration polarization was studied by finding the Milli-Q flux through the fouled membrane after one hour of fouling (J_{MQUF}). The study allows the derivation of R_{MQUF} that allows us to back calculate the R_{CP} as shown in Eqn. 6.6. As pH affects J_{UF} most significantly compared to flow and concentration, the study was only performed to the variation of solution pH (4.5, 5.4, and 7.4), with flow and feed concentration held constant.

Also, BSA passive adsorption test was carried out at pH 5.4 (Standard condition), to determine the effect of adsorption in causing flux decline. One hour BSA adsorption was performed at standard condition except at 0 TMP (gauge), and the Milli-Q flux (J_{MQP}) was determined after the adsorption to determine the final deposition and R_P.

6.3. Mass transfer study methods

6.3.1. Differentiating the resistances in the system

The procedures used to calculate resistance R_M, R_T, R_F and R_{CP} are described here. At pH 4.5, 5.4, and 7.4

i. Measure J_i (initial Milli-Q flux, 50kPa, 15min) and calculate R_M
ii. Measure J_{UF} (1 hour flux) and using Eqn 6.6 calculate R_T
iii. Measure J_{MQUF} (Milli-Q flux, 50kPa, 15min after fouling) and calculate R_F
iv. Obtain R_{CP} from $R_{CP} = R_T - R_F - R_M$
v. To obtain actual resistance from R_T and R_F, subtract R_M from each

6.3.2. Deriving osmotic pressure and theoretical wall concentrations

The osmotic pressure and wall concentrations were estimated using trial and error method for pH 4.5, 5.4 and 7.4. The experimental data available are final measured flux (J_{UF}), Milli-Q measured resistance after fouling (R_F) and membrane resistance (R_M). A spreadsheet was used to perform the estimation and the procedures are explained below.

i. Select a range of wall concentration, $C_{wi} < C_w < C_{wf}$
where
C_w is wall concentration (To be determined)
C_{wi} is initial wall concentration, 0.00105molm^{-3} BSA (Approximate $\approx$ 10 $\times$ less than C_b, 0.0105molm^{-3})
C_{wf} is the final concentration, 0.2 molm^{-3} BSA (Approximated)

ii. Calculate the corresponding $\prod(c)$ within the range of C_w using Vilker's Eqn.(6.3)

iii. Calculate the corresponding theoretical flux (J_{Theory}) within the range of C_w using Darcy's equation (Eqn. (6.6) from the known osmotic pressure ($\prod(c)$), and R_F
Two conditions were investigated when estimating osmotic pressure and theoretical flux. One is "Fouling" condition where the flux was estimated using Eqn. (6.12), and measured membrane resistance after fouling (R_F). The other is "Non-fouling" condition where the flux was estimated using Eqn. (6.13), and only the membrane resistance (R_M).

$$J_{Theory} = \frac{\Delta P - \Delta \pi}{\mu(R_F)} \tag{6.12}$$

$$J_{Theory} = \frac{\Delta P - \Delta \pi}{\mu(R_M)} \tag{6.13}$$

iv. Find the corresponding difference between experimental J_{uf} (Final measured UF flux) and J_{Theory} within the range of C_w (For both conditions)

v. The experimental C_w is the concentration when the difference between J_{uf} and J_{Theory} is zero (For both conditions). This is performed by trial and error using a spreadsheet.

6.3.3. Calculating diffusivity and mass transfer coefficient

Diffusivity and mass transfer coefficient were calculated from the known theoretical wall concentration C_w, and for both "fouling" and "non-fouling" conditions,

i. Obtain k by applying theoretical flux equation (stagnant film model) Eqn.(6.7)

ii. Calculate experimental diffusivity using Eqn.(6.11) at C_w

iii. Calculate diffusivity applied in the CFD study using Eqn.(6.4)

iv. Compare experimental diffusivity with diffusivity used in CFD at C_w

v. Calculate k_{id} at D_{id} (ideal conditions) and compare with k

vi. Compare "fouling" and "non-fouling" conditions

6.4. CFD study methods

In our CFD simulation, a transient, finite volume code was applied to solve the mass, momentum and species conservation equations, accounting for the solution physical properties strong dependence on protein concentration.

6.4.1. Membrane fouling model

The membrane is modelled as being fully permeable for the electrolyte. Therefore the solution can be treated as a binary mixture of BSA and salt solution. This allows for the description of the species transfer by the classical convection-diffusion equation. The physical properties therefore required for the description of mass transfer in the CFD program are the dynamic viscosity, density, osmotic pressure, gradient diffusion coefficient and the solubility/gelling

concentration. These physical property models are shown in Table 6.1 while the BSA properties are shown in Table 6.2.

The fouling model follows:

$$J = \frac{TMP - \pi(c_m)}{\mu_w \cdot (R_m + R_f[q])} \tag{6.14}$$

where the flux is described by a modified Darcy's law and a resistance-in-series approach, accounting for the clean membrane resistance and the fouling layer resistance. Accordingly the kinetics and the resistance of the forming protein layer are modelled based on previous studies (Gekas et al., 1993; Ruiz-Bevia, 1997)

$$\frac{dq}{dt} = Ac_m^k(q_{eq} - q) \tag{6.15}$$

$$R_f = Bq^n$$

Here, the rate of deposition is described as an irreversible adsorption reaction of order k with respect to the protein concentration at the membrane and first order with respect to 'surface saturation', i.e. the difference of equilibrium deposition and present deposition. There is evidence that the equilibrium deposition is dependent on the protein concentration next to the membrane. However, it is not yet clear which isotherm best describes the adsorption behaviour let alone empirical data being available for the present combination of protein and membrane (Nakanishi et al., 2001).

Here we assume that the equilibrium deposition is equivalent to an ideally packed protein monolayer, which agrees well with the measured depositions in our experimental conditions.

The shape of a BSA molecule is estimated to be rectangular shaped in an end-on configuration:

$$q_{eq} = q_{ml} \approx \frac{1}{a \cdot N_A} \tag{6.16}$$

These assumptions then allow us to calculate the rate constant A from the passive adsorption tests.

$$A = -\frac{\ln\left(1 - \frac{q_{passlh}}{q_{eq}}\right)}{c_m^k \cdot 3600}, \quad c_m = c_0 = \text{const.} \tag{6.17}$$

The resistance to flow is often described by a power law based on deposition. We used a linear relationship (n = 1) derived from passive adsorption data, assuming that the adsorption gradually blocks the membrane surface until a monolayer is built-up:

$$B = \left(\frac{TMP}{\mu_w J_{MQpasslh}} - R_m\right) \cdot \frac{1}{q_{passlh}} \tag{6.18}$$

The only missing parameter within this fouling model - the reaction order k – is adjusted for best agreement of the simulation with the experimental data (i.e. J_{exp} at standard conditions).

Table 6.4 summarizes the model parameters.

Table 6.4. Parameters for adsorption reaction

Property	Value	Units
K	0.6	-
q_{eq}	1.16×10^{-7}	mol m^{-2}
A	0.00225	$m^{1.8}$ s^{-1} $mol^{-0.6}$
N	1	-
B	7×10^{19}	m mol^{-1}

6.4.2. Hydrodynamic Model

Mass transfer within the membrane module is modelled with a transient finite volume code on a 2D grid assuming symmetry at half channel height. Figure 6.2 shows a schematic of the channel model used for the mass transfer simulations.

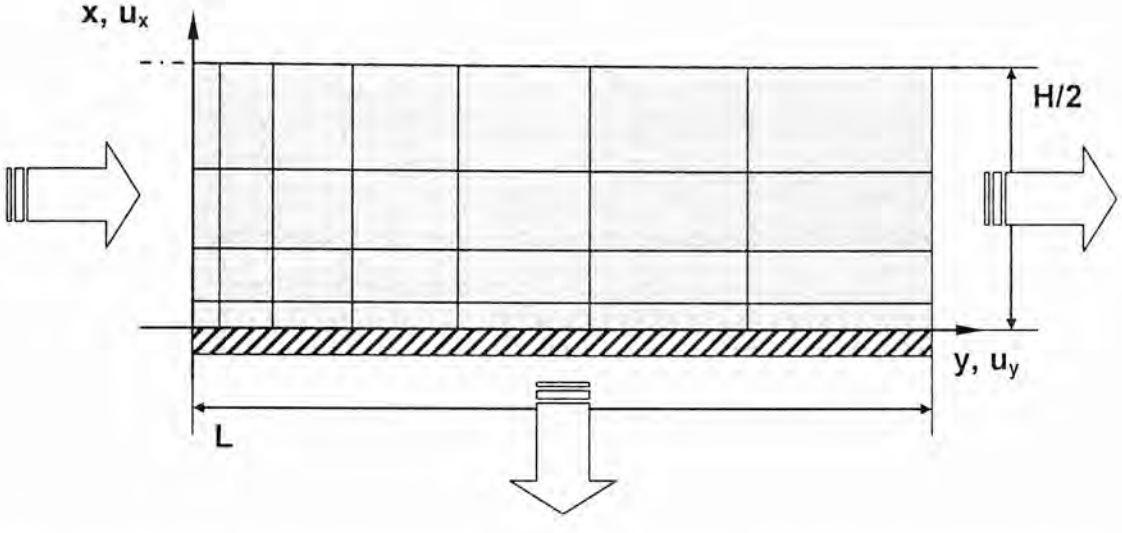

Figure 6.2. Schematic drawing of the channel as modelled for the simulations

By introducing a non-uniform grid, the resolution at the channel inlet and along the membrane can be increased to refine the results for entrance effects and the boundary layer. The simplification to two dimensions saves computational time and is reasonable due to the low aspect ratio of the channel. The equations to be solved are:

Mass conservation (constant density):

$$\frac{\partial u_x}{\partial x} + \frac{\partial u_y}{\partial y} = 0$$

Momentum conservation, x direction:

$$\frac{\partial u_x}{\partial t} = -\frac{\partial u_x u_x}{\partial x} - \frac{\partial u_x u_y}{\partial y} - \frac{1}{\rho}\frac{\partial p}{\partial x} + \frac{\partial}{\partial x}\cdot\left(\frac{\mu}{\rho}\cdot\left[\frac{\partial u_x}{\partial x} + \frac{\partial u_x}{\partial x}\right]\right) + \frac{\partial}{\partial y}\cdot\left(\frac{\mu}{\rho}\cdot\left[\frac{\partial u_y}{\partial x} + \frac{\partial u_x}{\partial y}\right]\right)$$

Momentum conservation, y direction:

$$\frac{\partial u_y}{\partial t} = -\frac{\partial u_y u_y}{\partial y} - \frac{\partial u_x u_y}{\partial x} - \frac{1}{\rho}\frac{\partial p}{\partial y} + \frac{\partial}{\partial y}\cdot\left(\frac{\mu}{\rho}\cdot\left[\frac{\partial u_y}{\partial y} + \frac{\partial u_y}{\partial y}\right]\right) + \frac{\partial}{\partial x}\cdot\left(\frac{\mu}{\rho}\cdot\left[\frac{\partial u_x}{\partial y} + \frac{\partial u_y}{\partial x}\right]\right)$$

Species conservation:

$$\frac{\partial c}{\partial t} = -\frac{\partial u_x c}{\partial x} - \frac{\partial u_y c}{\partial y} + \frac{\partial}{\partial x}\left(D\cdot\frac{\partial c}{\partial x}\right) + \frac{\partial}{\partial y}\left(D\cdot\frac{\partial c}{\partial y}\right)$$

The transient terms are solved using the Implicit Euler Method; the continuity condition (mass conservation) is established using the Semi-Implicit Method for Pressure-Linked Equations (SIMPLE) pressure correction method. The Hybrid Central Differences/Upwind Scheme is applied for the convective and diffusive terms:

- $|Pe|>2$: UDS (Upwind Differencing Scheme) for convection
- $|Pe|<2$: CDS (Central Differencing Scheme) for convection and diffusion

The latter choice agrees with results from (Geraldes et al., 2000). They compared different discretisation schemes for solution of the conservation laws in cross flow channels and found this hybrid scheme to be most suitable.

The boundary conditions for the conservation equations are of central importance and are discussed in detail.

Table 6.5. Spatial boundary conditions

Boundary	Momentum, x direction	Momentum, y direction	Concentration
y=0, ∀x	$u_x=0$	$u_y=u_{y0}$	$c=c_0$
y=L, ∀x	$\partial u_x/\partial y=0$	$\partial u_y/\partial y=0$	$\partial c/\partial y=0$
x=0, ∀y	$u_x=-J$	$u_y=0$	$D\cdot\partial c/\partial x=-J\cdot c + dq/dt$
x=H, ∀y	$u_x=0$	$\partial u_y/\partial x=0$	$\partial c/\partial x=0$

At the channel outlet, zero gradients for momentum and concentration with respect to the cross-flow direction are prescribed. This assumption seems to be suitable, as both the velocity and the concentration profiles are nearly constant at the channel outlet. For solution of the pressure correction, the pressure at channel outlet is prescribed. The boundary condition for the mass and momentum conservation equations at the membrane is calculated from the local water flux. The permeate pressure is assumed to be the surrounding atmospheric pressure. The scenario of gel or cake formation and the relevant boundary condition is not discussed here as the gelling limit was not reached in any case.

The transient boundary condition was chosen to agree with the empirical procedure (Start-up A): first the steady state cross-flow of protein solution without permeation (TMP = 0) is calculated to determine the conditions at $t = 0$. At $0 < t < t_R$ the start-up of filtration is simulated by a ramp function of TMP (by linearly decreasing the permeate pressure) followed by the transient calculation of concentration polarization and flux decline at constant TMP. A second scenario (Start-up B) was implemented to reveal the influence of start-up conditions on the simulation results: steady state calculation of cross flow and permeation of pure water at constant TMP ($c_0 = 0$) followed by a step function of BSA concentration at $t = 0$ and transient calculation of concentration polarization and flux decline at constant TMP.

6.4.3. Geometry and computational mesh

All simulations and corresponding experiments performed were based on the following channel geometry in Table 6.6.

Table 6.6. Channel geometry

Sections	Dimension, m
Length	0.5
Breadth	0.04
Height	0.0015

The spatial grid and the time step were optimized with respect to computational time by a grid-independence study. The parameter set of choice is 80 by 200 cells in the x and y – directions at a time step of 0.01 s. This corresponds to ~1 s computational time per time step on a Pentium 4 (2.5 GHz) CPU. The small time step is explained by the steep flux decline as the concentration polarization is building up. The calculations could be accelerated by variable time steps, which would be beneficial with respect to future long-term simulations at fully developed concentration profiles. The solution was found to be sensitive to the ratio of crossflow and permeate flow; the smaller the ratio the higher the grid resolution necessary in y – direction to achieve convergence.

6.5. Results and Discussions

6.5.1. Effects of operating conditions on final UF flux (J_{uf})

The effects of pH, concentration and cross-flow rate on relative fluxes (J_{uf}/J_i) are shown in Figures 6.3, 6.4 and 6.5 respectively, using solutions with and without added salt. The final UF flux (J_{uf}) was recorded after 1 hour of UF under various operating conditions. There were

generally trace amount of BSA detected in the permeate solution however a 100% rejection can be safely assumed. BSA rejection results are shown in Appendix D.

For both feed solutions with and without added salt, highest BSA concentration in the final feed was observed at pH 7.4, where the permeate flux is observed highest at constant TMP of 50kPa (Figures 6.3 and 6.4). The high flux was caused by reduction of concentration polarization due to the same charges between BSA and membrane causing electrostatic repulsion effect between them. It was found that the UF flux dependence with pH was more pronounced for no salt added solutions (Figure 6.3). On the other hand, the response of flux to feed concentration and flow was significant for solutions with added salt (Figures 6.4 and 6.5). In all three experiments, the flux declines instantly at the introduction of BSA, followed by a gradual decrease of flux with time. In addition, Figure 6.3 also shows the buffering effect of Na^+ and Cl^- ions in the added salt solution to small increase of relative flux to pH. On the whole, solutions with added salt have lower UF flux (J_{uf}) than solutions without added salt. The lowest relative flux was observed at pH 4.5 where strong concentration polarization and fouling occurs. At pH 7.4, the relative flux was the highest indicating low fouling and deposition.

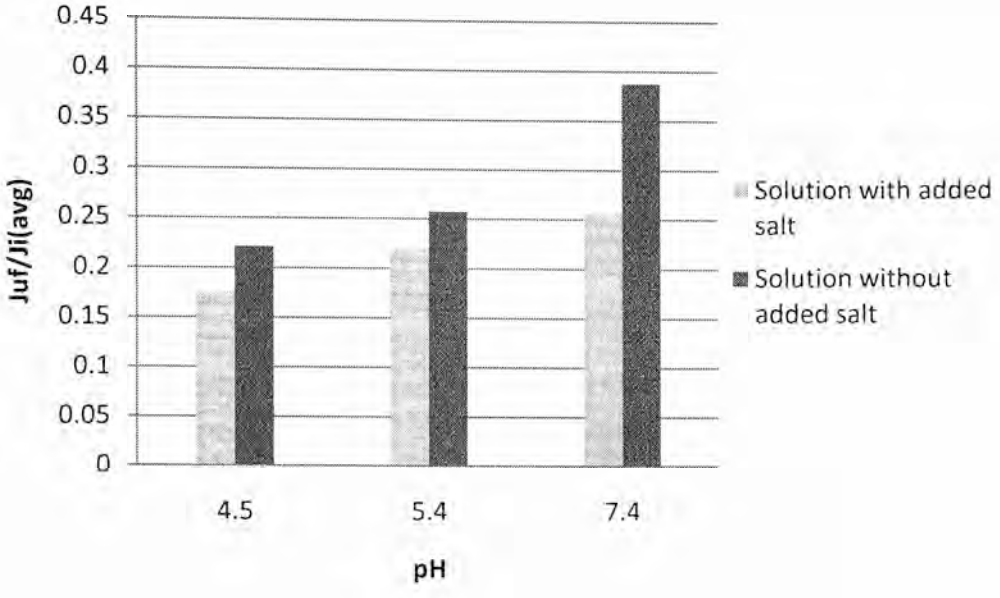

Figure 6.3 Relative fluxes (J_{uf}/j_i) Vs. Solution pH
(1hr, 50kPa TMP, 1.05×10^{-5}M BSA in 0.0M/0.15M NaCl, 500mL.min^{-1})

Figure 6.4 shows the effect BSA feed concentration to the relative flux demonstrating a trend of decreasing relative flux to increasing concentration. At 0.0714g.L^{-1}, the effect of added salt decreasing the relative flux as observed at 0.714 and 7.14g.L^{-1} concentrations did not occur. This was because the concentration of BSA was too low even to have any reaction with the added salt. Instead, an opposite effect of higher relative flux was observed at very low concentration. Also, from standard deviation measurements, feed concentration has the biggest effect in causing a flux decline due to the additional cake resistance on the membrane surface.

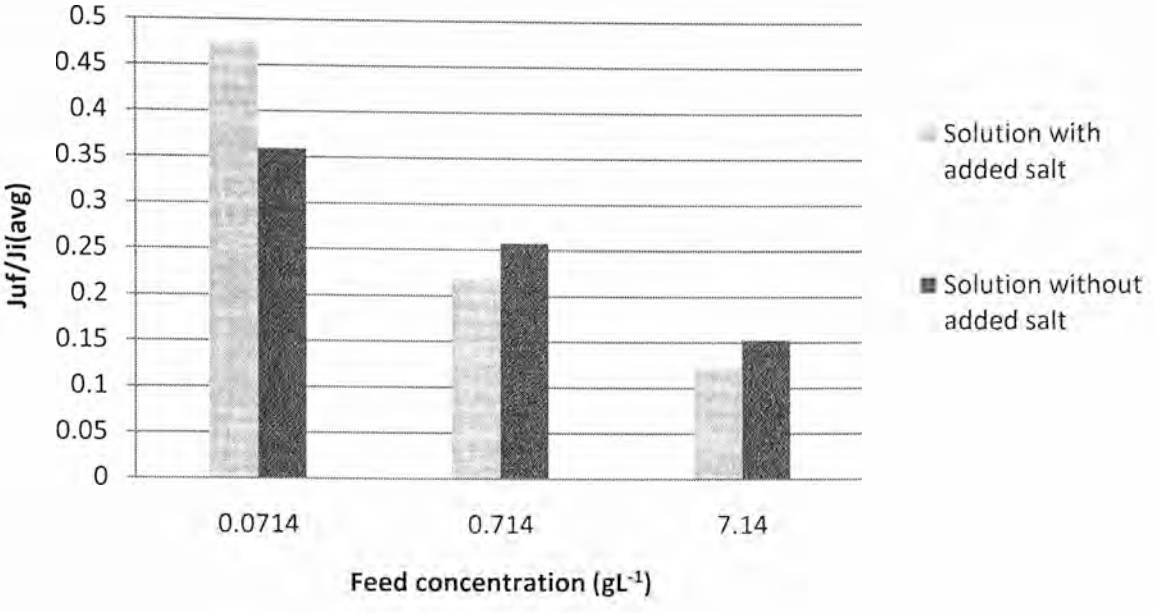

Figure 6.4 Relative fluxes vs. BSA feed concentration at pH 5.4 (1hr, 50kPa TMP, pH 5.4, 0.0M/0.15M NaCl, 500mL.min^{-1})

In Figure 6.5, high flow-rate (1000mL.min^{-1}, Re = 903, pH 5.4) causes high relative fluxes for both added or no added salt solutions proving that high flow lowers concentration polarization and fouling. Solutions with added salt were not as sensitive to cross flow rate as salt added solution which shows an increasing trend with flow-rate.

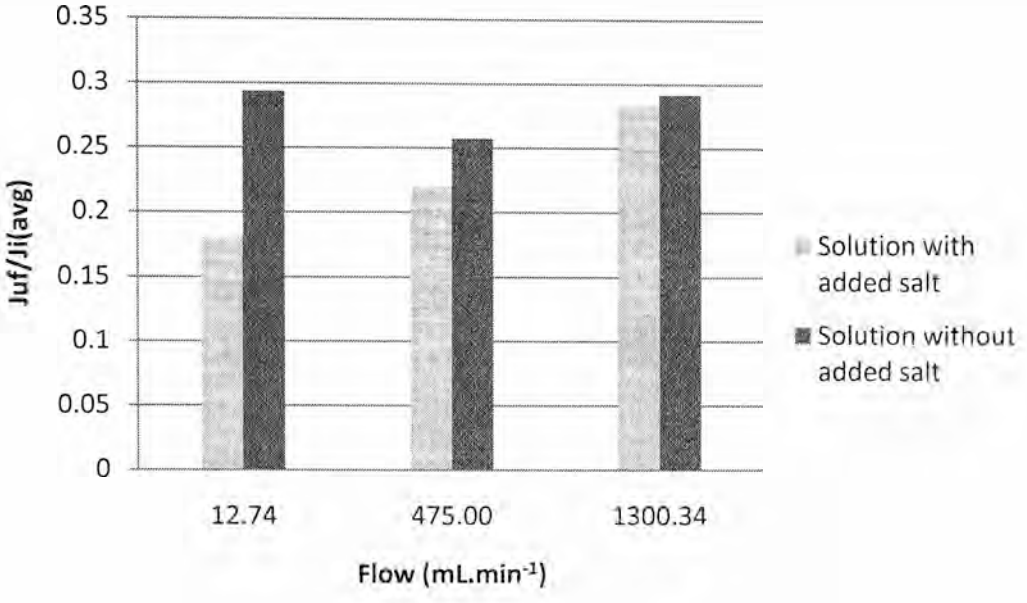

Figure 6.5 Relative fluxes vs. Cross flow-rate at pH 5.4
(1hr, 50kPa TMP, pH 5.4, 0.0M/0.15M NaCl)

In summary, steady state flux decreases with increasing feed protein concentration, increases with increasing feed volume flow, and slightly increases with increasing pH. Generally, solutions with no-added salt have higher fluxes than added salt at all the conditions tested.

6.5.2. BSA deposition after ultrafiltration and passive adsorption

The total BSA deposition was measured using Lowry method to analyse the effect of operating conditions on the horizontal deposition profile along the membrane. Figure 6.6 shows BSA deposition (per cm^2) along the membrane from the inlet to the outlet at various pH in no salt added solution. The deposition was randomly fluctuating in a range of about 0.8 – 1.4μgcm^{-2} along the membrane length because of aggregation and uneven initial deposition of BSA along the membrane surface. The average deposition (no-added salt) for pH 4.5, 5.4 and 7.4, are 1.04 ± 0.156, 1.07 ± 0.106 and 1.1 ± 0.096 μgcm^{-2}, respectively. As the difference in average deposition was small, we can safely conclude that BSA deposition on membrane

surface is independent of pH in solution without added salt at this operating condition.

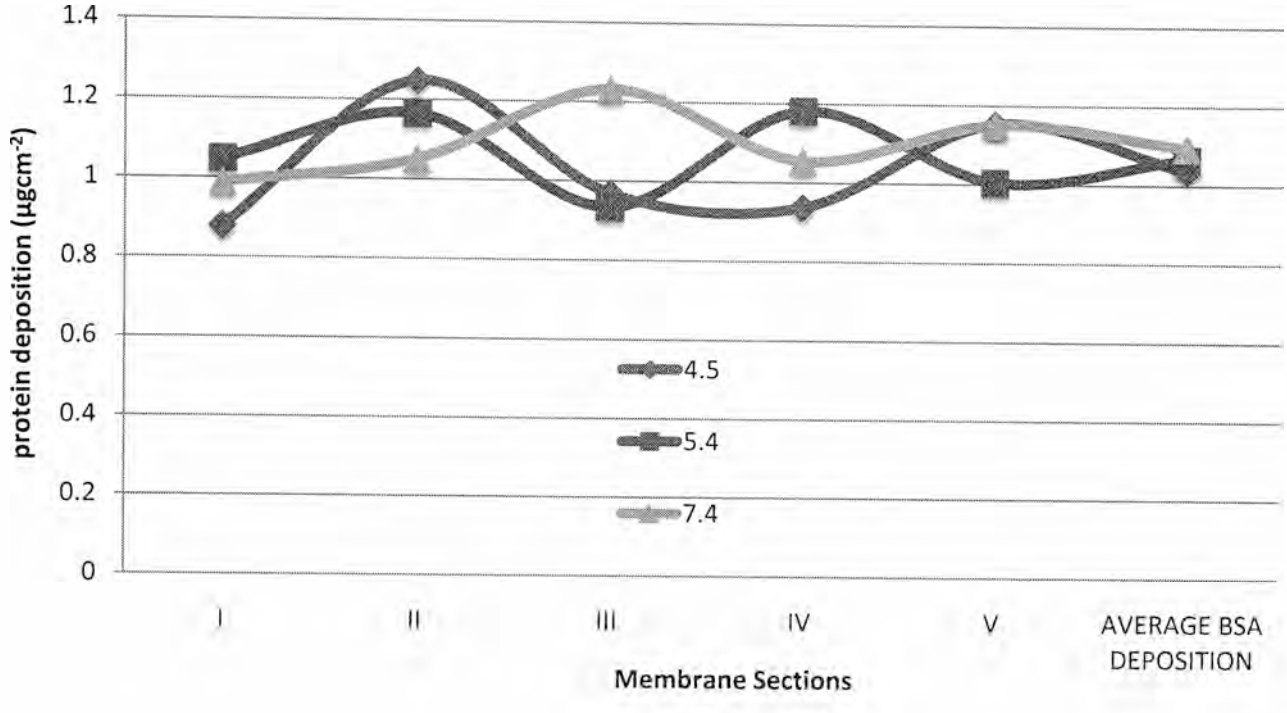

Figure 6.6 Deposition of BSA on the membrane at various pH after Ultrafiltration (Solution without added salt, 1hr, 50kPa TMP, pH 5.4, 0.0M NaCl, 500mL.min^{-1}, lines to guide the eye)

With solutions with added salt shown in Figure 6.7, there was a strong influence of pH on the protein deposition along the membrane surface. The average BSA deposition was the highest at pH 5.4 and it causes the low relative flux at pH 5.4 as observed earlier in Figure 6.3. Also at pH 5.4, the deposition looks flatter and smoother compared to the deposition at pH 4.5 and 7.4. Also, the fluctuations in solutions with added salt (Figure 6.7) were not as severe as no added salt solutions (Figure 6.6) showing the dampening effect of added salt to pH charges. Thus, similar to the UF flux, the shielding effect of salt also minimizes the effect of electrostatic charges to the BSA deposition. This shielding phenomenon was also observed in past studies (Suki et al., 1983). By looking at the average deposition for both figures, BSA deposition in solution with added salt was lower than solutions without added salt,

demonstrating the effect of salt in shielding electrostatic charges between the protein and membrane resulting in higher deposition. In addition, added salt may contribute to additional BSA solubility in solution if the pH is near the iso-electric point of BSA (i.e.p 4.9)(Chan and Chen, 2001). The relative flux for solution with salt added after 1 hour was the lowest at pH 4.5 (Figure 6.3) however the deposition is the lowest. Therefore, the BSA deposition on the membrane surface does not qualitatively reflect the final measured flux. This shows the complexities of BSA solutions and membrane interactions.

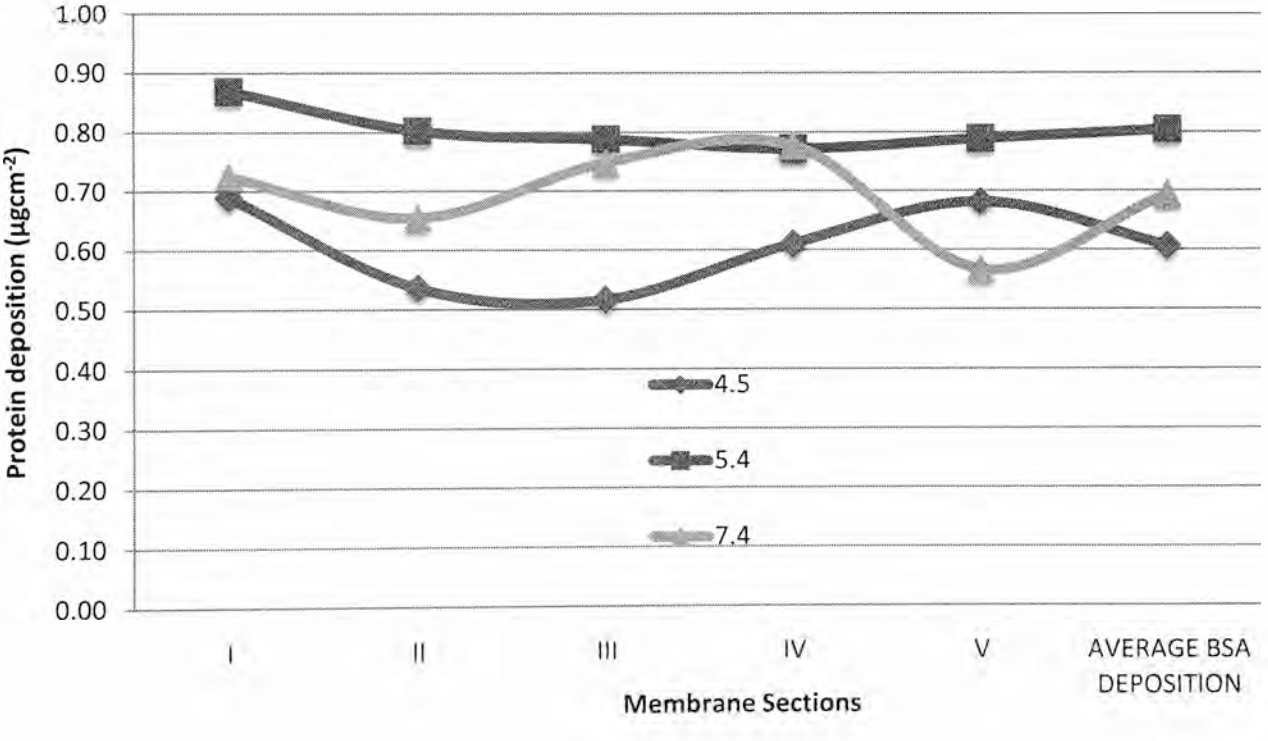

Figure 6.7 Deposition of BSA on the membrane at various pH after UF (Solutions with added salt,1hr, 50kPa TMP, pH 5.4, 0.15M NaCl, 500mL.min^{-1}, lines to guide the eye)

In conclusion, random deposition of BSA along the membrane surface was found with and without added salt. This has been observed in past studies and may be mainly caused by the

uneven initial deposition and aggregation of BSA on the membrane surface. In addition, the entrance and exit effect did not influence the deposition along the membrane. Solutions with added salt have a lower average final flux (J_{UF}) and however higher average deposition was measured. This shows that although the deposition was high, the flux was not affected.

In the following sections, experiments were performed mainly on BSA feed solution with added salt because of the availability of literature values for comparisons.

6.5.3. Resistance analysis

The steady state J_i, J_{UF}, and J_{MQUF} was measured and the resistances by concentration polarization, fouling and passive adsorption were calculated using Eqn. 6.6 and the method is described in Section 6.4.1. The resistances were plotted in Figure 6.8 showing the individual measured resistance contributed by concentration polarization, fouling and total resistance based on 1 hour of UF at various pH 4.5, 5.4 and 7.4. For all the pH tested, the contribution of fouling (R_F) was greater than concentration polarization (R_{CP}). R_F decreases with increasing pH while R_{CP} increases. Therefore, less deposition is expected at high pH, which is shown in Figure 6.7 where the BSA deposition was less at pH 7.4 than at pH 5.4. Interestingly, in Figure 6.8, R_F was the greatest at pH 4.5 compared to R_{CP} (although the deposition was lowest as shown in Figure 6.7) due to the opposite charges between the membrane and protein in solution. At pH 5.4, the R_{CP} was the highest compared to pH 4.5 and 7.4.

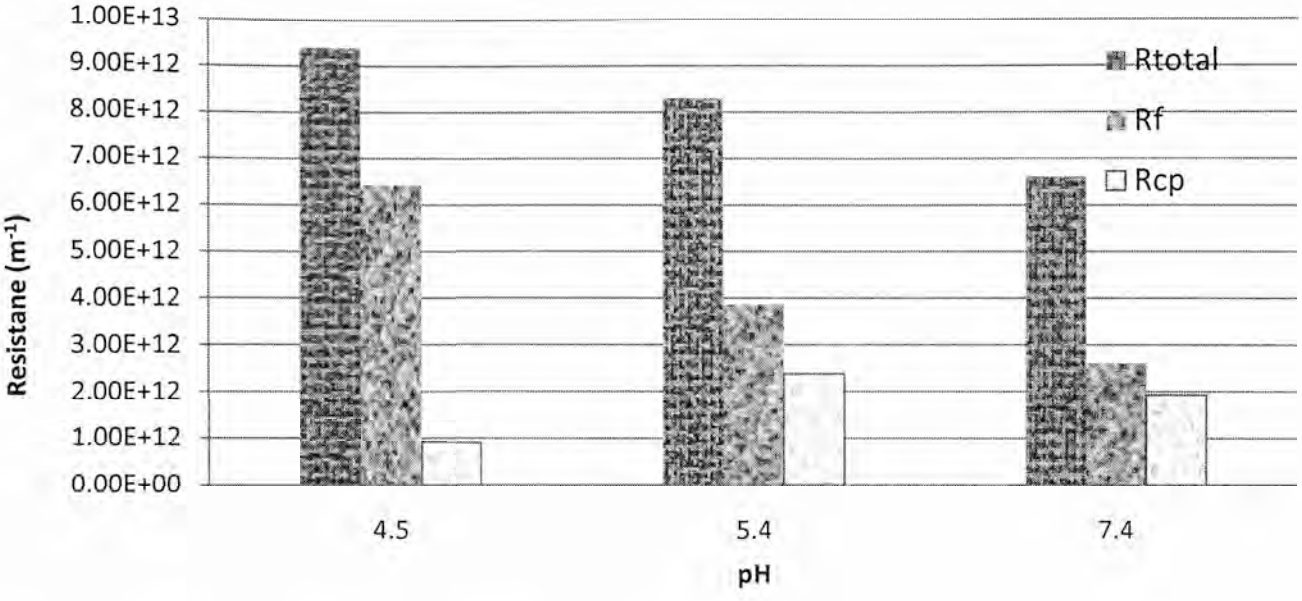

Figure 6.8 The variation of various resistances with pH
(1hr, 50kPa TMP, pH 5.4, 1.05×10^{-5}M BSA in 0.15M NaCl, 500mL.min^{-1})

Passive adsorption tests were carried out to determine the contribution of passive adsorption (R_P) to the total resistance (R_T). The membrane was exposed with BSA at standard conditions at atmospheric pressure for an hour, followed by a Milli-Q flux (J_{MQP}) measurement. J_{MQP} was used to calculate R_P. Analyses of various resistances – R_M, R_F, R_{CP}, R_P, and R_T are shown in different comparable cases (A and B) in Figure 6.9.

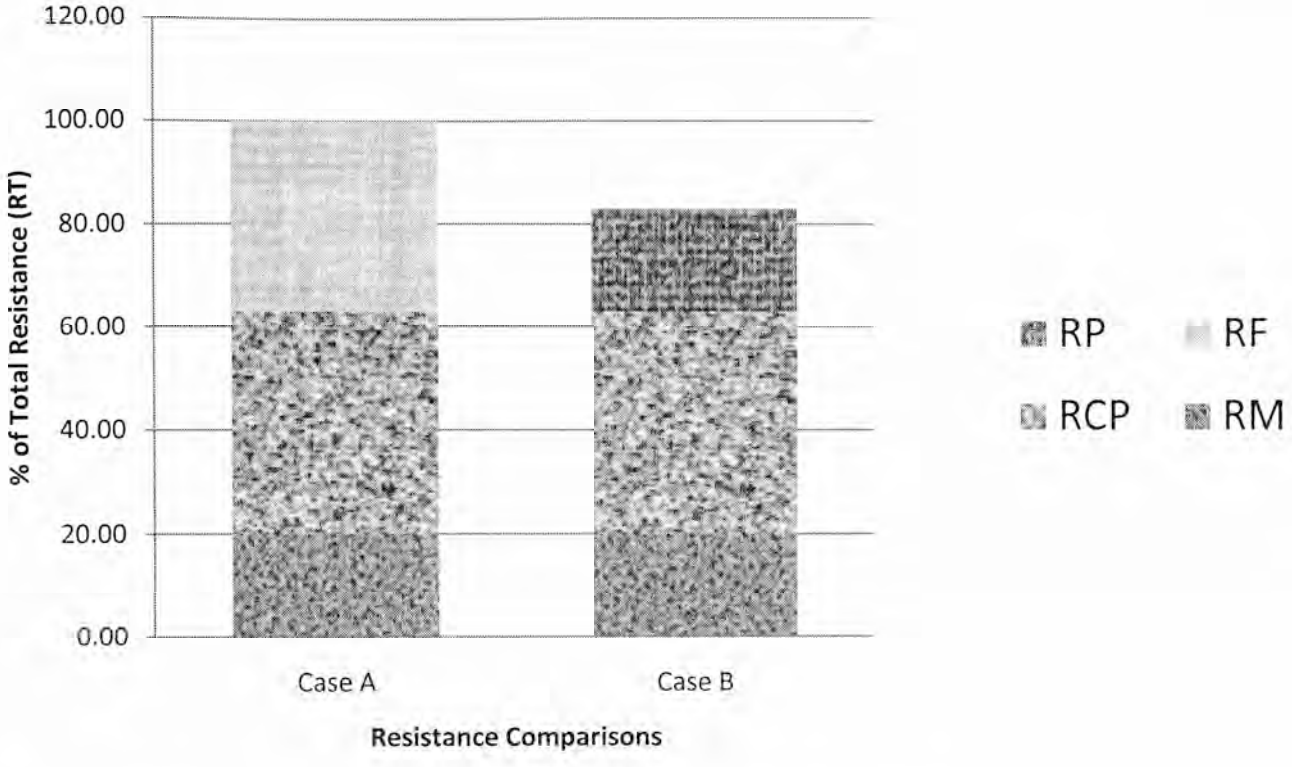

Figure 6.9 The variation of various resistances – R_P, R_F, R_{CP} and R_M.
(1hr, 50kPa TMP, pH 5.4, 1.05×10^{-5}M BSA in 0.15M NaCl, 500mL.min^{-1})

Case A distinguished the overall resistance (100% R_T) contributed during the UF of BSA solution at standard condition and is made up of R_M, R_{CP} and R_F. Case A shows that concentration polarization (R_{CP}) is the main contributor to the overall flux decline and R_T. Also, R_F and R_{CP} was almost equal for this case indicating the importance of both towards flux decline. Case B distinguishes the percent resistance of R_T provided by R_{CP} and R_P. Case B shows that R_{CP} is larger than R_P, however R_P was almost equivalent to R_M. The additional resistance might be a result of re-deposition of loose BSA during MQ flux measurement (J_{MQP}) to obtain R_P. Thus, under the absence of pressure, BSA still attaches itself strongly onto the membrane surface, causing resistance almost as high as fouling resistance with pressure.

6.5.4. CFD Simulation

The results of the CFD simulation are described in Table 6.7.

Table 6.7. Collected data, standard conditions printed bold

pH	V_0	c_0	J_{MQ0}	$J_{exp,1h}$	$J_{sim,nf,1h}$	$J_{sim,f,1h}$	$q_{exp,1h}$	$q_{sim,1h}$
-	$L\ h^{-1}$	$mmol\ m^{-3}$			$L\ m^{-2}\ h^{-1}$			$10^{-8}\ mol\ m^{-2}$
4.5	24.2	10.5	96.1	17.4	41.5	19.8	4.4	11.3
5.4	**19.1**	**10.5**	**94**	**19.3**	**43.3**	**19.6**	**5.8**	**11.3**
7.4	21.8	10.5	101.6	26	48.1	20	5	11.3
5.4	20.9	1.05	101.2	42.6	89	23.2	3.6	9.7
5.4	15.2	105.0	92.9	12	18	15.2	9.1	11.6
5.4	1.1	10.5	93	17.4	n.a.	n.a.	4.9	n.a.
5.4	73.9	10.5	94.9	25	64.3	20.5	5.4	10.8

The second set of calculations performed were the actual simulations of the experiments (see Table 6.7). Every experiment (exp) was simulated with fouling (sim,f) and without fouling (sim,nf, adsorption reaction deactivated). This way the contribution of concentration polarisation and fouling to flux decline, as well its dependence on the operating conditions were to be assessed. For all cases, the simulations revealed that the flux is governed by the solution osmotic pressure and that the gelling concentration was not exceeded.

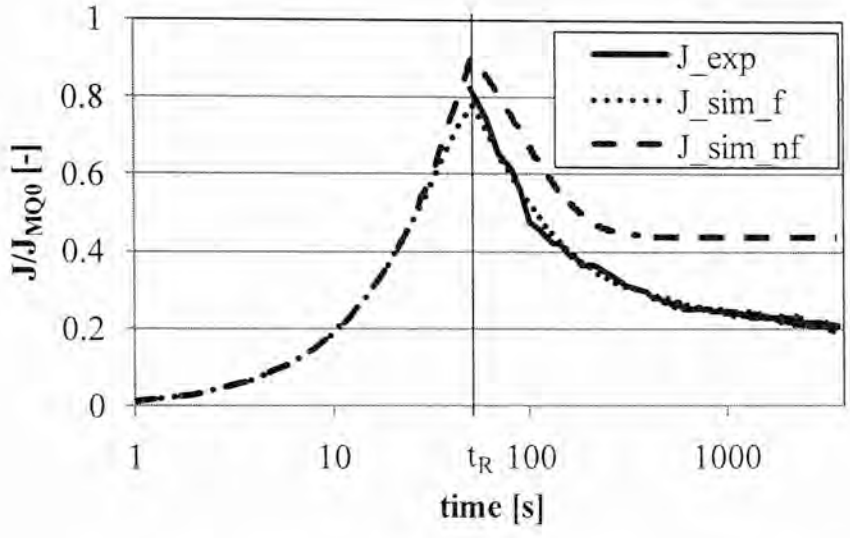

Figure 6.10 Experimental and simulated fluxes at standard conditions

Figure 6.10 shows the experimental and simulated fluxes as a function of time at standard conditions. The first reliable experimental data are produced at ~ 50 s; before that the flux - the gradient of weighed permeate mass with respect to time - is distorted by the dead volume of the permeate collection as well as start-up effects. As found by many researchers (e.g. (Gekas et al., 1993)), the flux decline is strong in the initial phase, tapering off towards experiment end.

Both simulated fluxes rise according to the installed ramp function for TMP. After t_R, the non-fouling flux decreases as the concentration boundary layer is forming until steady state is reached at ~ 300 s. The fouling flux reveals a considerable amount of fouling at t_R and agrees with the experimental flux. This agreement is remarkable as only one parameter – the reaction k – was adjusted.

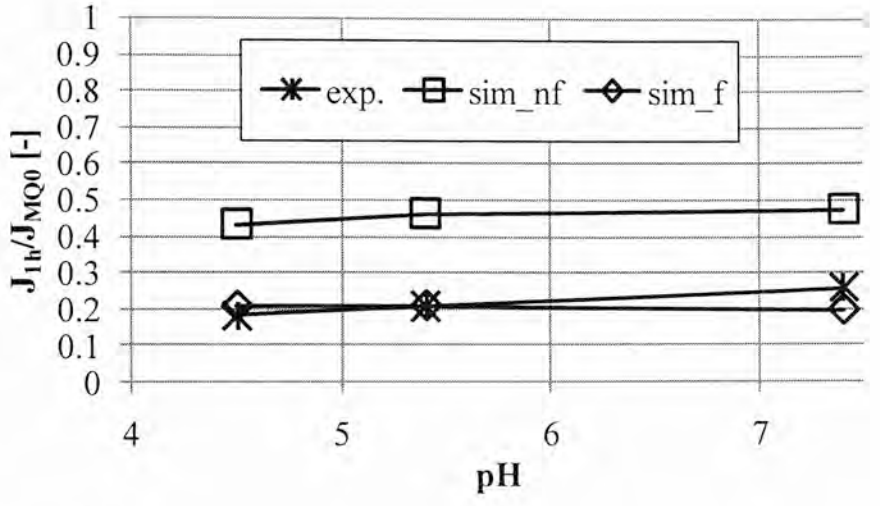
1
0.9
0.8
0.7
0.6
0.5
0.4
0.3
0.2
0.1
0
exp.
sim_nf
sim_f
J_{1h}/J_{MQ0} [-]
4
5
6
7
pH

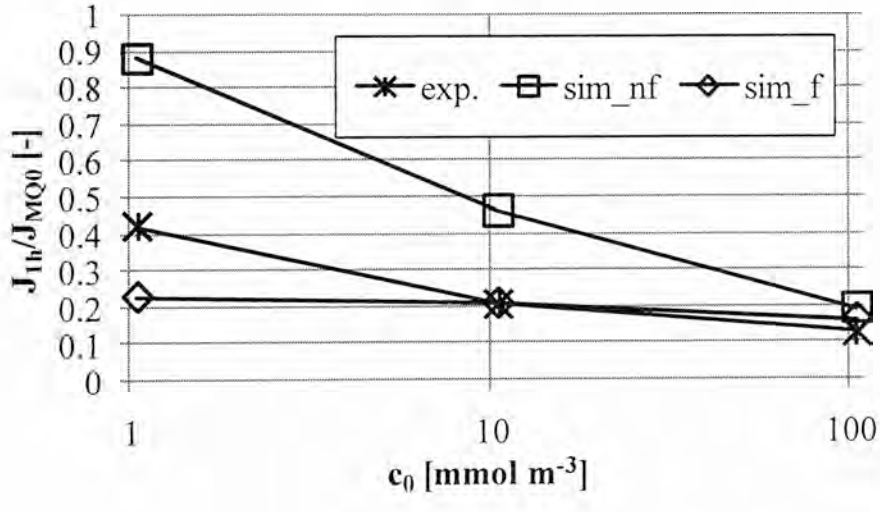
1
0.9
0.8
0.7
0.6
0.5
0.4
0.3
0.2
0.1
0
exp.
sim_nf
sim_f
J_{1h}/J_{MQ0} [-]
1
10
100
c_0 [mmol m^{-3}]

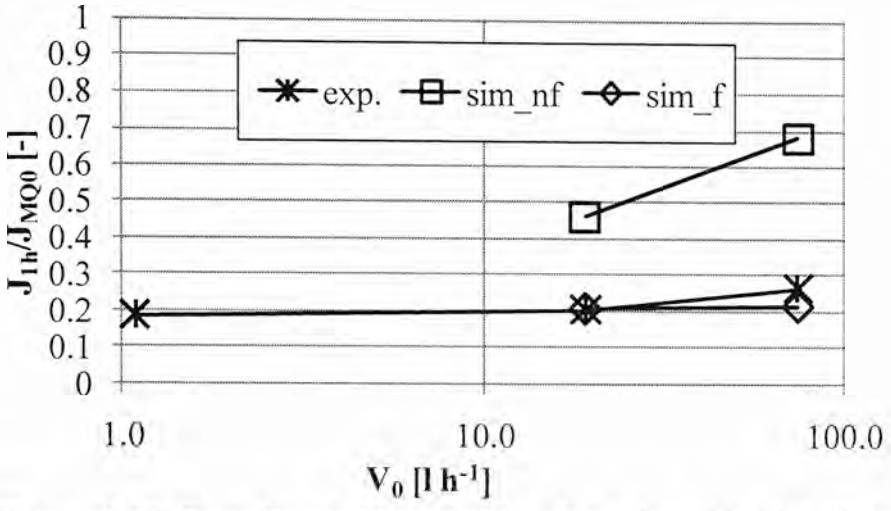

Figure 6.11. Experimental and simulated results with (sim_f) and without fouling (sim_nf) for the relative flux after one hour at varying operating conditions (lines to guide the eye)

Figure 6.11 shows the experimental results (also shown in Figure 6.4 and 6.5) and simulated results for the flux after one hour as listed in Table 6.7. The non-fouling simulations reached steady state after 120 to 600 s; the simulations for the low feed volume flow did not converge due to the very low ratio of cross-flow and permeate flow.

The experimental data reveals the following trends (listed with decreasing significance): flux decreases with increasing feed protein concentration, flux increases with increasing feed volume flow, flux slightly increases with increasing pH. The simulations qualitatively agree with these trends. The non-fouling simulations, i.e. the concentration polarization, show a very strong dependence on the operating conditions while the operating conditions are having only a minor impact on the fouling simulations; same is true for the simulated protein deposition ($q_{sim,\ 1h}$ in Table 6.7). These results imply that the concentration polarization is underestimated in the fouling simulations. This issue will now be discussed in detail. Rewriting equation 6.15 as follows allows the evaluation of the different resistances to trans-membrane flow (Eqn 6.19).

$$J = \frac{TMP - \pi(c_m)}{\mu_w \cdot (R_m + R_f[q])} = \frac{TMP}{\mu_w \cdot (R_m + R_f[q] + R_{CP})} \qquad (6.19)$$

R_{CP} in the experiment is determined by comparing the flux after one hour UF operation and the pure water flux through an equally fouled membrane. Remarkably, a fouling layer on the magnitude of a monolayer is causing nearly twice the clean membrane resistance. In the simulation, R_{CP} can be calculated as R_F in the simulation result. As shown in Figure 6.12, R_{CP} is underestimated in the simulation while R_F is over-predicted which is also evident from the deposition data in Table 6.7. Possible explanations for these deviations are (a) errors in the mass transfer model, i.e. the physical property models, (b) additional polarization effects not yet understood. As the physical property models were chosen very carefully, we tend to follow the latter option.

This finding together with the detailed analysis of the single resistances occurring revealed that the concentration polarisation was under predicted in the simulation. This phenomenon has been detected before; its most probable explanation is the neglect of membrane-solute-solvent interactions

The main conclusion from these findings was that concentration polarisation must be considered even at low trans-membrane fluxes. The next steps towards better prediction of this phenomenon are (a) replacing the convection-diffusion equation for BSA by suitable multi component transport equations for BSA and ionic species, (b) spatial resolution of the membrane including the corresponding conservation balances.

Concluding, a reliable predictive design tool for practical systems seems not yet to be within reach at the moment. However, we believe that simulation aiming for *ab initio* predictions provide a valuable service in understanding the complex phenomena involved at filtration separation of macromolecular solutions.

In the CFD simulation, R_{CP} was underestimated while R_F was over estimated. The comparison between CFD and experiment is shown in Figure 6.12 (Experiment also shown in Figure 6.9).

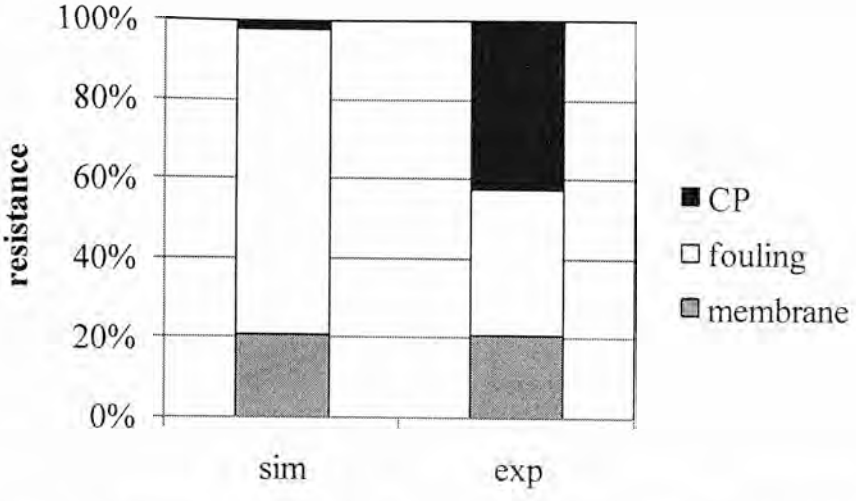

Figure 6.12 The Resistance to flux at 1h for standard conditions (1hr, 50kPa TMP, pH 5.4, 1.05×10^{-5}M BSA in 0.15M NaCl, 500mL.min^{-1})

6.5.5. Theoretical wall concentration, diffusivity and mass transfer coefficient

In this section, the wall concentration C_W, diffusivity, D and mass transfer coefficient, k are estimated at pH 4.5, 5.4 and 7.4. Two conditions were applied, "fouling" and "non-fouling" using subscripts $_{NF}$ and $_F$ respectively, as additional subscripts to C_W, D and k. At "non-fouling" condition, the theoretical J and C_W were estimated using R_M (Eqn. 6.13) while at "fouling" condition R_F was used (Eqn. 6.12). The methods of calculating J and C_W for "fouling" and "non-fouling" conditions are described in Section 6.4.2. The comparison between these two conditions was performed to determine the effect of neglecting the effect of fouling when estimating C_W, D, and k.

The findings are shown in Figure 6.13, where C_{WF} and C_{WNF} were plotted against pH. From the calculations, as pH increase, C_{WF} increases while C_{WNF} decreases.

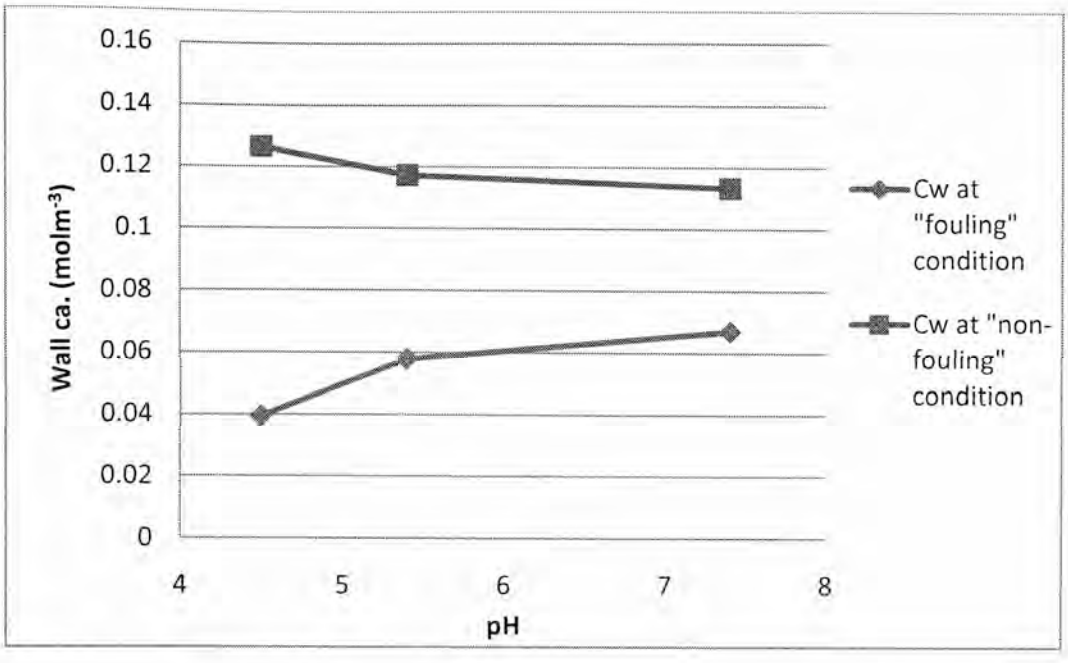

Figure 6.13 The variation of wall concentration with pH at fouling and non-fouling conditions (1hr, 50kPa TMP, pH 5.4, 1.05×10^{-5}M BSA in 0.15M NaCl, 500mL.min^{-1}, lines to guide the eye)

Under "fouling" condition, the estimated C_{WF} was dependent on the fouling resistance, R_F and osmotic pressure (Eqn. 6.12). In addition, J_F also increases with pH (Figure 6.3) while R_F decreases with pH (Figure 6.8). From Figure 6.13, it was found that C_{WF} decrease with the increase in pH.

In "non-fouling" condition, the theoretical flux (J_{Theory}) was not affected by R_M which stays constant with the increase in pH. However J_F increases with pH and osmotic pressure increases with C_W. Thus, to match i.e. obtain zero difference between J_{Theory} and J_F which increases with pH, the osmotic pressure and the C_{WNF} has to decrease with pH. Therefore, from Figure 6.13, a decrease in C_{WNF} occurs with the increase in pH. C_{WNF} is generally higher than C_{WF}, due to the neglect in fouling resistance R_F. Doing so adds an error to the estimation of wall concentration, thus "non-fouling" condition was unreliable.

The relative theoretical wall concentration under "fouling" condition (C_{WF}) and relative total BSA deposition measured by Lowry method are compared and shown in Figure 6.14 to look

for trends. Both instances shows an increasing trend with pH, however the increase in BSA deposition with pH is more gradual.

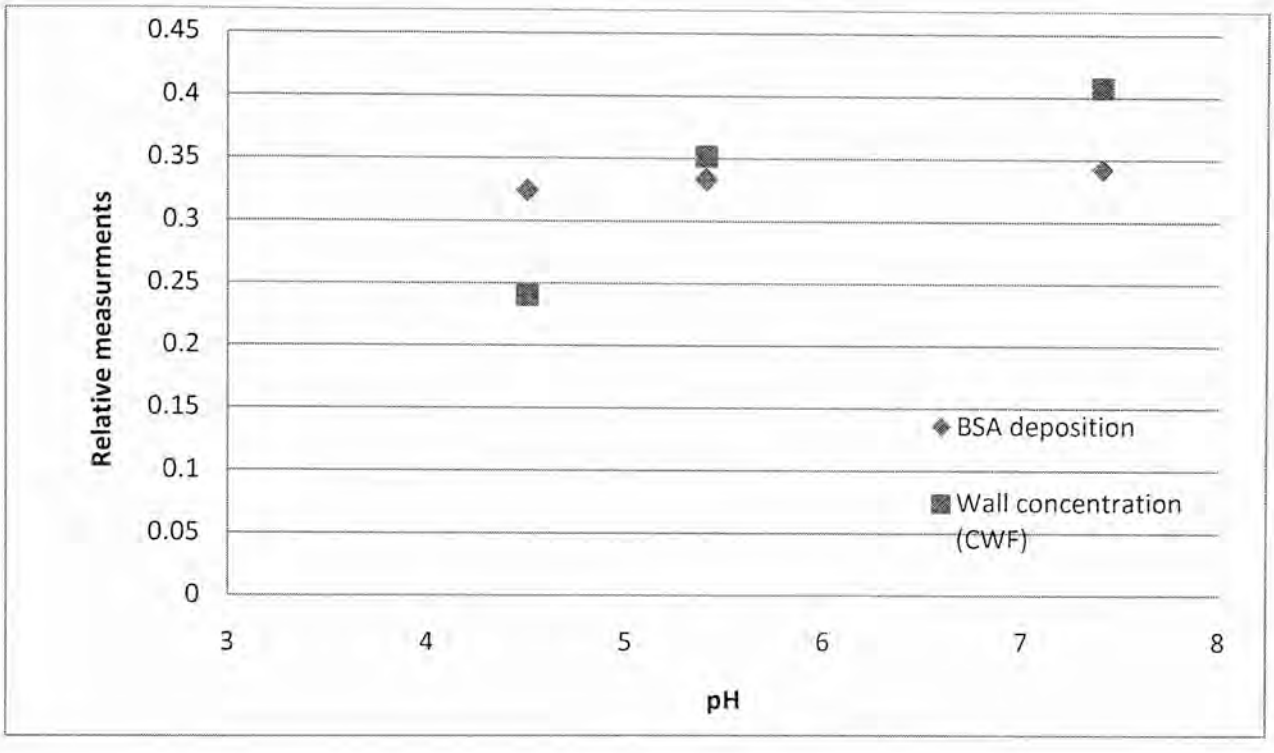

Figure 6.14 The variation of relative wall concentrations and deposition with pH (Fouling conditions, 1hr, 50kPa TMP, pH 5.4, 1.05×10^{-5}M BSA in 0.15M NaCl, 500mlmin^{-1})

The diffusivities (D) at "fouling condition" that correspond to the estimated C_{WF} using two different methods of calculations are shown in Figure 6.15. The equations applied to calculate "D from experiments" is (Eqn. 6.11) which is directly influenced by mass transfer models while "D from CFD" is (Eqn. 6.4) based on (Gaigalas et al., 1995). As shown in Figure 6.15, both methods gave almost similar diffusivities however "D from CFD" was generally lower than "D from experiments". The highest diffusivity from experiments occurred at pH 4.5 from the experiment with a reading of 2.935×10^{-10} m^{2}s^{-1}. The average diffusivity for all three pH was 2.8×10^{-10} m^{2}s^{-1}. The ideal diffusivity (at infinite dilution) was 6.7×10^{-11} m^{2}s^{-1} which was lower than the diffusivities obtained from these two methods (Shen and Probstein, 1977). This is because at ideal, the complex physical properties of BSA are not accounted for. The

diffusivity readings for all conditions were very similar to the literature (Chen, 1998). The calculated average k for "fouling" condition is 3.546×10^{-6} ms^{-1}.

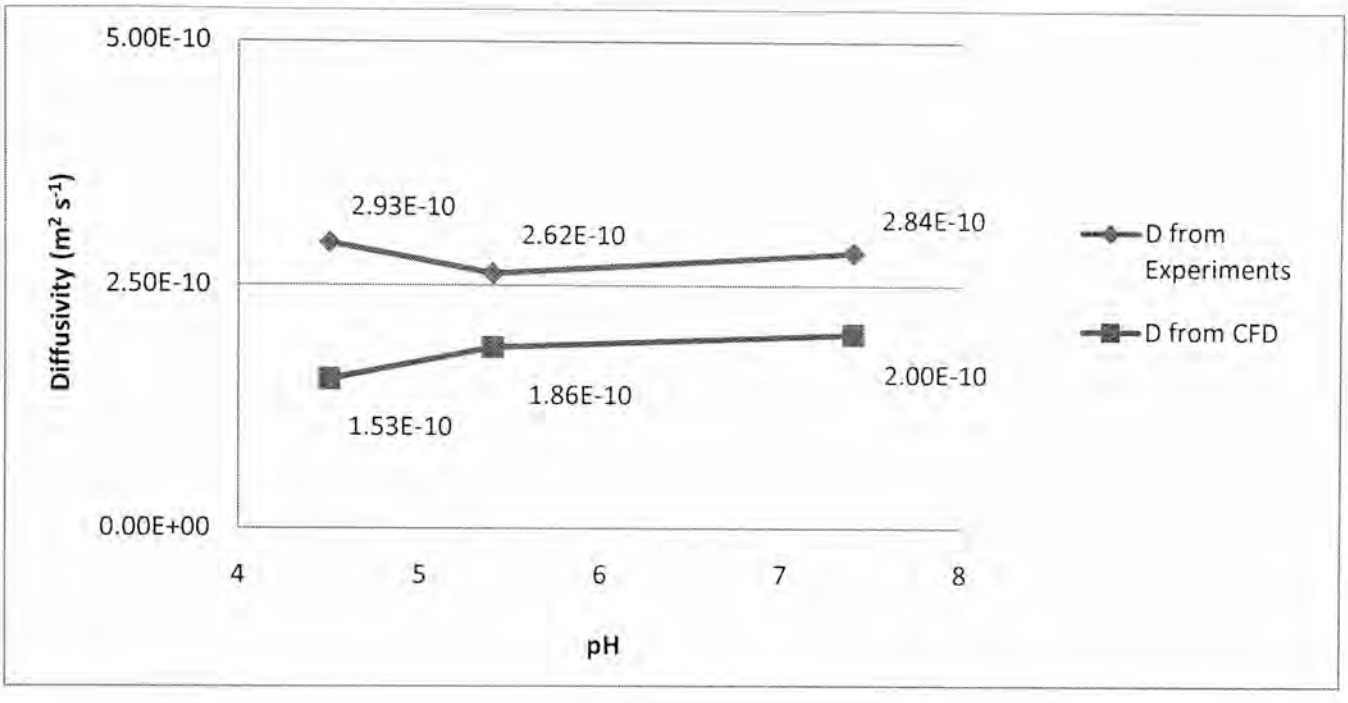

Figure 6.15 The variation of diffusivities with pH for experiments and CFD in fouling conditions

6.6. Conclusions

The operating parameters affecting concentration polarization and fouling of BSA solutions during ultrafiltration in a flat sheet cross flow system was theoretically investigated using Computational Fluid Dynamics (CFD) and empirical mass transfer equations. Computational Fluid Dynamics (CFD) simulates experimental data based on variable transport and physical properties. On the other hand, empirical mass transfer models assume constant physical properties when estimating diffusivity (D), mass transfer coefficient (k) and BSA wall concentration (C_w). Both CFD and mass transfer study distinguishes the individual contribution of concentration polarization and fouling towards flux decline, based on individual resistances, R_{CP} and R_F respectively. The agreement between mass transfer models (constant physical properties) and CFD (variable operating conditions) were discussed.

The contribution of fouling and concentration polarization were estimated from flux experiments using standard operating conditions of 0.15M NaCl, pH 5.4, 0.714gL^{-1}, and 500mL.min^{-1}. The standard condition was selected based on past studies (Suki et al., 1983; Waters et al., 1983; Vilker et al., 1984).

In all the ultrafiltration experiments, we have observed the common trend of BSA in solution, which includes immediate flux decline at the start of ultrafiltration and the strong effect of solution environment to the adsorption of BSA on the membrane surface. As expected, when we varied BSA concentration, flow, pH and salt concentration away from the standard condition, we found that concentration and pH were the dominant parameters that influences flux decline during ultrafiltration. Thus, for the mass transfer study, pH was the main parameter investigated. The relative flux measurements at variations of parameters indicated that the lowest relative flux for solutions with and without salt added conditions was at pH 4.5, where strong concentration polarization and fouling occurred, while the highest flux was observed at pH 7.4. BSA was totally rejected by the membrane during ultrafiltration, with pH 7.4 having the highest feed concentration of BSA at the end due to the high flux during ultrafiltration. Total BSA deposition per unit area on the membrane in added salt condition was lower than solutions without added salt, demonstrating the effect of salt in buffering electrostatic charges between the protein and membrane resulting in higher deposition. In addition, the spatial deposition profile in added salt condition is more even than without added salt condition. In added salt condition, the highest BSA deposition occurred at pH 5.4, while the lowest deposition occurred at pH 4.5.

In the analysis of concentration polarization and fouling using individual measured resistances at various pH, we found that at lower solution pH, the true resistance were mainly caused by fouling and while concentration polarization has less effect. Total resistance (R_T) was highest

at pH 4.5 consisted mainly of fouling resistance (R_F). The contribution of concentration polarization resistance (R_{CP}) was highest at pH 5.4. Passive adsorption measurement based on R_P at pH 5.4 shows that proteins readily adsorbed to the membrane surface without pressure intervention. We also found that R_P was higher than R_{CP}, in terms of percent R_T, and R_P is comparable to R_F in strength. This might be due to re-deposition of loose BSA during Milli-Q flux measurement (J_{MQP}) to obtain R_P. Thus BSA still attaches itself strongly to the membrane surface regardless of pressure.

In the mass transfer study, conditions "fouling" and "non-fouling" were used to calculate C_W, D and k. C_W increases while C_{WNF} decrease with the increase in pH. Relative BSA deposition and relative C_{WF} was also found to increase with pH. Therefore, C_W better represents the actual deposition occurring. When comparing the two conditions once again, "fouling" conditions have lower C_W, higher apparent "diffusivity from experiments", and lower predicted "diffusivity from CFD", compared to "non-fouling" condition. Also, k under "fouling condition" was higher than k under "non-fouling" conditions. The diffusivities from experiments were closely similar to the diffusivities from a related mass transfer calculations in the literatures (Chen, 1998).

In the CFD study, a remarkable agreement of the simulated and experimental fluxes over time was observed for standard conditions. The response to the varied operating conditions was only qualitatively correct. Particularly the dependence on the initial protein concentration was too low. This finding together with the detailed analysis of the single resistances occurring revealed that the concentration polarisation was under predicted in the simulation. This phenomenon has been detected before; its most probable explanation is the neglect of membrane-solute-solvent interactions (e.g. charge effects as revealed in (Noordman and Williams, 1996)). The main conclusion from the CFD findings is that concentration polarisation must be considered even at low TMP fluxes. The next steps towards better prediction of this phenomenon are (a) replacing the convection-diffusion equation for BSA by suitable multi component transport equations for BSA and ionic species, (b) spatial resolution of the membrane including the corresponding conservation balances. The mathematical

recipes are available (e.g. (Krishna and Wesselingh, 1997)) albeit the computational effort has to be kept in mind. A detailed thermodynamic description of the system water-protein-salt, maybe by activity coefficient models, could widen the simulations range of validity with respect to pH and buffer salt concentration. Furthermore this description together with kinetic experiments could support understanding the adsorption isotherms and the overall reaction correspondingly.

Concluding, a reliable predictive design tool for practical systems seems not yet to be within reach at the moment. However, we believe that simulation aiming for ab initio predictions provide a valuable service in understanding the complex phenomena involved at filtration separation of macromolecular solutions.

Chapter 7: Conclusions and Recommendations

7. Conclusions

In chapter four, the influence of cross-flow velocity, pH, filtration duration and spacer on binary protein fouling was reported. BSA and βLg solutions were used as model proteins and PES membranes of 30kDa MWCO was tested. The Lowry method was performed to quantify the total protein deposition while characterization of the proteins was performed by 1D SDS-PAGE. From these two methods, total protein extracted from the surface and pores are accounted for. Membranes from two sources, Pall Incorporated (PALL) and Synder Filtration (SYNDER) were tested to show the influence of membrane characteristics on fouling.

Although 90% flux decline was achieved at the end of ultrafiltration, the amount of protein measured on the membrane surface was small i.e. ≈ 1%, compared to the feed amount of 1g. This indicates strong protein adsorption and severe fouling occurring under the present condition. In addition, critical flux measurement showed that setting ultrafiltration at pH 4 and 50 kPa TMP can ensure irreversible fouling to occur that is crucial for cleaning studies to be performed. Using Lowry method, SYNDER membrane had more measured protein deposition compared to PALL membrane, which resulted in lower measured flux. The regularity of total protein deposition was derived from measuring the standard deviations of protein deposition in five pre-cut sections along the horizontal membrane surface. Lowry results show an absence of a consistent profile of total protein deposition along the SYNDER membrane surface. In addition, the individual deposition of BSA and βLg measured by 1D SDS-PAGE was also random. In addition, 1D SDS-PAGE also revealed that βLg deposition was found to be in higher than BSA for both membranes tested, signifying that lower molecular weight proteins dominates the total fouling deposition at the end of the ultrafiltration. The randomness in deposition was also experienced in the past using MALDI-MS method which measures the immediate uppermost protein layer. Therefore, our result confirms that random protein deposition along the horizontal membrane surface was inevitable during protein ultrafiltration and it occurs in the total layer. The randomness was a result of protein aggregation and

irregular initial deposition on the membrane surface. For PALL membranes, consistently higher protein deposition measured by Lowry method, occurred at the entrance of the rig where the proteins initially come in contact with the membrane. Spacer inserted in the channel, resting lightly above the membrane surface reduced flux and protein deposition by improving shear and turbulence. However the Milli-Q rinsing flux recovery with a spacer was less compared to the absence of spacer, showing that re-deposition of the loose proteins and trapping of the proteins have occurred while rinsing.

In Chapter 5, membrane cleaning studies using HCl, NaOH, sequential NaOH-HCl, and Protease M Amano on fouled PES membranes under controlled conditions were performed to understand the distribution and characteristics of residual fragments on the membrane surface. Whey Protein Isolate (WPI) and equimolar Bovine Serum Albumin (BSA) and Beta Lactoglobulin (βLg) was utilized as the protein foulant for this study. The protein residues deposited along the cross-flow membrane surface were characterized using Lowry method and 1D SDS-PAGE.

New discoveries were made during sequential NaOH-HCl cleaning of whey fouled membranes. In this study, the cleaning effects of NaOH and HCl cleaners were measured according to their individual Milli-Q flux increments (FRI_i) initiated and the flux results were repeatable in the experiments. NaOH cleaning alone recovered 47% (BSA and βLg fouled) and 33% (WPI fouled) of the initial Milli-Q flux of the membrane and was unable to effectively remove most deposits from the surface. Incorporating HCl cleaning during NaOH-HCl sequential cleaning added 11% to the flux recovered by NaOH cleaning. The additional flux recovered by HCl demonstrates that HCl during sequential cleaning was more effective for longer WPI fouling durations or fouled longer. This was due to the formation of a dense deposit layer after longer fouling that is not easily penetrable and solubilize by NaOH. However, the corrosive effect of HCl can penetrate this dense layer and assist in its removal from the membrane surface. Moreover, the flux recovered by HCl also improves as the number of fouling and cleaning cycles increases. The highest flux recovery obtained through sequential cleaning was 89% in repeated fouling and cleaning cycle. Although the measured

residues after sequential cleaning were 0.143μgcm^{-2} more than single NaOH cleaning, the flux recovered through sequential cleaning was higher. This shows that the total deposition does not necessarily reflect the flux recovery of the membrane after cleaning. Similarly, although the flux recovery was higher for sequential cleaning at 50°C than at 30°C, the deposition was slightly higher at 50°C. In addition, sequential cleaning have caused more re-deposition of the loose fragments back to the membrane surface after cleaning, thus measuring a higher protein amount. The amount of residues gradually increases as the fouling and cleaning cycle increases, accumulating at the end of each cycle, reducing the efficiency of cleaning. In addition, these residues of less than 20kDa MW were unknown and undistinguished by 1D SDS-PAGE due to its lack of sensitivity. The highest cleaning efficiency of 77% was achieved when 0.01% protease cleaning was performed for 40 mins for BSA and βLg fouled membrane. A higher protease concentration of 0.1% also resulted in a similar cleaning efficiency of 73%. A single distinct protein residue at 38kDa (protease) was observed on all protease cleaned membrane. Trypsin digestion and liquid chromatography and mass spectrometry (LCMS) was performed to identify the unknown residues after cleaning. Protease cleaning of binary fouled membranes resulted in high flux recovery, the highest identified at 77% for 0.01wt% protease and 1000mL.min^{-1} flow-rate. Protease cleaning leaves unknown residues of less than 10kDa and a single known protein residue at 38kDa, identified as alkaline proteinase by trypsin digestion. Cleaning efficiency during protease cleaning was affected by cross-flow rate and concentrations, where higher concentration and cross-flow resulted in lower residual concentration on the membrane surface. Protein deposition increases with increase in cleaning durations at the same concentration of 0.01wt% protease. The increase in protein deposition was most likely from the protease itself and not the protein residues from BSA and βLg.

In Chapter 6, the cross-flow Ultrafiltration (UF) of BSA solutions was studied using two methods, empirical mass transfer models at constant physical properties and Computational Fluid Dynamics (CFD) simulations at variable transport and physical properties. Experiments were performed to attain the final steady state flux at various feed concentrations, pH and volume flow. The Lowry method follows to measure the total protein adsorbed on the membrane. The contribution of concentration polarization and fouling towards flux decline

were distinguished in the CFD and mass transfer study. The standard condition selected for this study is 0.15M NaCl, pH 5.4, 0.714gL^{-1}, and 500mL.min^{-1}.

A common trend of BSA in solutions was observed in all the experiments to obtain the steady-state flux. The highest deposition on the membrane was measured at pH 5.4. Utilizing individual measured resistances at various pH, we found that at low pH, the true resistance were mainly caused by fouling and while concentration polarization has less effect. Total resistance (R_T) was highest at pH 4.5 consisted mainly of fouling resistance (R_F). The contribution of concentration polarization resistance (R_{CP}) was highest at pH 5.4 (Standard condition). Passive adsorption measurement based on R_P at pH 5.4 shows that proteins readily adsorbed to the membrane surface without pressure intervention. This is the reason for high concentration polarization observed. We also found that at pH 5.4, R_P was higher than R_{CP}, in terms of $\%R_T$, and R_P was comparable to R_F in strength. The similarity of R_P and R_F was caused by re-deposition of loose BSA during Milli-Q flux measurement (J_{MQP}) to obtain R_P. In the CFD study, a remarkable agreement of the simulated and experimental fluxes over time was observed for standard conditions. The response to the varied operating conditions was only qualitatively correct. Concentration polarisation was under predicted in the simulation as the importance of polarisation was shown in the single resistance studies. Therefore, concentration polarisation must be considered even at low TMP fluxes

7.1. Recommendations

Further studies can be performed using polyethersulphone membranes of other pore sizes as 10 and 100kDa MWCO. The results can be compared to the current study to analyse the effect of pore size on flux and deposition by BSA or BSA and βLg. The use of smaller pores may cause pore blocking while larger pores may cause internal pore plugging by these proteins.

Membranes of different materials can also be used to confirm that the fluctuations observed in the surface deposition of proteins on PES membranes are mainly caused by the irregular pore distribution in the membranes. These may include using cellulose acetate, Teflon, Polysulphone, Polycarbonate etc.

We can also use different variation of feed concentrations and the number of model proteins to analyse the interactions between BSA and βLg as well as competitive adsorption on the membrane surface. 1D SDS-PAGE and Lowry method can still be applied in the recommended study, as both methods measure the protein deposition by extracting and solubilising them in a solution first.

More studies can to be performed in the study of the residuals on the membrane surface after treatment using a variety of commercial cleaners since the current study is only limited to simple acid, base and protease solution. The surface can still be analysed using the current methods established.

A kinetic study can be performed if we have the cleaning efficiency variation with time. Also, a cleaning model can be derived from flux recovery data obtained from various cleaners to estimate the cleaning efficiency without actually performing the fouling and cleaning. More experiments are needed to obtain these set-points to be used in modelling.

A feed of whey protein concentrate can be used instead of WPI to better mimic the dairy and biological protein feeds in the industry although complexities may be higher.

Other studies that can be performed are deriving a model to predict flux decline based on fouling experiments. As pH was the main parameter varied in the study to distinguish R_{CP} and R_F at steady-state, it would be nice to also have a variation of feed concentration and flow.

A model can be derived to estimate the wall concentration and diffusivity of BSA at various conditions of pH, feed concentration and flow-rate.

Chapter 8: References

Andrews, A.T. (1986). Electrophoresis - Theory, Techniques and Biochemical and Clinical Applications. New York, Oxford University Press.

Arai, T. and Norde, W. (1990a). "The behaviour of some model proteins at solid-liquid interfaces 1. Adsorption from single protein solutions." Colloids and Surfaces **51**: 1-15.

Arai, T. and Norde, W. (1990b). "The behaviour of some model proteins at solid-liquid interfaces 2. Sequential and competitive adsorption." Colloids and Surfaces **51**: 17-28.

Bacchin, P., Aimar, P. and Sanchez, V. (1995). "Model for colloidal fouling of membranes." AIChE Journal **41**(2): 368-376.

Bansal, P. and Chen, D.C. (2006). "A Critical Review of Milk Fouling in Heat Exchangers." Comprehensive Reviews in Food Science and Food Safety **5**: 27-33.

Bartlett, M., Bird, M.R. and Howell, J.A. (1995). "An experimental study for the development of a qualitative membrane cleaning model." Journal of Membrane Science **105**(147-157).

Belfort, G., Pimbley, J.M., Greiner, A. and Chung, K.Y. (1993). "Diagnosis of membrane fouling using a rotating annular filter. 1. Cell culture media." Journal of Membrane Science **77**: 1-22.

Bird, M.R. (1992). Cleaning of food process plant. PhD Thesis. UK, University of Cambridge. **PhD Thesis**.

Bird, M.R. and Bartlett, M. (1995). "CIP Optimization for the Food Industry - Relationships between the detergent concentration, temperature and cleaning time." Food and Bioproducts Processing **73**(C2): 63-70.

Bird, M.R. and Bartlett, M. (2002). "Measuring and modelling flux recovery during the chemical cleaning of MF membranes for the processing of whey protein concentrate." Journal of Food Engineering **53**: 143-152.

Bird, M.R. and Fryer, P.J. (1991). "An experimental study of the cleaning surfaces fouled by whey proteins." Trans IChemE **69**: 13-21.

Blanpain-Avet, P., Migdal, J.F. and Benezech, T. (2004). "The effect of multiple fouling and cleaning cycles on a tubular ceramic microfiltration membrane fouled with a whey protein concentrate." Trans IChemE: Foods and Bioprocessing **82**(C3): 231-243.

Blatt, W., Dravid, A., Micheals, A.S. and Nelsen, L. (1970). Membrane Science and Technology. New York, Plenum.

Bohner, H.F. and Bradley Jr, R.L. (1992). "Effective Cleaning and Sanitizing of Polysulphone Ultrafiltration Membrane Systems." Journal of Dairy Science **75**: 718-724.

Bos, M.A., Shervani, Z., Anusiem, A.C.I., Giesbers, M., Norde, W. and Kleijn, J.M. (1994). "Influence of the electrical potential of the interface on the adsorption of proteins." Colloids and Surfaces B: Biointerfaces **3**: 91-100.

Bowen, W.R. and Gan, Q. (1991). "Properties of microfiltration membranes: Flux loss during constant pressure permeationof bovine serum albumin." Biotechnology and Bioengineering **38**: 688-696.

Bowen, W.R. and Jenner, F. (1995). "Theoretical descriptions of membrane filtration of colloids and fine particles: an assessment and review." Advances in Colloid and Interface Science **56**: 141-200.

Bowen, W.R., Liang, Y. and Williams, P.M. (2000). "Gradient diffusion coefficients -- theory and experiment." Chemical Engineering Science **55**(13): 2359-2377.

Burton, H. (1968). "Reviews of the progress of dairy science." Journal of Dairy Science **35**: 317-330.

Cabero, M.L., Riera, F.A. and Alvarez, R. (1999). "Rinsing of ultrafiltration ceramic membranes fouled with whey proteins: effects on cleaning procedures." Journal of Membrane Science **154**: 239-250.

Cao, Z., Wiley, D.E. and Fane, A.G. (2001). "CFD simulations with net-type turbulence promoters in a narrow channel." Journal of Membrane Science **185**: 157-176.

Chan, R. (2002). PhD Thesis, Fouling Mechanism in the Membrane Filtration of Single and Binary Protein Solution. Sydney, Australia, UNSW. **PhD**.

Chan, R. and Chen, V. (2001). "The effects of electrolyte concentration and pH on protein aggregation and deposition: critical flux and constant flux membrane filtration." Journal of Membrane Science **185**: 177-192.

Chan, R. and Chen, V. (2004). "Characterization of Protein Fouling on Membranes: Opportunities and Challenges." Journal of Membrane Science **242**: 169 - 188.

Chan, R., Chen, V. and Bucknall, M.P. (2002). "Ultrafiltration of protein mixtures: measurement of apparent critical flux, rejection performance, and identification of protein deposition." Desalination **146**: 83-90.

Chan, R., Chen, V. and Bucknall, M.P. (2004). "Quantitative Analysis of Membrane Fouling by protein Mixtures Using MALDI-MS." Biotechnology and Bioenegineering **85**: 190-201.

Changani, S.D., Belmar-Beiny, M.T. and Fryer, P.J. (1997). "Engineering and Chemical Factors Associated with Fouling and Cleaning in Milk Processing." Experimental Thermal and Fluid Science **14**: 392-406.

Chen, V. (1998). "Performance of partially permeable microfltration membranes under low fouling conditions." Journal of Membrane Science **147**: 265-278.

Chen, V., Chan, R., Li, H. and Bucknall, M.P. (2007). "Spatial distribution of foulants on membranes during ultrafiltration of protein mixtures and the influence of spacers in the feed channel." Journal of Membrane Science **287**: 79-87.

Chen, V., Li, H., Li, D., Tan, S. and Petrus, H.T.B.M. (2006). "Cleaning strategies for membrane fouled with protein mixtures." Desalination **200**(1-3): 198-200.

Cheryan, M. (1998). Ultrafiltration and Microfiltration Handbook. USA, Technomic Publishing Company.

Coolbear, T., Monk, C., Peek, K., Morgan, H.W. and Daniel, R.M. (1992). "Laboratory-scale investigations into the use of extremely thermophilic proteinases for cleaning ultrafiltration membranes fouled during whey processing." Journal of Membrane Science **67**: 93-101.

D' Souza, N.M. and Mawson, A.J. (2005). "Membrane cleaning in the dairy industry: A review." Critical Reviews in Food Science and Nutrition **45**: 125-134.

Da Costa, A.R., Fane, A.G., Fell, C.J.D. and Franken, A.C.M. (1991). "Optimal channel spacer design for ultrafiltration." Journal of Membrane Science **62**: 275-291.

Da Costa, A.R., Fane, A.G. and Wiley, D.E. (1993). "Ultrafiltration of whey protein solutions in spacer-filled flat channels." Journal of Membrane Science **76**: 245-254.

Daufin, G., Merin, U., Labbe, J.P., Quemerais, A. and Kerherve, F.L. (1991). "Cleaning of Inorganic Membrane After Whey and Milk Ultraflitration." Biotechnology and Bioengineering **38**: 82-89.

Dee, C.K., Puleo, D.A. and Bizios, R. (2002). An Introduction to Tissue-Biomaterial Interactions. New York, Wiley-Liss.

Deyl, Z. (1979). Electrophoresis, A survey of techniques and application, Part A: Techniques. Journal of Chromatography Library. Amsterdam, Netherlands, Elsevier Scientific Publishing Company. **18**.

Doonan, S. (2002). Peptides and Proteins. Cambridge UK, The Royal Society of Chemistry.

Fane, A.G. and Fell, C.J.D. (1987). "A Review of Fouling and Fouling Control in Ultrafiltration." Desalination **62**: 117-136.

Field, R., Hughes, D., Cui, Z. and Tirlapur, U. (2008). "Some observations on the chemical cleaning of fouled membranes." Desalination **227**: 132-138.

Field, R.W., Wu, D., Howell, J.A. and Gupta, B.B. (1995). "Critical flux concept for microfiltration fouling." Journal of Membrane Science **100**: 259-272.

Franks, F. (1993). Protein Biotechnology - Isolation, Characterization and Stabilization. Totowa, New Jersey, Humana Press.

Fryer, P.J., Christian, G.K. and Liu, W. (2006). "How hygiene happens: physics and chemistry of cleaning." International Journal of Dairy Technology **59**(2): 76-84.

Gaigalas, A.K., Reipa, V., Hubbard, J.B., Edwards, J. and Douglas, J. (1995). "A non-perturbative relation between the mutual diffusion coefficient, suspension viscosity, and osmotic compressibility: Application to concentrated protein solutions." Chemical Engineering Science **50**(7): 1107-1114.

Gekas, V., Aimar, P., Lafaille, J.-P. and Sanchez, V. (1993). "A simulation study of the adsorption-concentration polarisation interplay in protein ultrafiltration." Chemical Engineering Science **48**: 2753-2765.

Gekas, V. and Hallstrom, B. (1987). "Mass Transfer in the Membrane Concentration Polarization Layer Under Turbulent Cross Flow I. Critical Literature Review and Adaptation of Existing Sherwood Correlations to Membrane Operations." Journal of Membrane Science **30**: 153-170.

Geraldes, V., Semiao, V. and Pinho, M.N. (2000). "Numerical modelling of mass transfer in slits with semi-permeable membrane walls " Engineering Computations **17**(3): 192 - 218.

Ghidossi, R., Veyret, D. and Moulin, P. (2006). "Computational fluid dynamics applied to membranes: State of the art and opportunities." Chemical Engineering and Processing **45**(6): 437-454.

Ghosh, R. (2003). Protein Bioseparation Using Ultrafiltration: Theory, Applications and New Developments. London, Imperial College Press.

Gill, W.N., Wiley, D.E., Fell, C.J.D. and Fane, A.G. (1988). "Effect of viscosity on concentration polarization in ultrafiltration." AIChE Journal **34**(9): 1563-1567.

Gillham, C.R., Fryer, P.J., Hasting, A.P.M. and Wilson, D.I. (1999). "Cleaning-In-Place of Whey Protein Fouling Deposits: Mechanisms Controlling Cleaning." Food and Bioproducts Procesing **77**(C2): 127-135.

Grabhoff, A. (1989). Environmental efffects of the use of alkaline cleaning solutions. Fouling and cleaning in food processing. H. G. Kessler and D. B. Lund. Germany, University of Munich**:** 107-114.

Grabhoff, A. (1997). Cleaning of heat treatment equipment. Brussels, International Dairy Federation.

Grabhoff, A. (2002). "Enzymatic cleaning of milk pasteurizers." Transactions of IChemE **80**(Part C: Food and Bioproducts Processing): 247-252.

Hanemaaijer, J.H., Robbertsen, T., van den Boomgaard, T. and Gunnink, J.W. (1989). "Fouling of ultrafiltration membranes. The role of protein adsorption and salt precipitation." Journal of Membrane Science **40**(2): 199-217.

Harmant, P. and Aimar, P. (1998). "Coagulation of colloids in a boundary layer during cross-flow filtration." Colloids and Surfaces A: Physicochemical and Engineering Aspects **138**: 217-230.

Hess, H.H., Lees, M.B. and Derr, J.E. (1978). "A Linear Lowry-Folin Assay for Both Water-Soluble and Sodium Dodecyl Sulfate-Solubilized Proteins." Analytical Biochemistry **85**: 295-300.

Hoefer (1994). Hoefer Scientific Instruments: Protein Electrophoresis Applications Guide. USA.

Hoffmann, M.A.M. and Van Mil, P.J.J.M. (1997). "The dominating effect of ionic strength on the heat-induced denaturation and aggregation of β-lactoglobulin in simulated milk ultrafiltrate." Journal of Agricultural and Food Chemistry **45**: 2942-2948.

Hoffmann, M.A.M. and Van Mil, P.J.J.M. (1999). "Heat-induced aggregation of β-lactoglobulin as a function of pH." Journal of Agricultural and Food Chemistry **47**: 1898-1905.

Holland, F.A. and Bragg, R. (1995). Fluid Flow for Chemical Engineers. Great Britain, A division of Hodder Headline PLC, Edwards Arnolds.

Howell, J.A. (1995). "Sub-critical flux operation of microfiltration." Journal of Membrane Science **107**: 165-171.

Jeurnik, T.J.M. and Brinkman, D.W. (1994). "The cleaning of heat exchangers and evaporators after processing milk or whey." International Dairy Journal **4**: 347-368.

Karas, M. and Hillenkamp, F. (1988). "Laser Desorption Ionization of Proteins with Molecular Masses Exceeding 10000 Daltons." Analytical Chemistry **60**: 2299-2301.

Kim, K.J. and Fane, A.G. (1994). "Low voltage scanning electron microscopy in membrane research." Journal of Membrane Science **88**: 103-114.

Kim, K.J., Fane, A.G., Fell, C.J.D. and Joy, D.C. (1992). "Fouling mechanisms of membranes during protein ultrafiltration." Journal of Membrane Science **68**: 79-91.

Kim, K.J., Sun, P., Chen, V., Wiley, D.E. and Fane, A.G. (1993). "The Cleaning of ultrafiltration membranes fouled by protein." Journal of Membrane Science **80**: 241-249.

Kozinski, A.A. and Lightfoot, E.N. (1972). "Protein ultrafiltration: A general example of boundary layer filtration." AIChE Journal **18**(5): 1030-1040.

Krishna, R. and Wesselingh, J.A. (1997). "The Maxwell-Stefan Approach to Mass Transfer." Chemical Engineering Science **52**: 861-911.

Kuzmenko, D., Arkhangelsky, E., Belfer, S., Freger, V. and Gitis, V. (2005). "Chemical cleaning of UF membranes fouled with BSA." Desalination **179**: 323-333.

Labbe, J.P., Quemerais, A., Michel, F. and Daufin, G. (1990). "Fouling of Inorganic Membranes during Whey Ultrafiltration: Analytical Methodology." Journal of Membrane Science **51**(3): 293-307.

Larsen, B.S. and McEwen, C.N. (1998). Mass Spectrometry of Biological Materials. New York, Marcel Dekker.

Lassen, B. and Malmsten, M. (1996). "Structure of Protein Layers during Competitive Adsorption." Journal of Colloid and Interface Science **180**: 339-349.

Lee, D.N. and Merson, R.L. (1974). "Examination of cottage cheese whey proteins by scanning electron microscopy: relationship to membrane fouling during ultrafiltration." Journal of Dairy Science **58**(10): 1423-1432.

Lee, D.N. and Merson, R.L. (1975). "Examination of cottage cheese whey proteins by scanning electron microscopy: Relationship to membrane fouling during ultrafiltration." Journal of Dairy Science **58**(10): 1423.

Lee, D.N. and Merson, R.L. (1976). "Prefiltration of Cottage Cheese Whey to Reduce Fouling of Ultrafiltration Membranes." Journal of Food Science **41**: 403-410.

Leo, V. and Adams, A.L. (1969). "Identification of rapid changes at plasma-solids interfaces." Journal of Biomedical Material Research **3**: 43-67.

Li, H., Fane, A.G., Coster, H.G.L. and Vigneswaran, S. (2000). "An assessment of depolarisation models of crossflow microfiltration by direct observation through the membrane." **172**: 135-147.

Lowry, O.H., Rosebrough, N.J., Farr, A.l. and Randall, R.J. (1951). "Protein Measurement with the Folin Phenol Reagent." Journal of Biological Chemistry **193**: 265-275.

Maartens, A., Stewart, P. and Jacobs, E.P. (1996). "An enzymatic approach to the cleaning of ultrafiltration membranes fouled in abattoir effluent." Journal of Membrane Science **119**: 9-16.

Madaeni, S.S. and Sharifnia, S. (2000). "Chemical Cleaning of Ultrafiltration Membrane Fouled by Whey." Iranian Polymer Journal **9**(3): 143-151.

Matzinos, P. and Alvarez, R. (2002). "Effect of ionic strength on rinsing and alkaline cleaning of ultrafiltration inorganic membranes fouled with whey proteins." Journal of Membrane Science **208**: 23-30.

Meares, P. (1976). Membrane Separation Processes. Amsterdam, Elsevier Scientific Publishing Company.

Mercade-Prieto, R. and Chen, X.D. (2005). "Caustic-induced gelation of whey deposits in the alkali cleaning of membranes." Journal of Membrane Science **254**(1-2): 157-167.

Mercade-Prieto, R. and Chen, X.D. (2006). "Dissolution of whey protein concentrate gels in alkali." AIChE Journal **52**(2): 792-803.

Mercade-Prieto, R., Falconer, R.J., Paterson, W.R. and Wilson, D.I. (2006). "Probing the mechanisms limiting dissolution of whey protein gels during cleaning." Trans IChemE, Food and Bioproducts Processing **84**(C4): 311-319.

Mercade-Prieto, R., Falconer, R.J., Paterson, W.R. and Wilson, D.I. (2007). "Swelling and Dissolution of Beta-Lactoglobulin Gels in Alkali." Biomacromolecules **8**: 469-476.

Mercade-Prieto, R., Paterson, W.R., Chen, X.D. and Wilson, D.I. (2008). "Diffusion of NaOH into a protein gel." Chemical Engineering Science **63**: 2763-2772.

Metsamuuronen, S. (2003). Critical Flux and Fouling in Ultrafiltration of Proteins. Lappeenranta University of Technology. Finland. **Phd**.

Metsamuuronen, S., Howell, J. and Nystrom, M. (2002). "Critical flux in ultrafiltration of myoglobin and baker's yeast." Journal of Membrane Science **196**: 13-25.

Metsamuuronen, S. and Nystrom, M. (2000). Critical flux measurements by constant pressure method. Proceedings of 8th World Filtration Congress, Brighton, UK.

Miller, I., Crawford, J. and Gianazza, E. (2006). "Protein stains for proteomic applications: Which, when, why?" Proteomics **6**: 5385-5408.

Miquel, A. and Schock, G. (1987). "Mass transfer and pressure loss in spiral wound modules." Desalination **64**: 339-352.

Mulder, M. (2000). Basic Principles of Membrane Technology. Netherlands, Kluwer Academic Publisher.

Munoz-Aguado, M.J., Wiley, D.E. and Fane, A.G. (1996). "Enzymatic and detergent cleaning of a polysulfone ultrafiltration membrane fouled with BSA and whey." Journal of Membrane Science **117**: 175-187.

Nakanishi, K., Sakiyama, T. and Imagura, K. (2001). "Review: On the adsorption of Proteins on Solid Surfaces, a Common but Very Complicated Phenomenon." Journal of Bioscience and Bioengineering **91**(3): 233-244.

Nasir, A. and McGuire, J. (1998). "Sequential and competitive adsorption of bovine serum albumin and beta-lactoglobulin, and their resistance to exchange with alpha-lactalbumin and beta-casein." Food Hydrocolloids **12**: 95-103.

Neal, P.R., Li, H., Fane, A.G. and Wiley, D.E. (2003). "The effect of filament orientation on critical flux and particle deposition in spacer-filled channels." Journal of Membrane Science **214**: 165-178.

Noordman, W.R. and Williams, P.M. (1996). "The Osmotic Pressure of Electrostatically Stabilized Colloidal Dispersions." Journal of Colloid Interface Science **184**: 241-250.

Norde, W. and Anusiem, A.C.I. (1992). "Adsorption, desorption and re-adsorption of proteins on solid surfaces " Colloids and Surfaces **66**: 73-80.

Norde, W. and Favier, J.P. (1992). "Structure of adsorbed and desorbed proteins." Colloids and Surfaces **64**: 87-93.

Petrus, H.T.B.M. (2006). Enzymatic Cleaning of PES Ultrafiltration Membrane Fouled by Single and Binary Protein Mixtures. School of Chemical Sciences and Engineering. Sydney, Australia, UNSW. **M.E.**

Petrus, H.T.B.M., Li, H., Chen, V. and Norazman, N. (2008). "Enzymatic cleaning of ultrafiltration membranes fouled by protein mixture solutions." Journal of Membrane Science **325**: 783-792.

Plett, E. (1985). Cleaning of Fouled Surfaces in: Fouling and Cleaning in Food Processing. University of Wisconsin, Madison, WI, Extension Duplicating.

Robertson, B.C. and Zydney, A.L. (1990). "Protein Adsorption in Asymmetric Ultrafiltration Membranes with Highly Constricted Pores." Journal of Colloid Interface Science **134**: 563-575.

Romney, A.J.D. (1990). CIP: Cleaning in Place. London, Society of Dairy Technology.

Rosen, C. and Tragardh, C. (1993). "Computer simulations of mass transfer in the concentration boundary layer over ultrafiltration membranes." Journal of Membrane Science **85**(2): 139-156.

Ruiz-Bevia, F.e.a. (1997). "An improved model with time-dependent adsorption for simulating protein ultrafiltration." Chemical Engineering Science **52**: 2343-2352.

Sablani, S.S., Goosen, M.F.A., Al-Belushi, R. and Wilf, M. (2001). "Concentration polarization in ultrafiltration and reverse osmosis: a critical review." Desalination **141**: 269-289.

Sayed Razavi, S.K., Harris, J.L. and Sherkat, F. (1996). "Fouling and cleaning of membranes in the ultrafiltration of the aqueous extract of soya flour." Journal of Membrane Science **114**: 1996.

Schausberger, P., Norazman, N., Li, H., Chen, V. and Friedl, A. (2009). "Simulation of Protein Ultrafiltration Using CFD: Comparison of Concentration Polarization and Fouling Effects with Filtration and Protein Adsorption Experiments." Journal of Membrane Science **337**: 1-8.

Sheldon, J.M., Reed, I.M. and Hawes, C.R. (1991). "The fine structure of ultrafiltration membranes. II. Protein fouled membranes." Journal of Membrane Science **62**(1): 87-102.

Shen, J.J.S. and Probstein, R.F. (1977). "On the Prediction of Limiting Flux in Laminar Ultrafiltration of Macromolecular Solutions." Industrial and Engineering Chemistry Fundamentals **16**(4): 459-465.

Streitwieser, A.J. and Heathcock, C.H. (1976). Introduction to Organic Chemistry. New York, Macmillan Publishing Co., Inc.

Su, T.J., Lu, J.R., Cui, Z.F. and Thomas, R.K. (2000). "Fouling of ceramic membranes by albumins under dynamic filtration conditions." Journal of Membrane Science **173**: 167-178.

Suki, A., Fane, A.G. and Fell, C.J.D. (1983). "The effect of pH and ionic environment on the ultrafiltration of protein solutions with retentive membranes." Journal of Membrane Science **16**: 195-210.

Suki, A., Fane, A.G. and Fell, C.J.D. (1984). "Flux Decline in Protein Ultrafiltration." Journal of Membrane Science **21**: 269-283.

Timperley, D.A. and Smeulders, C.N.M. (1987). "Cleaning of Dairy High-Temperature-Short-Time Plate Heat Exchangers: Comparison of Single- and Two-Stage Procedures." Journal of the Society of Dairy Technology **40**: 4-7.

Tissier, J.P., Lalande, M. and Corrieu, G. (1984). A Study of Milk Deposit on Heat Exchange Surface during UHT Treatment. Engineering and Food. B. M. McKenna. London: 49-58.

Tragardh, G. (1989). "Membrane Cleaning." Desalination **71**: 325-335.

van Boxtel, A.J.B., Otten, Z.E.H. and van der Linden, H.J.L.J. (1991). "Evaluation of process models for fouling control of reverse osmosis of cheese whey." Journal of Membrane Science **58**: 89-111.

Vetier, C., Bennasar, M. and De la Fuente, B. (1988). "Study of the fouling of a mineral microfiltration membrane using scanning electron microscopy and physicochemical analyses in the processing of milk." Journal of Dairy Research **55**: 381-400.

Vilker, V.L., Colton, C.K., Smith, K.A. and Green, D.L. (1984). "The osmotic pressure of concentrated protein and lipoprotein solutions and its significance to ultrafiltration." Journal of Membrane Science **20**(1): 63-77.

Waters, A.G., Fane, A.G. and Fell, C.J.D. (1983). "Ultrafiltration of protein solutions through partially permeable membranes - The effect of adsorption and solution environment." Journal of Membrane Science **16**: 211-224.

Wu, A.R.W.L. (2007). Chemical Cleaning of Membranes Fouled by Whey Protein Isolates. School of Chemical Sciences and Engineering. Sydney, UNSW. **M. E.**

Xin, H., Chen, X.D. and Ozkan, N. (2002). "Whey protein-based gel as a model material for studying initial cleaning mechanisms of milk fouling." Journal of Food Science **67**(7): 2702-2711.

Xin, H., Chen, X.D. and Ozkan, N. (2004). "Removal of a model protein foulant from metal surfaces." AIChE Journal **50**(8): 1961-1973.

Ye, Y. (2005). Macromolecular Fouling During Membrane Filtration of Complex Fluids. School of Chemical Sciences and Engineering. Sydney, Australia, UNSW. **PhD**.

Zeman, L.J. and Zydney, A.L. (1996). Membrane Cleaning, Compaction, and Chemical Degradation. Microfiltration and Ultrafiltration Principles and Applications. New York, Marcel Dekker.

Appendix

1. Appendix A – Chapter 3

Materials and Methods

1.1. MALDI-MS method

1.1.1. Chemicals in MALDI-MS

MALDI-MS was used in several experiments along with Modified Lowry Assay and 1D SDS-PAGE. The chemicals used for MALDI-MS were Ovalbumin derived from chicken egg, Conalbumin, Sinapinic acid, 0.1% aqueous trifluoroacetic acid, and HPLC-grade acetonitrile. All chemicals were purchased from Sigma-Aldrich, Australia. Ovalbumin has a molecular mass of 45 kDa. Conalbumin, lysozyme and ovalbumin were used as standards in MALDI-MS method for analysing the protein deposited on the membrane surface. **Table 1.1** shows the characteristics of proteins such as molecular weights, molecular dimensions and iso-electric points (IEP).

Table 1.1
The characteristics of proteins used in the study

Proteins (Origin)	Mol. Weight (kDa)	Mol. Dimension (nm^3)	IEP
BSA	68	14.0 x 4.0 x 4.0	4.7
Lysozyme (chicken egg white)	14.4	4.5 x 3.0 x 3.0	11.0
βLg (bovine milk)	18.4	6.9 x 3.6 x 1.8	5.8
Conalbumin (chicken egg white)	80	5.5 x 2.8 x 2.8	6.6
Ovalbumin (chicken egg)	45	7.0 x 4.5 x 5.0	4.7

1.1.2. Equipments in MALDI-MS

The Voyager-DE^{TM} STR Biospectrometry Workstation was used for the MALDI-MS analysis of the proteins on the membrane samples. The machine is available in Bioanalytical and Mass Spectrometry Facility (BMSF) of UNSW. The settings were adjusted to fire 100 nitrogen laser shots per spectrum onto each membrane sample on the gold plated stainless steel target plate. It was operated in a positive ion linear mode with 25 kV accelerating voltage.

1.1.3. Procedures of MALDI-MS

The fouled and cleaned membranes were analysed using MALDI-MS. The metallic target plate was cleaned with 95% ethanol prior to sample preparation. In the cross-flow module, membrane samples were obtained at locations on the membrane as shown in **Figure 1.1**, in order to obtain an accurate description of the foulants along the membrane surface.

Membrane dissection for MALDI-MS

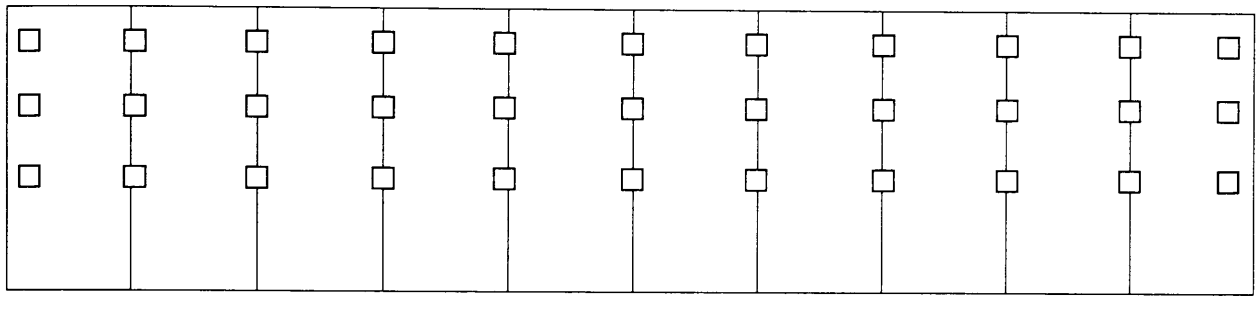

Figure 1.1 The top rectangle shows the locations where MALDI-MS samples are obtained from (small empty squares).

In stirred-cell module, membrane samples were taken at different radial distances from the centre. The samples were cut into square pieces measuring approximately 3mm by 3mm and were pasted onto the target plate (**Figure 1.2**) with the aid of double sided tape. The sinapinic acid matrix solution was prepared by adding 10 $mgml^{-1}$ sinapinic acid in a 1:1 mixture of 0.1% aqueous tri-fluoroacetic acid and HPLC-grade acetonitrile. 2 μl of Conalbumin internal standard was added and allowed to dry on each sample. Subsequently, 4 μl of matrix solution was added and allowed to dry in a fume hood. Finally, the samples were analysed on the Voyager-DE^{TM} STR Biospectrometry Workstation.

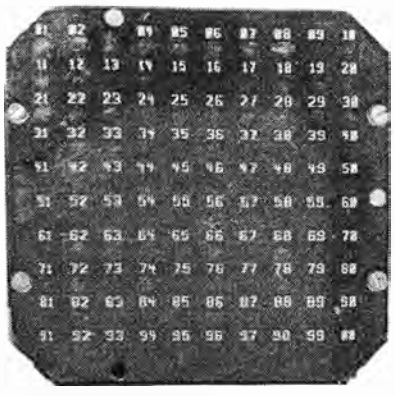

Figure 1.2 Gold plated MALDI-MS target plate.

1.1.4. MALDI-MS calibration graphs

The internal standard used for the analysis is 2 µl of 4pmolµl^{-1} of Conalbumin. The calibration procedure include Firstly, 1µl of BSA of known concentration were dropped onto a polyethylene backing, followed by 4 µl of matrix solution and 2 µl of internal standard. The micro mixture was mixed by the micro-syringe tip, to ensure that the matrix solution completely engulfs the protein analytes. The calibration curves for MALDI-MS method are shown in **Figure 1.3** and **1.4**.

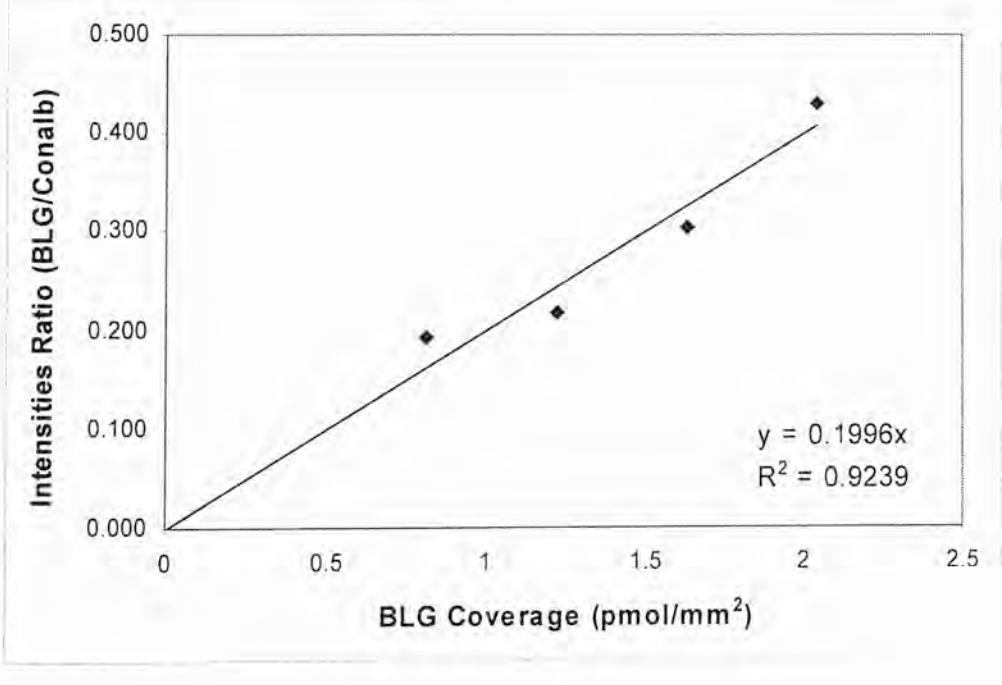

Figure 1.3 Calibration graph of Intensity ratio (βLg/Conalbumin) Vs βLg Coverage in MALDI–MS

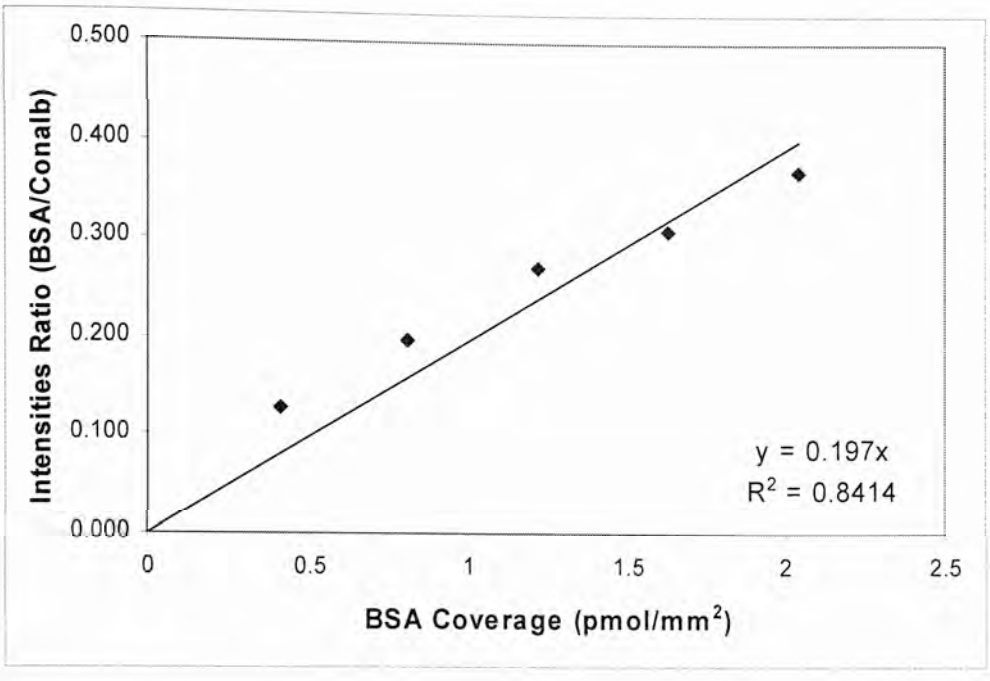

Figure 1.4 Calibration graph of Intensity ratio (BSA/Conalbumin) Vs BSA Coverage in MALDI–MS

1.2. Dead-end stirred-cell

A Perspex dead-end cell manufactured in our centre with an internal diameter of 4.45 cm and a capacity of 110 ml was used by a research colleague when performing some stirred-cell fouling and cleaning experiments covered. The rig consisted of a nitrogen gas feed cylinder, feed reservoir (1 litre), dead-end stirred-cell, magnetic stirrer (set 400 rpm), mass balance, permeate reservoir, computer, pressure gauge and differential pressure transmitter (TMP 100KPa). The photograph and the schematic of the set up are shown in **Figure 1.5**.

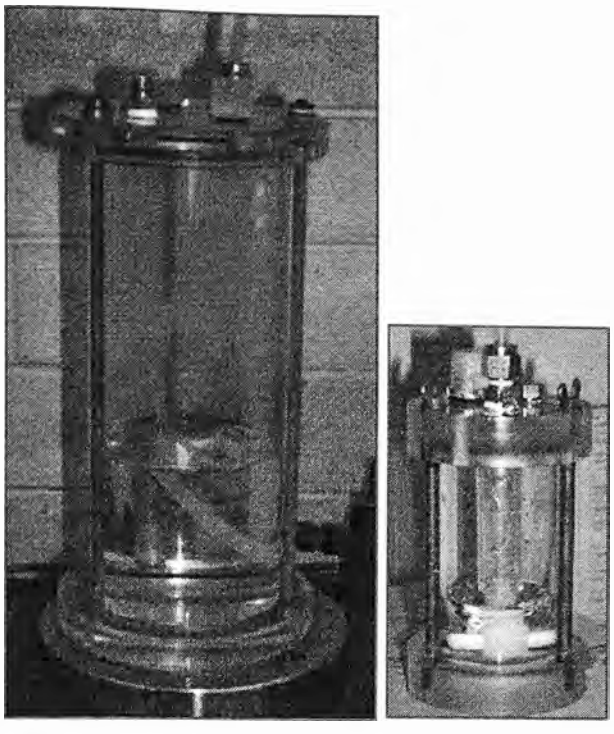

Figure 1.5 Feed reservoir (1 litre) and UF Dead-End Cell with magnetic stirrer (110ml). Photographs are not to scale for comparison.

1.3. 1D SDS-PAGE Method

1.3.1. Gel staining using CBB-R, CBB-G, and $AgNO_3$

De–staining of the gel is performed with a similar solution without the dye. The detection mode, limit and linearity range of these staining methods are shown in **Table 1.2**. These methods are compatible with mass spectrometry and thus further analysis of the peptides using MALDI-MS or liquid chromatography mass spectrometry (LC-MS) can be performed on the isolated proteins on the gels. **Table 1.3** contains the ingredients of CBB R-250. **Table 1.4** contains the procedure of performing silver staining of gels. The gels are stained overnight when using CBB R-250 and G-250, and then de-stained the following day. Amersham Pharmacia Biotech Image Scanner was used to scan the image of the gel for further analysis. Kodak Molecular Imaging Software was used to compare the intensities of the protein bands on the gel and quantify the amount of each protein component present

Table 1.2
Selected staining methods in the study

Staining method	Detection mode	Detection limit (ng)	Linearity range (orders of magnitude)
CBB-R	Colorimetry	8-10, 50-100	1–1.3
CBB-G (Colloidal)	Colorimetry	8-10, 10-20, 30-100	3, 1–1.3
Silver nitrate	Colorimetry	1,3-5	2, 1

Table 1.3
CBB R-250 stain

Constituent	Concentration	Requirements for 100ml
CBB	0.5% w/v	0.5g
Methanol	40% (v/v)	40ml
Acetic acid	10% (v/v)	10ml
MQ water		Make up to 100ml

Table 1.4
Ingredients and procedures of silver staining

Steps	Solution	Constituent	Volume (ml)	Operation	Time
1	A	50% methanol 10% acetic acid	100ml	Fix	30 min
2	B	5% methanol	100ml	Incubate	20 min
3	-	Milli-Q		Wash 3 times	3 x 5 min
4	C* = stock	Sodium thiosulphate ($Na_2S_2O_3.5H_2O$) 0.2g/10ml	Dilute 1:100 Working solution 100ml	Incubate	120 s
5	-	Milli-Q		Wash 3 times	3 x 30 s
6	D*	Silver nitrate ($AgNO_3$)	0.2g/100ml 100ml	Incubate	25 min
7	-	Milli-Q	100ml	Wash 3 times	3 x 60 s
8	E*	Sodium Carbonate solution (Na_2CO_3) 37% HCOH $Na_2S_2O_3.5H_2O$	For 100ml 3g Na_2CO_3 50µl Formaldehyde 20µl stock=C	Develop	10 min max
9	F	5% Acetic Acid by volume	100ml	Stop develop Wash	10 min
10	-	Milli-Q	100ml	Rinse	5 min

1.4. Trypsin digestion and LCMS

Ammonium bicarbonate (AMBIC), Dithiothreitol (DTT), Iodoacetamide (IAA), and trypsin are the main chemicals used in running the digestion of the proteins in gel pieces. Make 500mM stock solution of AMBIC. AMBIC was photosensitive, and was wrapped with aluminum foil. AMBIC is used for making the solvent for DTT, IAA and Trypsin enzyme.

100mM is used for making DTT, 100mM is used in making IAA and 50mM is used for making trypsin solution (pH 8). Make 100mM of AMBIC stock solution, 0.1M DTT (0.015424g in 1ml of Milli-Q water), and 0.2M IAA (0.037g of IAA in 1 ml of Milli-Q water). Make 10mM DTT and 25mM IAA using the 100mM AMBIC solution. Make 12 $ng\mu l^{-1}$ trypsin solutions.

Table 1.5
General trypsin digestion (Long method)

Steps	Actions
1	Under sterile conditions, slice the gel band containing the peptide into small pieces and put the gel pieces into eppendorf tubes
2	Add MQ water just enough to cover samples and vortex and let sit for 10 mins
3	Remove MQ water and reduce in 10mM DTT for 30 mins. Use volume ≈10µl or enough to cover the gel pieces
4	Remove DTT and alkylate bands in 10µl 25mM IAA for 30 mins at 37°C.
5	Remove IAA and add 10µl acetonitrile (CH_3CN).
6	Remove acetonitrile with pipette, poke a hole on the eppendorf lid, and then dry down with speed vac.
7	Add 10 µl trypsin and leave overnight at 37°C.

Table 1.6
General trypsin digestion (Short method)

Steps	Actions
1	Under sterile conditions, slice the gel band containing the peptides into small pieces and put the gel pieces into eppendorf tubes
2	Dehydrate the gel pieces in 100% acetonitrile for 10 mins
3	Remove acetonitrile and SpeedVac until dry

4	Make buffer containing 2µl trypsin and 128µl AMBIC (pH 8 checked) Equiv.: 12ng trypsin/µl buffer)
5	Reswell gel pieces in 10µl of trypsin buffer at 4°C for 45mins
6	Digest overnight at 37°C

Table 1.7
Peptide extraction from gel pieces (Following Table 1.5)

Steps	Actions
1	Add 10µl of 50% acetonitrile and 5% Formic acid to the gel pieces and leave at room temperature for 20 mins. This acidifies the solution.
2	Remove the peptide solution from the gel pieces and transfer to new tubes
3	Repeat step 1 to 2 three times to get all the peptides out.
4	Dry down peptides using speed vac close to dry ≈ 5µl
5	Freeze till ready for LCMS
6	When ready for LCMS, resuspend peptides in 0.05% Heptafluorobutyric Acid (HFBA)/1% formic acid
7	Put samples in special vials for Q-Star

Table 1.8
Peptide extraction from gel pieces (following Table 1.6)

Steps	Actions
1	Extract peptides for 3 × 20mins washes with 15µl of 5% formic acid in 50% acetonitrile at room temperature. Acid stops the trypsin digestion while the acetonitrile extracts the proteins.
2	SpeedVac pooled supernatants until dry
3	Store at -20°C, but do not keep it for months.

In the short trypsin digestion method, use the same long tip pipette for the same sample to transfer the solvent with the peptides to a new micro tube. Micro tubes instead of larger 2ml tubes are used to reduce surface area and loss of peptides.

1.4.1. LCMS (Q-Star) settings

Digested proteins by trypsin were separated by Nano-LC using an Ultimate HPLC and Famos auto-sampler system (LC-Packings, Amsterdam, Netherlands). Samples (5 µl) were concentrated and desalted using a micro C18 pre-column (500 µm × 2 mm, Michrom Bioresources, Auburn, CA) with H_2O:CH_3CN (98:2, 0.1 % formic acid) at 20 µlmin^{-1}. After a 4 min wash the pre-

column was switched (Switchos, LC Packings) into line with a fritless nano column. Peptides were eluted using a linear gradient of H2O:CH3CN (95:5, 0.1 % formic acid) to H_2O:CH_3CN (50:50, 0.1 % formic acid) at a flow rate of ~200 $nlmin^{-1}$ over 30 min. High voltage (2300 V) was applied to low volume tee (Upchurch Scientific) and a column tip positioned ~ 1 cm from the orifice of an API Q-Star Pulsar i hybrid tandem mass spectrometer (Applied Biosystems, Foster City, CA). Positive ions were generated by Electrospray and the Q-Star operated in information dependent acquisition mode (IDA). A TOF MS survey scan was acquired (m/z 350 – 1700, 1 s). The 2 largest multiply charged ions (counts >15) were sequentially selected by Q1 for MS/MS analysis. Nitrogen was used as collision gas and an optimum collision energy chosen (based on charge state and mass). Tandem mass spectra were accumulated for 2.5 s (m/z 65 – 2000). Peak lists were generated using Mascot Distiller (Matrix Science, London, England) using the default parameters, and submitted to the Mascot database search program (version 2.1, Matrix Science). Search parameters were: precursor and product ion tolerances ± 0.25 and 0.2 Da respectively; Met (O) specified as variable modification, enzyme specificity was trypsin, 1 missed cleavage was possible and the NCBInr database searched. Confidence in identified proteins was based on scores > X, meaning these proteins were present with a 95% confidence ($P < 0.05$).

2. Appendix B – Chapter 4

Fouling Study of Single and Binary Protein Solutions in a Cross-flow UF System

2.1. UV-Vis Spectrometry of protein solution

2.1.1. 280 Nm Calibration curve for BSA solutions

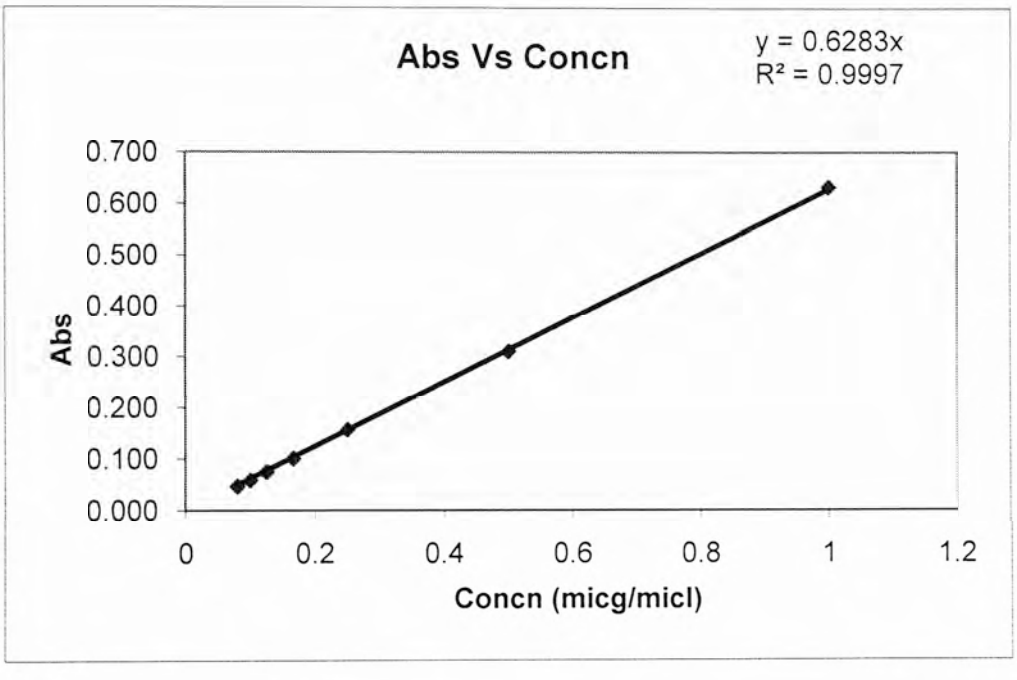

Figure 2.1 UV absorbance calibration curve for aqueous BSA measured at 280Nm.

2.2. Critical flux measurement at pH 3 for BSA solution

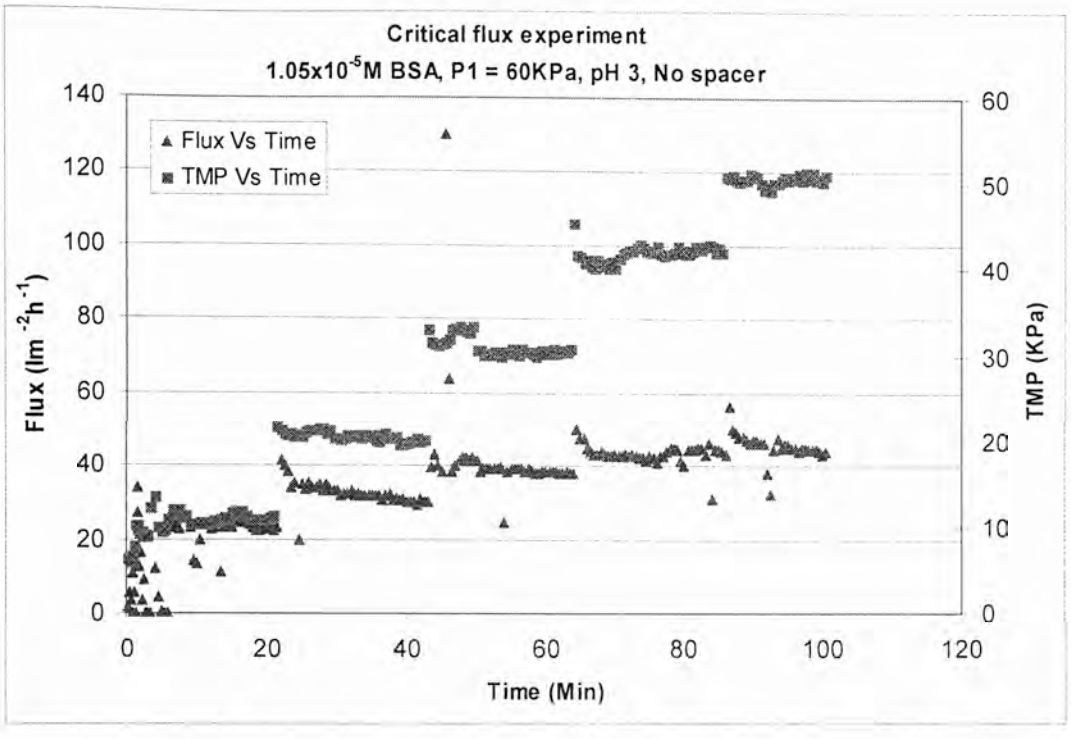

Figure 2.2 Flux stepping experiment at pH 3 for $1.05x10^{-5}$M BSA
(Abt 120 mins, pH 3, P_{inlet} = 60Kpa, No spacer Membrane IEP, BSA +ve)

2.3. Analysis of surface protein deposited on membrane with MALDI-MS

2.3.1. Surface coverage after 8 hours of fouling (SYNDER)

MALDI-MS was used to analyse the surface deposition on the membrane after 4 and 8 hours of UF (feed concentration, pH and cross-flow rate remained the same) with and without spacer. The deposition profile with spacer and without spacer after 8 hours of UF is shown in **Figure 2.3** and **Figure 2.4** respectively. It was found that the βLg coverage on the surface was higher than BSA coverage after 8 hours of UF with and without spacer. The deposition profile of BSA is smoother than the βLg on the surface. 4 hour deposition profile also has a higher coverage of βLg than BSA similar to 8 hour deposition.

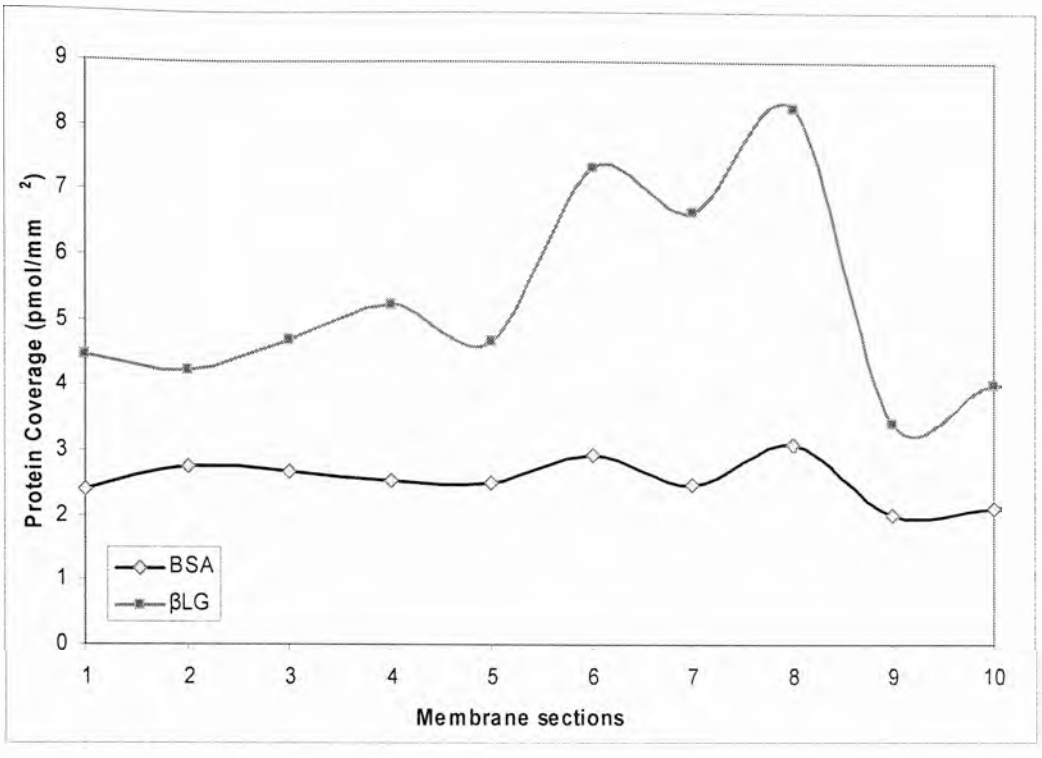

Figure 2.3 BSA and βLg profile along the membrane strip after 8 hours of fouling (feed, pH, flowrate) with spacer (SYNDER) in the membrane channel

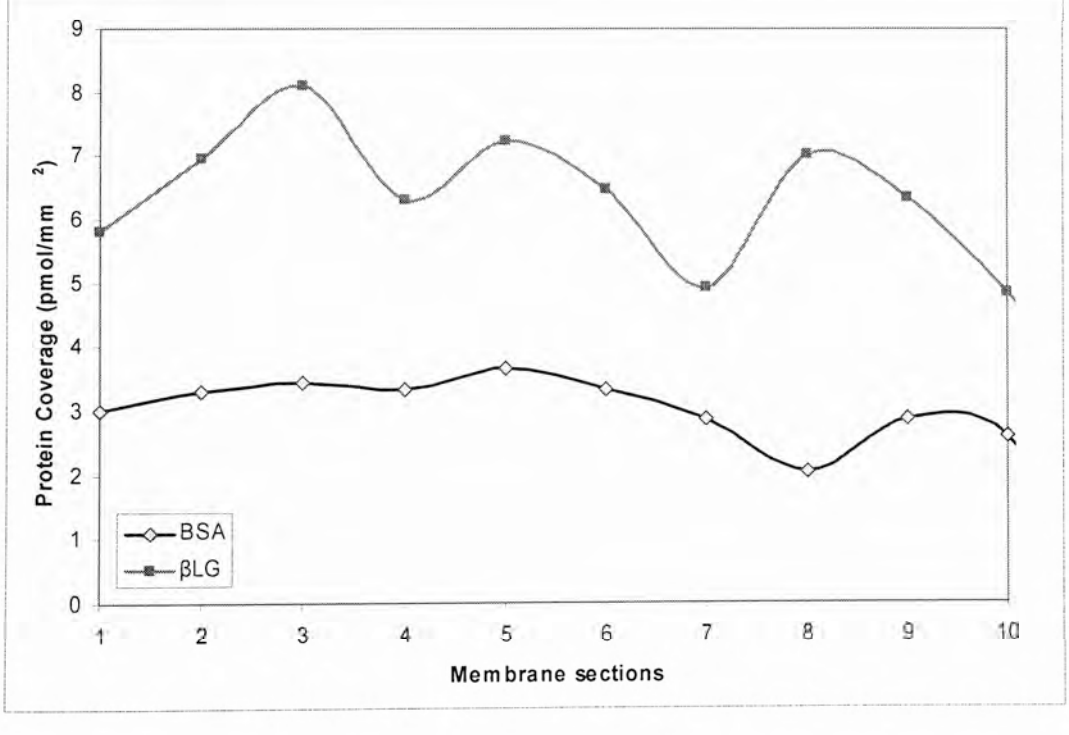

Figure 2.4. BSA and βLg profile along the membrane strip after 8 hours of fouling without spacer (SYNDER) in the membrane channel

The coverage of βLg was more erratic, while the BSA coverage was more or less stable. The maximum coverage for BSA on the surface was about 3 to 4 $pmolmm^{-2}$ while the βLg was about 8 to 9 $pmolmm^{-2}$. The extent of coverage between 4 and 8 hours were similar, indicating the independence from duration of fouling. Spacers caused more coverage of βLg in the central section of the membrane for 8 hours fouling with spacers (**Figure 2.4**). From the results, the βLg could be concluded to be the topmost sheet enveloping the BSA on the surface of the gel. MALDI-MS describes the top-surface deposition while 1D SDS-PAGE and Modified Lowry represents the whole layer of deposition on the membrane surface.

2.4. Analysis of feed and permeate using 1D SDS-PAGE

The permeate and the final feed solution obtained from the UF experiments were analysed using 1D SDS-PAGE with the objective of identifying and measuring the approximate amount of proteins in the feed solution and permeate after 4 and 8 hours of UF with and without spacer. The constituents of the feed are mainly BSA and βLg as shown in **Figure 2.5**, while no proteins are detected in the permeate stream. We can see that PES 30KDa membrane was able to fully retain BSA (68KDa) and βLg (18.5KDa) from the feed solution. The relative quantification of BSA and βLg in the feeds after 4 hr with spacer, and 8 hour with and without spacer is shown in **Table 2.1**. The standards on the far right contains equimolar 1 wt% mixed BSA/βLg (78.88μg/21.344μg) and 0.1wt% mixed BSA/βLg (7.88μg/2.134μg).

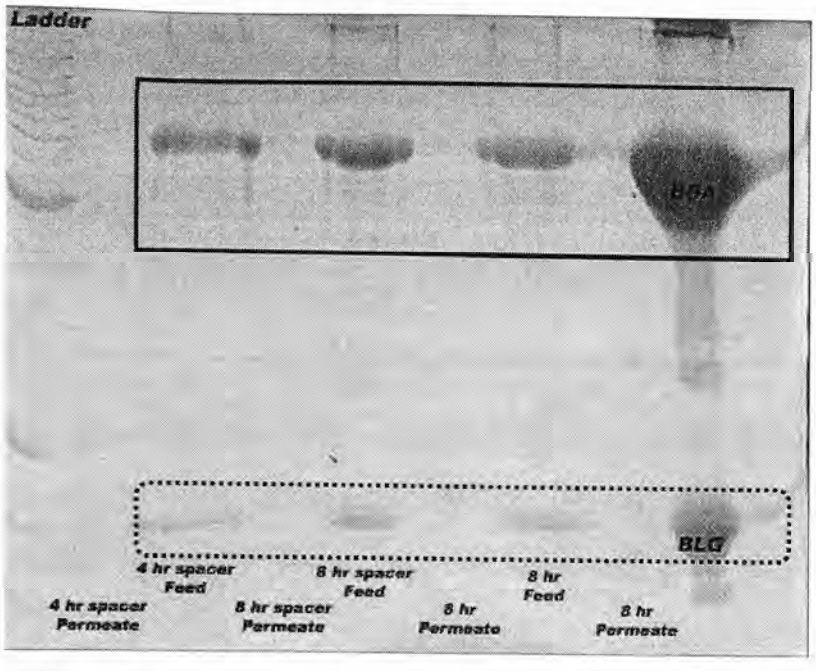

Figure 2.5 1D SDS-PAGE transmissive gel scan of feed and permeate indicating the presence of BSA (Rectangle box) and βLg (Rectangle dotted box). The annotations at the base indicate the individual contents in the lane.

As observed in **Table 2.1**, there was more BSA and βLg in the recycled feed solution when spacer is present during UF. Based on the standard intensity of BSA, there was an excess of 24% of BSA in the final feed solution with spacer compared with no spacer, indicating more BSA available in the feed solution. On the other hand, based on the standard intensity of βLg, 61% more βLg was observed in the final feed solution with spacer compared to no spacer present. However, these readings do not make sense as there should not be change in the BSA and βLg concentration in the feed as from the mass balance, very small amount of proteins were deposited on the membrane (**Chapter 4, Section 4.3.1**). These might be caused by errors during measurements.

Table 2.1
Relative protein quantification of the feed solution after filtration from band intensity measurements of 1D SDS-PAGE Coomassie G-250 stained gel. The linear standards are: BSA (μg) = 1.3098 Intensity (R^2 = 0.9549); and βLg (μg) = 2.473 Intensity (R^2 = 0.9638) give the amount of BSA and BLg in the original feed

	Experimental Settings		
	4 hr spacer	8 hr spacer	8 hr no spacer
Protein	Relative Protein Mass (μg) in 20μl electrophoresis solution		
BSA	21.00	76.92	58.47
βLg	16.61	51.96	20.09

The standards used are equimolar 1 wt% mixed BSA/βLg (39.44μg/10.672μg) and 0.1wt% mixed BSA/βLg (3.944μg/1.0672μg). The gel was dyed with Coomassie blue (CBB G250) to enable relative quantification to be performed due to the excellent linearity range of 1 – 1.3 and detection limit of 30 – 100ng proteins

The graph shows the relative masses for BSA and βLg on the surface based on the standards injected in each gel and by comparing the intensities of the BSA and βLg bands with the known standards. The known masses of standards are 3.519μg of BSA and 0.9696μg of βLg and

2.5. 4 hours of UF no spacer SYNDER

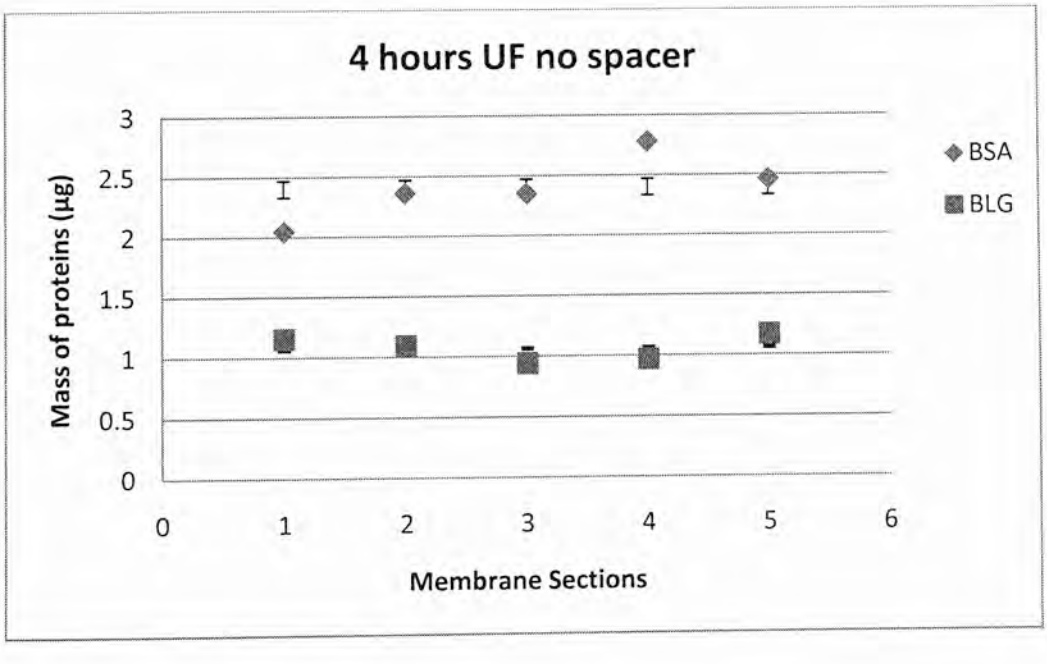

Figure 2.6 BSA and βLg profile along the membrane strip after 4 hours of fouling without spacer (SYNDER) using 1D SDS-PAGE.

2.6. The calculations of pressure losses on the UF rig

2.6.1. Procedures

Diameter of entrance and exit, d = 0.01 m = d_{i1}
Hydraulic diameter of channel without spacer, dh = 0.003 m = d_{i2}
Reynold's number, Re = 451
Fanning friction factor, f = $\frac{16}{Re}$ = 0.0355

1. Pressure drop at the entrance:

A contraction occurred at the entrance of the channel,

Using $\Delta P_c = \Delta P_{ent} = K\left(\frac{\rho u_2^2}{2}\right)$, where K = $0.4\left[1.25 - \left(\frac{d_{i2}}{d_{i1}}\right)^2\right]$ when $\frac{d_{i2}^2}{d_{i1}^2} < 0.715$

$\Delta P_c = 4.5472\ Pa$

2. Pressured drop along the channel:

Using $\Delta P_f = \frac{2fL\rho u^2}{d_i}$ = 231.93 Pa

3. Pressure drop at the exit:

Using $\Delta P_{ex} = \frac{\rho u_1^2}{2}\left[1 - \left(\frac{d_{i1}}{d_{i2}}\right)^2\right]^2$ = 8.115 Pa

2.7. FESEM

These are some of the images obtained using electron microscopy. The membrane was rinsed with MQ water prior to fixation, dehydration and critical point drying. **Figure 2.7** shows the FESEM images of clean PALL membrane. Image 1 and 2 shows the surface of a clean membrane at 250× and 500× magnification respectively. Here the membrane surface looks relatively smooth with many small fracture lines occurring in most areas. Zooming in on the smooth areas previously at 5000×, image 3 the area is covered with globules embedded into the surface. The globules originated from the chemical pre-treatment of the membrane surface. We

can conclude that the globules are chemical coatings found on the membrane that might help to reduce fouling or bacteria growth. The crack was magnified at ×10000, (image 4) and no globules can be found inside. Globules are magnified at ×30000 (image 4) and ×100K (image 6) times. The globules are confirmed to be etched on the membrane surface and at ×100K (image 6), we can observe that the smooth skin of the membrane.

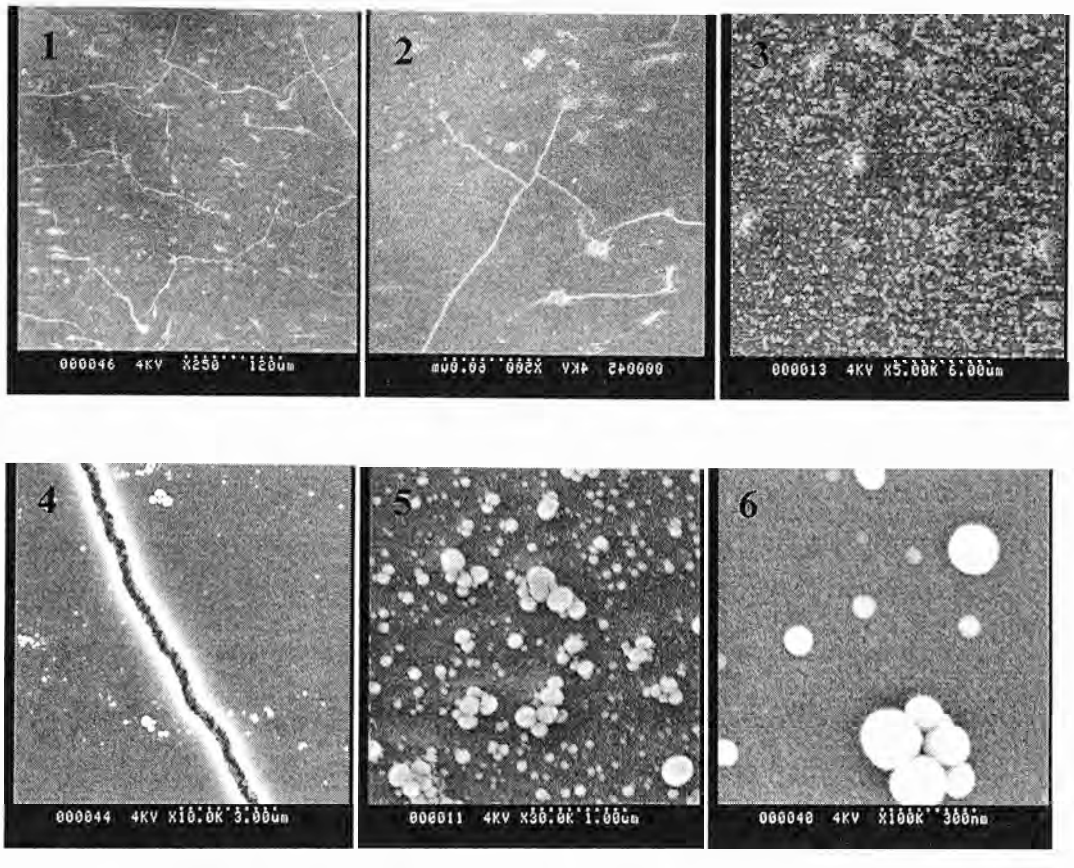

Figure 2.7 Image of Clean PALL Membrane at different magnification. 1: ×250, 2: ×500, 3: ×5K, 4: ×10K, 5: ×30K, 6: ×100K

Figure 2.8 shows the FESEM images of clean and unused SYNDER membrane. Image 1 and 2 was observed at ×30000 mag. The surface of SYNDER membrane was not significantly covered with globules as observed in **Figure 2.6**. The surface at this magnification is smooth and relatively clean. Zooming in on the surface at ×100K (image 3) and ×200K (image 4), we can see that the surface is closely similar to the skin observed in **Figure 2.6** (image 6). however the surface is more wrinkled.

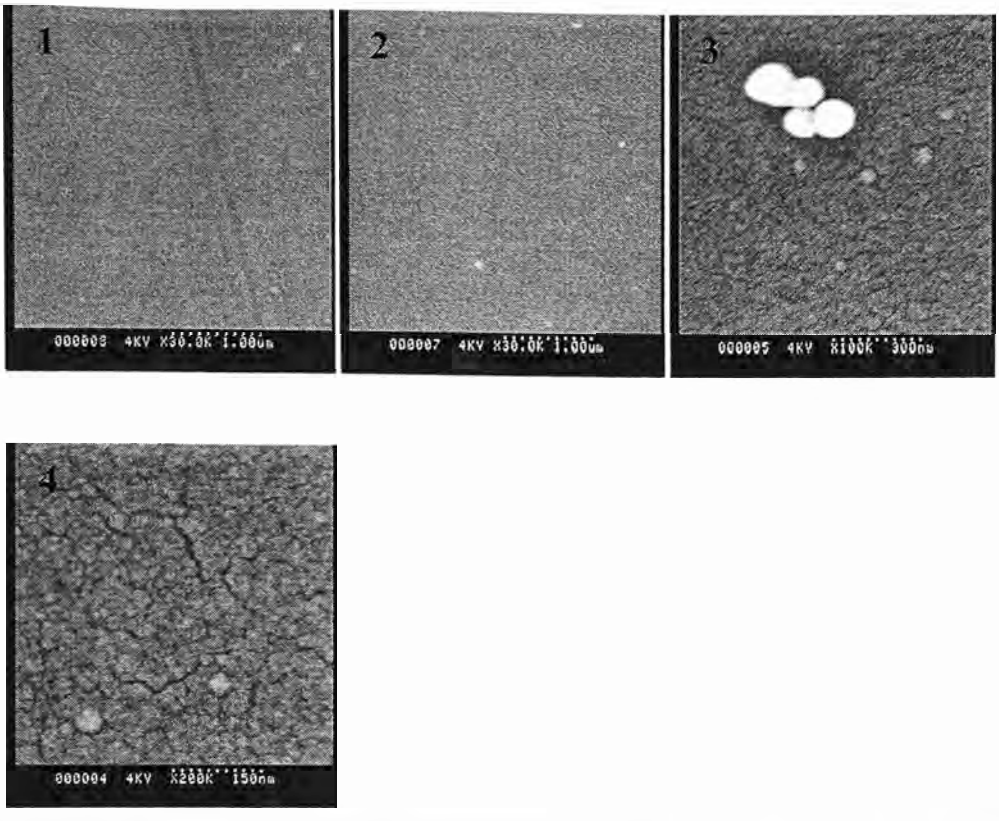

Figure 2.8 Image of Clean SYNDER Membrane at different magnification. 1: ×30K, 2: ×30K, 3: ×100K, 4: ×200K

Figure 2.9 shows the images of protein adsorbed SYNDER membranes. The membranes are cut into small $10mm^2$ pieces and soaked in 0.1% BSA solutions for 1 hour. Image 1, 2 and 3 are membranes adsorbed by BSA under static adsorption (No TMP). We can observe that in most sections, the surface is covered with proteins. Image 3 shows an interesting artefact of BSA adsorption. The results indicate the strong attraction of BSA to the membrane surface. Image 4 shows a zoomed image at ×30000 magnification. Image 5 and 6 are binary protein adsorbed membranes viewed at ×30000. The deposition was layered and wave-like.

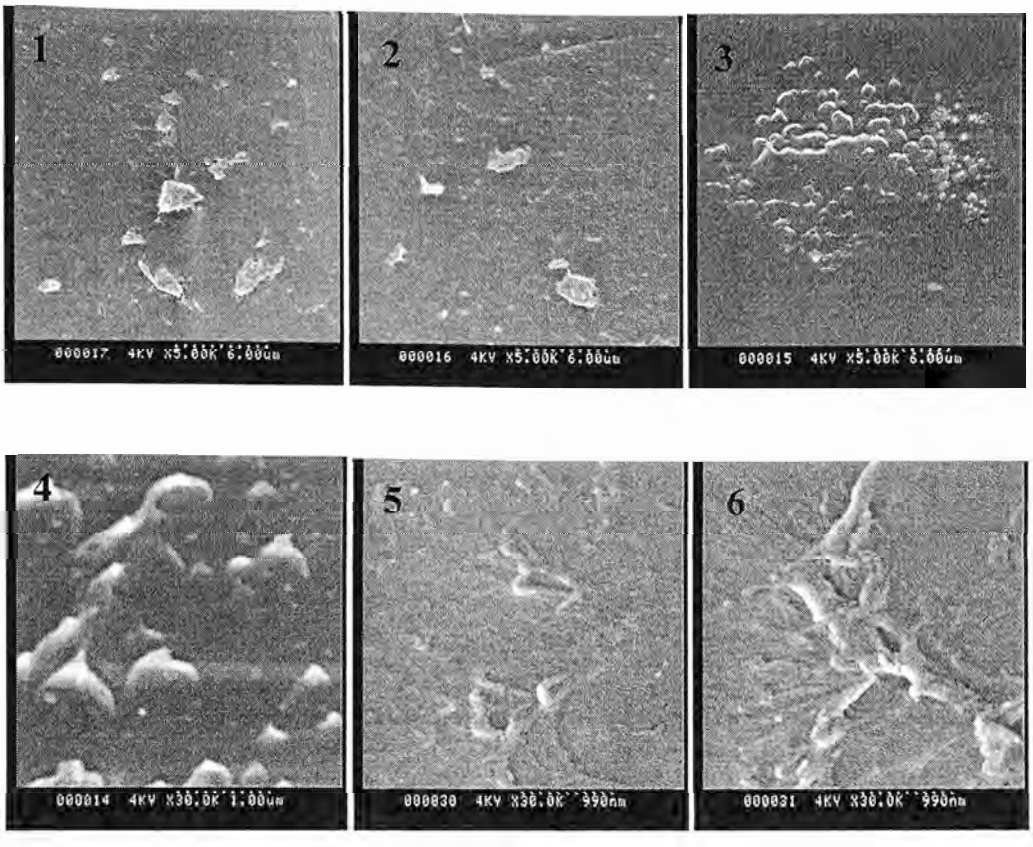

Figure 2.9. Images of fouled SYNDER Membrane at different magnification. 1: ×5K BSA adsorbed, 2: ×5K BSA adsorbed, 3: ×5K BSA adsorbed, 4: 30K BSA adsorbed, 5: ×30K Binary BSA & βLg adsorbed, 6: ×30K Binary BSA & βLg adsorbed,.

Figure 2.10 shows the FESEM images of protein adsorbed PALL membranes. The globules are identified as pre-treatment impurities coming from the clean membrane (Figure 4.23). Image 1 and 2 shows BSA adsorbed membrane observed at ×10000. The deposition was layered and wave-like. The surface is covered with pot holes originated from the caused by the impurities found on the membrane. There are close similarity between BSA and binary protein adsorbed membranes (Image 4 and 5). The impurities are seen embedded into protein deposits on the surface.

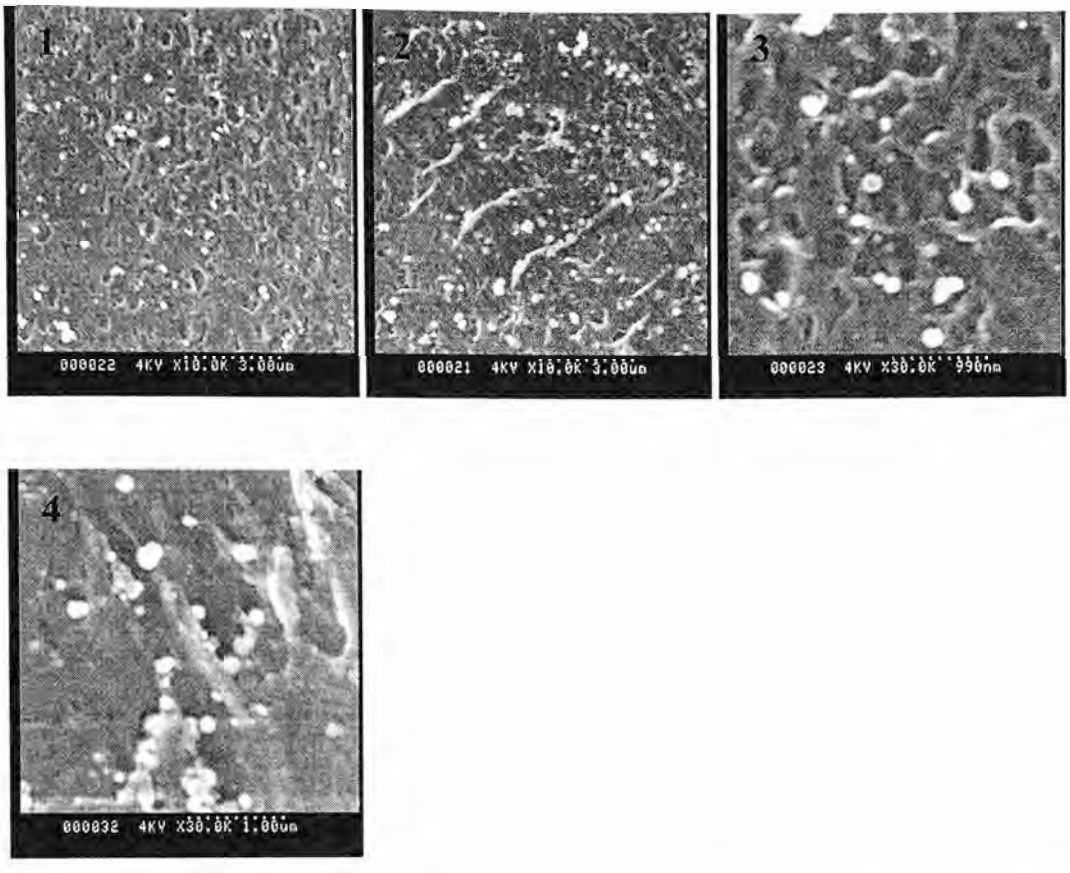

Figure 2.10 Image of protein adsorbed Pall Membrane at different magnification. 1: ×10K BSA adsorbed, 2: ×10K BSA adsorbed, 3: ×30K BSA adsorbed, 4: ×30K Binary BSA & βLg adsorbed, ×30K)

3. Appendix C – Chapter 5

Investigating the Residues after Chemical Cleaning of Ultrafiltration Membrane Fouled with Whey Isolate and Binary BSA and βLg Solutions

3.1. Observation of membrane surface using FESEM

The surface of a clean PALL membranes were analysed using FESEM in photographs (1 – 5) of **Figure 3.1**. Clean PALL membrane was smooth at 20,000× (photo 1), however the surface was less homogeneous and rougher at 100,000× (photos 2 and 3). In addition, small openings of 60nm diameter could be seen on the surface of the membrane. However these openings were not pores as they were still too big for the specified MWCO of 30KDa. Also, it could be observed that SYNDER membranes (photo 5) were more granulated than PALL membrane (photos 1 – 4). The pores were not visible at a high magnification, even up to 200,000×. The membranes were relatively clean and pure as neither foreign particles nor bacteria could be detected on the membrane surface.

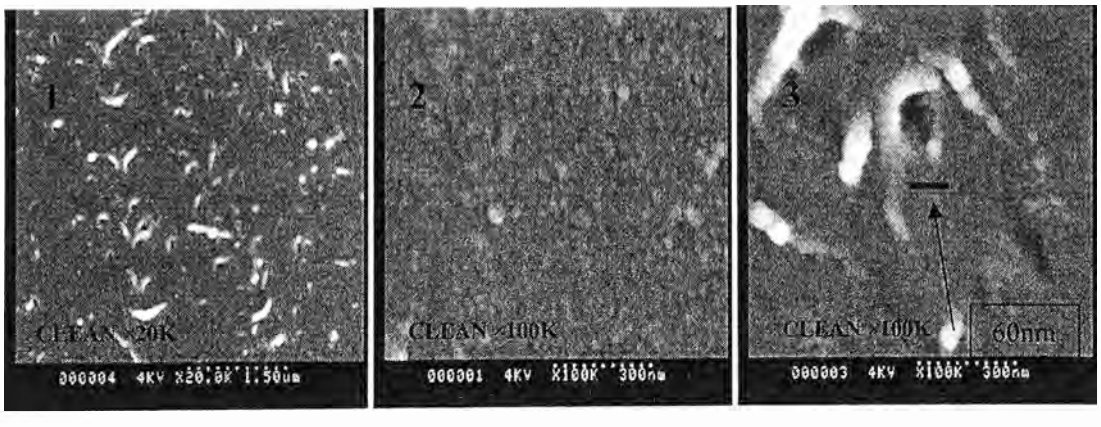

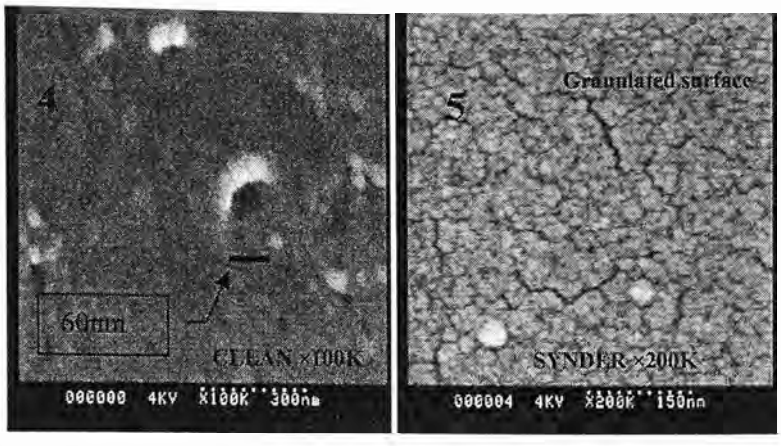

Figure 3.1 Surface FESEM photographs of unused 30,000 MWCO, Pall membranes (Photos 1 – 4) and Synder Filtration membrane (Photo 5).

The surface of WPI fouled membranes (0.1wt%, 4 hours, 500ml/min, 50KPa) are shown in Photos (1 – 3) in **Figure 3.2**. We could observe spherical deposition and cake–like semi–solid deposition on the membrane surface. The globules were fats/lipids present in the WPI (0.6g/100g) that 0.06g in the fouling mixture. The largest of these globules have a diameter of about 0.250μm (250nm). These globules were randomly spread, absent in some regions and clumped together in other areas. There were also scattered circular prints present on the fouled surface where globules were absent. These circular prints were footprints of the globules when they were removed by flow. Some globules were also trapped in between the cake structure.

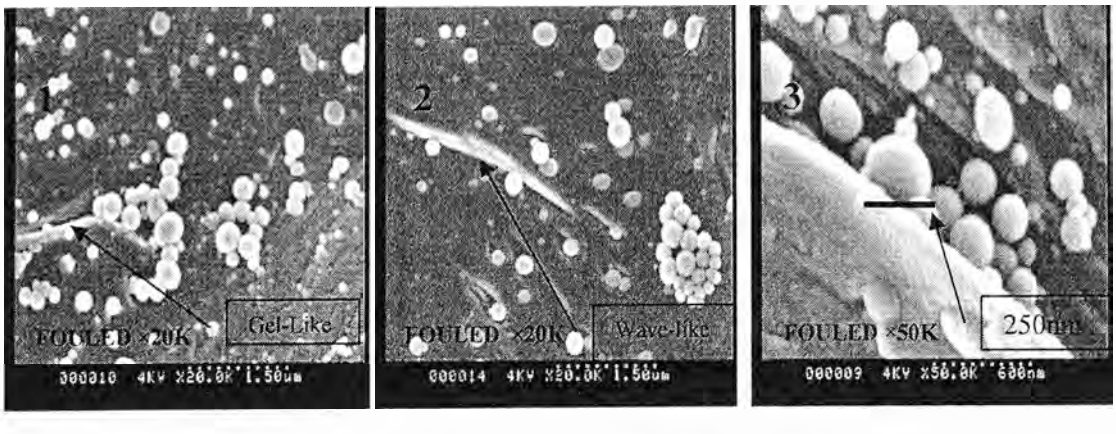

Figure 3.2 Surface FESEM photographs of WPI fouled 30,000 MWCO, Pall membranes (1 – 3)

The surface of HCl treated (0.1M HCl soaked under agitation, 30 mins) membranes are shown in Photos (1 – 3) in **Figure 3.3**. The fat globules were removed from the surface leaving behind circular footprints on the gel surface. Fragments that originated from the hydrolysis treatment could be observed on the surface of the HCl treated membrane. The photos shows that the gel were not completely removed from the membrane surface after the treatment and the membrane did not resemble the clean membranes in **Figure 3.1**.

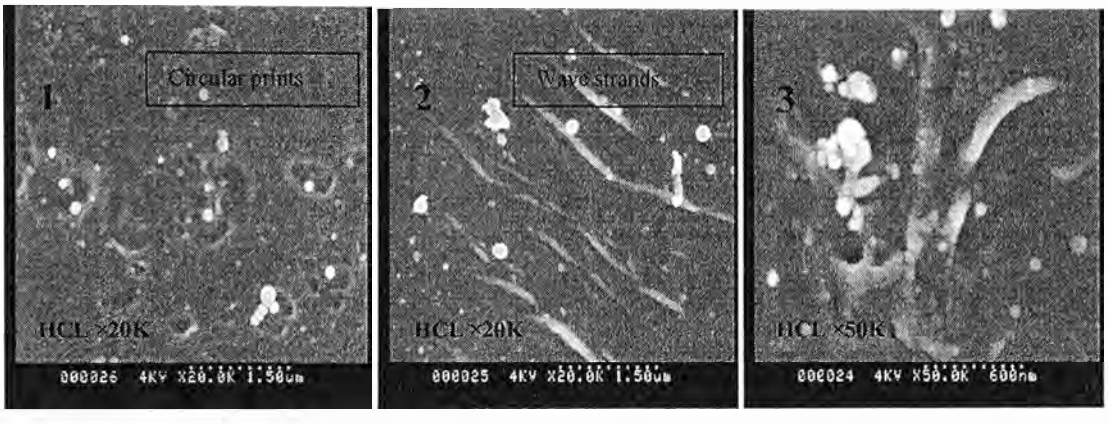

Figure 3.3 Surface FESEM photographs of HCl treated of WPI fouled 30,000 MWCO, Pall membranes (1 – 3)

The surface of NaOH treated (0.1M NaOH soaked under agitation, 30 mins) membranes are shown in Photos (1 – 2) in **Figure 3.4**. Similar to HCl treatment, the fat globules were removed from the surface leaving behind circular footprints on the gel surface. Fragments originated from the hydrolysis treatment could be seen on the surface of the NaOH treated membrane. Again, the gel are not completely removed from the membrane surface.

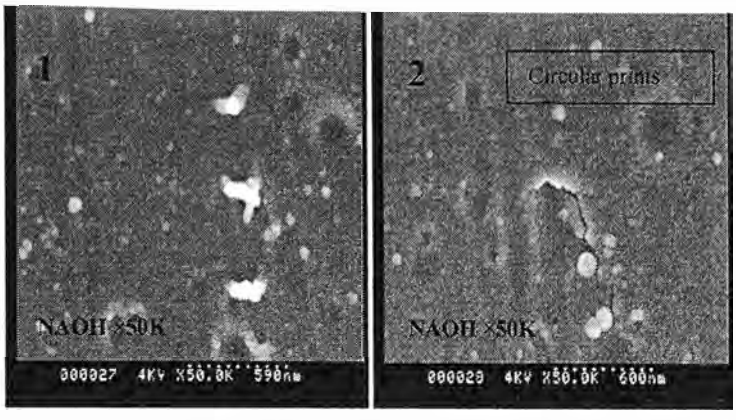

Figure 3.4 Surface FESEM photographs of NaOH treated of WPI fouled 30,000 MWCO, Pall membranes (1 – 2)

The surface of PMA treated (0.1% PMA soaked under agitation, 30 mins) membranes are shown in Photos (1 – 3) in **Figure 3.5**. At 50,000×, the photos were similar to HCl and NaOH treatment, where most of the fat globules were removed from the surface leaving behind circular footprints on the gel surface. However, the fragments present in **Figure 3.3** were absent and at 100,000×, the surface was rougher and granulated.

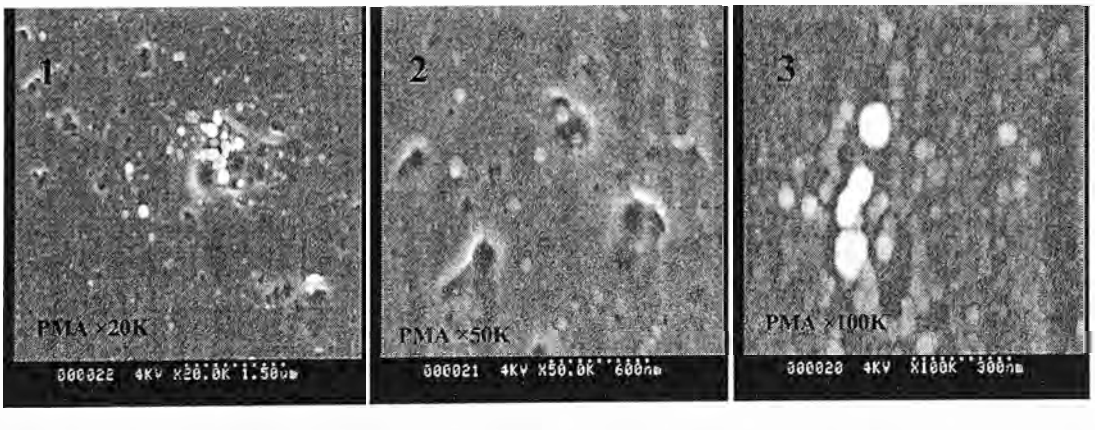

Figure 3.5 Surface FESEM photographs of Protease M Amano treated mof WPI fouled 30,000 MWCO, Pall membranes (1 – 3)

Static adsorption of proteins, BSA or BSA and βLg (1 hour, under agitation) was performed on SYNDER membranes and the results were analysed using FESEM (**Figure 3.6**). In BSA adsorbed membranes (photos 1 – 3), there were fragments and agglomeration of BSA on the surface. In photo 3, the protein agglomeration resembles "shallots" gel-like deposition. On the other hand, in BSA and βLg (photos 4 and 5) adsorbed membranes, the deposition resembles a more cake-like deposition.

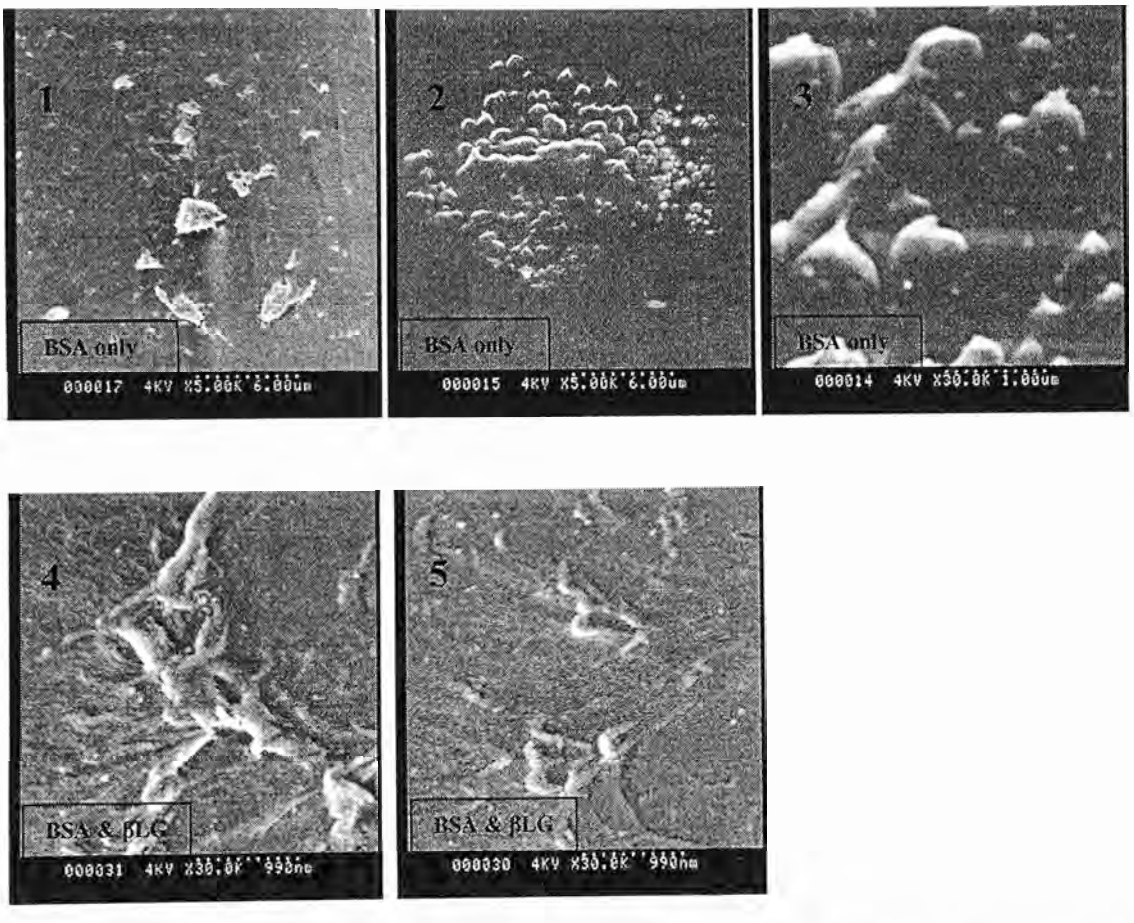

Figure 3.6 Surface FESEM micrographs of protein (BSA or BSA and βLg) adsorbed on 30,000 MWCO Synder membranes

4. Appendix D – Chapter 6

Investigating Concentration Polarization and Fouling on the Steady State Flux in the Cross–flow UF of BSA Solutions

4.1. Methods to derive stagnant-film equation

In our current study, a mass balance equation was used to describe the change in concentration during UF near the membrane wall

$$\frac{\partial C}{\partial t} + v \cdot \nabla C = D\nabla^2 C$$

Where C is the concentration of the solute and D is the diffusivity of the solute in the solvent phase (water) with assumptions:

i. No concentration gradient exists in the z-direction (axial)
ii. The concentration gradient in the direction of the product flow $^{\partial C}/_{\partial x}$ can be considered negligible in comparison with $^{\partial C}/_{\partial y}$

Using these assumptions and considering the relation $v_y = -J_v$, equation becomes

$$\frac{\partial C}{\partial t} - J_v \frac{\partial C}{\partial y} = D \frac{\partial^2 C}{\partial y^2}$$

The boundary conditions

At t = 0, $C = C_{w,0} = C_{b,0}$

At y = δ, $C = C_b$

At y = 0, $J_v C_w = -D \left(\frac{\partial C}{\partial y}\right)_{y=0}$

Under steady state conditions, the equation becomes [Chapter 6, Eqn. (8)],

$$J_v = \frac{D}{\delta} ln \frac{C_w}{C_b} = k ln \frac{C_w}{C_b} \quad (8)$$

where k represents the mass transfer coefficient and δ is for layer thickness for solute transport through the membrane cell.

4.2. BSA rejection during UF

The BSA concentration in the feed solution and permeate was measured using UV-Vis Spectrophotometer and the results are shown in **Figure 4.1 and 4.2** for unsalted and salted solutions respectively. As shown, there were generally trace amount of BSA detected in the permeate solution however a 100% rejection can be safely assumed. For both un-buffered and buffered, highest BSA concentration in the final feed was observed at pH 7.4, where the permeate flux is highest at constant TMP of 50KPa. Thus, at pH 4.5, the final feed concentration is the lowest, where the flux is the lowest due to electrostatic charges.

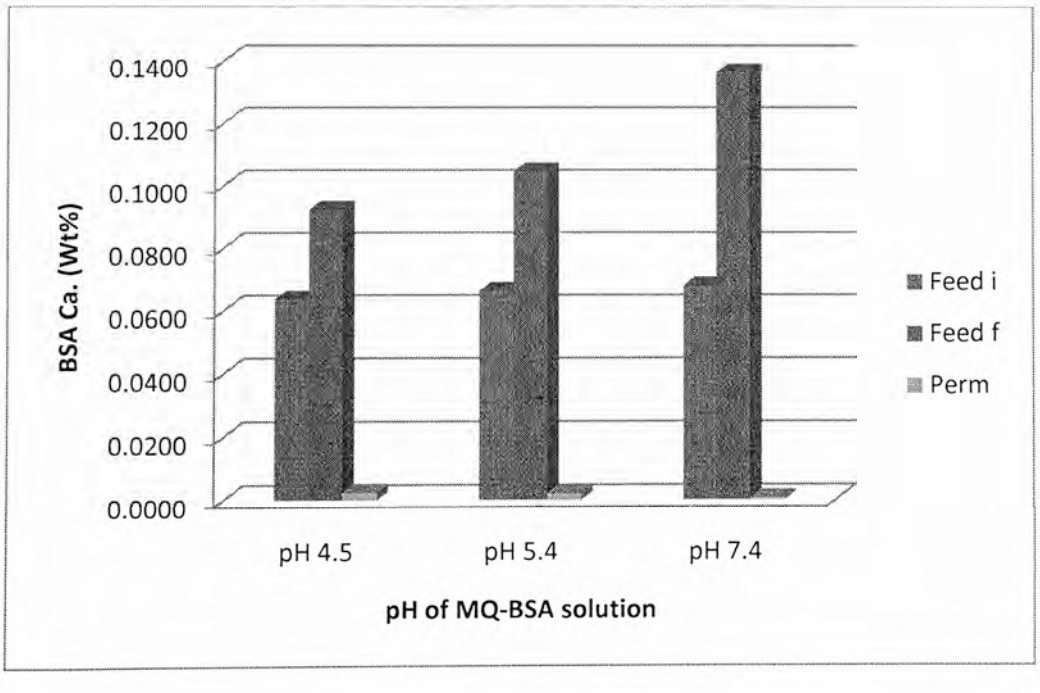

Figure 4.1 Effects of pH during UF on the final feed and permeate concentration (1hr, 50KPa TMP, 1.05×10^{-5}M BSA, 500ml/min, unsalted).

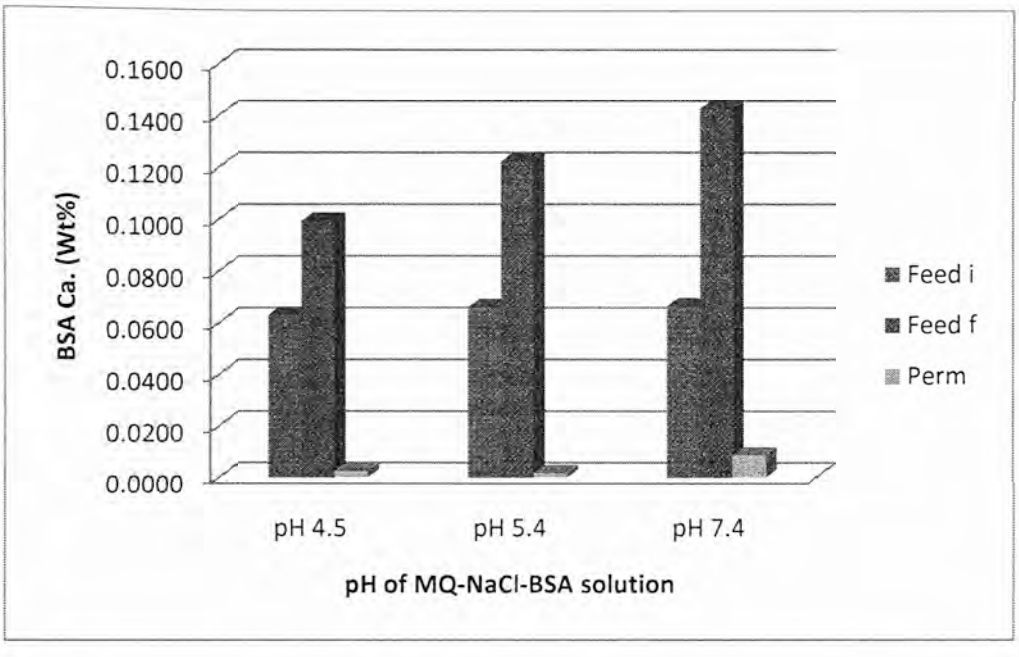

Figure 4.2 Effects of pH during UF on the final feed and permeate concentration (1hr, 50KPa TMP, 1.05×10^{-5}M BSA, 500ml/min, salted).

By comparing the two figures again, for salted feed and unsalted feed solutions respectively, there was higher BSA concentration measured in the salted feed solution of buffered. Thus the fluxes are generally higher for unsalted solutions causing a higher final concentration of the feed solution.

4.3. Effect of feed and flow on BSA deposition

Figures 4.3 shows the BSA deposition along the membrane surface at pH 5.4 and 500mlmin^{-1} under different feed concentrations.

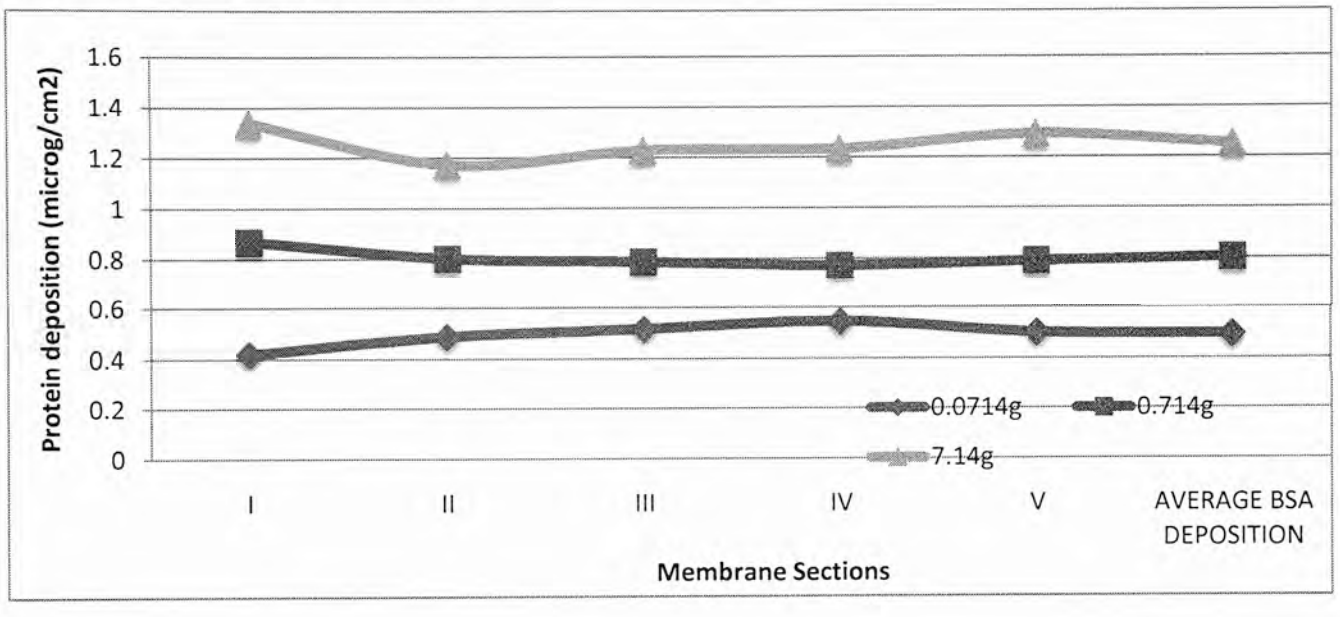

Figure 4.3 Deposition of BSA on the membrane at various feed concentration after UF (salted) (1hr, 50KPa TMP, pH 5.4, 0.15M NaCl, 500mlmin^{-1}, lines to guide the eye)

Figure 4.4 shows BSA deposition along the membrane surface at pH 5.4 and 1.016×10^{-5}M, under various cross-flow rates

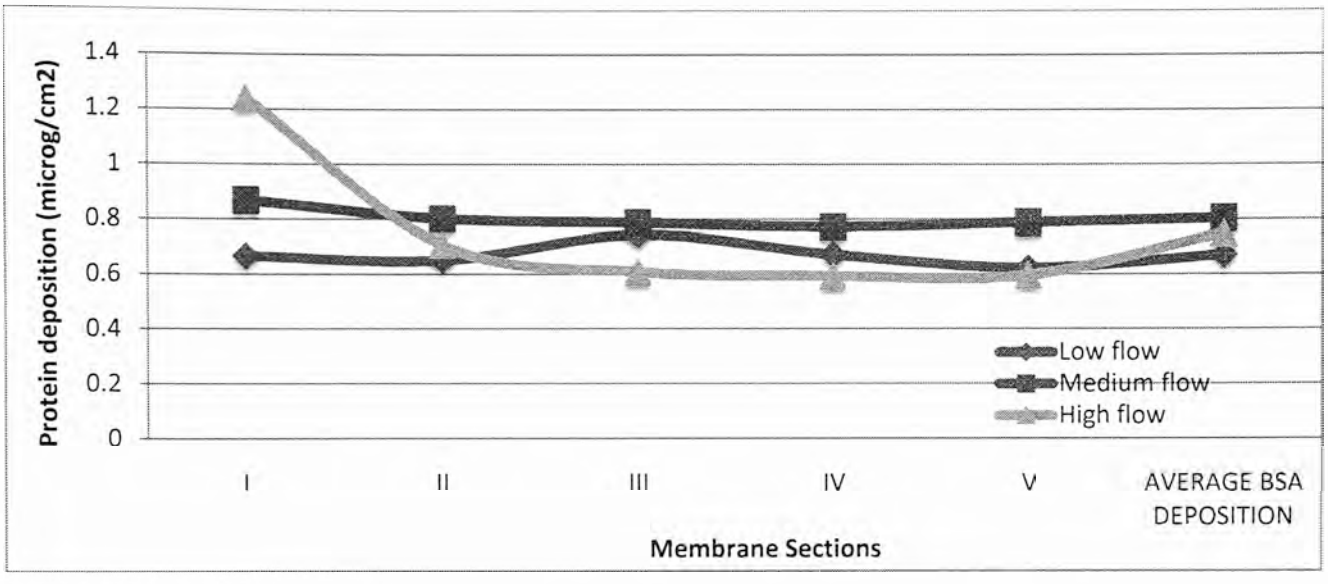

Figure 4.4 Deposition of BSA on the membrane at various flow after UF (salted)
(1hr, 50KPa TMP, pH 5.4, 0.15M NaCl, 500mlmin^{-1}, lines to guide the eye)

FINAL HARDBOUND LIBRARY COPY